N 70 35821

NASA CR-72687
U-C R-957

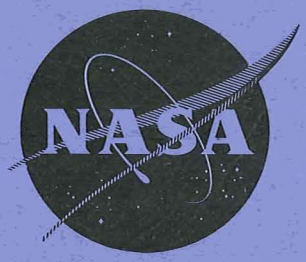


# WROUGHT NICKEL-BASE SUPERALLOYS

by

W. B. Kent

UNIVERSAL-CYCLOPS SPECIALTY STEEL DIVISION
CYCLOPS CORPORATION

prepared for

NATIONAL AERONAUTICS AND SPACE ADMINISTRATION

NASA Lewis Research Center
Contract NAS 3-11155
Fredric H. Harf, Project Manager
Robert L. Dreshfield, Research Advisor

CASE FILE
COPY

**NOTICE**

This report was prepared as an account of Government-sponsored work. Neither the United States, nor the National Aeronautics and Space Administration (NASA), nor any person acting on behalf of NASA:

A.) Makes any warranty or representation, expressed or implied, with respect to the accuracy, completeness, or usefulness of the information contained in this report, or that the use of any information, apparatus, method, or process disclosed in this report may not infringe privately-owned rights; or

B.) Assumes any liabilities with respect to the use of, or for damages resulting from the use of, any information, apparatus, method or process disclosed in this report.

As used above, "person acting on behalf of NASA" includes any employee or contractor of NASA, or employee of such contractor, to the extent that such employee or contractor of NASA or employee of such contractor prepares, disseminates, or provides access to any information pursuant to his employment or contract with NASA, or his employment with such contractor.

Requests for copies of this report should be referred to

National Aeronautics and Space Administration
Scientific and Technical Information Facility
P.O. Box 33
College Park, Md. 20740

NASA CR-72687
U-C R-957

FINAL REPORT

# WROUGHT NICKEL-BASE SUPERALLOYS

by

W. B. Kent

UNIVERSAL-CYCLOPS SPECIALTY STEEL DIVISION
CYCLOPS CORPORATION
Bridgeville, Pennsylvania

prepared for

NATIONAL AERONAUTICS AND SPACE ADMINISTRATION

March 26, 1970

CONTRACT NAS 3-11155

NASA Lewis Research Center
Cleveland, Ohio
Fredric H. Harf, Project Manager
Robert L. Dreshfield, Research Advisor
Materials and Structures Division

# FOREWORD

The work described herein was conducted by the Research and Development Department of the Universal-Cyclops Specialty Steel Division, Bridgeville, Pennsylvania, under NASA Contract NAS 3-11155. The contract was administered under the management of the NASA Project Manager, Mr. F. H. Harf, Materials and Structures Division, NASA Lewis Research Center. Mr. R. L. Dreshfield served as the NASA Research Advisor.

The Project Engineer for the program was Mr. W. B. Kent of Universal-Cyclops Specialty Steel Division. Mr. L. W. Lherbier served as Program Supervisor, and technical assistance was provided by Mr. H. L. Black and Mr. F. J. Rizzo.

ABSTRACT

Six highly alloyed nickel-base compositions were evaluated to select a base for the development of a new wrought high temperature alloy with improved strength characteristics. Four of the compositions were successfully extruded and rolled to bar stock. Tensile strengths from room temperature to 1800°F (982°C), stress rupture properties to 1900°F (1038°C), sulfidation and oxidation resistance and phase stability were evaluated. It was concluded that a composition of 0.13 C, 10 Cr, 10 Co, 2 Mo, 5.5 W, 8 Ta, 4.5 Al, 1 Ti, 1 V, 1 Hf, and balance nickel offered excellent potential for the development of a new wrought superalloy.

TABLE OF CONTENTS


| | | Page |
|---|---|---|
| I. | SUMMARY | 1 |
| II. | INTRODUCTION | 3 |
| III. | PROCEDURE | 4 |
| | A. Task I | 4 |
| | 1. Materials | 4 |
| | 2. Melting | 4 |
| | 3. Chemical Analysis | 4 |
| | 4. As-Cast Hot Workability Studies | 5 |
| | 5. Processing | 5 |
| | a. Single Extrusions | 5 |
| | b. Double Extrusions | 6 |
| | c. Rolling and Forging | 6 |
| | d. Workability Studies of Extruded Material | 7 |
| | 6. Inspection | 7 |
| | 7. Structural Examination | 7 |
| | a. Metallographic Analysis | 8 |
| | b. X-Ray Phase Analysis | 8 |
| | c. Electron Beam Microprobe Analysis | 8 |
| | B. Task II | 9 |
| | 1. Heat Treatment Evaluation | 9 |
| | a. Heat Treatment Studies | 9 |
| | b. Structural Examination | 10 |
| | 2. Mechanical Testing | 10 |
| | a. Tensile Tests | 11 |
| | b. Stress Rupture Testing | 11 |
| | (1) Testing Procedure | 11 |
| | (2) Structural Examinations | 11 |
| | c. Interrupted Low Cycle Fatigue Tests | 12 |
| | 3. Evaluation of Processing Variations | 12 |
| | a. Rolling | 12 |
| | (1) As-Cast Material | 12 |
| | (2) Single Extruded Material | 12 |
| | b. Forging | 13 |
| | 4. Thermal Stability Studies | 13 |
| | a. Thermal Exposures | 13 |
| | b. Stress Rupture Tests | 13 |
| | c. Structural Examinations | 13 |
| | 5. Oxidation Testing | 13 |
| | a. Cyclic Testing | 13 |
| | (1) Testing Procedure | 13 |
| | (2) Structural Examinations | 14 |
| | b. Continuous Oxidation Tests | 14 |
| | 6. Sulfidation Testing | 14 |
| | a. Testing Procedure | 14 |
| | b. Structural Examination | 15 |

TABLE OF CONTENTS (Continued)


| | | Page |
|---|---|---|
| | 7. Thermal Cycling Fatigue Testing | 15 |
| IV. | RESULTS AND DISCUSSION | 16 |
| | A. Task I | 16 |
| | 1. Melting | 16 |
| | 2. Chemical Analyses | 16 |
| | 3. As-Cast Hot Workability Studies | 16 |
| | 4. Processing | 17 |
| | a. Single Extrusions | 17 |
| | b. Double Extrusions | 18 |
| | c. Rolling and Forging | 19 |
| | d. Hot Workability Studies - Extrusions | 20 |
| | 5. Structural Examinations | 20 |
| | a. As-Cast Material | 21 |
| | b. Material Quenched From the Optimum Working Temperature | 22 |
| | c. Extruded Material | 22 |
| | B. Task II | 23 |
| | 1. Heat Treatment Evaluation | 23 |
| | a. Determination of Optimum Temperatures | 23 |
| | (1) Solution Treatments | 23 |
| | (2) Intermediate Aging Treatments | 24 |
| | (3) Final Aging Treatments | 25 |
| | b. Structural Examinations | 25 |
| | 2. Mechanical Testing | 26 |
| | a. Tensile Tests | 26 |
| | b. Stress Rupture Tests | 27 |
| | (1) Rupture Life and Ductility Data | 27 |
| | (2) Structural Evaluation | 28 |
| | c. Interrupted Low Cycle Fatigue Tests | 30 |
| | 3. Processing Studies | 30 |
| | a. Rolling | 30 |
| | b. Forging | 32 |
| | 4. Thermal Stability Studies | 32 |
| | a. Phase Identification | 32 |
| | b. Microstructure | 33 |
| | c. Stress Rupture Testing | 35 |
| | 5. Oxidation Testing | 36 |
| | a. Continuous Tests | 36 |
| | b. Cyclic Testing | 36 |
| | (1) Weight Change Data | 36 |
| | (2) Microstructural Examinations | 36 |
| | (3) Examination of Oxide Scales | 38 |
| | 6. Sulfidation Testing | 39 |
| | 7. Thermal Cycling Fatigue Testing | 39 |
| V. | SUMMARY OF RESULTS | 40 |
| VI. | CONCLUDING REMARKS | 42 |
| | REFERENCES | 43 |

LIST OF TABLES


| Table | |
|---|---|
| 1 | Chemical Analyses of Fifty Pound Heats. |
| 2 | Chemical Analyses of One Hundred Pound Heats. |
| 3 | Gleeble Hot Ductility Results For As-Cast Unitemp AF 2-1DA. |
| 4 | Gleeble Hot Ductility Results For As-Cast I 5. |
| 5 | Gleeble Hot Ductility Results For As-Cast IIb. |
| 6 | Gleeble Hot Ductility Results For As-Cast IIIg mod. |
| 7 | Gleeble Hot Ductility Results For As-Cast IId. |
| 8 | Gleeble Hot Ductility Results For As-Cast IIIg. |
| 9 | Gleeble Inherent Ductility Profiles For Single and Double Extruded Unitemp AF 2-1DA. |
| 10 | Gleeble Inherent Ductility Profiles For Single and Double Extruded I 5. |
| 11 | Gleeble Inherent Ductility Profiles For Single and Double Extruded IIb. |
| 12 | Gleeble Inherent Ductility Profiles For Single and Double Extruded III g mod. |
| 13 | Gleeble Inherent Ductility Profile For Single Extruded IId. |
| 14 | Gleeble Inherent Ductility Profile For Single Extruded IIIg. |
| 15 | X-Ray Diffraction Studies of Residues Extracted From Specimens for Task I Structural Evaluations. |
| 16 | X-Ray Diffraction Studies of Residues Extracted from Task II Alloys After Each Stage of Heat Treatment. |
| 17 | Tensile Properties of Unitemp AF 2-1DA. |
| 18 | Tensile Properties of I 5. |
| 19 | Tensile Properties of IIb. |

LIST OF TABLES (continued)


| Table | |
|---|---|
| 20 | Tensile Properties of III g mod. |
| 21 | Stress Rupture Properties of Unitemp AF 2-1DA. |
| 22 | Stress Rupture Properties of I 5. |
| 23 | Stress Rupture Properites of IIb. |
| 24 | Stress Rupture Properties of III g mod. |
| 25 | X-Ray Diffraction Studies of Residues Extracted From Task II Alloys After Stress Rupture Testing at Various Conditions. |
| 26 | Interrupted Low Cycle Fatigue Data for Task II Alloys. |
| 27 | Stress Rupture Properties for Unitemp AF 2-1DA and I 5 Rolled Material. |
| 28 | Stress Rupture Properties for Task II Alloys in the Single Extruded and Rolled Condition. |
| 29 | X-Ray Diffraction Studies of Residues Extracted From Task II Thermal Stability Specimens. |
| 30 | 1400°F/90,000 psi Stress Rupture Data for Task II Stability Exposure Specimens. |
| 31 | Oxidation Data for Task II Alloys Subjected to Cyclic Testing at 1875°F. |
| 32 | Oxidation Data for Task II Alloys Subjected to Cyclic Testing at 1950°F. |
| 33 | Oxidation Data for Task II Alloys Subjected to Cyclic Testing at 2100°F. |
| 34 | Sulfidation Data for Task II Alloys. |

## LIST OF FIGURES


| Figure | |
|---|---|
| 1 | Schematic Diagrams of Two Types of Canned Billets for Extrusion to Two Sizes. |
| 2 | Test Specimen Configurations. |
| 3 | Gleeble Hot Workability Curves for As-Cast Unitemp AF 2-1DA and I 5. |
| 4 | Gleeble Hot Workability Curves for As-Cast IIb and IIIg mod. |
| 5 | Gleeble Hot Workability Curves for As-Cast IId and IIIg. |
| 6 | Results of Series I Single Extrusions. |
| 7 | Results of Series II Single Extrusions. |
| 8 | Results of Series III Single Extrusions. |
| 9 | Results of Series IV Single Extrusions. |
| 10 | Results of First Phase of Double Extrusions. |
| 11 | Results of Second Phase of Unitemp AF 2-1DA Double Extrusions. |
| 12 | Results of Second Phase of I 5 Double Extrusions. |
| 13 | Results of Second Phase of IIb Double Extrusions. |
| 14 | Results of Second Phase of IIIg mod Double Extrusions |
| 15 | Unitemp AF 2-1DA and I 5 Bars Rolled From 3 1/8 Inch Diameter Ingots to One Inch Diameter Round Cornered Square Bars. |
| 16 | Gleeble Hot Workability Curves For Extruded Unitemp AF 2-1DA and I 5. |
| 17 | Gleeble Hot Workability Curves For Extruded IIb and IIIg mod. |
| 18 | Gleeble Hot Workability Curves For Extruded IId and IIIg. |
| 19 | Photomicrographs Representing the Basic Variations in the As-Cast Microstructures of the Experimental Alloys. |
| 20 | Photomicrographs of IIIg and Unitemp AF 2-1DA Illustrating the Similarity to the As-Cast Structure After Quenching From the Optimum Working Temperature. |

LIST OF FIGURES (continued)


| Figure | |
|---|---|
| 21 | Photomicrographs Comparing the Structures of Three Alloys After Extrusion to Three Inch Diameter and One Inch Diameter Billets. |
| 22 | Optical Micrographs of Double Extruded Unitemp AF 2-1DA Illustrating the Effect of Various Solution Treatments on Grain Size. |
| 23 | Optical Micrographs of Double Extruded I 5 Illustrating the Effect of Various Intermediate Aging Treatments on Gamma Prime and Grain Boundary Carbide Precipitation. |
| 24 | Electron Micrographs of Unitemp AF 2-1DA Illustrating the Variations in Structure After Each Stage of Heat Treatment. |
| 25 | Electron Micrographs of I 5 Illustrating the Variations in Structure After Each Stage of Heat Treatment. |
| 26 | Electron Micrographs of IIb Illustrating the Variations in Structure After Each Stage of Heat Treatment. |
| 27 | Electron Micrographs of IIIg mod Illustrating the Variations in Structure After Each Stage of Heat Treatment. |
| 28 | Ultimate Tensile Strength versus Test Temperature for Task II Alloys. |
| 29 | 0.2 Percent Yield Strength versus Test Temperature for Task II Alloys. |
| 30 | Tensile Ductility versus Test Temperature for Task II Alloys. |
| 31 | Larson-Miller Parameter Curves Showing Stress Rupture Properties of Task II Alloys. |
| 32 | Stress Rupture Ductility versus Test Temperature for Task II Alloys. |
| 33 | Microstructures of Double Extruded Unitemp AF 2-1DA After Stress Rupture Testing at Various Conditions. |
| 34 | Microstructures of Double Extruded I 5 After Stress Rupture Testing at Various Conditions. |
| 35 | Microstructures of Double Extruded IIb After Stress Rupture Testing at Various Conditions. |

LIST OF FIGURES (continued)


| Figure | |
|---|---|
| 36 | Microstructures of Double Extruded IIIg mod After Stress Rupture Testing at Various Conditions. |
| 37 | Task II Alloys Rolled From 1 1/8 Inch Diameter Canned Single Extruded Billets to 0.6 Inch Diameter Bars. |
| 38 | Larson-Miller Parameter Curves Showing Stress Rupture Properties of Unitemp AF 2-1DA After Various Methods of Processing. |
| 39 | Larson-Miller Parameter Curves Showing Stress Rupture Properties of I 5 After Various Methods of Processing. |
| 40 | Larson-Miller Parameter Curves Showing Stress Rupture Properties of IIb After Various Methods of Processing. |
| 41 | Optical Micrographs of I 5 Stress Rupture Samples Illustrating the Structural Variations Which Occur Depending on the Method of Processing. Same Heat Treatment Was Used for Both Samples. |
| 42 | Optical Micrographs of IIb Stress Rupture Samples Illustrating the Structural Variations Which Occur Depending on the Method of Processing. Same Heat Treatment Was Used for Both Samples. |
| 43 | Electron Micrographs Illustrating the Microstructure of Unitemp AF 2-1DA After 1500 Hours Exposure at Various Temperatures. |
| 44 | Electron Micrographs Illustrating the Microstructure of I 5 After 1500 Hours Exposure at Various Temperatures. |
| 45 | Electron Micrographs Illustrating the Microstructure of IIb After 1500 Hours Exposure at Various Temperatures. |
| 46 | Electron Micrographs Illustrating the Microstructure of IIIg mod After 1500 Hours Exposure at Various Temperatures. |
| 47 | Scanning Electron Micrograph of a IIb Sample After a 1600°F/ 1500 Hour Exposure Showing Heavy Grain Boundary Precipitate and Needle-Like Platelets. |
| 48 | Oxidation Rates of Task II Alloys for Continuous Testing at 1950°F. |

LIST OF FIGURES (continued)


| Figure | |
|---|---|
| 49 | Samples Resulting From 1000 Hour Static Oxidation Tests Conducted at 1875, 1950 and 2100°F. |
| 50 | Optical Micrographs Illustrating the Effects of 1000 Hour Cyclic Oxidation Tests Conducted at Various Temperatures on the Microstructure of Unitemp AF 2-1DA. |
| 51 | Optical Micrographs Illustrating the Effects of 1000 Hour Cyclic Oxidation Tests Conducted at Various Temperatures on the Microstructure of I 5. |
| 52 | Optical Micrographs Illustrating the Effects of 1000 Hour Cyclic Oxidation Tests Conducted at Various Temperatures on the Microstructure of IIb. |
| 53 | Optical Micrographs Illustrating the Effects of 1000 Hour Cyclic Oxidation Tests Conducted at Various Temperatures on the Microstructure of IIIg mod. |
| 54 | Electron Beam Microprobe Scans Showing Element Distribution in Matrix and Oxide Scale of a Unitemp AF 2-1DA Cyclic Oxidation Sample Tested for 1000 Hours at 1950°F. |
| 55 | Optical Micrograph of Unitemp AF 2-1DA Illustrating Grain Boundary Attack After Sulfidation Testing for One Hour at 1800°F. |

# I. SUMMARY

The object of this program was to determine the potential of six highly alloyed wrought nickel-base alloys for use in advanced gas turbine engines. The six alloys were I 5, IIb, IIIg mod, IId, IIIg and Unitemp AF 2-1DA. The program was divided into two tasks. The fabrication characteristics of the alloys were evaluated in Task I. Based upon the workability exhibited by the alloys in Task I, four compositions were selected for detailed property evaluations in Task II.

In Task I, optimum hot working temperatures were chosen for each of the six alloys based on inherent ductility profiles and actual extrusion studies. The results of the hot workability studies indicated that, with the exception of IId and IIIg, all of the alloys could be successfully fabricated to wrought bar product by extrusion or hot rolling. Radiographic inspection of IId and IIIg extrusion billets indicated that internal damage had been experienced during the extrusion operation. As a result, I 5, IIb, IIIg mod, and Unitemp AF 2-1DA were chosen for the Task II studies.

In Task II, a solution treatment, an intermediate aging treatment and a final aging treatment were selected for each alloy. Material for Task II testing was heat treated by the optimum method determined for each alloy and property evaluations were conducted. These included tensile tests over the range from room temperature to 1800°F (982°C); stress rupture tests at a variety of conditions from 1300°F/100,000 psi (704°C/688 $N/mm^2$) to 1900°F/15,000 psi (1038°C/103 $N/mm^2$); interrupted low cycle fatigue tests; 100 hour continuous oxidation tests conducted at 1950°F (1066°C); 1000 hour cyclic oxidation tests conducted at 1875°, 1950°, and 2100°F (1024°, 1066°, and 1149°C); sulfidation tests conducted at 1600° and 1800°F (871° and 982°C); thermal cycling fatigue tests from room temperature to 1800°F (982°C); detailed thermal stability evaluations; and stress rupture testing of material fabricated by various methods. Detailed structural studies were conducted throughout the program to examine the effects of structure on resultant properties. These studies included optical and electron microscopy, X-ray diffraction studies of electrolytically extracted residues, and electron beam microprobe studies. The results of the Task II studies showed IIb to possess high temperature strength properties significantly better than those exhibited by any commercially available wrought alloy up to 1900°F (1038°C). Deficiencies of the alloy included low tensile and rupture ductility, poor oxidation characteristics at 2100°F (1149°C), and phase instability after 1500 hours exposure at 1500°, 1600° and 1700°F (816°, 871°, and 927°C). The high strengths exhibited by IIb indicate that the alloy has excellent potential for use in advanced gas turbines if the noted deficiencies can be corrected while maintaining or even improving strength via thermomechanical techniques. The strength properties of Unitemp AF 2-1DA were second to those exhibited by IIb, but it had higher ductility and better oxidation resistance, and the alloy remained stable after 1500 hours exposure at all

temperatures evaluated. Although IIIg mod exhibited tensile strengths similar to Unitemp AF 2-1DA and good sulfidation resistance, the rupture strength of the alloy was low, as was its ductility. The alloy which exhibited the best resistance to both cyclic and continuous oxidation was I 5; however, its strength properties were the lowest of the four alloys evaluated in Task II.

## II. INTRODUCTION

The aircraft industry has taken tremendous strides towards the development of gas turbine engines capable of yielding increased thrusts and efficiencies. The primary means of achieving these increases has been to raise the operating temperature within the hot section of the engine. However, continued progress in this area has been seriously retarded by materials limitations. Currently available materials are not capable of maintaining the combination of properties required for efficient service at increased operating temperatures. Therefore, further improvements in turbine engine technology will be dependent upon the development of new materials capable of maintaining strength, creep and stability properties while exhibiting good oxidation resistance at increased operating temperatures.

This program was initiated to evaluate the potential of six nickel base alloys for use in advanced gas turbines at increased operating temperatures. Five of the alloys were originally developed on NASA Contract NAS 3-7267 by TRW[1] and the sixth alloy, Unitemp AF 2-1DA, was developed under Air Force Contract AF33(615)-1729 by Universal-Cyclops Specialty Steel Division[2]. The primary problem with these alloys is that they are not commercially available at the present time and little information is available concerning their overall capabilities. This program was designed to evaluate the fabricability, mechanical and corrosive properties, thermal stability, and general metallurgy of the six alloys. The specific objective of the program was to determine which of these alloys could be fabricated by common production techniques, and to select the best composition for the development of a wrought nickel base superalloy substantially stronger than those currently available.

This report covers the work performed during the twenty months of NASA Contract NAS 3-11155. It includes a review of the overall program, descriptions of pertinent equipment, a review of the experimental procedures, details of the results obtained, and a discussion of these results.

## III. PROCEDURE

### A. Task I

#### 1. Materials

Virgin raw materials were used for all heats melted to minimize the level of impurity elements and to reduce their effects on resulting properties. A minimum purity level of 99.9 percent was specified for all alloying elements.

#### 2. Melting

Each of the six alloy compositions was double vacuum melted as one 50-pound (22.7 kg) and one 100-pound (45.4 kg) heat. Second 100-pound (45.4 kg) heats of IIb and IIIg mod were later melted to provide additional material. The initial melting operations were conducted in vacuum induction furnaces. The as-cast electrodes were then vacuum consumable-arc remelted to obtain the final cast product.

The general procedure for vacuum induction melting was the same for both the 50- (22.7 kg) and the 100-pound (45.4 kg) heats. The first step was the melting of the main charge which consisted of nickel, chromium, tantalum, molybdenum, tungsten, and one-half of the total carbon addition. After the initial melt-down, cobalt and the remainder of the carbon were added. The bath was then allowed to cool and form a thin "skin" on the surface prior to the addition of the reactive elements, titanium and aluminum. After the titanium and aluminum were added, power was slowly increased allowing these elements to melt in slowly with a minimum of reaction. Zirconium and nickel-boron were then added along with rhenium, hafnium, columbium, and vanadium, if required. Each heat was deoxidized by plunging magnesium into the bath after the temperature had stabilized at 2850°F (1566°C). The bath was then cooled to approximately 2750°F (1510°C), and the product was cast into steel electrode molds.

The 50-pound (22.7 kg) heats were cast into 2-1/2 inch (0.063 m) diameter round electrodes. The resulting electrodes were vacuum consumable-arc remelted into two 3-1/8 inch (0.079 m) diameter ingots weighing approximately 25 pounds (11.4 kg) each. The 100-pound (45.4 kg) heats were cast into four inch (0.10 m) diameter electrodes, and were vacuum consumable-arc remelted into 5-3/4 inch (0.145 m) diameter ingots.

#### 3. Chemical Analysis

A one-half inch (0.013 m) slice was sectioned from each vacuum induction melted electrode for X-ray spectographic analysis. The slices were also lathe turned to provide chips for wet chemical analysis. Carbon, boron, hafnium, and zirconium were analyzed by wet chemistry techniques.

X-ray spectographic techniques were employed to analyze the remainder of the elements.

4. As-Cast Hot Workability Studies

As-cast Gleeble hot workability studies were conducted on material from the 100-pound (45.4 kg) double vacuum melted heats. A three inch (0.076 m) thick slice was sectioned from the 5-3/4 inch (0.145 m) diameter ingots of each of the six experimental compositions. Sixteen transverse Gleeble hot ductility specimens were sectioned and machined to the required dimensions of one-quarter inch (0.006 m) diameter and 5-1/2 inches (0.140 m) long. Eight specimens from each ingot were used to develop inherent ductility profiles for each alloy over the temperature range of 1850° to 2100°F (1010° to 1149°C). For these tests, the specimens were heated at a rate of 85°F (45°C) per second to the specified temperature in the hot working range, held for five minutes, and pulled in tension at a nominal strain rate of five seconds $^{-1}$. This strain rate approximates the rate of extrusion. Ultimate tensile strength and reduction of area were measured and recorded for each specimen. The ductility data were plotted versus temperature to provide an inherent ductility profile for each alloy in the cast condition.

Four specimens from each alloy were used to develop hot work simulation profiles. Specimens were heated to the optimum ductility temperature (as derived from the inherent ductility profiles), held for five minutes, cooled to a lower "working" temperature, and pulled in tension. The same data were developed as before, and ductility versus temperature was plotted to provide a hot work simulation profile.

Four specimens were also used to evaluate the potential of homogenization heat treatments to improve workability. All specimen blanks were heated to 2250°F (1232°C) and were held at temperature for 20 hours. After this treatment, the blanks were finish machined to size, and hot work simulation profiles were developed as described above. The strain rate for this test was increased to 20 seconds $^{-1}$, which more closely approximates rolling and hammer forging rates.

5. Processing

a. Single Extrusions

Material from one of the two 25-pound (11.4 kg) vacuum consumable-arc remelted ingots of each alloy was used for the single extrusions. One 3-1/8 inch (0.079 m) diameter ingot of each alloy was cut in half. Each piece was turned to 2-1/2 inches (0.063 m) in diameter and canned in 1/2 inch (0.013 m) thick mild steel in preparation for extrusion at Air Force Materials Laboratory (AFML), Wright-Patterson Air Force Base. A schematic representation of the type of container used is shown in Figure 1A. The two canned pieces of each alloy composition were coated

with a glass slurry, heated to the desired extrusion temperature, soaked for a minimum of one hour, and extruded to a canned diameter of 1-1/8 inches (0.028 m). The first canned piece from each composition was extruded from the optimum temperature derived from the Gleeble inherent ductility profiles. The temperatures were increased for the extrusion of the second piece from each heat in an effort to achieve better workability. Alloys IIb, IIIg mod, IIIg, and IId required additional test extrusions due to their poor workability and the remaining 25-pound (11.4 kg) ingot of each of these alloys (which had been scheduled for rolling and forging studies) was prepared as described above for additional trial extrusions. These eight additional extrusions were conducted at working temperatures above those originally derived from the Gleeble hot ductility tests.

b. Double Extrusions

The six 5-3/4 inch (0.145 m) diameter ingots from the 100-pound (45.4 kg) heats were turned to 5-1/2 inch (0.140 m) diameter and were placed in three mild steel cans (two ingots per can). The ingots were arranged in the cans based on the optimum extrusion temperatures for each alloy derived from the as-cast Gleeble inherent ductility profiles. A schematic representation of the canned ingots is shown in Figure 1B. The extrusions were performed at the Canton Drop Forging and Manufacturing Company. The canned ingots were preheated a minimum of four hours at 1200°F (649°C) and then transferred to salt bath furnaces and soaked a minimum of two hours at the desired working temperature. The 7-1/2 inch (0.19 m) diameter canned ingots were extruded to 3-1/2 inch (0.089 m) diameter canned billets to complete the first step of the double extrusion. Because the first extrusions for IIb and IIIg mod were unsuccessful, additional extrusions for these alloys were performed at a later date. These extrusions used material from the second 100-pound (45.4 kg) heat of each of the alloys, however, the original extrusion temperatures were increased.

The second phase of the double extrusion was conducted at AFML. The 3-1/2 inch (0.089 m) diameter canned billets were decanned, turned to 2-1/2 inches (0.063 m) in diameter, sectioned into approximately five inch (0.127 m) lengths, and recanned to 2.92 inches (0.074 m) in diameter in preparation for extrusion at AFML. The schematic illustration of a canned billet is shown in Figure 1A. This operation was conducted only for the four alloys selected for the Task II studies: Unitemp AF 2-1DA, I 5, IIb, and IIIg mod. The canned billets were glass coated, heated to the desired extrusion temperature, soaked, and extruded to a canned diameter of 1-1/8 inches (0.028 m).

c. Rolling and Forging

Due to the additional extrusion studies required for alloys IIb, IIIg mod, IIIg, and IId, the evaluation of rolling and forging of as-cast material was limited to Unitemp AF 2-1DA and I 5. One half of

the remaining 25-pound (11.4 kg) ingot from each alloy was used for the rolling evaluation, and the other half was used for forging.

Both ingots were soaked at 2050°F (1121°C) for a minimum of one hour prior to initiating rolling. The 3-1/8 inch (0.079 m) diameter ingots were rolled without cans to one inch (0.025 m) round corner square bars using a reduction per pass of 0.010 to 0.015 inch (0.0002 to 0.0004 m) with three to four passes per reheat. The material was reheated to 2050°F (1121°C) as necessary to maintain a minimum working temperature of 1850°F (1010°C).

The forging studies were conducted on uncanned material using a hammer forging unit. The soaking and reheating temperature used for both Unitemp AF 2-1DA and I 5 was again 2050°F (1121°C) and the working temperature was maintained above 1850°F (1010°C). Although the reductions could not be controlled as closely as in rolling, the operation began with small reductions, which increased slowly as the piece received more work.

d. Workability Studies of Extruded Material

Eight Gleeble specimens were sectioned from one inch (0.025 m) diameter bars in both the single and double extruded conditions. These specimens were used to develop inherent ductility profiles for the experimental alloys in the wrought form. Testing was conducted on all six of the alloys in the single extruded condition. However, only those alloys later selected for Task II studies (AF 2-1DA, I 5, IIb, and IIIg mod) were tested in the double extruded condition. The test procedure was the same as previously described for developing inherent ductility profiles, except that the strain rate was increased to 20 seconds $^{-1}$ to more closely represent rolling and forging operations.

6. Inspection

A radiographic inspection technique was used to examine single extruded bars of IIb, IIIg mod, IIg, and IId to detect possible subsurface defects. The bars were first sectioned into six inch (0.15 m) long segments and the rough, scaled surface of the can was machined to a smooth finish. The bars were radiographed in two positions, the second representing a 90° rotation around the longitudinal axis from the initial position. This method is effective for detecting porosity, cracks, and other types of voids which may have resulted from processing operations.

7. Structural Examination

Detailed structural examinations were conducted on samples from each of the six alloy compositions in three conditions: 1) as-cast, 2) as-extruded, and 3) quenched from the optimum working temperature. The structural examination consisted of optical metallography, X-ray phase analysis, and electron beam microprobe analysis.

a. Metallographic Analysis

The samples were prepared for optical microscopy examination by mechanical polishing and etching in one of the following solutions, depending on the response to the solution and the desired effect:

1) 60 percent water
   15 percent sulfuric acid
   15 percent hydrofluoric acid
   9 percent nitric acid
   1 percent hydrogen peroxide

2) 85 percent water
   14 percent hydrochloric acid
   1 percent hydrogen peroxide

Photomicrographs were taken at 200X and 500X for each of the samples examined.

b. X-Ray Phase Analysis

Samples for X-ray phase analysis were prepared for electrolytic extraction by first sandblasting the piece at low pressure. The samples were then cleaned electrolytically in a solution of ten percent hydrochloric acid in methanol for ten minutes. The samples were rinsed and extractions were conducted in a new ten percent hydrochloric acid in methanol solution. The samples were extracted for one-half hour using a current density of 0.25 amps per square inch (400 amps per square meter). The residues were cleaned in methanol, dried, mounted on glass slides and subjected to X-ray diffraction analyses to identify the phases present.

c. Electron Beam Microprobe Analysis

Microprobe samples were sectioned, mounted in copper-epoxy, and polished through 0.5 micron diamond in preparation for study. These studies were designed to determine the degree and type of segregation in specimens in the cast, extruded, and quenched conditions. Several types of studies were conducted, depending on the condition of the sample. These studies included point counts, element scans, and X-ray and specimen current image photography.

The point count method consists of focusing the beam to a diameter of ten microns and counting the X-ray intensity of a particular element in that area for five seconds. After the five second count, the sample is shifted six microns in the desired direction and counts are registered in that area for the same element. The sample continues shifting in the same direction until the desired stopping point is reached. The same path is repeated for each element to be evaluated. These counts are then plotted for each step to determine any significant variations. This is the most sensitive technique, and was used to detect segregation across dendritic areas and within grains.

The procedure for element scans varies somewhat from the point count procedure, although the end result is very similar. This technique is not as sensitive as the point count method, but it is faster for long distance traverses. For this method, the specimen is traversed under a one micron diameter beam at a speed of 15 microns per minute. Deviations in element concentration are recorded simultaneously on a chart incorporated into the unit. This method can be used for examining areas which would be too large to employ point counts, and to determine segregation on a microscopic scale.

X-ray and specimen current image photography was used to detect element deviations over a relatively large area. For this method, the beam scans an area of approximately 320 square microns. Fluctuations in element concentration within the area under examination are viewed on an oscilloscope screen. Photographs representing the concentrations of each element are taken directly from the screen. This is a technique which is easy to interpret and illustrate, but it is the least sensitive.

## B. Task II

### 1. Heat Treatment Evaluation

#### a. Heat Treatment Studies

A heat treatment evaluation was conducted on double extruded bar material representing the Unitemp AF 2-1DA, I 5, IIb, and IIIg mod compositions. The bars were decanned and cut into six inch (0.15 m) long segments for gradient bar studies. The bars were ground flat on parallel sides to provide a surface for hardness measurements. Three optimum temperatures, including a solution treatment temperature, an intermediate aging temperature, and a final aging temperature were determined for each composition.

The gradient bar treatments were performed in a special gradient furnace. The desired temperature gradient to be maintained from one end of the bar to the other was monitored and controlled by thermocouples attached at one inch (0.025 m) intervals. The actual temperature at any point on the bar can be determined from the thermocouple record.

Solution treatment temperatures were evaluated by treating gradient bars over the range of 1800° to 2300°F (982° to 1260°C) for two hours and air cooling. After removing the bars from the furnace, the location for each temperature was marked and hardness readings were taken across the flat surface at various temperatures following a light surface grinding operation to remove the scale. The bars were then sectioned at 100°F (55°C) intervals and were prepared for examination by optical microscopy. Approximately five one-quarter inch (0.006 m) square specimens from each composition were sectioned and heat treated within the optimum range determined from the gradient bar studies in order to

verify the gradient results. In several cases, the heat treatment times were modified in an effort to achieve the desired structural characteristics. From this information, an optimum solution treatment temperature was chosen for each alloy. The temperatures were chosen based upon the degree of carbide and gamma prime solutioning and especially on grain size. A uniform grain size of ASTM 4 to 5 was the desired aim in order to maintain a constant grain size in all alloy compositions for subsequent testing.

Optimum intermediate aging temperatures were determined for each alloy in a similar manner. The bars were first solution treated according to the optimum conditions selected from the above studies. Intermediate aging temperatures over the range of 1500° to 2000°F (816° to 1093°C) were evaluated at aging times of two and sixteen hours. Again one-quarter inch (0.006 m) square specimens were heat treated within the general range determined from the gradient bar studies and examined by optical microscopy to verify the optimum intermediate aging temperatures. Optimum temperatures were chosen based upon the degree of gamma prime nucleation and carbide precipitation.

The final aging temperature studies were conducted on gradient bars which were solution treated and intermediate aged according to the conditions previously established. The gradient bars were subjected to sixteen hour aging treatments over the range of 1100° to 1600°F (593° to 871°C). Optimum final aging temperatures were determined for each alloy by electron microscopy based upon the morphology of the carbide and gamma prime constituents.

Electron microscopy specimens were mechanically polished through a 600 grit silicon carbide abrasive and electrolytically polished in a perchloric acid in alcohol solution. The specimens were etched in a variety of solutions, namely perchloric, hydrochloric and sulfuric acids, to emphasize the desired structural characteristics. The polished and etched specimens were then single stage replicated using a one percent solution of parlodion in isoamylacetate. Shadowing was performed with chromium at an angle of approximately 15°. All electron micrographs were taken at a magnification of 2500X, and were photographically enlarged to 5000X.

b. Structural Examination

After the optimum heat treatments were selected for each alloy, the structural characteristics after each stage of the heat treatment were determined by optical and electron microscopy, X-ray diffraction of extracted residues, and electron beam microprobe techniques. The procedures used were detailed in previous sections.

2. Mechanical Testing

All specimens for mechanical testing were sectioned from double extruded bar material, rough machined, radiographically inspected, heat

treated by the optimum method, and finish machined and polished to the prescribed dimensions. The test specimen configurations and dimensions are illustrated in Figure 2. Tensile tests, stress rupture tests and interrupted low cycle fatigue tests, were included in this evaluation.

a. Tensile Tests

Duplicate tensile tests were conducted at room temperature, 1000°, 1200°, 1400°, 1600°, and 1800°F (538°, 649°, 760°, 871°, and 982°C). All tensile tests were conducted on a 50,000 pound (2270 kg) capacity Baldwin-Emery tensile testing machine. The specimens were pulled at a nominal strain rate of 0.005 minute $^{-1}$ up to the 0.2 percent yield point, where the strain rate was increased to 0.05 minute $^{-1}$. The yield point was measured by use of a deflectometer. Special furnaces were employed for elevated temperature testing and the specimens were held at temperature for a minimum of 20 minutes before testing.

b. Stress Rupture Testing

1) Testing Procedure

Stress rupture tests were conducted in duplicate at the following conditions:

| Temperature | Stress |
|---|---|
| 1300°F (704°C) | 100,000 psi (690 N/mm$^2$) |
| 1400°F (760°C) | 90,000 psi (620 N/mm$^2$) |
| 1400°F (760°C) | 85,000 psi (585 N/mm$^2$) |
| 1500°F (816°C) | 70,000 psi (483 N/mm$^2$) |
| 1600°F (871°C) | 55,000 psi (380 N/mm$^2$) |
| 1750°F (954°C) | 30,000 psi (207 N/mm$^2$) |
| 1800°F (982°C) | 25,000 psi (173 N/mm$^2$) |
| 1800°F (982°C) | 20,000 psi (138 N/mm$^2$) |
| 1900°F (1038°C) | 15,000 psi (103 N/mm$^2$) |

The tests were conducted on lever arm testing machines. The samples were loaded into the furnace, heated to the desired temperature, and held for 15 minutes prior to the load being applied. Rupture life was measured from the time the load was applied. Sample temperature was controlled to $\pm$ 5°F (3°C).

2) Structural Examinations

Three stress rupture test specimens from each composition were selected for detailed structural examinations. The selected specimens consisted of a high temperature test, 1900°F/15,000 psi (1038°C/ 103 N/mm$^2$); a moderate temperature test, 1600°F/55,000 psi (871°C/ 380 N/mm$^2$); and a low temperature test, 1400°F/90,000 psi (760°C/ 620 N/mm$^2$). The structural examinations included optical and electron

microscopy and X-ray diffraction of electrolytically extracted residues. These procedures were conducted as previously described.

c. Interrupted Low Cycle Fatigue Tests

Duplicate interrupted low cycle fatigue tests were conducted on each alloy at the following conditions:

| Temperature | Stress |
|---|---|
| 1300°F (704°C) | 110,000 psi (758 $N/mm^2$) |
| 1350°F (732°C) | 100,000 psi (690 $N/mm^2$) |
| 1450°F (788°C) | 80,000 psi (550 $N/mm^2$) |

The tests were conducted on an Instron Universal testing machine equipped for this type of test. The specimens were notched to give a stress concentration factor ($K_t$) of 2.5. Each testing cycle consisted of increasing the load on the specimen from zero to the desired value in ten seconds, holding for 90 seconds, and reducing the load to zero in ten seconds. Test duration and number of cycles to failure were recorded for each specimen.

3. Evaluation of Processing Variations

a. Rolling

1) As-Cast Material

Stress rupture specimens were sectioned and machined from the Unitemp AF 2-1DA and I 5 one inch (0.025 m) round cornered square bars, which were rolled directly from 3-1/8 inch (0.079 m) diameter ingots during Task I. The specimens were heat treated by the optimum methods previously determined, and single tests were conducted at the following conditions:

| Temperature | Stress |
|---|---|
| 1300°F (704°C) | 100,000 psi (690 $N/mm^2$) |
| 1400°F (760°C) | 90,000 psi (620 $N/mm^2$) |
| 1500°F (816°C) | 70,000 psi (483 $N/mm^2$) |
| 1600°F (871°C) | 55,000 psi (380 $N/mm^2$) |
| 1800°F (982°C) | 25,000 psi (173 $N/mm^2$) |
| 1900°F (1038°C) | 15,000 psi (103 $N/mm^2$) |

2) Single Extruded Material

A six inch (0.15 m) long piece was sectioned from a 1-1/2 inch (0.038 m) diameter single extruded bar of each of the alloys selected for Task II study. The bars were rolled to 0.60 inch (0.015 m) diameter. Soaking and reheating temperatures were the same as those

derived from the extrusion studies. These included 2050°F (1121°C) for Unitemp AF 2-1DA and I 5 and 2100°F (1149°C) for the remaining alloys. Reductions were approximately 0.010 to 0.015 inch (0.0002 to 0.0004 m) per pass and the working temperatures were maintained above 1850°F (1010°C).

Stress rupture specimens were sectioned and machined from the single extruded rolled material and heat treated by the optimum methods. Single tests were conducted at the conditions summarized in the previous section.

b. Forging

Six inch (0.15 m) long segments were sectioned from the 1-1/2 inch (0.038 m) diameter single extruded bars of each alloy. The pieces were heated to their optimum working temperatures as determined from the extrusion studies and attempts were made to forge the bars to 0.60 inch (0.015 m) diameter. The forging was conducted on a hammer forging unit, and the working temperatures were maintained above 1850°C (1010°C). Stress rupture testing was to be conducted at the same conditions described above if sound material could be obtained.

4. Thermal Stability Studies

a. Thermal Exposures

Specimens of double extruded bars representing each composition were heat treated and subjected to 1500 hours exposure at 1400°, 1500°, 1600°, and 1700°F (760°, 816°, 871°, and 927°C).

b. Stress Rupture Tests

One stress rupture sample was sectioned and machined from each bar of the thermally exposed material. All tests were run at 1400°F/90,000 psi (760°C/620 $N/mm^2$).

c. Structural Examinations

The effects of the thermal exposures on microstructure were evaluated through electron microscopy. In addition, exposed specimens were subjected to electrolytic extraction and microprobe studies to determine variations in minor phases and also to detect the formation of any new phases. These procedures were detailed in a previous section.

5. Oxidation Testing

a. Cyclic Testing

1) Testing Procedure

Samples for cyclic oxidation tests were sectioned from

double extruded material heat treated by the optimum methods. The samples were machined and finished to a size of one-half inch (0.013 m) diameter by one-half inch (0.013 m) long using 150 grit silicon carbide paper. A platinum wire was welded to each sample. The samples were ultrasonically degreased and each sample was suspended in a quartz crucible assembly by the platinum wire. The assembly was designed to collect spalling oxides during testing, while also permitting air to circulate around the samples. The crucible assemblies, including the samples, were weighed prior to initiating testing.

Duplicate samples from each heat were subjected to 1000 hour cyclic oxidation tests at 1875°, 1950°, and 2100°F (1024°, 1066°, and 1149°C). The assemblies were removed from the furnace after 100 hour intervals and cooled and weighed. The crucibles were covered during cooling to insure containment of all spalling oxides. Weight changes were recorded and oxidation rates were calculated in milligrams per square centimeter for each sample. Testing was discontinued after a total of ten 100-hour exposures, or 1000 total hours.

2) Structural Examinations

After testing, all samples were mounted, polished, and etched for optical microscopy. Photographs of each sample were taken at 500X. One sample of each alloy tested at 1950°F (1066°C) was subjected to microprobe studies to determine the mechanism of oxidation and to identify possible element depletion near the surface. Element line scans and specimen current and X-ray photography were among the techniques employed in evaluating the samples.

b. Continuous Oxidation Tests

One specimen from each composition was heat treated, machined, and finished to a size of one-half inch (0.013 m) diameter by one inch (0.025 m) long using 150 grit silicon carbide paper. The sample was welded to a long platinum wire, ultrasonically degreased, and subjected to continuous oxidation testing for 100 hours at 1950°F (1066°C). During testing, the sample was suspended in a vertical tube type furnace equipped with an external balance in such a manner that the sample could be weighed at desired intervals without removing it from the heat zone. Approximately 25 weighings were made in the 100 hour interval, although the majority of the weighings were taken during the first several hours to properly monitor the most rapid oxidation rates.

6. Sulfidation Testing

a. Testing Procedure

Two specimens from each composition were heat treated and machined and finished to a size of one-half inch (0.013 m) diameter by one inch (0.025 m) long using 150 grit silicon carbide paper. The

samples were ultrasonically degreased, weighed, and subjected to sulfidation testing at 1600° and 1800°F (871° and 982°C). Each sample was placed in a crucible containing a mixture of 99 percent sodium sulfate and one percent sodium chloride. The crucibles were heated to the desired temperature and held for one hour at temperature. After testing, the samples were then cleaned in methanol and weighed, and a sulfidation rate was calculated.

b. Structural Examinations

The above test procedure was repeated at 1800°F (982°C) for one sample from each composition; however, the samples were not descaled. The samples were sectioned and one half was used for optical microscopy examination and the other was used for microprobe studies.

7. Thermal Cycling Fatigue Testing

Samples for thermal cycling fatigue tests were sectioned, heat treated, and ground and polished to standard size as shown in Figure 2. Three samples of each composition were attached to a rotating drum unit capable of heating the specimens by gas flame impingement to the desired temperature and cooling to room temperature by air blast. The cycle consisted of slowly heating to a maximum temperature of 1800°F (982°C), then cooling by air blast to room temperature. Each cycle required approximately 40 seconds for heating to 1800°F (982°C) and an equal amount of time for cooling to room temperature. The criteria for failure was thermal cracking; therefore, the samples were periodically inspected by optical microscopy to examine for microscopic cracks. At the completion of the testing, the samples were mounted, polished, and etched for optical microscopy, and photographs were taken at 500X.

# IV. RESULTS AND DISCUSSION

## A. Task I

### 1. Melting

The vacuum induction melting, casting, and vacuum arc remelting proceeded well for the six compositions. No irregularities were exhibited by any of the compositions which required deviation from the standard melting procedures previously established for alloys of this type. During vacuum induction melting, no problems were encountered in dissolving high melting point elements. In addition, pouring was conducted at normal tapping temperatures and rates. No indications of premature solidification were exhibited by any of the compositions. In casting the vacuum induction melted material into electrode molds, a normal amount of ingot piping was detected. However, by reducing voltage and amperage during vacuum arc remelting, the final ingots were hot topped, essentially eliminating piping in these ingots.

### 2. Chemical Analyses

The alloy designations, heat numbers, and aim and actual chemical compositions for the 50- and 100-pound (22.7 and 45.4 kg) heats melted in Task I are summarized in Tables 1 and 2, respectively. In general, the values previously established concerning the recovery of alloying elements for standard nickel base compositions proved to be quite accurate for these highly alloyed compositions. Alloy compositions involving hafnium were found to exhibit slightly higher than normal zirconium levels due to the residual zirconium contained in the hafnium. All heats were within the normally acceptable analysis range.

### 3. As-Cast Hot Workability Studies

The results of the Gleeble hot workability tests conducted on the six alloys in the as-cast condition are summarized in Tables 3 to 8. Each table includes the inherent ductility profile and the hot work simulation profile for each alloy. These data were plotted as reduction of area versus test temperature to determine an optimum working temperature and the widest possible hot working range for each alloy. The resultant curves are shown in Figures 3, 4, and 5 for the six alloys.

The data showed the inherent ductility of all the alloys to be quite low, with IIb exhibiting the highest ductility of 19.7 percent at 1900°F (1038°C). Reduction of area values for the hot work simulation profiles were also very low. Maximum reduction of area values for the remaining alloys varied considerably with Unitemp AF 2-1DA reaching its maximum ductility of 14.5 percent at 1900°F (1038°C); I 5, 7.3 percent at 1850°F (1010°C); IIIg mod, 13.0 percent at 1850°F (1010°C); IId, 11.7 percent at 1950°F (1066°C); and IIIg, 10.5 percent at 2050°F (1121°C).

Past experience has shown that alloys of this type generally require at least 30 percent reduction of area at any given temperature before they can be considered to have good workability in rolling or forging operations. The reduction of area values for the six alloys not only fell well below the 30 percent minimum, but the alloys also exhibited very narrow hot working ranges.

A series of specimens was subjected to a homogenization treatment in an attempt to improve the ductility of the alloys by solutioning regions of primary gamma prime in the as-cast structure. The results of these tests are included in the preceding tables and figures. The data showed no significant improvement in ductility for any of the alloys after the homogenization treatment.

Based upon the data available, the determination of optimum working temperatures for each alloy was very difficult. For example, past experience has shown that Unitemp AF 2-1DA is readily workable by extrusion from a temperature of 2050°F (1121°C)[3]. However, the Unitemp AF 2-1DA Gleeble data indicated the optimum working temperature for the alloy was considerably lower. A maximum reduction of area value of 14.5 percent was achieved at 1900°F (1038°C), while at the expected optimum working temperature of 2050°F (1121°C), the reduction of area was only 6.2 percent. This indicated that the data for the other alloys also might be misleading.

As a result of this problem, optimum working temperatures for the alloys were chosen based on a combination of the Gleeble data derived for each alloy and the generally accepted principles concerning the hot processing of alloys of this type. In general, the minimum temperature range which would be realistic for processing such superalloys is approximately 1950°F (1066°C) to 2000°F (1093°C). Therefore, for the alloys which exhibited Gleeble data favoring optimum working temperatures within or below this range, the temperature chosen for subsequent working operations was 2000°F (1093°C). These alloys included I 5, IIb, IId, and IIIg mod. A working temperature of 2050°F (1121°C) was selected for the remaining two alloys, Unitemp AF 2-1DA and IIIg.

## 4. Processing

### a. Single Extrusions

The one inch (0.025 m) diameter bars fabricated by single extrusion at Wright-Patterson Air Force Base are shown in Figures 6 to 9. It should be noted that in the photographs a portion of the mild steel can which is approximately 0.06 inch (0.0015 m) thick still surrounds each billet. Also, the rounded segment at one end of each billet, which appears to be breakage, represents the mild steel nose section which was welded into the original can. A somewhat shorter segment on the opposite end of the billet represents the mild steel tail section. These sections appear on all the photographs, and are not considered breakage in the extrusion workability evaluation.

The purpose of the extrusions was to evaluate the fabricability of the six alloys. Based upon the Gleeble hot ductility data and the generally accepted principles for processing alloys of this type, a temperature of 2000°F (1093°C) was selected as the extrusion temperature for alloys I 5, IIb, IIIg mod, and IId; 2050°F (1121°C) was selected as the extrusion temperature for Unitemp AF 2-1DA and IIIg. The extrusions were conducted in four series. The Series I and II extrusions involved all six of the alloys and the Series III and IV extrusions were conducted only on alloys IIb, IIIg mod, IId and IIIg to further investigate the workability potential of these alloys at higher extrusion temperatures. The one inch (0.025 m) billets resulting from the Series I extrusions are shown in Figure 6. The Unitemp AF 2-1DA and I 5 billets, which were extruded from temperatures of 2050°F (1121°C) and 2000°F (1093°C) respectively, extruded well. The IIIg billet was extruded from 2050°F (1093°C) and experienced quite severe breakage, as did the IId, IIb, and IIIg mod billets.

The poor workability exhibited by IId, IIb, and IIIg mod during the Series I extrusions was believed to be due to the relatively low extrusion temperature of 2000°F (1093°C) which was chosen for these alloys. Therefore, for the Series II extrusions, the extrusion temperature for these alloys was increased to 2050°F (1121°C). The bars resulting from the Series II extrusions are shown in Figure 7. The condition of the IId, IIb, and IIIg mod billets was considerably improved as compared with the initial extrusions; however, the condition of the billets was only fair, as some breakage occurred. The IIIg and I 5 billets also experienced slight breakage in this series, while the Unitemp AF 2-1DA billet again extruded satisfactorily.

In an attempt to further improve the workability exhibited by IIIg, IId, IIb, and IIIg mod, additional extrusion studies were conducted for these alloys. Material which was originally scheduled for as-cast rolling and forging studies was diverted to these extrusion studies due to the importance of developing an optimum extrusion temperature for each of the alloys. Series III and Series IV extrusions were conducted on the four above mentioned alloys from extrusion temperatures of 2100 (1149°C) and 2150°F (1177°C), respectively. The bars resulting from these extrusions are shown in Figures 8 and 9. Due to the limited amount of material available for these studies, the ingots were shorter than for the Series I and II extrusions. Therefore, the mild steel nose section was made considerably larger to make up for the difference in length. The extruded mild steel nose sections appear at the right side of these photographs. The only billet which experienced any breakage outside of the nose and tail sections was the IId billet extruded from 2100°F (1149°C). The remainder of the billets extruded satisfactorily at both temperatures.

b. Double Extrusions

The bars resulting from the double extrusions are shown in Figures 10 to 14. The thin mild steel can still remains on the billets

after extrusion; the actual material is not visible in the photographs. The first part of the double extrusion consisted of a reduction from the original 5-1/2 inch (0.140 m) ingot diameter to a billet size of approximately three inches (0.076 m) in diameter. The ingots were canned and extruded as two ingots per can, and were paired according to their originally selected extrusion temperatures. The Unitemp AF 2-1DA and IIIg ingots were paired in Can No. 1 and were extruded from a temperature of 2050°F (1121°C). The ingots representing the I 5 and IIb compositions were placed in Can No. 2, and the IIIg mod and IId ingots were grouped in Can No. 3. Both Can No. 2 and Can No. 3 were extruded from a temperature of 2000°F (1093°C). The bars resulting from these extrusions are shown in Figure 10A. As was the case for the previously described single extrusions, only Unitemp AF 2-1DA and I 5 extruded satisfactorily. The remaining alloys experienced severe breakage.

Because only Unitemp AF 2-1DA and I 5 extruded well enough to provide sufficient material for the second part of the double extrusion and subsequent Task II studies, a decision was made to re-extrude alloys IIb and IIIg mod using a higher extrusion temperature. This decision was made based upon the improved condition of the IIb and IIIg mod single extrusions (described in the previous section) when the extrusion temperature was increased from 2000°F (1093°C) to 2100°F (1149°C). The alloys were remelted, canned together and extruded to three inch (0.076 m) diameter billet from an extrusion temperature of 2100°F (1149°C). The bars resulting from this extrusion are shown in Figure 10B. Both alloys extruded satisfactorily and provided sufficient material to continue with the second phase of the double extrusion.

The second phase of the double extrusions involved sectioning and decanning of the three inch (0.076 m) diameter Unitemp AF 2-1DA, I 5, IIb, and IIIg mod extruded billets. The billets were then lathe turned to 2-1/2 inch (0.063 m) diameter, recanned, and extruded to one inch (0.025 m) diameter bars from the optimum extrusion temperature for each alloy. The Unitemp AF 2-1DA and I 5 billets were extruded from a temperature of 2050°F (1121°C), and the IIb and IIIg mod billets from 2100°F (1149°C). The bars resulting from these extrusions are shown in Figures 11, 12, 13, and 14, respectively. Six one inch (0.025 m) diameter billets approximately three feet (0.9 m) long were obtained from the I 5 and IIb double extrusions, and seven billets were obtained from the Unitemp AF 2-1DA and IIIg mod double extrusions. The condition of all billets was very good.

c. Rolling and Forging

Due to the additional material required for the IIb, IId, IIIg, and IIIg mod single extrusion studies, rolling and forging studies on as-cast material were only conducted for Unitemp AF 2-1DA and I 5. Both the Unitemp AF 2-1DA and I 5 ingots were rolled to one inch (0.025 m) round cornered square bars with moderate success. The resulting bars from the rolling operation are shown in Figure 15. The Unitemp AF 2-1DA

bar experienced somewhat more severe edge cracking, although the depth of the cracks was not significant. The severe crack across one section of the I 5 bar is believed to have been caused by a shrink cavity from the melting operation rather than as a result of the rolling operation. The material used for this study was from the top half of a 25-pound (11.4 kg) ingot, which might have some degree of shrinkage. The remainder of the I 5 bar rolled quite satisfactorily.

Forging of as-cast Unitemp AF 2-1DA and I 5 was unsuccessful. After reducing the ingots from their original 3-1/8 inch (0.079 m) diameter to near 2-1/2 inches (0.063 m), the ingots failed due to severe center bursts.

d. Hot Workability Studies - Extrusions

The results of the Gleeble inherent ductility tests conducted on extruded material representing each of the six alloys are shown in Tables 9 to 14. Data on both single and double extruded material are presented for Unitemp AF 2-1DA, I 5, IIb, and IIIg mod; and, as the double extrusion of IId and IIIg was not accomplished, only data on single extruded material are reported for these alloys. These data are also illustrated in Figures 16, 17, and 18.

The information indicated that several of the alloys exhibited very low ductilities within their hot working ranges in the single and double extruded conditions. The alloys included single and double extruded IIb and IIIg mod and single extruded Unitemp AF 2-1DA, IId and IIIg. Although alloys IId and IIIg were not evaluated in the double extruded condition, it is quite probable that the ductilities would also be low, as was the case for IIb and IIIg mod. Unitemp AF 2-1DA in the double extruded condition and I 5 in both the single and double extruded conditions exhibited good ductilities over a rather wide range of temperatures. The best hot working characteristics were exhibited by I 5 in the double extruded condition. This material displayed ductilities between fifty and sixty percent over the range from 1900 (1038°C) to 2150°F (1177°C). Reduction of area values near seventy percent were exhibited by I 5 in the single extruded condition. However, the values were not consistently high over a range as wide as the one exhibited by the double extruded material.

5. Structural Examinations

The results of the structural evaluations conducted on each of the six alloys in the as-cast condition, quenched from the optimum working temperature and in the as-extruded condition are presented below. The structural examination of the six alloys in each of the three conditions included optical microscopy, X-ray phase identification and electron beam microprobe studies. The results of the examinations are summarized in Table 15 and Figures 19, 20, and 21.

a. As-Cast Material

Minor phases present in the extracted residues from each of the as-cast alloys were identified by X-ray diffraction. The results are shown in Table 15. Due to the heavy concentrations of gamma prime present in the cast structures of each of the alloys, the X-ray data indicate the presence of some gamma prime, even though the ten percent hydrochloric acid in methanol solution was designed to dissolve the phase during the extraction. The only other major phase identified was the MC-type carbide, which was present in heavy concentrations in each of the alloys.

Three representative photomicrographs from the metallographic examination of as-cast material are shown in Figure 19. The alloys pictured include I 5, Unitemp AF 2-1DA, and IId. These microstructures represent the three basic structural variations exhibited by the six alloys. The as-cast microstructures for I 5 and IIIg mod were very similar. As shown in Figure 19 for I 5, the main characteristics of the structure included an abundance of script MC-type carbides in a coarse gamma prime matrix. Photomicrographs taken at 200X and 500X were included to illustrate both the overall structure and the texture of the gamma prime. The carbides were widely dispersed and were located at the dendritic grain boundaries and within the individual grains.

The as-cast structure of Unitemp AF 2-1DA was somewhat different than the structure exhibited by any of the other alloys. A very coarse gamma prime phase was evident in the microstructure in combination with rather large blocky MC-type carbides. The number and size of the carbides in the Unitemp AF 2-1DA microstructure were much larger than for any of the other alloys.

The basic as-cast microstructures of IId, IIb, and IIIg were similar. Each consisted of both blocky and script MC-type carbides in a coarse gamma prime matrix. The unique characteristic of these microstructures was an abundance of massive, primary gamma prime particles. Although the primary gamma prime was evident to a limited degree in the Unitemp AF 2-1DA microstructure, the particles exhibited in these microstructures were found in much greater abundance and were of a larger size.

The results of the electron beam microprobe studies conducted on as-cast material indicated that no significant pattern of segregation was evident for any of the alloys. Electron beam microprobe point count and X-ray photography methods were used in this evaluation. The samples were examined near dendritic grain boundaries and across individual grains to detect possible fluctuations in element concentrations which would indicate micro and macro segregation. The only significant variations in element concentration were caused by the beam traversing small carbide particles and primary gamma prime particles.

b. Material Quenched From the Optimum Working Temperature

The results of the X-ray diffraction studies of samples quenched from their working temperatures are shown in Table 15. It should be noted that the working temperatures used in this evaluation were the ones originally chosen, and do not take into account the temperature increases which were later found necessary. The results of the X-ray diffraction data indicate small concentrations of gamma prime in the extracted residues for each of the alloys. Also, as was the case for the as-cast samples, a heavy concentration of MC-type carbides was detected for each of the alloys. The relatively low working temperatures evaluated caused no significant changes in the minor phases present after heating and quenching material in the as-cast condition. However, it is believed that if the revised 2050°F (1121°C) and 2100°F (1149°C) working temperatures had been used, the quantity of the MC-type carbides and gamma prime would have been slightly reduced due to solutioning.

The microstructural examination indicated very little variation in the quenched structures as compared with the as-cast structures. The dendritic patterns were undisturbed by the heating and quenching operations, probably due to the low working temperatures. The photomicrographs in Figure 20 for IIIg and Unitemp AF 2-1DA illustrate the similarity to the as-cast structures. The massive primary gamma prime particles present in the as-cast IIIg microstructure were not solutioned during the treatment, and are evident in the photographs.

Electron microprobe techniques were again employed on quenched samples to detect possible areas of segregation. No significant variations in element concentrations were discovered in any of the samples.

c. Extruded Material

Samples for the structural examination of extruded material were sectioned near the area of the failure for alloys which exhibited poor workability. Samples were sectioned from both the three inch (0.076 m) diameter and the one inch (0.025 m) diameter single extruded billets. This procedure was followed to determine possible structural causes for the poor workability. The results of the X-ray diffraction studies of extruded material are summarized in Table 15. These results were similar to the X-ray results previously obtained for as-cast material and material quenched from optimum working temperature. The major phase identified was an MC-type carbide, and some quantity of gamma prime was also detected for each of the alloys.

The results of the metallographic examination of one (0.025 m) and three inch (0.076 m) diameter single extruded billets are shown in Figure 21. The basic structural variation between the two sizes of extrusions was that the as-cast structure was completely broken up and recrystallization had occurred after the extrusion from 5-1/2 inch (0.140 m)

diameter ingots to three inch (0.076 m) diameter billets. On the other hand, the extrusions from 2-1/2 inch (0.063 m) diameter ingots to one inch (0.025 m) diameter billets left some evidence of the cast structure. As illustrated in Figure 21 for I 5 and IIIg, no dendritic patterns were evident after the extrusions to three inch (0.076 m) diameter billets. However, after the extrusion to one inch (0.025 m) diameter billets, five of the alloys still displayed the cast structure. As shown in the photographs, Unitemp AF 2-1DA was the only alloy which did not exhibit a dendritic structure after the single extrusion to one inch (0.025 m) diameter.

The results of the electron beam microprobe studies conducted on the extruded billets in the areas of failure did not detect any structural variations as a reason for the breakage. No evidence of segregation, carbide clustering, or variations in element concentration, was detected near or along the cracked billets. Therefore, it was concluded that the reason for the failures was due to low working temperatures, rather than structural effects or inherent poor workability.

## B. Task II

The four alloys chosen for Task II studies included Unitemp AF 2-1DA, I 5, IIb, and IIIg mod. These alloys were chosen based upon their workability as exhibited in the Task I studies. Alloys IId and IIIg were not included in the Task II evaluations.

### 1. Heat Treatment Evaluation

The results of the heat treatment evaluation of Task II double extruded alloys are summarized in Table 16 and Figures 22 to 27. Optimum solution treatment and intermediate and final aging temperatures were determined for each of the four alloys. These temperatures were chosen based upon the results of an in-depth structural examination of specimens subjected to a variety of treatments. Optical and electron microscopy, X-ray diffraction studies and electron beam microprobe techniques were employed in the structural examinations to arrive at the optimum temperatures.

#### a. Determination of Optimum Temperatures

##### 1) Solution Treatments

Optimum solution treatment temperatures were chosen for the alloys based upon the degree of carbide and gamma prime solutioning and on grain size. A grain size of ASTM 4 to 5 was chosen as the aim for each of the alloys, based upon past experience with alloys of this type. This grain size does not favor either tensile or rupture properties, and was chosen because it usually provides a fair representation of the overall properties of each alloy. Due to the importance of developing the same target grain size, one-half inch (0.013 m) square cubes were sectioned and heat treated at various time and temperature conditions

within the general range suggested from the gradient bar studies. An example of the effect of various solution treatments on ASTM grain size is shown in Figure 22 for Unitemp AF 2-1DA. In this case, changing the solution treatment conditions from 2175°F (1191°C) for four hours to 2250°F (1231°C) for two hours resulted in an increase in the grain size from ASTM 6 to 7 to ASTM 3 to 4. For Unitemp AF 2-1DA, the optimum solution treatment was found to be two hours at 2200°F (1204°C); for I 5, one hour at 2225°F (1218°C); and for IIb and IIIg mod, two hours at 2225°F (1218°C).

In each of these alloys, the grains formed during the solution treatment were not uniform in size. An average grain size of ASTM 4 to 5 was achieved, but randomly distributed grains ranged from ASTM 2 to ASTM 7.

2) Intermediate Aging Treatments

Optimum intermediate aging temperatures for each alloy were chosen based upon the degree of grain boundary carbide precipitation and gamma prime nucleation. The gradient bar samples were solution treated by the optimum method determined from the previous evaluation. After subjecting the bars to the gradient aging treatments, they were sectioned to represent every 100°F (55°C) variation in temperature and mounted, polished, and etched for structural examination. They were examined by optical microscopy at magnifications ranging from 500X to 1000X as required.

Satisfactory intermediate aging temperatures were developed from the gradient bars for Unitemp AF 2-1DA, and IIb; however, for I 5 and IIIg mod, some difficulties were encountered. The major problem was the inability to achieve proper grain boundary carbide precipitation with conventional intermediate aging treatments. These problems were solved by employing longer aging times (up to 16 hours) at relatively high temperatures, but these treatments caused the gamma prime particles to become coarsened, or overaged. Therefore, for I 5 and IIIg mod, a decision was made to achieve the most acceptable degree of grain boundary carbide distribution without causing an overaging of the gamma prime particles.

A 1950°F (1066°C) age for two hours developed a satisfactory structure for Unitemp AF 2-1DA, and a treatment at 1900°F (1038°C) for two hours was acceptable for IIb. However, neither of these treatments were satisfactory for I 5. The micrographs in Figure 23 illustrate the problem in developing the desired structure in I 5. After aging I 5 at 1950°F (1066°C) for two hours, very little gamma prime nucleation and carbide precipitation resulted. A treatment at 2000°F (1093°C) for 16 hours resulted in relatively good carbide precipitation; however, the gamma prime particles became coarsened. The procedure finally chosen was an aging treatment at 1950°F (1066°C) for 16 hours. This treatment resulted in some degree of carbide precipitation and did not detrimentally affect the morphology of the gamma prime particles.

This treatment at 1950°F (1066°C) for 16 hours proved to be too severe for IIIg mod as overaging of the gamma prime particles was experienced. Extreme difficulty was encountered in obtaining any degree of grain boundary carbide precipitation for IIIg mod by aging at any temperature. Even the high temperature 16 hour treatments failed to effect a satisfactory degree of precipitation. Therefore, a treatment at 1950°F (1066°C) for two hours was selected for this alloy to produce an acceptable gamma prime morphology, even though the degree of carbide precipitation was not optimum.

3) Final Aging Treatments

Final aging temperatures for each alloy were chosen based upon carbide and gamma prime precipitation. Gradient bar samples were solution treated and intermediate aged according to the treatments previously derived. After gradient final aging, the bars were sectioned to represent every 100°F (55°C) increment, mounted, and prepared for electron microscopy studies. For each of the alloys, a final aging treatment at 1400°F (760°C) for 16 hours was considered optimum. This temperature was selected because it produced what is considered in other alloys of this type to be an optimum gamma prime morphology for each of the alloys.

b. Structural Examinations

After the proper heat treatments had been determined for each alloy, samples after each stage of heat treatment were subjected to a structural examination using electron microscopy and X-ray diffraction and electron beam microprobe techniques. Samples from each of the four compositions were examined in the solution treated condition, the solution treated plus intermediate aged condition, and the solution treated plus intermediate aged plus final aged condition.

The results of the phase identification work conducted on Unitemp AF 2-1DA after various stages of heat treatment are summarized in Table 16. Electron micrographs of Unitemp AF 2-1DA after each stage of its heat treatment are illustrated in Figure 24. The X-ray data indicated that the only phase present in the solution treated condition was the MC-type carbide. Intermediate aging resulted in the precipitation of $M_6C$-type carbides, which were also present in an equivalent amount in the final aged or fully heat treated condition.* These trends can also be observed in the electron micrographs. The solution treated structure exhibited large and small MC-type carbides which were surrounded by extremely fine gamma prime particles throughout the matrix. The grain boundaries contained no carbides

*Gamma prime, present in almost all specimens, is not detected by X-ray analysis because the solution for digestion, ten percent hydrochloric acid in methanol, dissolves this phase.

in this condition. After intermediate aging, the most significant structural effect was the growth of the gamma prime particles. Another significant effect was the precipitation of the $M_6C$-type carbides in the grain boundaries. These carbides formed as a result of the decomposition of the MC-type carbides as shown in EM1620 of Figure 24. The final aged or fully heat treated microstructure also exhibited the MC and $M_6C$-type carbides surrounded by gamma prime particles. The most significant change from the intermediate aged structure was the gamma prime morphology. The blocky particles were much sharper, and interspersed between those particles were very fine precipitates, commonly referred to as second generation gamma prime.(4)

In general, the results of the X-ray phase analyses for the remaining three alloys after each stage of heat treatment were similar. The I 5 intermediate aging treatment resulted in the formation of $M_{23}C_6$-type grain boundary carbides, and $M_6C$-type carbides were formed in IIb. The only alloy which did not form any detectable amount of grain boundary carbides was IIIg mod.

The effects of the heat treatment on the microstructures of I 5, IIb, and IIIg mod are shown in Figures 25, 26, and 27, respectively. The general structural changes were similar to those described above for Unitemp AF 2-1DA, although some variations did occur. For example, the grain boundary carbides were extremely fine in these three alloys, even after full heat treatment. Also, I 5 and IIb exhibited a eutectic-like gamma prime structure even in the fully heat treated condition. The solution treatment temperatures for these alloys were quite high at 2225°F (1218°C), thus indicating the solutioning temperature of these eutectic-like constituents is above 2225°F (1218°C). Higher solution temperatures than used are not recommended as they would result in extremely large grain sizes and possibly incipient melting. With respect to gamma prime morphology, the extremely fine size of the individual gamma prime particles in the IIb and IIIg mod fully heat treated samples should be noted. These particles were much smaller than were the particles in the Unitemp AF 2-1DA and I 5 structures.

2. Mechanical Testing

Material for mechanical testing was taken from double extruded stock and was heat treated by the optimum methods determined from the heat treatment evaluations described in the previous section.

a. Tensile Tests

The results of the tensile tests conducted on Unitemp AF 2-1DA, I 5, IIb, and IIIg mod are shown in Tables 17 to 20, respectively. The effect of test temperature on ultimate tensile strength, 0.2 percent yield strength, and tensile ductility are illustrated in Figures 28, 29, and 30 respectively. The data points plotted on these figures represent an average of the two tests.

As shown in Figures 28 and 29, with respect to ultimate tensile and yield strengths, IIb exhibited the highest strength values over the temperature range investigated. The ultimate tensile strength for IIb ranged from approximately 217,000 psi (1500 $N/mm^2$) at room temperature to 81,000 psi (558 $N/mm^2$) at 1800°F (982°C); and, yield strength values ranged from approximately 174,000 psi (1198 $N/mm^2$) at room temperature to 61,000 psi (420 $N/mm^2$) at 1800°F (982°C). Tensile and yield strengths exhibited for Unitemp AF 2-1DA and IIIg mod were very similar throughout the temperature range investigated and were an average of 10,000 to 15,000 psi (69 to 103 $N/mm^2$) lower than the strengths exhibited by IIb. From room temperature to 1000°F (538°C), IIIg mod had slightly higher strength values than Unitemp AF 2-1DA; however, from 1200°F (649°C) to 1800°F (982°C), Unitemp AF 2-1DA became slightly stronger. The weakest of the four alloys, with respect to ultimate tensile and yield strengths was I 5. Strength values for I 5 varied with temperature, but were 20,000 to 50,000 psi (138 to 344 $N/mm^2$) less than the corresponding strengths exhibited by the strongest alloy, IIb.

As shown in Figure 30, tensile reduction of area values varied considerably for the alloys over the temperature range investigated. The general trend for I 5, IIb, and IIIg mod was for ductility to decrease as the test temperature increased. The best low temperature ductility was exhibited by I 5, and was approximately 25 percent at room temperature. However, beyond 1000°F (538°C), the tensile ductility of I 5 dropped to a low of about six percent for the 1800°F (982°C) test. The ductility values for IIIg mod were lower than for I 5, and a similar decrease in ductility occurred with increasing temperature. In this case, the decrease was from about 18 percent at room temperature to two percent at 1800°F (982°C). The tensile ductility of IIb was consistently low, even at low test temperatures. Reduction of area values were approximately 12 percent from room temperature to 1400°F (760°C); however, these values steadily decreased at temperatures above 1400°F (760°C) to eight percent at 1600°F (871°C) and three percent at 1800°F (982°C). The best overall tensile ductility was exhibited by Unitemp AF 2-1DA. From a low room temperature ductility near 10 percent, the reduction of area values increased to 17 percent at 1000°F (538°C) and remained steady between 16 and 18 percent from 1000°F (538°C) to 1800°F (982°C).

b. Stress Rupture Tests

1) Rupture Life and Ductility Data

The stress rupture test data for the four alloys are listed in Tables 21 to 24 and are illustrated in Figures 31 and 32. The data plotted in the figures represent the average of two or three tests.

With respect to rupture strength, as shown in the Larson-Miller parameter plot in Figure 31, IIb exhibited the best properties over the entire range of temperature and stress conditions evaluated. The rupture properties exhibited by Unitemp AF 2-1DA were very close to those

exhibited by IIb, although slightly lower over the range evaluated. Both I 5 and IIIg mod exhibited rupture properties considerably lower than the IIb or Unitemp AF 2-1DA values. Of the two alloys, I 5 appeared to exhibit better rupture life at low temperature-high stress conditions, while IIIg mod exhibited better properties at high temperature-low stress conditions.

From the rupture ductility data represented in Figure 32, as measured by reduction of area, Unitemp AF 2-1DA displayed the best rupture ductility of the four Task II alloys evaluated at each test temperature. The rupture ductility values for Unitemp AF 2-1DA were only slightly greater than values exhibited by the other alloys at low temperatures; however, this effect became much more significant as the temperature increased. The other alloys also displayed the trend for increasing ductility with increasing temperature, although the values for these alloys were considerably lower than the values for Unitemp AF 2-1DA.

2) Structural Evaluation

The stress rupture testing was supplemented by a structural examination of specimens of each alloy after testing at three conditions. Specimens from each of the four alloys were examined by optical and electron microscopy and by phase analysis through X-ray diffraction techniques. Specimens were examined after testing at the following conditions: a) 1400°F/ 90,000 psi (760°C/620 $N/mm^2$), b) 1600°F/55,000 psi (871°C/380 $N/mm^2$) and c) 1900°F/15,000 psi (1038°C/103 $N/mm^2$). These specimens were selected to examine the structural effects of low temperature-high stress conditions, moderate temperature-moderate stress conditions, and high temperature-low stress conditions, respectively. The results of examinations are shown in Figures 33 to 36 and Table 25.

The results of the X-ray diffraction studies of extracted residues are summarized in Table 25. Also included in the table is the time each sample was exposed to the test conditions until rupture occurred. This time is important and must be factored into the X-ray phase analysis, as the time a material is exposed to temperature-stress conditions has a significant effect on the microstructural changes which can occur.

The phase identification data for Unitemp AF 2-1DA samples after testing indicated the presence of the three major carbide phases: MC-, $M_6C$-, and $M_{23}C_6$-type carbides. The relative concentration of these phases varied depending upon the test temperature. As the test temperature increased, the MC-type carbide decomposition rate increased. This decomposition of MC-type carbides was accompanied by an increase in the concentration of $M_6C$ and $M_{23}C_6$-type carbides. This effect can be observed in the electron micrographs shown in Figure 33. With increasing test temperatures, the massive MC-type carbides present in the as-heat treated microstructure began to decompose into smaller grain boundary carbides. The sample which was tested at 1900°F (1038°C) exhibited extremely large grain boundary $M_6C$- and $M_{23}C_6$-type carbides. The increasing temperature also had a significant effect on the gamma prime morphology. The very fine, blocky gamma prime

particles in the as-heat treated microstructure tended to grow with increasing temperature. After testing at 1900°F (1038°C), the coarsened gamma prime particles became elongated in the direction of the stress. Several unidentified lines were present in the Unitemp AF 2-1DA X-ray scans. These lines were also present in several I 5 and IIb samples and were tentatively identified as a cubic $M_2M$-type phase. In all cases, the relative intensity of the lines was very weak, making exact identification impossible.

The phase identification work conducted on I 5 stress rupture specimens revealed only a slight decrease in the concentration of MC-type carbides with increasing test temperature. No grain boundary $M_6C$- or $M_{23}C_6$- type carbides were detected in any of the samples. It is believed that the decomposition of the MC-type carbides resulted in the formation of some carbide phase; however, the concentration of this phase was not significant enough to detect by normal electrolytic extraction and X-ray diffraction techniques. The results of the electron microscopy studies of the I 5 stress rupture samples are shown in Figure 34. As was the case for the Unitemp AF 2-1DA samples, increasing temperature caused a coarsening of the gamma prime particles, especially after testing at 1900°F (1038°C). Also, the near-complete absence of grain boundary carbides suggested from the X-ray data was confirmed in these studies. Note the extremely fine boundaries, even in the sample tested at 1900°F (1038°C). The boundaries appear to be entirely free of grain boundary carbides, except for several extremely small, widely dispersed particles.

The results of the phase identification work conducted on the IIb stress rupture specimens were very similar to those derived for Unitemp AF 2-1DA. The major carbide phase, the MC-type, decomposed with increasing temperature and resulted in the formation of progressively larger concentrations of $M_6C$- and $M_{23}C_6$-type carbides. After testing at 1400°F (760°C), only MC- and $M_6C$-type carbides were identified in the extracted residue. However, a slightly greater decomposition of the MC-type carbides after testing at 1600°F (871°C) resulted in the formation of a moderate amount of $M_{23}C_6$-type carbides, in addition to the MC- and $M_6C$-type. The most significant change occurred after testing at 1900°F (1038°C). A much more significant decomposition of MC-type carbides resulted in the formation of a large amount of $M_6C$-type carbides. The amount of $M_{23}C_6$-type carbides formed was less than formed during the 1600°F (871°C) test, probably due to the higher temperature which does not favor the formation of the less stable $M_{23}C_6$-type carbides. These effects can be observed in the microstructures as shown in Figure 35. After testing at 1400°F (760°C), the very fine grain boundary carbides were predominantly the $M_6C$-type. After testing at 1600°F (871°C), the grain boundaries became thicker with an increase in the amount of the $M_{23}C_6$-type carbide, which at this temperature was the major grain boundary precipitate. After the 1900°F (1038°C) test, the gamma prime precipitate again became coarsened; however, the most significant change was the thickened grain boundaries. These carbides were almost continuous, separated only in places by areas of gamma prime.

The effect of temperature on the phase changes in III g mod after stress rupture testing was very similar to the behavior of I 5. Increasing test temperature resulted only in a decrease in the concentration of the MC-type carbide. Even after testing at 1900°F (1038°C), no significant amount of grain boundary carbides were detected. Again it is believed that some small degree of grain boundary carbide precipitation occurred; however, the amount was not significant enough to be detected by normal extraction and X-ray diffraction techniques. As shown in the electron micrographs in Figure 36, no appreciable grain boundary carbide precipitate was evident in the microstructures. The random dispersion of MC-type carbides occasionally resulted in the formation of an MC-type carbide in the grain boundary, as shown in one of the photographs after testing at 1600°F (871°C); however, the only significant microstructural changes which occurred in IIIg mod were the decomposition of the MC-type carbides and the coarsening of the gamma prime particles with increasing test temperature.

c. Interrupted Low Cycle Fatigue Tests

The results of the interrupted low cycle fatigue tests conducted on the four Task II double extruded alloys are summarized in Table 26. The results indicate that IIb exhibited the best low cycle fatigue strength of the four alloys at all temperature-stress conditions evaluated. With the exception of the I 5 test at 1300°F (704°C), which survived a larger number of cycles to failure than the corresponding Unitemp AF 2-1DA test, Unitemp AF 2-1DA exhibited the second best properties, followed by I 5 and IIIg mod, respectively. The properties obtained on the III g mod samples were very low as compared with the other three alloys.

3. Processing Studies

a. Rolling

The bars resulting from the Task I rolling studies conducted on Unitemp AF 2-1DA and I 5 in the as-cast condition were previously shown in Figure 15. Bars of Unitemp AF 2-1DA, I 5, IIb, and IIIg mod after single extrusion and rolling are pictured in Figure 37.

The results of the Task I rolling studies conducted on Unitemp AF 2-1DA and I 5 as-cast material were previously discussed. Stress rupture specimens were sectioned from each bar, heat treated by the optimum methods derived from the heat treatment study, and subjected to testing at various temperature/stress conditions ranging from 1300°F/100,000 psi (704°C/690 $N/mm^2$) to 1900°F/15,000 psi (1038°C/103 $N/mm^2$). The test conditions were similar to those used in the stress rupture testing of double extruded material. The results of these tests are summarized in Table 27.

Additional rolling studies were conducted on the four Task II alloys in the single extruded condition. A six inch (0.15 m) long segment was sectioned from a one inch (0.025 m) diameter canned single extruded billet from each composition. The pieces were rolled to 0.60 inch (0.015 m)

diameter bars, and the results of the rolling are pictured in Figure 37. The condition of the Unitemp AF 2-1DA, I 5, and IIb bars was satisfactory; however, the IIIg mod bar experienced very deep cracking during the rolling operation, and processing was discontinued after reducing the bar to approximately 0.85 inch (0.022 m) diameter. The condition of this bar was too poor to recover stress rupture samples; however, samples were sectioned from the remaining three bars, heat treated and subjected to stress rupture testing at the same conditions specified for the material rolled directly from ingot. The results of these tests are shown in Table 28.

The rupture data for Unitemp AF 2-1DA and I 5 in the double extruded condition, the single extruded and rolled condition, and the as-cast and rolled condition were plotted on Larson-Miller parameter curves and are shown for the two alloys in Figures 38 and 39, respectively. The rupture data for IIb in the double extruded, and single extruded and rolled condition were also plotted on parameter curves, and the curves are presented in Figure 40.

No extreme variation in rupture strength occurred for Unitemp AF 2-1DA processed by the three methods, although the double extruded material exhibited slightly better rupture strengths than the material rolled directly from ingot or the single extruded and rolled material.

The rupture strength data for I 5 and IIb, however, exhibited condiderable variation depending on the processing method. The rupture strength of the I 5 material rolled directly from ingot was considerably improved over the strength of I 5 produced by double extrusion. These properties were very close to the strengths achieved by double extruded IIb, which exhibited the best rupture strength of any of the alloys in the double extruded condition. However, I 5 processed by single extrusion and rolling exhibited very poor rupture strengths. The data for IIb also varied considerably, with the material in the single extruded and rolled condition exhibiting considerably lower rupture strengths than the double extruded IIb.

These variations can be explained by examining the microstructures of I 5 and IIb material processed by the various methods and subjected to the standard heat treatments for the alloys. The structural appearance after the standard heat treatments varied considerably depending on the method the alloys were processed. These structural effects are shown in Figures 41 and 42 for I 5 and IIb, respectively. The two I 5 samples shown in Figure 41 were both heat treated using the same cycle and were tested at the same conditions of 1300°F/100,000 psi (704°C/690 $N/mm^2$). The samples differ only in that one was taken from material directly rolled from ingot form and the other was taken from single extruded and rolled material. The sample from the material which was rolled directly from ingot had a very uniform grain size in the area of ASTM 4 to 5. However, the sample from the single extruded and rolled material had a variable grain size. Most of the area exhibited very fine grain size of ASTM 7 to 9 or finer, although some areas of larger grains (ASTM 2 to 5) were present.

This variation was significant enough to cause the 1400°F/90,000 psi (760°C/620 N/mm$^2$) rupture life to decrease from 841.5 hours for the sample with a relatively large, uniform grain size to 138.2 hours for the sample with the smaller, variable grain size.

Figure 42 shows a similar situation was encountered for IIb. The 1400°F/90,000 psi (760°C/620 N/mm$^2$) stress rupture life of double extruded IIb was 201.7 hours; however, the life was decreased to 69.7 hours for single extruded and rolled material heat treated using the same cycle. The grain size of the double extruded material after heat treatment was ASTM 3 to 5, while a variable grain size from ASTM 1 to 7 was exhibited by the single extruded and rolled material. Also present in the microstructure of the single extruded and rolled sample was a stringer-type dispersion of undissolved carbide particles. These particles were especially concentrated in the finer grain size areas, and suggest the reason the grains did not grow to an acceptable size was due to the undissolved carbide particles concentrated in certain areas.

b. Forging

Forging studies were conducted on 1-1/8 inch (0.028 m) diameter single extruded bars representing each of the Task II alloys. The results of these studies were unsuccessful as the bars failed due to severe center bursting. These failures were similar to the results of the Task I forging studies on Unitemp AF 2-1DA and I 5 ingots, and were believed to be due to the inability to adequately control reductions on the hammer forging unit. No bars were successfully reduced to the aim 0.60 inch (0.015 m) diameter without failure. Therefore, no material was available to conduct the scheduled stress rupture testing on forged material.

4. Thermal Stability Studies

a. Phase Identification

The results of the X-ray diffraction studies conducted on thermal stability specimens representing each of the Task II alloys are summarized in Table 29. The stability samples from each alloy were subjected to 1500 hours exposure at 1400, 1500, 1600, and 1700°F (760, 816, 871, 927°C). The effects of the stability treatments on Unitemp AF 2-1DA and I 5 were similar. No detrimental phases were formed during the exposures in either of the alloys. However, the concentrations of the major carbide phases were significantly affected by the treatments. As the exposure temperature was increased from 1400°F (760°C) to 1700°F (927°C), each of the alloys experienced a decrease in the concentration of the MC-type carbide. This decrease was accompanied by a significant increase in the concentration of the grain boundary $M_{23}C_6$-type carbide. No additional phases were identified in the I 5 samples; however, the $M_6C$-type carbide was identified in each of the Unitemp AF 2-1DA samples. The concentration of the carbide decreased from a medium concentration after exposure at 1400°F (760°C) to a weak concentration after exposure at the three higher temperatures.

The results of the phase identification studies conducted on IIb are presented in Table 29. This alloy also experienced a decrease in the concentration of the MC-type carbides with increasing exposure temperature. The concentration of the $M_6C$-type carbide increased from weak after the 1400°F (760°C) and 1500°F (816°C) exposures to very strong after the 1600°F (871°C) exposure. A medium concentration of the $M_6C$-type carbide formed during the 1700°F (927°C) exposure. The concentration of the $M_{23}C_6$-type carbide varied from weak to medium after the 1400, 1500, and 1700°F (760, 816, and 927°C) exposures, but was very weak after the 1600°F (871°C) exposure. This decrease in concentration after the 1600°F (871°C) exposure was attributed to the very strong concentration of stable $M_6C$-type carbides which formed at this temperature, thereby reducing the preferred elements available to combine and form the $M_{23}C_6$-type carbides. A detrimental $M_7M_6$-type mu phase was identified in increasing amounts after exposure at 1500, 1600, and 1700°F (816, 871, 927°C). The relative concentration of this phase increased from weak, to medium strong, to strong with increasing exposure temperatures.

The results of the phase analysis of IIIg mod exposure samples indicated that the behavior of the alloy varies considerably when compared to the other three alloys. No detrimental phases were definitely identified after exposure at any of the temperatures. However, several unidentified lines in the 1700°F (927°C) residue suggested the presence of a possible weak concentration of mu phase. The unique feature of this alloy was that it did not experience a decrease in the concentration of the MC-type carbides with increasing temperature. No significant degree of grain boundary carbide precipitation occurred until the 1700°F (927°C) exposure. Weak concentrations of $M_6C$ and $M_{23}C_6$-type carbides were identified after the 1500 and 1600°F (816 add 871°C) exposures. However, medium amounts were not formed until the 1700°F (927°C) exposure, and no accompanying decrease in the MC-type carbide concentration was detected.

b. Microstructure

The effects of the 1500 hour exposures at 1400, 1500, 1600, and 1700°F (760, 816, 871, and 927°C) on the microstructures of Unitemp AF 2-1DA and I 5 are shown in Figures 43 and 44, respectively. The increasing concentration of grain boundary carbides as the exposure temperature increased was evident in the microstructure of both of the alloys. The gamma prime morphology also changed with increasing exposure temperature as the individual particles became coarsened. For Unitemp AF 2-1DA, the most drastic structural change occurred between 1500 and 1600°F (816 add 871°C). After the 1500°F (816°C) exposure, the structure was relatively fine although there was a definite increase in grain boundary carbides; however, after the 1600°F (871°C) exposure, the structure became extremely coarsened. Also, the degree of grain boundary carbide precipitation increased considerably, resulting in thickened grain boundary envelopes. These effects became more severe after the 1700°F (927°C) exposure, with the grain boundary envelopes becoming extremely thickened and containing near continuous carbides as shown in EM1966 of Figure 43. The severe structural

change for I 5 did not occur until the 1700°F (927°C) exposure, as illustrated in Figure 44. This treatment resulted in extreme gamma prime coarsening and thickened grain boundary envelopes. Note the decomposition of a massive MC-type carbide shown in EM2012 of Figure 44.

The results of the microstructural examination of IIb thermal stability specimens are shown in Figure 45. The pools of undissolved gamma prime which were present in the as-heat treated condition were not solutioned after the 1500 hour exposure at any of the temperatures. After the 1400°F (760°C) exposure, the gamma prime morphology remained relatively fine, although some degree of increased grain boundary carbide precipitation occurred. The formation of very thin $M_7M_6$-type mu platelets occurred after the 1500°F (816°C) exposure, and the degree of grain boundary carbide precipitation also increased somewhat. A very significant structural change occurred after the exposure at 1600°F (871°C). This change was identified by the X-ray data as a sharp increase in the concentration of $M_6C$-type carbides and a corresponding decrease in the concentration of $M_{23}C_6$-type carbides. Although the $M_6C$-type carbide usually forms as a grain boundary precipitate, the electron micrographs showed that the amount of grain boundary precipitate did not significantly increase from that which occurred after the 1500°F (816°C) exposure; however, there was a considerable increase in the amount of the needle-like precipitates dispersed throughout the matrix. Electron beam microprobe techniques and scanning electron microscopy studies indicated that many of the needle-like particles were $M_6C$-type carbides. The major elements contained in these carbide particles were found to be chromium and molybdenum; additional elements present in weaker concentrations were cobalt, nickel, tantalum, and tungsten. The needle-like mu platelets were also analyzed and their composition was very similar to the $M_6C$-type carbide particles. The mu platelets appeared to contain a substantial amount of chromium and were richer in tungsten than the $M_6C$ platelets. The mu platelets also contained weak concentrations of cobalt, nickel, and molybdenum[5]. Neither phase was large enough for quantitative microprobe analysis.

A sample exposed at 1600°F (871°C) was prepared for electron microscopy using special techniques to differentiate between the two needle-like phases. This sample was replicated and photographed as shown in EM2443. The gamma prime structure was not properly accentuated so the needles could be viewed more clearly. The photograph definitely shows two types of platelets. A group of thin, symmetrically-shaped platelets are visible in the upper left corner of the photograph. These platelets appear to be growing along preferential planes, and were identified as the mu phase. The remaining thicker, non-symmetrical platelets do not appear to be aligned along preferential planes and were identified as the $M_6C$-type carbide phase. The abundant formation of the mu and $M_6C$-type carbide phases during exposure at 1600°F (871°C) explained the decrease in the concentration of the $M_{23}C_6$-type grain boundary carbide. The $M_{23}C_6$-type carbide contains a heavy concentration of chromium as its primary constituent. Both the mu and the $M_6C$-type carbide phases contain very heavy concentrations of chromium, thereby significantly decreasing the amount of chromium

available to form the less stable $M_{23}C_6$-type carbides. The 1600°F (871°C) IIb exposure sample examined by scanning electron microscopy showing the heavy grain boundary precipitation and needle-like phases is shown in Figure 47. After exposure at 1700°F (927°C), the concentration of the mu phase increased slightly; however, the concentration of the needle-like $M_6C$-type carbide phase significantly decreased. This change resulted in more chromium being available to combine and form $M_{23}C_6$-type grain boundary carbides; and, as shown in the micrographs, the grain boundary precipitation of the $M_{23}C_6$-type carbide was significantly increased over the slight amount which occurred during the 1600°F (871°C) exposure. The 1700°F (927°C) exposure also resulted in a coarsening of the gamma prime particles and a corresponding increase in the thickness of the grain boundary envelopes.

The results of the electron microscopy studies of IIIg mod thermal stability specimens are shown in Figure 46. The degree of grain boundary carbide precipitation in this alloy was much less than for any of the other alloys. Even after the 1700°F (927°C) exposure, which resulted in heavy grain boundary precipitation and envelope thickening for the other three alloys, no significant precipitation occurred. Note the grain boundaries in EM2469 after the 1700°F (927°C) exposure which are almost entirely free of carbides. The most significant structural change experienced by the alloy was an increasing degree of gamma prime particle agglomeration with increasing exposure temperature from 1600°F (871°C) to 1700°F (927°C). Also, the particles which did not agglomerate experienced coarsening and changed from a blocky to a rounded configuration.

c. Stress Rupture Testing

The results of the stress rupture tests conducted for each of the Task II alloys after 1500 hours thermal exposure at various temperatures are presented in Table 30. All tests were run at 1400°F/90,000 psi (760°C/620 $N/mm^2$) conditions. Each of the alloys exhibited decreasing stress rupture lives with increasing exposure temperature with one exception. The exception was a Unitemp AF 2-1DA sample subjected to 1500 hours exposure at 1600°F (871°C). The reason for the improved rupture strength of this sample was unexplained. Each of the samples exposed at 1700°F (927°C) for 1500 hours experienced failure by brittle fracture. This was probably due to the extreme thickening of the grain boundaries and heavy grain boundary carbide precipitation effected by exposure at this temperature. The rupture strengths of Unitemp AF 2-1DA and I 5 were not reduced considerably with exposures up to 1600°F (871°C). However, the rupture strengths of IIb and IIIg mod were considerably decreased after the 1600°F (871°C) treatment. For IIb, the decrease was probably due to a combination of the very heavy $M_6C$-type carbide precipitation and the $M_7M_6$-type mu phase formation. The mu phase probably has the most detrimental effect on rupture strength, as its initial formation after the 1500°F (816°C) treatment caused a reduction in rupture strength and its progressively increasing concentration with increasing exposure temperature was accompanied by corresponding decreases in rupture life. The concentration of the $M_6C$-type

carbide phase was variable with increasing exposure temperature and could not be correlated as the cause of the decreasing rupture strengths. However, the increase in the degree of $M_{23}C_6$-type grain boundary carbide precipitation after the 1700°F (927°C) exposure probably can be cited as the cause for the brittle failure of the specimen exposed at 1700°F (927°C) as the heavy grain boundary precipitates in Unitemp AF 2-1DA and I 5 effected the same results.

5. Oxidation Testing

a. Continuous Tests

The results of the 100 hour continuous oxidation tests conducted at 1950°F (1066°C) for the Task II alloys are illustrated in Figure 48. The data are plotted as weight gain versus time at temperature. IIb exhibited the poorest resistance to oxidation, although the oxidation rate of Unitemp AF 2-1DA was slightly more rapid up to approximately two hours exposure. I 5 and IIIg mod exhibited similar rate curves, both of which were considerably less severe than the Unitemp AF 2-1DA and IIb curves. The data indicated that some degree of spalling occurred for at least three of the alloys. These alloys were I 5, IIb, and IIIg mod, and the spalling for each of the alloys seemed to occur near the end of the 100 hour tests.

b. Cyclic Testing

1) Weight Change Data

The results of the cyclic oxidation tests conducted on the Task II alloys at 1875, 1950, and 2100°F (1024, 1066, and 1149°C) are summarized in Tables 31 to 33, respectively. These data were very difficult to analyze due to weight losses experienced by many of the samples during the periodic weighings. Although the sample assemblies were designed to retain all spalling oxides within the crucibles, it is believed that in some instances, scale may have spalled through the air circulation holes in the crucibles. This loss of scale for some of the samples made correlation of the weight change data very difficult.

Figure 49 shows the samples after testing and the scale collected in the crucible assembly for each of the samples. Using the scale formation as a measure of oxidation resistance, I 5 appeared to exhibit good resistance to oxidation at each test temperature; although, in general, increasing test temperature seemed to result in increased scale formation for each of the alloys. Unitemp AF 2-1DA exhibited the next best cyclic oxidation resistance followed by IIIg mod and IIb, respectively. The oxidation resistance of IIb was poor at 1950°F (1066°C) and the alloy was susceptible to severe attack at 2100°F (1149°C).

2) Microstructural Examinations

Samples of each alloy were examined by optical microscopy after testing at 1875, 1950, and 2100°F (1024, 1066, and 1149°C) for a

total of 1000 hours. The results of these studies are illustrated in Figures 50 to 53 for Unitemp AF 2-1DA, I 5, IIb, and IIIg mod, respectively. The photographs were not taken on the edge of the samples, as the only samples which experienced any significant internal oxidation were the IIIg mod samples tested at 1950 and 2100°F (1066 and 1149°C). The actual microstructural changes which occurred in each alloy after testing at the various temperatures were more significant.

The structure of Unitemp AF 2-1DA varied considerably with increasing test temperature as shown in Figure 50. After cycling for a total of 1000 hours at 1875°F (1024°C), the amount of grain boundary carbide precipitation was considerable. These carbides are probably primarily the $M_{23}C_6$-type with a much lesser amount of $M_6C$-type carbides. The gamma prime particles also became coarsened, forming thick grain boundary envelopes. After the testing at 1950°F (1066°C), the amount of MC-type carbides visibly decreased causing a considerable increase in the amount of grain boundary carbide particles. The carbides were nearly continuous within the grain boundaries. Gamma prime coarsening was more severe than after the 1875°F (1024°C) testing and the grain boundary envelopes were considerably thickened. A severe structural change occurred after testing at 2100°F (1149°C). The gamma prime and grain boundary carbides were almost completely solutioned after the testing. The microstructure resembled that of a fully solution treated sample.

The results of the I 5 examinations as illustrated in Figure 51 were similar to the Unitemp AF 2-1DA results at 1875°F (1024°C). The structure consisted of matrix MC-type and grain boundary $M_{23}C_6$-type carbides, while the gamma prime particles were coarsened. I 5 behaved somewhat differently than Unitemp AF 2-1DA after the 1950°F (1066°C) testing. The grain boundary carbides did not form in thick envelopes as for the 1875°F (1024°C) sample. The gamma prime particles were considerably coarsened and showed signs of some degree of agglomeration. The amount of grain boundary carbide precipitation was less at this temperature, as the $M_{23}C_6$-type carbide in I 5 was apparently not as stable as the composition which formed in Unitemp AF 2-1DA. After the 2100°F (1149°C) testing, the structure was not fully solutioned as was the case for Unitemp AF 2-1DA; however, extreme coarsening and agglomeration of the gamma prime particles occurred with no grain boundary carbide precipitation.

The results of the IIb microscopic evaluations conducted on oxidation samples tested at the three temperatures are illustrated in Figure 52. The structural changes experienced by I 5 with increasing test temperature were almost identical to those which occurred for IIb. The only significant variation from the I 5 pattern occurred for the IIb sample tested at 2100°F (1149°C). Much more severe gamma prime agglomeration occurred in IIb. This agglomeration occurred in the area of the grain boundaries, and the particles were not continuous, but were agglomerated into individual large patches of gamma prime. Although the agglomerated gamma prime particles in the I 5 sample tested at 2100°F (1149°C) were randomly distributed throughout the matrix and along the grain boundaries,

IIb experienced larger particle agglomeration, especially along the grain boundaries. The particles within the grains were not as coarsened as were the I 5 particles within the grains.

The microstructural variations which occurred for IIIg mod with increasing oxidation test temperature are shown in Figure 53. This alloy experienced only gamma prime coarsening with increasing temperature up to 1950°F (1066°C). No grain boundary carbide precipitation was evident after testing at either 1875 or 1950°F (1024 or 1066°C). The structure after testing at 2100°F (1149°C) became fully solutioned similar to the Unitemp AF 2-1DA sample tested at 2100°F (1149°C). A significant feature evident in the IIIg mod sample after testing at 2100°F (1149°C) was the penetration of the internal oxide attack. These particles penetrated the entire sample area. A much lesser degree of internal oxidation occurred for the IIIg mod sample tested at 1950°F (1066°C).

3) Examination of Oxide Scales

Samples representing each of the four Task II alloys were subjected to an electron beam microprobe examination after 1000 hour cyclic oxidation testing at 1950°F (1066°C). The samples were evaluated by X-ray and specimen current image photography. The oxidation mechanisms for each of the alloys were found to be very similar. An example of a typical series of X-ray photographs is shown in Figure 54 for Unitemp AF 2-1DA. Also included is an optical micrograph of the area examined. The X-ray photographs were taken at 400X and the optical micrograph at 500X. For the Unitemp AF 2-1DA sample, the surface oxide was broken down into two separate layers. The layer nearest the metal surface was very rich in aluminum and also contained a greater concentration of titanium than was present in the sample matrix. In addition, a moderate concentration of cobalt was present. Although slight traces of other elements were present in this layer to a minor extent, the layer was significantly depleted in chromium and nickel. The second, or outermost oxide layer was predominantly a chromium-rich oxide. This oxide also contained a significant concentration of nickel.

As previously mentioned, the results of the studies conducted on the other three samples were very similar, with the exception of a few minor variations. Due to the higher percentages of tantalum present in I 5, IIb, and IIIg mod, this element had more influence in the oxide layers of these alloys than it did for Unitemp AF 2-1DA. For example, a moderate amount of tantalum was present in the outermost scaled layers of these three alloys. Also, although the Unitemp AF 2-1DA exhibited no signs of internal oxidation, IIIg mod experienced some attack directly beneath the outer oxide layers along the surface of the sample. A few small areas along the surface of the I 5 and IIb samples also experienced some internal attack. In all cases, the internal oxide particles were found to have a composition similar to the aluminum-rich oxide layer found at the metal-oxide interface in each of the samples.

Also of interest were the white particles in the matrix in the sample current image photograph of Figure 54. These particles are MC-type carbides which contain primarily titanium and tantalum. The scans for IIb indicated the additional presence of hafnium and vanadium in the carbides.

6. Sulfidation Testing

The results of the sulfidation tests conducted at 1600 and 1800°F (871 and 982°C) for each of the Task II alloys are shown in Table 34. The sulfidation rate was calculated in inches penetration per year. In general, the sulfidation rate for each of the alloys at 1800°F (982°C) was higher than for 1600°F (871°C) testing except for IIIg mod. The variation in the IIIg mod tests is believed to be due to an unsatisfactory descaling operation for the sample tested at 1800°F (982°C). The alloy most severely attacked was Unitemp AF 2-1DA, and a microscopic examination revealed that Unitemp AF 2-1DA was the only alloy susceptible to preferential grain boundary attack. This attack is illustrated in Figure 55. I 5 and IIIg mod also experienced rather heavy attack, while the best resistance to sulfidation was exhibited by IIb.

Samples of each alloy tested at 1800°F (982°C) were examined by electron beam microprobe techniques. These studies were not successful in identifying the mechanism of attack for any of the samples. The reason for this problem was the heavy amounts of sodium sulfate which tightly adhered to the samples. The presence of this compound made the studies very difficult to interpret, in that the actual attack near the metal's surface was disguised.

7. Thermal Cycling Fatigue Testing

The thermal cycling fatigue tests were discontinued after approximately 70,000 cycles from room temperature to 1800°F (982°C). None of the samples experienced macrocracking, and due to a time limitation, the testing was discontinued. The specimens were sectioned and examined by optical microscopy; no evidence of microcracking was seen.

## V. SUMMARY OF RESULTS

The object of this program was to determine the feasibility of melting and processing a series of six highly alloyed nickel base alloys to bar stock, and to determine the potential of these alloys for use in advanced gas turbine engines by evaluating the properties of the resultant wrought product. The program was conducted in two tasks, and the alloys evaluated were I 5, IIb, IIIg mod, IId, IIIg, and Unitemp AF 2-1DA. Task I involved an evaluation of fabricability via actual and simulated hot workability testing. Task II involved a detailed study of selected compositions which included mechanical property tests, oxidation tests, phase stability evaluations and structural analyses. The results can be summarized as follows:

1. Based on actual hot working studies, four of the alloys were found to be workable to bar product by extrusion and/or hot rolling. These alloys included I 5, IIb, IIIg mod, and Unitemp AF 2-1DA. Reliable hot working parameters for single and double extruded material were obtained by Gleeble testing. None of the alloys were successfully processed by hammer forging operations.

2. The general structure of the alloys consisted mainly of MC-type carbides and undissolved gamma prime in the as-cast condition. After full heat treatment, the MC-type carbides dissolved resulting in the precipitation of $M_6C$-and/or $M_{23}C_6$-type grain boundary carbides surrounded by a gamma prime precipitate.

3. The best tensile and rupture strengths over the temperature range investigated were exhibited by IIb. Tensile strengths for Unitemp AF 2-1DA and IIIg mod were second to those exhibited by IIb, and ranged from an average of 10,000 to 15,000 psi (60 to 103 $N/mm^2$) lower than those exhibited by IIb. The rupture strength of Unitemp AF 2-1DA was only slightly less than that exhibited by IIb, while IIIg mod displayed much lower rupture properties. I 5 exhibited low tensile and rupture strengths.

4. The best overall tensile and rupture ductility was exhibited by Unitemp AF 2-1DA over the temperature range investigated. IIb exhibited low ductility, especially near 1800°F (982°C), and I 5 and IIIg mod experienced a decrease in ductility with increasing test temperature.

5. The effect of the optimum heat treatments on structure and resultant properties varied depending upon the method of processing. Different structures and properties resulted from processing the material by double extrusion, single extrusion,

and/or hot rolling. In general, the target average grain size of ASTM 4 to 5 was achieved in all of the alloys through solution treatments; however, randomly dispersed grains from ASTM 2 to ASTM 7 were also present.

6. IIb experienced phase instability after long time thermal exposures when a needle-like $M_7M_6$-type mu phase was formed. However, heavy precipitation of $M_{23}C_6$-type grain boundary carbides after exposure at 1700°F (925°C) resulted in low rupture strengths and brittle failures in all of the alloys.

7. Of the four alloys evaluated, I 5 exhibited the best resistance to oxidation. All of the alloys were attacked to some degree during oxidation, especially the IIb sample tested at 2100°F (1149°C), which experienced very severe attack.

8. The best resistance to sulfidation was displayed by IIb. Sulfidation attack was particularly severe on Unitemp AF 2-1DA, which experienced grain boundary attack.

## VI. CONCLUDING REMARKS

The high strength properties exhibited by IIb indicate that this alloy has a potential for use in advanced gas turbine engines. However, the alloy lacks sufficient ductility near 1800°F (982°C), has poor oxidation characteristics and displays phase instability after 1500 hours exposure between 1500 and 1700°F (816 and 927°C). Improvements must be effected for these deficiencies by methods which will not decrease the strength capabilities of the alloy. It is therefore recommended that chemistry modifications of the IIb composition be investigated to eliminate the deficiencies of the alloy in addition to thermomechanical processing techniques to maintain or improve current strength levels.

## REFERENCES


1. Collins, H. E., "Development of High Temperature Nickel Base Alloys for Jet Engine Turbine Bucket Applications", Summary Report issued under NASA Contract NAS 3-7276, June 20, 1967.

2. Rizzo, F. J., and Lherbier, L. W., "Research Directed Towards the Development of a Wrought Superalloy", Technical Report AFML-TR-66-364, November, 1966.

3. Rizzo, F. J., Black, H. L., and Lherbier, L. W., "Development of a Wrought Nickel Base Superalloy for Turbine Wheel/Bucket Applications", Technical Report AFML-TR-69-25, February, 1969.

4. Collins, H. E., "Research on Microstructural Instability of Nickel Base Superalloys", Technical Report AFML-TR-68-256, October, 1968.

5. Radavich, J. F., Micro-Met Laboratories. Private Communication, February, 1970.

TABLE 1

Chemical Analyses of Fifty Pound Heats

| Alloy Designation | Heat Number | Chemical Analyses (Weight Percent) For: | | | | | | | | | | | | | | |
|---|---|---|---|---|---|---|---|---|---|---|---|---|---|---|---|---|
| | | C | Cr | Co | Mo | W | Ta | Al | Ti | B | Zr | Cb | V | Hf | Re | Ni |
| Unitemp | Aim | 0.35 | 12.00 | 10.00 | 3.00 | 6.00 | 1.50 | 4.60 | 3.00 | 0.015 | 0.100 | -- | -- | -- | -- | Bal |
| AF 2-1DA | KC1635 | 0.33 | 12.19 | 10.00 | 2.96 | 5.98 | 1.46 | 4.64 | 3.00 | 0.020 | 0.099 | -- | -- | -- | -- | Bal |
| I 5 | Aim | 0.13 | 10.00 | 10.00 | 1.00 | 5.50 | 4.50 | 6.30 | 1.00 | 0.020 | 0.030 | -- | -- | -- | -- | Bal |
| | KC1643 | 0.11 | 10.10 | 10.14 | 0.76 | 5.70 | 4.20 | 6.50 | 1.00 | 0.020 | 0.020 | -- | -- | -- | -- | Bal |
| II b | Aim | 0.13 | 10.00 | 10.00 | 2.00 | 5.50 | 8.00 | 4.50 | 1.00 | 0.020 | 0.030 | -- | 1.00 | 1.00 | -- | Bal |
| | KC1637 | 0.11 | 9.95 | 9.90 | 1.85 | 5.60 | 7.93 | 4.44 | 0.93 | 0.020 | 0.030 | -- | 0.99 | 0.95 | -- | Bal |
| III g mod | Aim | 0.13 | 10.00 | 10.00 | 2.00 | 5.50 | 8.00 | 4.50 | 1.00 | 0.020 | 0.030 | -- | -- | -- | -- | Bal |
| | KC1631 | 0.10 | 9.65 | 10.00 | 1.80 | 5.43 | 7.60 | 4.45 | 0.88 | 0.020 | 0.023 | -- | -- | -- | -- | Bal |
| II d | Aim | 0.13 | 10.00 | 10.00 | 2.00 | 5.50 | 8.00 | 4.50 | 1.00 | 0.020 | 0.030 | 1.00 | -- | 1.00 | -- | Bal |
| | KC1639 | 0.10 | 9.85 | 10.05 | 1.85 | 5.65 | 8.02 | 4.48 | 0.93 | 0.020 | 0.035 | 0.95 | -- | 1.00 | -- | Bal |
| III g | Aim | 0.13 | 10.00 | 10.00 | 2.00 | 5.50 | 8.00 | 4.50 | 1.00 | 0.020 | 0.030 | -- | -- | -- | 4.00 | Bal |
| | KC1641 | 0.13 | 9.75 | 9.91 | 1.80 | 5.90 | 7.87 | 4.57 | 0.90 | 0.020 | 0.022 | -- | -- | -- | 3.98 | Bal |

TABLE 2

Chemical Analyses of One Hundred Pound Heats

| Alloy Designation | Heat Number | Chemical Analyses (Weight Percent) For: | | | | | | | | | | | | | | |
|---|---|---|---|---|---|---|---|---|---|---|---|---|---|---|---|---|
| | | C | Cr | Co | Mo | W | Ta | Al | Ti | B | Zr | Cb | V | Hf | Re | Ni |
| Unitemp AF 2-1DA | Aim | 0.35 | 12.00 | 10.00 | 3.00 | 6.00 | 1.50 | 4.60 | 3.00 | 0.015 | 0.100 | -- | -- | -- | -- | Bal |
| | KC1646 | 0.36 | 12.50 | 9.95 | 2.94 | 6.05 | 1.53 | 4.58 | 3.01 | 0.020 | 0.090 | -- | -- | -- | -- | Bal |
| I 5 | Aim | 0.13 | 10.00 | 10.00 | 1.00 | 5.50 | 4.50 | 6.30 | 1.00 | 0.020 | 0.030 | -- | -- | -- | -- | Bal |
| | KC1647 | 0.11 | 10.10 | 10.23 | 0.88 | 5.68 | 4.30 | 6.22 | 0.96 | 0.020 | 0.024 | -- | -- | -- | -- | Bal |
| II b | Aim | 0.13 | 10.00 | 10.00 | 2.00 | 5.50 | 8.00 | 4.50 | 1.00 | 0.020 | 0.030 | -- | 1.00 | 1.00 | -- | Bal |
| | KC1658 | 0.13 | 9.71 | 10.05 | 1.80 | 5.78 | 8.26 | 4.62 | 0.90 | 0.020 | 0.038 | -- | 0.99 | 1.03 | -- | Bal |
| III g mod | Aim | 0.13 | 10.00 | 10.00 | 2.00 | 5.50 | 8.00 | 4.50 | 1.00 | 0.020 | 0.030 | -- | -- | -- | -- | Bal |
| | KC1659 | 0.13 | 9.53 | 10.10 | 1.86 | 5.72 | 8.01 | 4.48 | 0.95 | 0.020 | 0.010 | -- | -- | -- | -- | Bal |
| II d | Aim | 0.13 | 10.00 | 10.00 | 2.00 | 5.50 | 8.00 | 4.50 | 1.00 | 0.020 | 0.030 | 1.00 | -- | 1.00 | -- | Bal |
| | KC1651 | 0.12 | 10.08 | 10.07 | 1.84 | 5.60 | 7.96 | 4.63 | 0.99 | 0.020 | 0.041 | 0.95 | -- | 1.02 | -- | Bal |
| III g | Aim | 0.13 | 10.00 | 10.00 | 2.00 | 5.50 | 8.00 | 4.50 | 1.00 | 0.020 | 0.030 | -- | -- | -- | 4.00 | Bal |
| | KC1650 | 0.10 | 9.70 | 9.99 | 1.79 | 5.77 | 7.79 | 4.54 | 0.93 | 0.020 | 0.024 | -- | -- | -- | 4.19 | Bal |

TABLE 3

Gleeble Hot Ductility Results For As-Cast Unitemp AF 2-1DA

INHERENT DUCTILITY PROFILE

| Test Temperature (°F) | Test Temperature (°C) | Ultimate Strength (psi) | Ultimate Strength ($N/mm^2$) | Reduction of Area (%) |
|---|---|---|---|---|
| 2050 | 1121 | 50,200 | 346 | 6.2 |
| 2025 | 1107 | 62,500 | 431 | 8.2 |
| 2000 | 1093 | 56,300 | 388 | 3.9 |
| 2000 | 1093 | 52,000 | 359 | 4.5 |
| 1975 | 1080 | 74,000 | 510 | 9.1 |
| 1950 | 1066 | 83,000 | 572 | 12.7 |
| 1900 | 1038 | -- | - | -- |
| 1900 | 1038 | 90,000 | 621 | 14.5 |

Conditions: Heat to indicated test temperature, hold five minutes and test at a nominal strain rate of 5"/"/seconds$^{-1}$.

HOT WORK SIMULATION PROFILE

| Preheat Temperature (°F) | Preheat Temperature (°C) | Test Temperature (°F) | Test Temperature (°C) | Nominal Strain Rate (seconds$^{-1}$) | Ultimate Strength (psi) | Ultimate Strength ($N/mm^2$) | Reduction of Area (%) |
|---|---|---|---|---|---|---|---|
| 2075 | 1135 | 2000 | 1093 | 5 | 64,400 | 445 | 7.8 |
| 2050 | 1121 | 2000 | 1093 | 5 | 66,300 | 457 | 9.5 |
| 2050 | 1121 | 1950 | 1066 | 5 | 77,500 | 534 | 12.9 |
| 2050 | 1121 | 1900 | 1038 | 5 | 92,000 | 634 | 11.7 |
| 2075* | 1135 | 2000 | 1093 | 20 | 48,100 | 332 | 4.0 |
| 2050* | 1121 | 2000 | 1093 | 20 | 65,700 | 453 | 2.4 |
| 2050* | 1121 | 1950 | 1066 | 20 | 29,600 | 204 | 2.4 |
| 2050* | 1121 | 1900 | 1038 | 20 | 81,500 | 562 | 8.6 |

Conditions: Heat to preheat temperature, hold five minutes, cool to test temperature and test at indicated nominal strain rate.

* Homogenized at 2250°F (1232°C) for 20 hours.

TABLE 4

Gleeble Hot Ductility Results For As-Cast I 5

INHERENT DUCTILITY PROFILE

| Test Temperature (°F) | Test Temperature (°C) | Ultimate Strength (psi) | Ultimate Strength ($N/mm^2$) | Reduction of Area (%) |
|---|---|---|---|---|
| 2050 | 1121 | 58,200 | 401 | 4.0 |
| 2000 | 1093 | 73,000 | 503 | 5.5 |
| 1975 | 1080 | 74,000 | 510 | 3.1 |
| 1950 | 1066 | 83,000 | 572 | 3.9 |
| 1950 | 1066 | 75,500 | 521 | 3.5 |
| 1900 | 1038 | 93,700 | 646 | 5.5 |
| 1350 | 1010 | 90,000 | 621 | 7.3 |
| 1850 | 1010 | 103,000 | 710 | 3.5 |

Conditions: Heat to indicated test temperature, hold five minutes and test at a nominal strain rate of 5 seconds $^{-1}$.

HOT WORK SIMULATION PROFILE

| Preheat Temperature (°F) | Preheat Temperature (°C) | Test Temperature (°F) | Test Temperature (°C) | Nominal Strain Rate (seconds$^{-1}$) | Ultimate Strength (psi) | Ultimate Strength ($N/mm^2$) | Reduction of Area (%) |
|---|---|---|---|---|---|---|---|
| 2050 | 1121 | 2000 | 1093 | 5 | 73,200 | 505 | 7.6 |
| 2000 | 1093 | 1950 | 1066 | 5 | 87,000 | 600 | 9.7 |
| 2000 | 1093 | 1900 | 1038 | 5 | 91,000 | 627 | 8.5 |
| 2000 | 1093 | 1850 | 1010 | 5 | 91,500 | 631 | 5.3 |
| 2050* | 1121 | 2000 | 1093 | 20 | 45,000 | 310 | 5.0 |
| 2000* | 1093 | 1950 | 1066 | 20 | 78,000 | 538 | 6.9 |
| 2000* | 1093 | 1900 | 1038 | 20 | 89,500 | 617 | 3.2 |
| 2000* | 1093 | 1850 | 1010 | 20 | 88,000 | 607 | 2.7 |

Conditions: Heat to preheat temperature, hold five minutes, cool to test temperature and test at indicated nominal strain rate.

*Homogenized at 2250°F (1232°C) for 20 hours.

TABLE 5

Gleeble Hot Ductility Results For As-Cast IIb

INHERENT DUCTILITY PROFILE

| Test Temperature (°F) | Test Temperature (°C) | Ultimate Strength (psi) | Ultimate Strength ($N/mm^2$) | Reduction of Area (%) |
|---|---|---|---|---|
| 2050 | 1121 | 72,200 | 498 | 11.5 |
| 2000 | 1093 | 82,000 | 565 | 15.4 |
| 1950 | 1066 | 89,000 | 614 | 15.6 |
| 1925 | 1052 | 91,500 | 631 | 13.3 |
| 1925 | 1052 | 90,500 | 624 | 16.3 |
| 1900 | 1038 | 93,500 | 645 | 19.7 |
| 1875 | 1024 | 94,000 | 648 | 15.4 |
| 1850 | 1010 | 115,000 | 793 | 14.9 |

Conditions: Heat to indicated test temperature, hold five minutes and test at a nominal strain rate of 5"/"/$seconds^{-1}$.

HOT WORK SIMULATION PROFILE

| Preheat Temperature (°F) | Preheat Temperature (°C) | Test Temperature (°F) | Test Temperature (°C) | Nominal Strain Rate ($seconds^{-1}$) | Ultimate Strength (psi) | Ultimate Strength ($N/mm^2$) | Reduction of Area (%) |
|---|---|---|---|---|---|---|---|
| 2050 | 1121 | 2000 | 1093 | 5 | 73,800 | 509 | 8.4 |
| 2000 | 1093 | 1950 | 1066 | 5 | 87,000 | 600 | 18.1 |
| 2000 | 1093 | 1900 | 1038 | 5 | 91,300 | 630 | 17.2 |
| 2000 | 1093 | 1850 | 1010 | 5 | 93,500 | 645 | 14.4 |
| 2050* | 1121 | 2000 | 1093 | 20 | 57,800 | 399 | 4.3 |
| 2000* | 1093 | 1950 | 1066 | 20 | 83,500 | 576 | 5.1 |
| 2000* | 1093 | 1900 | 1038 | 20 | 98,000 | 676 | 14.5 |
| 2000* | 1093 | 1850 | 1010 | 20 | 99,800 | 688 | 7.0 |

Conditions: Heat to preheat temperature, hold five minutes, cool to test temperature and test at indicated nominal strain rate.

*Homogenized at 2250°F (1232°C) for 20 hours.

TABLE 6

Gleeble Hot Ductility Results For As-Cast III g mod

INHERENT DUCTILITY PROFILE

| Test Temperature (°F) | Test Temperature (°C) | Ultimate Strength (psi) | Ultimate Strength ($N/mm^2$) | Reduction of Area (%) |
|---|---|---|---|---|
| 2050 | 1121 | 67,000 | 462 | 6.5 |
| 2000 | 1093 | 83,000 | 572 | 9.2 |
| 1975 | 1080 | 88,000 | 607 | 9.6 |
| 1950 | 1066 | 91,000 | 627 | 8.4 |
| 1950 | 1066 | -- | - | - |
| 1925 | 1052 | 101,500 | 700 | 7.9 |
| 1900 | 1038 | 93,000 | 641 | 8.7 |
| 1850 | 1010 | 91,700 | 632 | 13.0 |

Conditions: Heat to indicated test temperature, hold five minutes and test at a nominal strain rate of 5 $seconds^{-1}$.

HOT WORK SIMULATION PROFILE

| Preheat Temperature (°F) | Preheat Temperature (°C) | Test Temperature (°F) | Test Temperature (°C) | Nominal Strain Rate ($seconds^{-1}$) | Ultimate Strength (psi) | Ultimate Strength ($N/mm^2$) | Reduction of Area (%) |
|---|---|---|---|---|---|---|---|
| 2050 | 1121 | 2000 | 1093 | 5 | 78,800 | 543 | 13.1 |
| 2000 | 1093 | 1950 | 1066 | 5 | 87,700 | 605 | 16.9 |
| 2000 | 1093 | 1900 | 1038 | 5 | 86,500 | 596 | 12.0 |
| 2000 | 1093 | 1850 | 1010 | 5 | 97,000 | 669 | 10.8 |
| 2050* | 1121 | 2000 | 1093 | 20 | 63,700 | 439 | 5.4 |
| 2000* | 1093 | 1950 | 1066 | 20 | 43,200 | 298 | 4.9 |
| 2000* | 1093 | 1900 | 1038 | 20 | 40,200 | 277 | 3.7 |
| 2000* | 1093 | 1850 | 1010 | 20 | 73,000 | 503 | 3.4 |

Conditions: Heat to preheat temperature, hold five minutes, cool to test temperature and test at indicated nominal strain rate.

*Homogenized at 2250°F (1232°C) for 20 hours.

TABLE 7

Gleeble Hot Ductility Results For As-Cast II d

INHERENT DUCTILITY PROFILE

| Test Temperature (°F) | Test Temperature (°C) | Ultimate Strength (psi) | Ultimate Strength ($N/mm^2$) | Reduction of Area (%) |
|---|---|---|---|---|
| 2075 | 1135 | 50,500 | 348 | 4.8 |
| 2050 | 1121 | 49,700 | 343 | 5.7 |
| 2025 | 1107 | 64,700 | 446 | 5.2 |
| 2000 | 1093 | 72,200 | 498 | 8.2 |
| 1975 | 1080 | 53,000 | 365 | 3.4 |
| 1975 | 1080 | 85,300 | 588 | 11.5 |
| 1950 | 1066 | 91,000 | 627 | 11.7 |
| 1900 | 1038 | 92,800 | 640 | 10.1 |

Conditions: Heat to indicated test temperature, hold five minutes and test at nominal strain rate of 5 $seconds^{-1}$.

HOT WORK SIMULATION PROFILES

| Preheat Temperature (°F) | Preheat Temperature (°C) | Test Temperature (°F) | Test Temperature (°C) | Nominal Strain Rate ($seconds^{-1}$) | Ultimate Strength (psi) | Ultimate Strength ($N/mm^2$) | Reduction of Area (%) |
|---|---|---|---|---|---|---|---|
| 2050 | 1121 | 2000 | 1093 | 5 | 68,500 | 472 | 4.5 |
| 2000 | 1093 | 1950 | 1066 | 5 | 85,000 | 586 | 8.5 |
| 2000 | 1093 | 1900 | 1038 | 5 | 89,000 | 614 | 7.8 |
| 2000 | 1093 | 1850 | 1010 | 5 | 95,000 | 655 | 9.3 |
| 2050* | 1121 | 2000 | 1093 | 20 | 40,000 | 276 | 2.4 |
| 2000* | 1093 | 1950 | 1066 | 20 | 39,000 | 269 | 2.2 |
| 2000* | 1093 | 1900 | 1038 | 20 | 56,000 | 386 | 2.7 |
| 2000* | 1093 | 1850 | 1010 | 20 | 74,500 | 514 | 3.1 |

Conditions: Heat to preheat temperature, hold five minutes, cool to test temperature and test at indicated nominal strain rate.

*Homogenized at 2250°F (1232°C) for 20 hours.

TABLE 8

Gleeble Hot Ductility Results For As-Cast III g

INHERENT DUCTILITY PROFILE

| Test Temperature (°F) | Test Temperature (°C) | Ultimate Strength (psi) | Ultimate Strength ($N/mm^2$) | Reduction of Area (%) |
|---|---|---|---|---|
| 2150 | 1177 | 24,200 | 167 | 0 |
| 2100 | 1149 | 61,500 | 424 | 4.9 |
| 2075 | 1135 | 60,700 | 419 | 6.3 |
| 2050 | 1121 | 77,800 | 536 | 10.5 |
| 2025 | 1107 | 79,500 | 548 | 6.5 |
| 2000 | 1093 | 75,800 | 523 | 5.8 |
| 1950 | 1066 | 89,000 | 614 | 8.4 |
| 1900 | 1038 | 118,000 | 814 | 7.6 |

Conditions: Heat to indicated test temperature, hold five minutes and test at a nominal strain rate of 5 $seconds^{-1}$.

HOT WORK SIMULATION PROFILE

| Preheat Temperature (°F) | Preheat Temperature (°C) | Test Temperature (°F) | Test Temperature (°C) | Nominal Strain Rate ($seconds^{-1}$) | Ultimate Strength (psi) | Ultimate Strength ($N/mm^2$) | Reduction of Area (%) |
|---|---|---|---|---|---|---|---|
| 2075 | 1135 | 2000 | 1093 | 5 | 84,500 | 583 | 9.3 |
| 2050 | 1121 | 2000 | 1093 | 5 | 71,400 | 492 | 6.0 |
| 2050 | 1121 | 1950 | 1066 | 5 | 82,800 | 571 | 7.8 |
| 2050 | 1121 | 1900 | 1038 | 5 | 94,000 | 648 | 10.1 |
| 2075* | 1135 | 2000 | 1093 | 20 | 42,700 | 294 | 4.0 |
| 2050* | 1121 | 2000 | 1093 | 20 | 39,000 | 269 | 4.5 |
| 2050* | 1121 | 1950 | 1066 | 20 | 60,500 | 417 | 6.2 |
| 2050* | 1121 | 1900 | 1038 | 20 | 69,300 | 478 | 9.8 |

Conditions: Heat to preheat temperature, hold five minutes, cool to test temperature and test at indicated nominal strain rate.

*Homogenized at 2250°F (1232°C) for 20 hours.

TABLE 9

Gleeble Inherent Ductility Profiles For Single and Double Extruded Unitemp AF2-1DA

| Material Condition | Test Temperature (°F) | (°C) | Ultimate Strength (psi) | ($N/mm^2$) | Reduction of Area (%) |
|---|---|---|---|---|---|
| Single Extruded | 2150 | 1177 | 16,800 | | 0.0 |
| Single Extruded | 2100 | 1149 | 52,000 | | 29.8 |
| Single Extruded | 2050 | 1121 | 60,200 | | 14.0 |
| Single Extruded | 2000 | 1093 | 72,500 | | 13.2 |
| Single Extruded | 1950 | 1066 | 94,500 | | 11.3 |
| Single Extruded | 1900 | 1038 | 103,000 | | 6.6 |
| Double Extruded | 2150 | 1177 | 43,300 | | 7.0 |
| Double Extruded | 2125 | 1163 | 46,200 | | 42.2 |
| Double Extruded | 2100 | 1149 | 41,500 | | 39.0 |
| Double Extruded | 2050 | 1121 | 58,300 | | 42.0 |
| Double Extruded | 2000 | 1093 | 73,200 | | 39.0 |
| Double Extruded | 1950 | 1066 | 85,500 | | 30.4 |

Condition: Heat to indicated test temperature, hold five minutes and test at a nominal strain rate of 20 $seconds^{-1}$.

TABLE 10

Gleeble Inherent Ductility Profiles For Single and Double Extruded I 5

| Material Condition | Test Temperature (°F) | Test Temperature (°C) | Ultimate Strength (psi) | Ultimate Strength ($N/mm^2$) | Reduction of Area (%) |
|---|---|---|---|---|---|
| Single Extruded | 2250 | 1232 | 18,200 | 125 | 0.0 |
| Single Extruded | 2200 | 1204 | 40,800 | 281 | 51.5 |
| Single Extruded | 2150 | 1177 | 44,300 | 305 | 63.5 |
| Single Extruded | 2100 | 1149 | 45,500 | 314 | 18.5 |
| Single Extruded | 2050 | 1121 | 51,000 | 352 | 14.0 |
| Single Extruded | 1950 | 1066 | 87,400 | 603 | 28.0 |
| Double Extruded | 2200 | 1204 | 16,400 | 113 | 0.0 |
| Double Extruded | 2150 | 1177 | 44,500 | 307 | 57.2 |
| Double Extruded | 2100 | 1149 | 42,000 | 290 | 55.0 |
| Double Extruded | 2050 | 1121 | 44,500 | 307 | 57.2 |
| Double Extruded | 1950 | 1066 | 80,500 | 555 | 54.0 |
| Double Extruded | 1900 | 1038 | 74,500 | 514 | 60.0 |
| Double Extruded | 1850 | 1010 | 105,000 | 724 | 27.2 |

Condition: Heat to indicated test temperature, hold five minutes and test at a nominal strain rate of 20 $seconds^{-1}$.

TABLE 11

Gleeble Inherent Ductility Profiles For Single and Double Extruded IIb

| Material Condition | Test Temperature (°F) | Test Temperature (°C) | Ultimate Strength (psi) | Ultimate Strength ($N/mm^2$) | Reduction of Area (%) |
|---|---|---|---|---|---|
| Single Extruded | 2150 | 1177 | 26,100 | 180 | 0.0 |
| Single Extruded | 2100 | 1149 | 52,200 | 360 | 23.5 |
| Single Extruded | 2050 | 1121 | 60,800 | 419 | 8.7 |
| Single Extruded | 2050 | 1121 | 84,300 | 581 | 10.5 |
| Single Extruded | 2000 | 1093 | 69,800 | 481 | 30.8 |
| Single Extruded | 1900 | 1038 | 100,500 | 693 | 14.0 |
| Double Extruded | 2200 | 1204 | 14,100 | 97 | 0.0 |
| Double Extruded | 2150 | 1177 | 48,500 | 334 | 19.2 |
| Double Extruded | 2100 | 1149 | 44,500 | 307 | 4.0 |
| Double Extruded | 2100 | 1149 | 50,700 | 350 | 26.3 |
| Double Extruded | 2050 | 1121 | 67,200 | 463 | 30.9 |
| Double Extruded | 2000 | 1093 | 77,000 | 531 | 27.0 |
| Double Extruded | 1950 | 1066 | 89,200 | 615 | 21.2 |
| Double Extruded | 1850 | 1010 | 112,000 | 772 | 17.6 |

Condition: Heat to indicated test temperature, hold five minutes and test at a nominal strain rate of 20 $seconds^{-1}$.

TABLE 12

Gleeble Inherent Ductility Profiles For Single and Double Extruded III g mod

| Material Condition | Test Temperature (°F) | Test Temperature (°C) | Ultimate Strength (psi) | Ultimate Strength ($N/mm^2$) | Reduction of Area (%) |
|---|---|---|---|---|---|
| Single Extruded | 2200 | 1204 | 37,200 | 256 | 5.8 |
| Single Extruded | 2200 | 1204 | 33,700 | 232 | 7.8 |
| Single Extruded | 2150 | 1177 | 48,800 | 336 | 33.4 |
| Single Extruded | 2100 | 1149 | 59,500 | 410 | 27.4 |
| Single Extruded | 2050 | 1121 | 59,000 | 407 | 20.8 |
| Single Extruded | 2000 | 1093 | 77,500 | 534 | 27.9 |
| Double Extruded | 2200 | 1204 | 23,900 | 165 | 0.0 |
| Double Extruded | 2150 | 1177 | 47,300 | 326 | 8.3 |
| Double Extruded | 2125 | 1163 | 54,200 | 374 | 28.6 |
| Double Extruded | 2100 | 1149 | 53,200 | 367 | 35.4 |
| Double Extruded | 2075 | 1135 | 64,200 | 443 | 25.6 |
| Double Extruded | 2050 | 1121 | 70,500 | 486 | 10.8 |
| Double Extruded | 1950 | 1066 | 87,000 | 600 | 8.0 |
| Double Extruded | 1850 | 1010 | 106,000 | 731 | 10.5 |

Condition: Heat to indicated test temperature, hold five minutes and test at a nominal strain rate of 20 $seconds^{-1}$.

TABLE 13

Gleeble Inherent Ductility Profile For Single Extruded II d

| Test Temperature (°F) | Test Temperature (°C) | Ultimate Strength (psi) | Ultimate Strength ($N/mm^2$) | Reduction of Area (%) |
|---|---|---|---|---|
| 2150 | 1177 | 22,200 | 153 | 0.0 |
| 2100 | 1149 | 50,800 | 350 | 7.0 |
| 2050 | 1121 | 62,000 | 427 | 12.3 |
| 2000 | 1093 | 73,000 | 503 | 17.5 |
| 1950 | 1066 | 80,000 | 552 | 28.4 |
| 1900 | 1038 | 94,000 | 648 | 13.8 |

Condition: Heat to indicated test temperature, hold five minutes and test at a nominal strain rate of 20 $seconds^{-1}$.

TABLE 14

Gleeble Inherent Ductility Profile For Single Extruded III g

| Test Temperature (°F) | (°C) | Ultimate Strength (psi) | (N/mm$^2$) | Reduction of Area (%) |
|---|---|---|---|---|
| 2200 | 1204 | 42,500 | 293 | 22.4 |
| 2150 | 1177 | 52,800 | 364 | 31.0 |
| 2100 | 1149 | 65,000 | 448 | 32.3 |
| 2050 | 1121 | 68,500 | 472 | 28.1 |
| 1950 | 1066 | 94,000 | 648 | 17.0 |

Condition: Heat to indicated test temperature, hold five minutes and test at a nominal strain rate of 20 seconds$^{-1}$.

TABLE 15

X-Ray Diffraction Studies of Residues Extracted From Specimens for Task I Structural Evaluations

| | | Phase* | | | | |
|---|---|---|---|---|---|---|
| | | MC | $\gamma'$ | HfN | $M_3B_4$ | $Ta_2N$ |
| Unitemp AF 2-1DA | As-Cast | S | W | | | |
| | Quenched from 2050°F (1121°C) | S | M | | | ?VW |
| | Extruded | S | VW | | | |
| I 5 | As-Cast | S | W | | | |
| | Quenched from 2000°F (1093°C) | S | VW | | | |
| | Extruded | S | VW | | | |
| IIb | As-Cast | S | VW | | | |
| | Quenched from 2000°F (1093°C) | S | VW | | | |
| | Extruded | S | VW | ?W | | |
| III g mod | As-Cast | S | W | | | |
| | Quenched from 2000°F (1093°C) | S | W | | | |
| | Extruded | S | S | | ?VW | |
| IId | As-Cast | S | VW | | | |
| | Quenched from 2000°F (1093°C) | S | VW | | | |
| | Extruded | S | M | ?M | ?VW | |
| IIIg | As-Cast | S | W | | | ?W |
| | Quenched from 2050°F (1121°C) | S | W | | | |
| | Extruded | M | S | | | |

*Residues Extracted Electrolytically in a 10% HCl Methanol Solution.
S Represents Strong; M, Medium; W, Weak; and V, Very.

TABLE 16

X-Ray Diffraction Studies of Residues Extracted from Task II Alloys After Each Stage of Heat Treatment

| Alloy Designation | Condition | Relative Concentration of Phases Present* | | |
|---|---|---|---|---|
| | | MC** | $M_6C$ | $M_{23}C_6$ |
| Unitemp AF2-1DA | 2200°F/2 hrs | S | | |
| | 2200°F/2 hrs + 1950°F/2 hrs | S | W | |
| | 2200°F/2 hrs + 1950°F/2 hrs + 1400°F/16 hrs | M | W | |
| I 5 | 2225°F/1 hr | M | | |
| | 2225°F/1 hr + 1950°F/16 hrs | M | | VW |
| | 2225°F/1 hr + 1950°F/16 hrs + 1400°F/16 hrs | M | | VW |
| IIb | 2225°F/2 hrs | S | | |
| | 2225°F/2 hrs + 1900°F/2 hrs | S | W | |
| | 2225°F/2 hrs + 1900°F/2 hrs + 1400°F/16 hrs | S | W | |
| III g mod | 2225°F/2 hrs | VS | | |
| | 2225°F/2 hrs + 1950°F/2 hrs | S | | |
| | 2225°F/2 hrs + 1950°F/2 hrs + 1400°F/16 hrs | S | | |

* S Represents Strong; M, Moderate; W, Weak; and V, Very.

** MC-type carbides displayed varying parameters, depending on the elements present. Major elements identified included titanium, tantalum and hafnium.

TABLE 16

X-Ray Diffraction Studies of Residues Extracted from Task II Alloys After Each Stage of Heat Treatment

| Alloy Designation | Condition | Relative Concentration of Phases Present* MC** | $M_6C$ | $M_{23}C_6$ |
|---|---|---|---|---|
| Unitemp | 1204°C/2 hrs | S | | |
| AF2-1DA | 1204°C/2 hrs + 1066°C/2 hrs | S | W | |
| | 1204°C/2 hrs + 1066°C/2 hrs + 760°C/16 hrs | M | W | |
| I 5 | 1219°C/1 hr | M | | |
| | 1219°C/1 hr + 1066°C/16 hrs | M | | VW |
| | 1219°C/1 hr + 1066°C/16 hrs + 760°C/16 hrs | M | | VW |
| IIb | 1219°C/2 hrs | S | | |
| | 1219°C/2 hrs + 1038°C/2 hrs | S | W | |
| | 1219°C/2 hrs + 1038°C/2 hrs + 760°C/16 hrs | S | W | |
| III g mod | 1219°C/2 hrs | VS | | |
| | 1219°C/2 hrs + 1066°C/2 hrs | S | | |
| | 1219°C/2 hrs + 1066°C/2 hrs + 760°C/16 hrs | S | | |

* S Represents Strong; M, Moderate; W, Weak; and V, Very.

** MC-type carbides displayed varying parameters, depending on the elements present. Major elements identified included titanium, tantalum and hafnium.

TABLE 17

Tensile Properties of Unitemp AF 2-1DA

| Temperature (°F) | Temperature (°C) | Ultimate Tensile Strength (psi) | Ultimate Tensile Strength ($N/mm^2$) | Yield Strength (psi) | Yield Strength ($N/mm^2$) | Elongation (%) | Reduction of Area (%) |
|---|---|---|---|---|---|---|---|
| Room | Room | 193,900 | 1337 | 152,300 | 1050 | 12.4 | 12.6 |
| | | 183,700 | 1267 | 152,700 | 1052 | 6.3 | 7.9 |
| 1000 | 538 | 193,600 | 1334 | 155,900 | 1075 | 13.2 | 16.0 |
| | | 195,200 | 1345 | 159,400 | 1099 | 14.0 | 18.0 |
| 1200 | 649 | 199,400 | 1375 | 159,300 | 1098 | 14.5 | 14.4 |
| | | 195,700 | 1349 | 152,000 | 1048 | 12.4 | 17.0 |
| 1400 | 760 | 166,200 | 1146 | 144,200 | 994 | 10.3 | 17.0 |
| | | 168,600 | 1162 | 146,800 | 1012 | 6.9 | 14.1 |
| 1600 | 871 | 118,200 | 815 | 102,900 | 709 | 7.4 | 16.7 |
| | | 122,200 | 843 | 102,900 | 709 | 9.6 | 14.8 |
| 1800 | 982 | 65,200 | 450 | 47,500 | 328 | 13.6 | 17.7 |
| | | 66,300 | 457 | 48,100 | 332 | 13.2 | 18.9 |

Heat Treatment: 2200°F/2 hours/RAC + 1950°F/2 hours/RAC + 1400°F/16 hours/AC
1204°C/2 hours/RAC + 1066°C/2 hours/RAC + 760°C/16 hours/AC

TABLE 18

Tensile Properties of I 5

| Temperature (°F) | Temperature (°C) | Ultimate Tensile Strength (psi) | Ultimate Tensile Strength ($N/mm^2$) | Yield Strength (psi) | Yield Strength ($N/mm^2$) | Elongation (%) | Reduction of Area (%) |
|---|---|---|---|---|---|---|---|
| Room | Room | 194,800 | 1343 | 139,700 | 963 | 23.0 | 24.3 |
| | | 195,800 | 1350 | 138,400 | 954 | 22.1 | 25.5 |
| 1000 | 538 | 180,000 | 1241 | 134,800 | 929 | 19.7 | 24.2 |
| | | 177,200 | 1222 | 131,400 | 906 | 21.6 | 24.0 |
| 1200 | 649 | 175,500 | 1210 | 138,500 | 955 | 15.8 | 20.4 |
| | | 170,000 | 1172 | 133,100 | 918 | 12.5 | 17.1 |
| 1400 | 760 | 141,900 | 978 | 124,400 | 858 | 3.0 | 8.9 |
| | | 149,200 | 1029 | 124,900 | 861 | 4.6 | 12.6 |
| 1600 | 871 | 115,800 | 798 | 90,800 | 626 | 4.0 | 10.3 |
| | | 112,700 | 777 | 88,400 | 610 | 8.5 | 11.4 |
| 1800 | 982 | 55,800 | 385 | 36,800 | 254 | 7.8 | 7.1 |
| | | 52,600 | 363 | 35,300 | 243 | 7.5 | 5.7 |

Heat Treatment: 2225°F/1 hour/RAC + 1950°F/16 hours/RAC + 1400°F/16 hours/AC
1219°C/1 hour/RAC + 1066°C/16 hours/RAC + 760°C/16 hours/AC

TABLE 19

Tensile Properties of IIb

| Temperature (°F) | Temperature (°C) | Ultimate Tensile Strength (psi) | Ultimate Tensile Strength ($N/mm^2$) | Yield Strength (psi) | Yield Strength ($N/mm^2$) | Elongation (%) | Reduction of Area (%) |
|---|---|---|---|---|---|---|---|
| Room | Room | 217,700 | 1501 | 173,400 | 1196 | 11.7 | 13.1 |
| | | 215,600 | 1487 | 174,500 | 1203 | 10.8 | 11.8 |
| 1000 | 538 | 203,200 | 1401 | 177,200 | 1222 | 7.8 | 11.4 |
| | | 202,900 | 1399 | 168,100 | 1159 | 8.4 | 11.4 |
| 1200 | 649 | 208,500 | 1438 | 166,700 | 1149 | 6.9 | 11.3 |
| | | 210,900 | 1454 | 170,100 | 1173 | 7.3 | 11.7 |
| 1400 | 760 | 181,600 | 1252 | 159,500 | 1100 | 8.0 | 12.8 |
| | | 181,300 | 1250 | 160,900 | 1109 | 6.8 | 11.4 |
| 1600 | 871 | 133,500 | 920 | 109,400 | 754 | 5.3 | 7.1 |
| | | 132,700 | 915 | 110,800 | 764 | 5.4 | 8.3 |
| 1800 | 982 | 80,900 | 558 | 60,700 | 419 | 3.7 | 4.2 |
| | | 80,100 | 552 | 61,800 | 426 | 3.6 | 2.3 |

Heat Treatment: 2225°F/2 hours/RAC + 1900°F/2 hours/RAC + 1400°F/16 hours/AC.
1219°C/2 hours/RAC + 1038°C/2 hours/RAC + 760°C/16 hours/AC.

TABLE 20

Tensile Properties of III g mod

| Temperature (°F) | Temperature (°C) | Ultimate Tensile Strength (psi) | Ultimate Tensile Strength ($N/mm^2$) | Yield Strength (psi) | Yield Strength ($N/mm^2$) | Elongation (%) | Reduction of Area (%) |
|---|---|---|---|---|---|---|---|
| Room | Room | 209,300 | 1443 | 152,000 | 1048 | 17.2 | 19.1 |
| | | 213,000 | 1469 | 158,300 | 1091 | 17.9 | 17.6 |
| 1000 | 538 | 202,000 | 1393 | 158,000 | 1089 | 13.5 | 16.9 |
| | | 209,100 | 1442 | 159,300 | 1098 | 18.1 | 20.1 |
| 1200 | 649 | 202,100 | 1394 | 158,500 | 1093 | 10.8 | 15.3 |
| | | 193,400 | 1333 | 150,700 | 1039 | 10.8 | 14.8 |
| 1400 | 760 | 166,700 | 1149 | 140,100 | 966 | 3.1 | 7.0 |
| | | 168,700 | 1163 | 150,300 | 1036 | 5.6 | 6.7 |
| 1600 | 871 | 103,400 | 713 | 98,500 | 679 | 2.0 | 1.4 |
| | | 110,100 | 759 | 106,300 | 733 | 2.0 | 4.2 |
| 1800 | 982 | 66,600 | 459 | 51,200 | 353 | 2.5 | 2.2 |
| | | 65,100 | 449 | 55,500 | 382 | 2.7 | 1.4 |

Heat Treatment: 2225°F/2 hours/RAC + 1950 °F/2 hours/RAC + 1400°F/16 hours/AC.
1219°C/2 hours/RAC + 1066°C/2 hours/RAC + 760°C/16 hours/AC.

TABLE 21

Stress Rupture Properties of Unitemp AF 2-1DA

| Temperature (°F) | Temperature (°C) | Stress (psi) | Stress ($N/mm^2$) | Rupture Life (hours) | Elongation (%) | Reduction of Area (%) |
|---|---|---|---|---|---|---|
| 1300 | 704 | 100,000 | 690 | 510.2 | 2.5 | 1.2 |
| | | | | 888.1 | 3.8 | 6.8 |
| 1400 | 760 | 85,000 | 586 | 223.0 | 4.4 | 8.5 |
| | | | | 210.7 | 4.9 | 8.5 |
| 1400 | 760 | 90,000 | 621 | 111.2 | 3.5 | 5.5 |
| | | | | 85.0 | 4.5 | 5.1 |
| | | | | 119.8 | 4.1 | 8.5 |
| 1500 | 816 | 70,000 | 483 | 85.9 | 5.5 | 12.9 |
| | | | | 82.2 | 5.9 | 9.6 |
| 1600 | 871 | 55,000 | 379 | 53.3 | 4.8 | 2.6 |
| | | | | 45.5 | 6.0 | 9.0 |
| | | | | 38.9 | 5.0 | 14.6 |
| | | | | 53.1 | 7.4 | 9.0 |
| 1750 | 954 | 30,000 | 207 | 61.8 | 10.6 | 20.6 |
| | | | | 61.0 | 10.5 | 15.5 |
| 1800 | 982 | 20,000 | 138 | 105.1 | 18.4 | 38.6 |
| | | | | 102.5 | 9.8 | 27.5 |
| 1800 | 982 | 25,000 | 172 | 53.2 | 13.4 | 25.2 |
| | | | | 40.6 | 14.8 | 26.0 |
| 1900 | 1038 | 15,000 | 103 | 27.7 | 15.3 | 24.8 |
| | | | | 24.9 | 16.3 | 34.6 |

Heat Treatment: 2200°F/2 hours/RAC + 1950°F/2 hours/RAC + 1400°F/16 hours/AC.
1204°C/2 hours/RAC + 1066°C/2 hours/RAC + 762°C/16 hours/AC.

TABLE 22

Stress Rupture Properties of I 5

| Temperature (°F) | Temperature (°C) | Stress (psi) | Stress ($N/mm^2$) | Rupture Life (hours) | Elongation (%) | Reduction of Area (%) |
|---|---|---|---|---|---|---|
| 1300 | 704 | 100,000 | 690 | 747.0 | 4.6 | 4.5 |
| | | | | 178.7 | 2.0 | --* |
| | | | | 205.0 | 1.8 | 3.1 |
| 1400 | 760 | 85,000 | 586 | 9.6** | 1.1 | 5.0 |
| | | | | 82.7 | 1.6 | --* |
| | | | | 53.0 | 1.6 | 5.3 |
| | | | | 103.2 | 2.4 | 1.8 |
| 1400 | 760 | 90,000 | 621 | 119.2 | 2.0 | 3.6 |
| | | | | 34.4 | 1.7 | 2.9 |
| | | | | 54.6 | 2.3 | 3.7 |
| 1500 | 816 | 70,000 | 483 | 43.6 | 3.5 | 4.4 |
| | | | | 41.3 | 2.6 | 3.6 |
| 1600 | 871 | 55,000 | 379 | 11.0 | 3.4 | 4.7 |
| | | | | 10.7 | 5.0 | 1.8 |
| | | | | 14.4 | 3.9 | 1.2 |
| 1750 | 954 | 30,000 | 207 | 3.9 | 4.9 | 7.6 |
| | | | | 13.2 | 4.0 | 6.5 |
| 1800 | 982 | 20,000 | 138 | 84.4 | 4.3 | 5.5 |
| | | | | 37.2 | 5.6 | 6.2 |
| | | | | 69.6 | 4.4 | 4.5 |
| 1800 | 982 | 25,000 | 172 | 9.8 | 4.9 | 5.0 |
| | | | | 5.0 | 5.1 | 4.5 |
| 1900 | 1038 | 15,000 | 103 | 7.9 | 5.0 | 8.1 |
| | | | | 9.7 | 3.7 | 3.1 |

Heat Treatment: 2225°F/1 hour/RAC + 1950°F/16 hours/RAC + 1400°F/16 hours/AC.
1219°C/1 hour/RAC + 1066°C/16 hours/RAC + 760°C/16 hours/AC.

*Specimen broke in shoulder.

**Cracked specimen.

TABLE 23

Stress Rupture Properties of IIb

| Temperature (°F) | Temperature (°C) | Stress (psi) | Stress ($N/mm^2$) | Rupture Life (hours) | Elongation (%) | Reduction of Area (%) |
|---|---|---|---|---|---|---|
| 1300 | 704 | 100,000 | 690 | 1860.8 | 2.3 | 2.8 |
| | | | | 1760.9 | 1.6 | 1.3 |
| 1400 | 760 | 85,000 | 586 | 316.0 | 1.3 | 0.5 |
| | | | | 418.4 | 1.3 | 2.4 |
| 1400 | 760 | 90,000 | 621 | 179.9 | 2.0 | 3.3 |
| | | | | 201.7 | 1.2 | 2.6 |
| 1500 | 816 | 70,000 | 483 | 66.3 | 1.2 | 0.6 |
| | | | | 74.3 | 1.7 | -- |
| 1600 | 871 | 55,000 | 379 | 61.8 | 3.2 | 0.9 |
| | | | | 67.6 | 2.9 | -- |
| 1750 | 954 | 30,000 | 207 | 65.3 | 4.0 | 4.0 |
| | | | | 87.9 | 6.5 | 3.4 |
| 1800 | 982 | 20,000 | 138 | 110.5 | 5.4 | 15.8 |
| | | | | 73.0 | 4.0 | 12.1 |
| 1800 | 982 | 25,000 | 172 | 33.0 | 2.7 | 11.7 |
| | | | | 44.9 | 5.0 | 6.2 |
| 1900 | 1038 | 15,000 | 103 | 50.1 | 5.3 | 13.2 |
| | | | | 26.2 | 6.2 | 14.0 |

Heat Treatment: 2225°F/2 hours/RAC + 1900°F/2 hours/RAC + 1400°F/16 hours/AC
1219°C/2 hours/RAC + 1038°C/2 hours/RAC + 760°C/16 hours/AC

TABLE 24

Stress Rupture Properties of III g mod

| Temperature (°F) | Temperature (°C) | Stress (psi) | Stress ($N/mm^2$) | Rupture Life (hours) | Elongation (%) | Reduction of Area (%) |
|---|---|---|---|---|---|---|
| 1300 | 704 | 100,000 | 690 | 18.5 | 0.9 | -- |
| | | | | 130.1 | 1.1 | --* |
| 1400 | 760 | 85,000 | 586 | 40.6 | 1.0 | -- |
| | | | | 30.1 | 1.5 | --* |
| 1400 | 760 | 90,000 | 621 | 18.3 | 1.5 | -- |
| | | | | 38.5 | 0.6 | -- |
| 1500 | 816 | 70,000 | 483 | 23.4 | 1.7 | --* |
| | | | | 28.6 | 1.1 | --* |
| 1600 | 871 | 55,000 | 379 | 16.1 | 1.6 | 1.3 |
| | | | | 25.6 | 1.8 | 1.5 |
| 1750 | 954 | 30,000 | 207 | 27.8 | 2.3 | 2.5 |
| | | | | 21.0 | 4.0 | 3.1 |
| 1800 | 982 | 20,000 | 138 | 74.0 | 5.8 | 5.1 |
| | | | | 69.6 | 5.0 | 3.8 |
| 1800 | 982 | 25,000 | 172 | 18.8 | 2.5 | 1.8 |
| | | | | 19.8 | 3.8 | 3.3 |
| 1900 | 1038 | 15,000 | 103 | 16.8 | 3.5 | 1.0 |
| | | | | 76.4 | 15.7 | 16.6 |

*Broke in shoulder.

Heat Treatment: 2225°F/2 hours/RAC + 1950°F/2 hours/RAC + 1400°F/16 hours/AC.
1219°C/2 hours/RAC + 1060°C/2 hours/RAC + 760°C/16 hours/AC.

TABLE 25

X-Ray Diffraction Studies of Residues Extracted From
Task II Alloys After Stress Rupture Testing at Various Conditions

| Alloy Designation | Stress Rupture Conditions (°F/psi) | (°C/N/mm$^2$) | Time in Test (hours) | Relative Concentration of Phases Present* MC** | $M_6C$ | $M_{23}C_6$ | $M_2M$ |
|---|---|---|---|---|---|---|---|
| Unitemp | 1400/90,000 | 760/621 | 111.2 | S | W | VW | ?VW |
| AF 2-1DA | 1600/55,000 | 871/379 | 53.3 | MS | W | W | ?VW |
| | 1900/15,000 | 1038/103 | 27.7 | M | M | M | ?VW |
| I 5 | 1400/90,000 | 760/621 | 119.2 | MS | | | |
| | 1600/55,000 | 871/379 | 10.7 | M | | | ?VW |
| | 1900/15,000 | 1038/103 | 7.9 | M | | | ?VW |
| IIb | 1400/90,000 | 760/621 | 201.7 | VS | W | | |
| | 1600/55,000 | 871/379 | 67.6 | S | W | M | ?VW |
| | 1900/15,000 | 1038/103 | 50.1 | MS | VS | VW | ?VW |
| IIIg mod | 1400/90,000 | 760/621 | 38.5 | VS | | | |
| | 1600/55,000 | 871/379 | 25.6 | VS | | | |
| | 1900/15,000 | 1038/103 | 76.4 | S | | | |

* S represents Strong; M, Medium; W, Weak; and V, Very.
**MC-type carbides displayed varying parameters, depending on the elements present.
Major elements identified included titanium, tantalum, and hafnium.

TABLE 26

Interrupted Low Cycle Fatigue Data for Task II Alloys

| Test Conditions | Average Cycles to Failure for: Unitemp AF 2-1DA | I 5 | IIb | III g mod |
|---|---|---|---|---|
| 1300°F / 110,000 psi<br>704°C / 758 N/mm$^2$ | 519 | 1244 | 1337 | 170 |
| 1350°F / 100,000 psi<br>732°C / 690 N/mm$^2$ | 736 | 486 | 1850 | 60 |
| 1450°F / 80,000 psi<br>788°C / 552 N/mm$^2$ | 685 | 368 | 935 | 160 |

Heat Treatments:

Unitemp AF 2-1DA - 2200°F/2hours/RAC+1950°F/2 hours/RAC+1400°F/16 hours/AC
1204°C/2hours/RAC+1066°C/2 hours/RAC+ 760°C/16 hours/AC

I 5 - 2225°F/1hour /RAC+1950°F/16hours/RAC+1400°F/16 hours/AC
1219°C/1hour /RAC+1066°C/16hours/RAC+ 760°C/16 hours/AC

IIb - 2225°F/2hours/RAC+1900°F/2 hours/RAC+1400°F/16 hours/AC
1219°C/2hours/RAC+1038°C/2 hours/RAC+ 760°C/16 hours/AC

IIIg mod - 2225°F/2hours/RAC+1950°F/2 hours/RAC+1400°F/16 hours/AC
1219°C/2hours/RAC+1066°C/2 hours/RAC+ 760°C/16 hours/AC

TABLE 27

Stress Rupture Properties for Unitemp AF 2-1DA and I 5 Rolled Material*

| Alloy Designation | Temperature (°F) | Temperature (°C) | Stress (psi) | Stress ($N/mm^2$) | Rupture Life (hours) | Elongation (%) | Reduction of Area (%) |
|---|---|---|---|---|---|---|---|
| Unitemp AF 2-1DA | 1300 | 704 | 100,000 | 690 | 522.0 | 2.6 | 2.1 |
| | 1400 | 760 | 90,000 | 621 | 41.6 | 1.3 | 1.3 |
| | 1500 | 816 | 70,000 | 483 | 107.3 | 3.6 | 7.2 |
| | 1600 | 871 | 55,000 | 379 | 44.2 | 7.7 | 11.1 |
| | 1800 | 982 | 25,000 | 172 | 40.7 | 7.2 | 14.2 |
| | 1900 | 1038 | 15,000 | 103 | 31.0 | 13.1 | 30.2 |
| I 5 | 1300 | 704 | 100,000 | 690 | 841.5 | 4.1 | 9.5 |
| | 1400 | 760 | 90,000 | 621 | 167.3 | 4.1 | 6.0 |
| | 1500 | 816 | 70,000 | 483 | 113.3 | 4.7 | 8.3 |
| | 1600 | 871 | 55,000 | 379 | 49.4 | 4.9 | 5.3 |
| | 1800 | 982 | 25,000 | 172 | 47.8 | 5.7 | 10.5 |
| | 1900 | 1038 | 15,000 | 103 | 32.1 | 3.3 | 3.1 |

Heat Treatment: Unitemp AF 2-1DA - 2200°F/2 hours/RAC + 1950°F/2 hours/RAC + 1400°F/16 hours/AC
1204°C/2 hours/RAC + 1066°C/2 hours/RAC + 760°C/16 hours/AC
2225°F/1 hour/RAC + 1950°F/16 hours/RAC + 1400°F/16 hours/AC
1219°C/1 hour/RAC + 1066°C/16 hours/RAC + 760°C/16 hours/AC

*Rolled from 3-1/8 inch (0.079 m) diameter to one inch (0.025 m) diameter.

TABLE 28

Stress Rupture Properties for Task II Alloys in the Single Extruded and Rolled Condition*

| Alloy Designation | Temperature (°F) | Temperature (°C) | Stress (psi) | Stress ($N/mm^2$) | Rupture Life (hours) | Elongation (%) | Reduction in Area (%) |
|---|---|---|---|---|---|---|---|
| Unitemp AF 2-1DA | 1300 | 704 | 100,000 | 690 | 388.6 | 3.1 | 1.4 |
| | 1400 | 760 | 90,000 | 621 | 57.1 | 3.9 | 5.5 |
| | 1500 | 816 | 70,000 | 483 | 42.1 | 3.2 | 5.2 |
| | 1600 | 871 | 55,000 | 379 | 34.4 | 7.5 | 15.1 |
| | 1800 | 982 | 25,000 | 172 | 17.2 | 14.8 | 35.2 |
| I 5 | 1300 | 704 | 100,000 | 690 | 138.2 | 1.1 | 4.2 |
| | 1400 | 760 | 90,000 | 621 | 11.4 | 2.1 | 1.9 |
| | 1500 | 816 | 70,000 | 483 | 9.4 | 4.3 | 2.1 |
| | 1600 | 871 | 55,000 | 379 | 3.6 | 7.0 | 12.0 |
| | 1800 | 982 | 25,000 | 172 | 1.4 | 16.8 | 19.5 |
| | 1900 | 1038 | 15,000 | 103 | 1.3 | 18.0 | 18.9 |
| IIb | 1300 | 704 | 100,000 | 690 | 786.1 | 0.8 | 0.5 |
| | 1400 | 760 | 90,000 | 621 | 69.7 | 1.2 | 1.5 |
| | 1500 | 816 | 70,000 | 483 | 29.1 | 0.7 | -- |
| | 1600 | 871 | 55,000 | 379 | 7.0 | 1.9 | -- |
| | 1800 | 982 | 25,000 | 172 | 15.8 | 1.9 | 4.7 |
| | 1900 | 1038 | 15,000 | 103 | 16.9 | 5.2 | 13.3 |

*Extruded from three inch diameter to one inch (0.025 m) diameter, and rolled to 0.5 inch (0.013 m) diameter.

Heat Treatment: Unitemp AF 2-1DA - 2200°F/2 hours/RAC + 1950°F/2 hours/RAC + 1400°F/16 hours/AC
1204°C/2 hours/RAC + 1066°C/2 hours/RAC + 760°C/16 hours/AC

I 5 - 2225°F/1 hour /RAC + 1950°F/16 hours/RAC + 1400°F/16 hours/AC
1219°C/1 hour /RAC + 1066°C/16 hours/RAC + 760°C/16 hours/AC

IIb - 2225°F/2 hours/RAC + 1900°F/2 hours/RAC + 1400°F/16 hours/AC
1219°C/2 hours/RAC + 1038°C/2 hours/RAC + 760°C/16 hours/AC

TABLE 29

X-Ray Diffraction Studies of Residues Extracted From Task II Thermal Stability Specimens

| Alloy Designation | Thermal Exposure (°F-Hours) | Thermal Exposure (°C-Hours) | Relative Concentration of Phases Present* MC** | $M_6C$*** | $M_{23}C_6$ | $M_7M_6$ |
|---|---|---|---|---|---|---|
| Unitemp AF 2-1DA | 1400-1500 | 760-1500 | S | M | VW | |
| | 1500-1500 | 816-1500 | MS | W | M | |
| | 1600-1500 | 871-1500 | M | W | S | |
| | 1700-1500 | 927-1500 | W | W | VS | |
| I5 | 1400-1500 | 760-1500 | VS | | VW | |
| | 1500-1500 | 816-1500 | VS | | W | |
| | 1600-1500 | 871-1500 | S | | M | |
| | 1700-1500 | 927-1500 | S | | S | |
| IIb | 1400-1500 | 760-1500 | S | W | W | |
| | 1500-1500 | 816-1500 | S | W | M | W |
| | 1600-1500 | 871-1500 | M | VS | VW | MS |
| | 1700-1500 | 927-1500 | W | M | M | S |
| III g mod | 1400-1500 | 760-1500 | VS | | | |
| | 1500-1500 | 816-1500 | VS | | W | |
| | 1600-1500 | 871-1500 | VS | VW | VW | |
| | 1700-1500 | 927-1500 | VS | M | M | VW? |

* S represents Strong; M, Medium; W, Weak; and V, Very.

** MC-type carbides displayed varying parameters, depending on the elements present. Major elements identified included titanium, tantalum, and hafnium.

***$M_6C$-type carbide parameters also varied, depending on the elements present.

TABLE 30

1400°F/90,000 psi (760°C/621 N/mm$^2$) Stress Rupture Data for Task II Stability Exposure Specimens

| Alloy Designation | Exposure After Regular Heat Treatment | Rupture Life (hours) | Elongation (%) | Reduction of Area (%) |
|---|---|---|---|---|
| Unitemp AF 2-1DA | 1400°F (760°C)/1500 hours | 99.7 | 9.0 | 11.8 |
| | 1500°F (816°C)/1500 hours | 81.1 | 6.0 | 19.9 |
| | 1600°F (871°C)/1500 hours | 124.2 | 6.1 | 9.7 |
| | 1700°F (927°C)/1500 hours | 48.4 | --* | --* |
| I 5 | 1400°F (760°C)/1500 hours | 72.8 | 6.1 | 8.4 |
| | 1500°F (816°C)/1500 hours | 67.6 | 5.2 | 8.3 |
| | 1600°F (871°C)/1500 hours | 62.5 | 3.1 | 7.5 |
| | 1700°F (927°C)/1500 hours | --** | --** | --** |
| IIb | 1400°F (760°C)/1500 hours | 261.4 | 2.0 | 3.3 |
| | 1500°F (816°C)/1500 hours | 209.9 | 6.5 | 3.7 |
| | 1600°F (871°C)/1500 hours | 89.8 | 4.2 | 3.4 |
| | 1700°F (927°C)/1500 hours | --** | --** | --** |
| III g mod | 1400°F (760°C)/1500 hours | 84.2 | 3.1 | 2.2 |
| | 1500°F (816°C)/1500 hours | 72.0 | 4.1 | 2.3 |
| | 1600°F (871°C)/1500 hours | 6.4 | 0.4 | 0.3 |
| | 1700°F (927°C)/1500 hours | 3.1* | --* | --* |

*Specimen broke at shoulder.

**Specimen broke on loading.

Heat Treatments:

Unitemp AF 2-1DA - 2200°F/2 hours/RAC + 1950°F/2 hours/RAC + 1400°F/16 hours/AC
1204°C/2 hours/RAC + 1066°C/2 hours/RAC + 760°C/16 hours/AC

I 5 - 2225°F/1 hour/RAC + 1950°F/16 hours/RAC + 1400°F/16 hours/AC
1219°C/1 hour/RAC + 1066°C/16 hours/RAC + 760°C/16 hours/AC

IIb - 2225°F/2 hours/RAC + 1900°F/2 hours/RAC + 1400°F/16 hours/AC
1219°C/2 hours/RAC + 1038°C/2 hours/RAC + 760°C/16 hours/AC

III g mod - 2225°F/2 hours/RAC + 1950°F/2 hours/RAC + 1400°F/16 hours/AC
1219°C/2 hours/RAC + 1066°C/2 hours/RAC + 760°C/16 hours/AC

TABLE 31

Oxidation Data for Task II Alloys
Subjected to Cyclic Testing at 1875°F (1024°C)

| Alloy Designation | Cumulative Weight Change ($mg/cm^2$) after testing for: | | | | | | | | | |
|---|---|---|---|---|---|---|---|---|---|---|
| | 100 hours | 200 hours | 300 hours | 400 hours | 500 hours | 600 hours | 700 hours | 800 hours | 900 hours | 1000 hours |
| Unitemp AF 2-1DA | 1.06 | 1.84 | -0.17 | -0.24 | 0.20 | 0.55 | 0.77 | 0.91 | 1.15 | 1.47 |
| | 1.25 | 2.28 | 0.05 | 0.19 | 0.49 | 0.89 | 1.15 | 1.27 | 1.46 | 1.78 |
| I 5 | 0.33 | 0.42 | 0.64 | --* | 0.73 | 0.94 | 1.11 | 1.19 | 1.32 | 1.61 |
| | 0.35 | 0.35 | 0.69 | --* | 0.69 | 1.10 | 1.31 | 1.42 | 1.42 | 1.73 |
| IIb | 1.77 | 1.72 | 2.18 | 2.17 | 2.36 | 2.66 | 2.92 | 2.94 | 3.04 | 3.27 |
| | 1.87 | 0.96 | 1.07 | --* | 1.21 | 1.34 | 1.55 | 3.37 | 3.96 | 3.49 |
| III g mod | 0.43 | 1.35 | 1.78 | 1.63 | 1.78 | 1.92 | 2.11 | 2.15 | 2.31 | 2.65 |
| | 0.44 | 1.42 | 2.12 | 2.34 | 2.56 | 2.73 | 2.96 | 2.99 | 3.16 | 3.48 |

*No data available due to cracked container. The container was replaced for the remaining measurements.

TABLE 32

Oxidation Data for Task II Alloys
Subjected to Cyclic Testing at 1950°F (1066°C)

| Alloy Designation | Cumulative Weight Change ($mg/cm^2$) after testing for: | | | | | | | | | |
|---|---|---|---|---|---|---|---|---|---|---|
| | 100 hours | 200 hours | 300 hours | 400 hours | 500 hours | 600 hours | 700 hours | 800 hours | 900 hours | 1000 hours |
| Unitemp AF 2-1DA | 1.23 | 1.44 | 0.12 | -0.15 | -0.29 | -0.29 | -0.29 | 0.37 | 0.49 | 0.77 |
| | 1.28 | 1.24 | 1.14 | 0.86 | 0.72 | 0.77 | 0.58 | 0.70 | 0.70 | 0.77 |
| I 5 | 0.57 | 0.94 | 0.72 | 0.24 | -0.13 | -0.07 | -0.26 | -0.25 | -0.25 | -0.21 |
| | 0.60 | 0.89 | 0.52 | 0.05 | -0.26 | -0.17 | -0.25 | -0.20 | -0.35 | -0.25 |
| IIb | 2.30 | 2.42 | 1.51 | 0.78 | 0.26 | 0.33 | -0.10 | 0.25 | 0.46 | 0.48 |
| | 2.21 | 2.16 | 2.11 | 1.81 | 1.92 | 1.96 | 1.59 | 1.60 | 1.73 | 2.17 |
| III g mod | 0.90 | 2.25 | 2.40 | 2.17 | 2.11 | 2.22 | 2.67 | 2.83 | 2.85 | 3.31 |
| | 1.05 | 1.48 | 1.76 | 1.02 | 0.77 | 0.32 | 0.31 | 0.35 | 0.32 | 0.43 |

TABLE 33

Oxidation Data for Task II Alloys
Subjected to Cyclic Testing at 2100°F (1149°C)

| Designation | Cumulative Weight Change ($mg/cm^2$) after testing for: | | | | | | | | | |
|---|---|---|---|---|---|---|---|---|---|---|
| | 100 hours | 200 hours | 300 hours | 400 hours | 500 hours | 600 hours | 700 hours | 800 hours | 900 hours | 1000 hours |
| Unitemp | -1.96 | -2.77 | -2.89 | -2.46 | -2.44 | -2.34 | -1.28 | -1.18 | 2.21 | 2.51 |
| AF 2-1DA | 1.94 | -2.08 | -2.20 | -1.56 | -1.46 | -1.15 | 0.72 | 1.10 | 2.53 | 2.84 |
| I 5 | 0.96 | 0.99 | 1.43 | 1.73 | 1.90 | 1.96 | 3.81 | 3.58 | 3.58 | 3.39 |
| | -0.08 | -0.29 | 0.09 | 0.09 | 0.09 | -0.10 | 2.31 | 2.38 | 4.54 | 3.97 |
| IIb | 19.70 | 59.34 | 88.34 | 120.41 | 149.50 | 173.52 | 189.99 | 212.27 | 236.27 | 257.20 |
| | 2.19 | 42.99 | 84.73 | 115.94 | 143.48 | 170.33 | 187.78 | 208.08 | 222.67 | 241.95 |
| III g mod | 0.20 | -0.98 | -1.16 | -0.30 | 0.03 | 1.10 | 4.11 | 4.14 | 3.98 | 3.93 |
| | 0.92 | -0.01 | 0.44 | 1.93 | 3.65 | 5.38 | 7.82 | 9.58 | 10.65 | 13.61 |

TABLE 34

Sulfidation Data for Task II Alloys

| Alloy Designation | Temperature (°F) | Temperature (°C) | Sulfidation Rate (inches per year) | Sulfidation Rate (meters per year) |
|---|---|---|---|---|
| Unitemp AF 2-1DA | 1600 | 871 | 45.0 | 1.14 |
| | 1800 | 982 | 64.2 | 1.63 |
| I 5 | 1600 | 871 | 23.3 | 0.59 |
| | 1800 | 982 | 60.8 | 1.54 |
| IIb | 1600 | 871 | 17.2 | 0.44 |
| | 1800 | 982 | 49.8 | 1.26 |
| IIIg mod | 1600 | 871 | 21.6 | 0.55 |
| | 1800 | 982 | 12.7 | 0.32 |

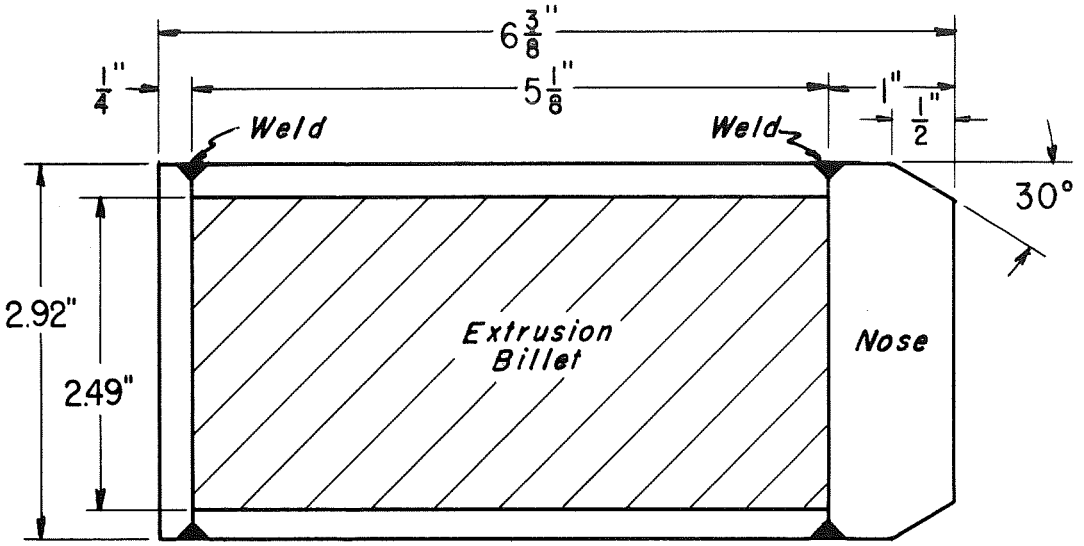


A. FOR EXTRUSION TO ONE INCH DIAMETER

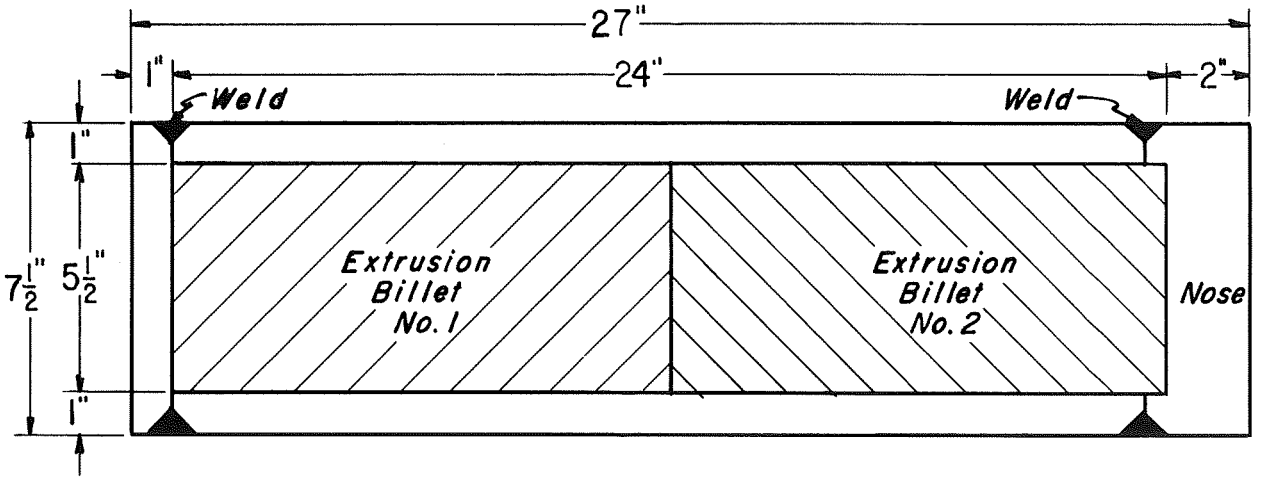


B. FOR EXTRUSION TO THREE INCH DIAMETER

FIGURE 1 : SCHEMATIC DIAGRAMS OF TWO TYPES OF CANNED BILLETS FOR EXTRUSION TO TWO SIZES.

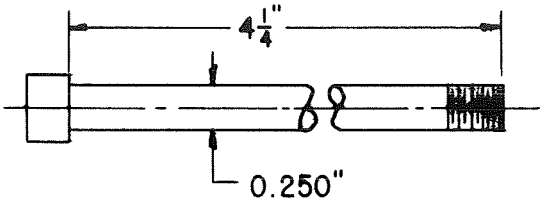


A. GLEEBLE

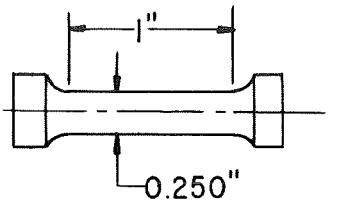


B. TENSILE

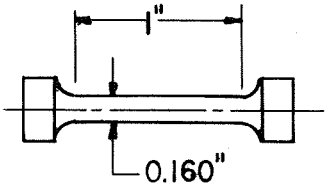


C. STRESS RUPTURE

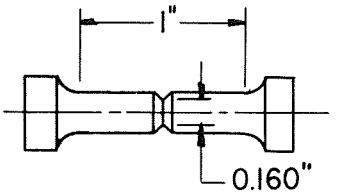


D. INTERRUPTED LOW CYCLE FATIGUE
$K_t = 2.5$

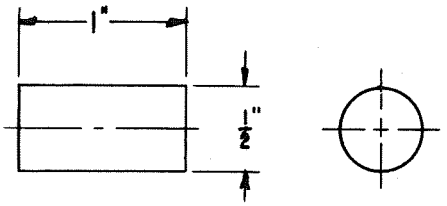


E. CONTINUOUS OXIDATION

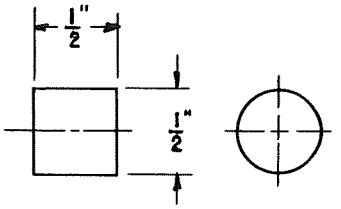


F. CYCLIC OXIDATION

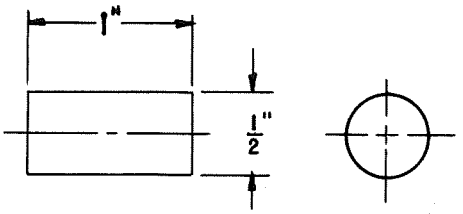


G. SULFIDATION

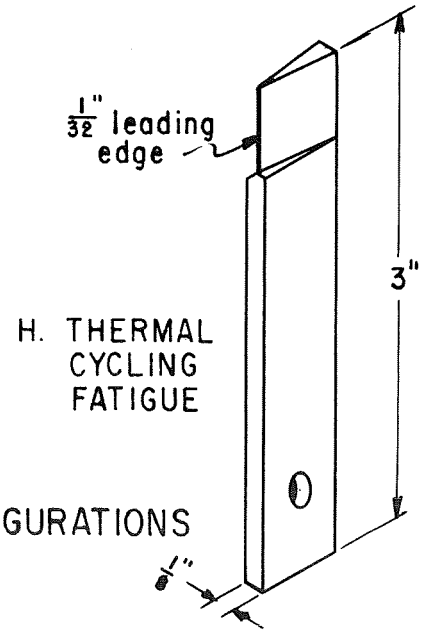


H. THERMAL CYCLING FATIGUE

FIGURE 2: TEST SPECIMEN CONFIGURATIONS

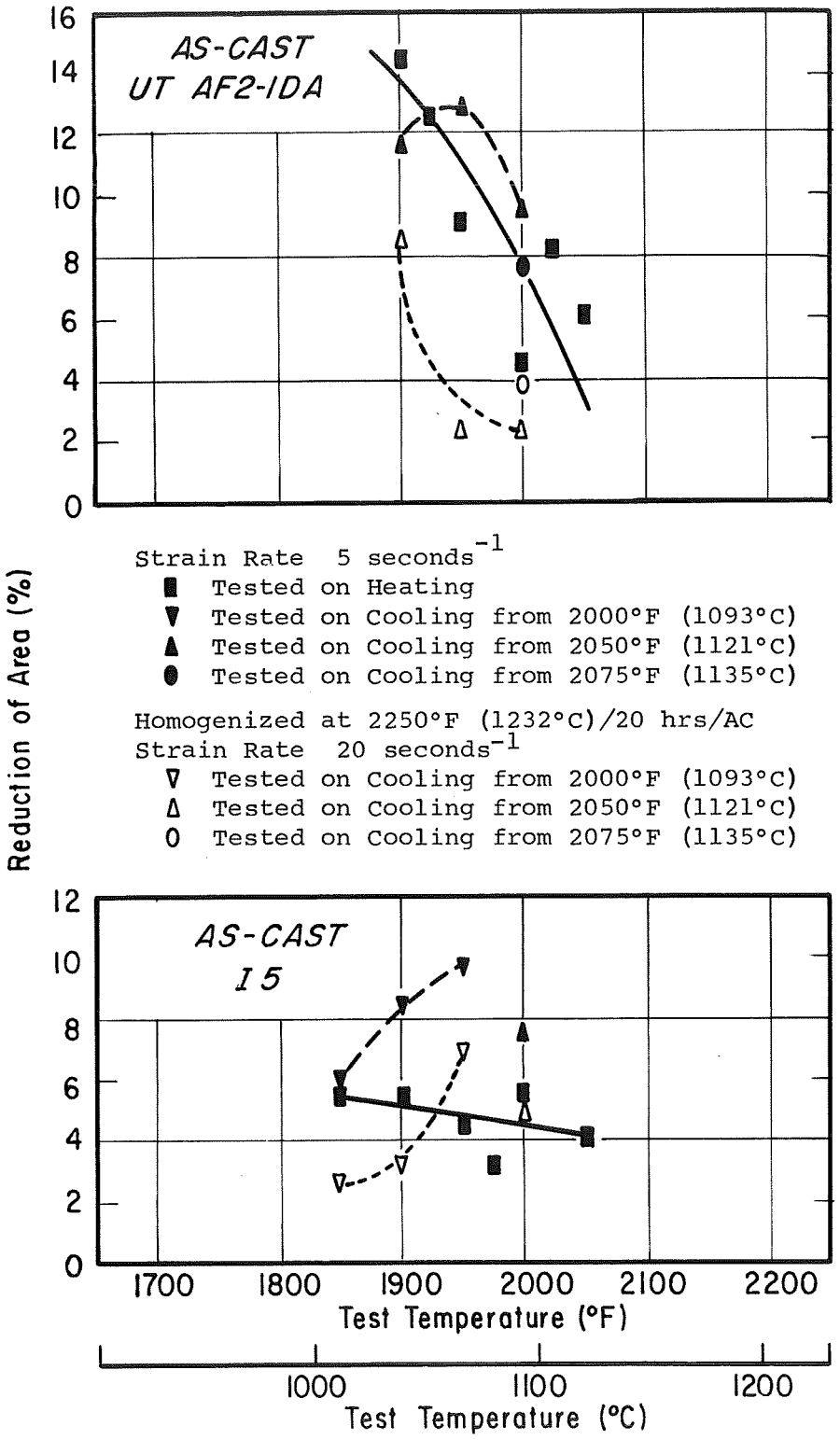


FIGURE 3: GLEEBLE HOT WORKABILITY CURVES FOR AS-CAST UNITEMP AF2-IDA AND I 5.

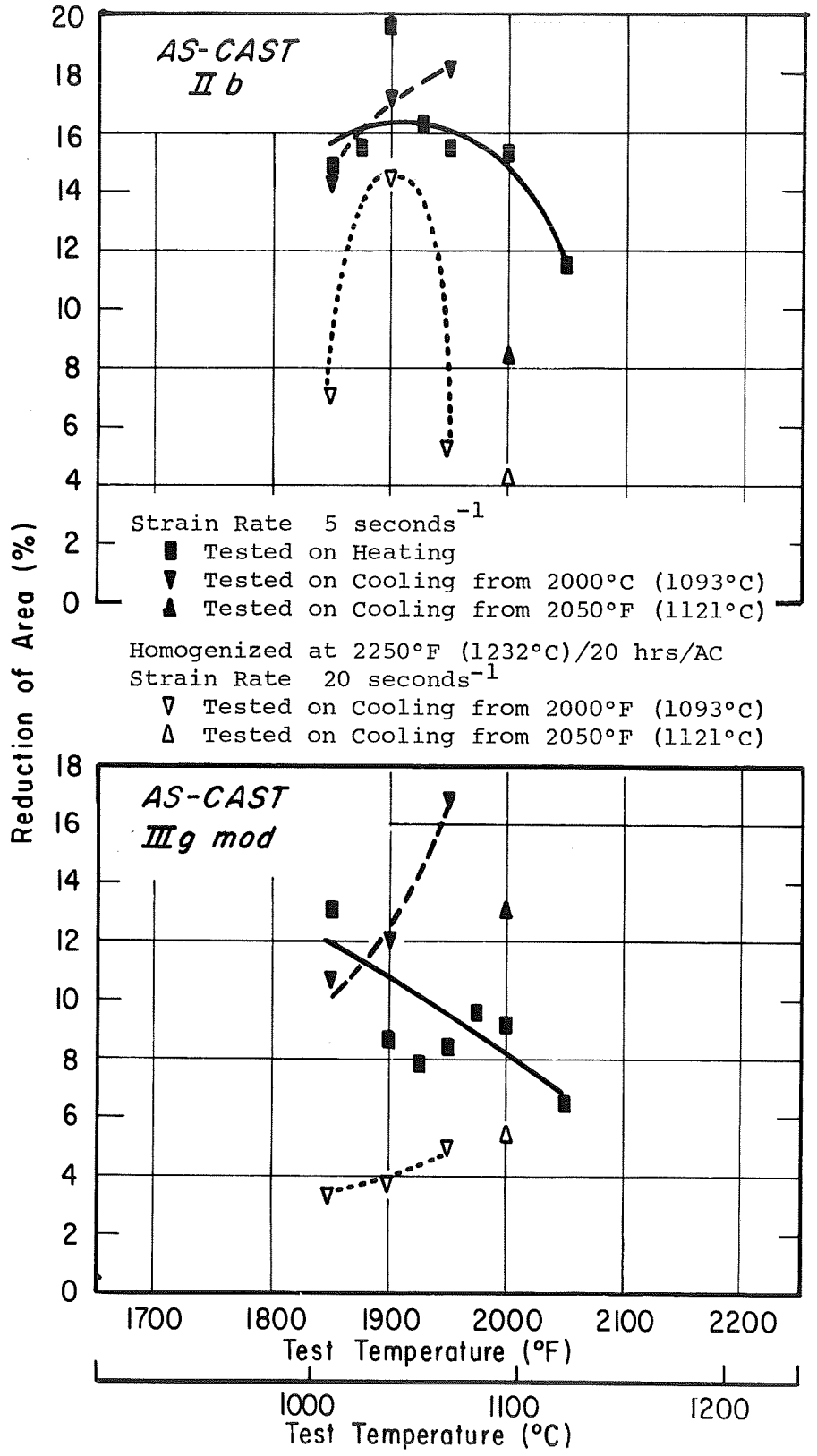


FIGURE 4 : GLEEBLE HOT WORKABILITY CURVES FOR AS-CAST II b AND IIIg mod.

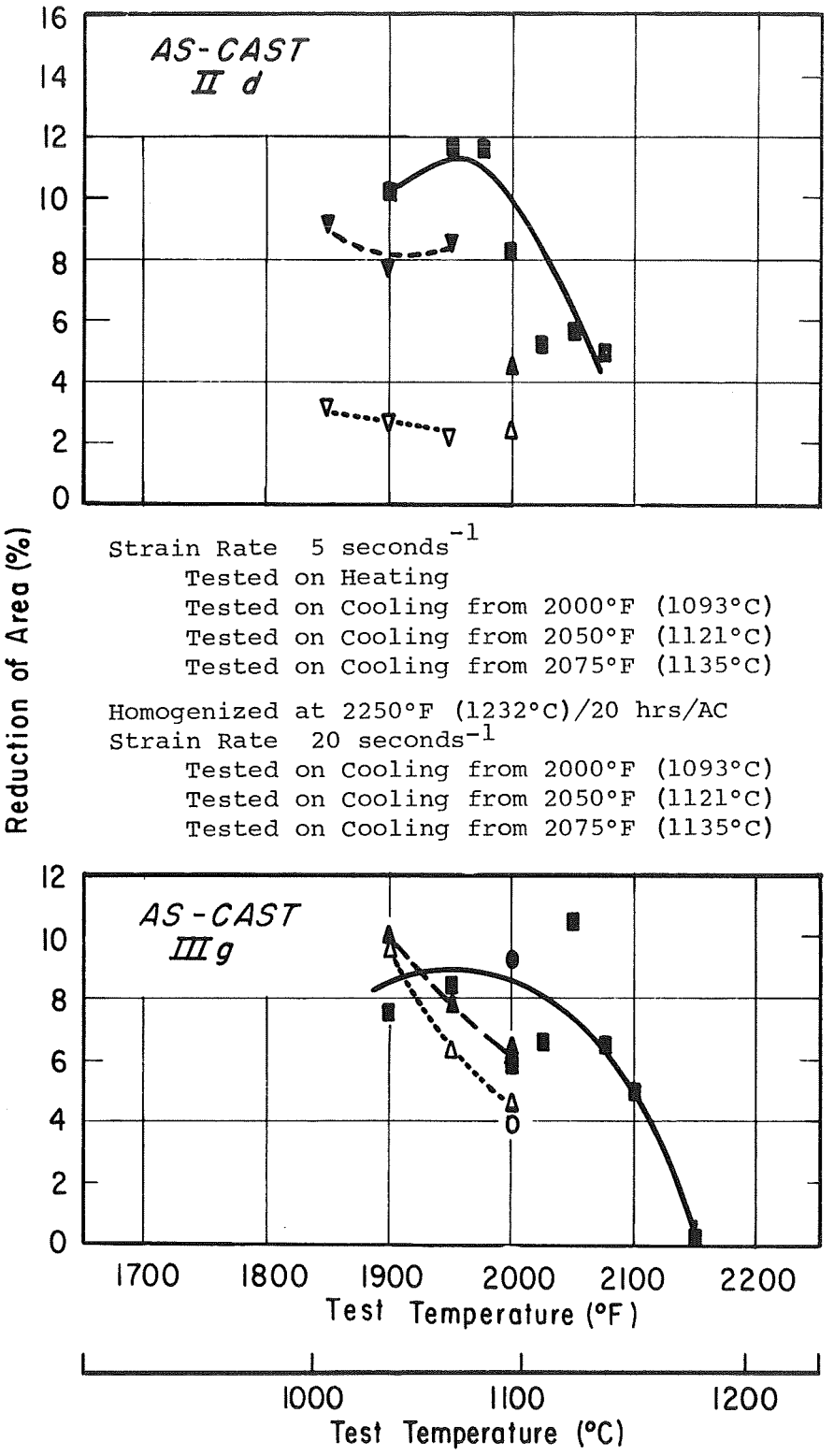


FIGURE 5: GLEEBLE HOT WORKABILITY CURVES FOR AS-CAST II d AND III g.

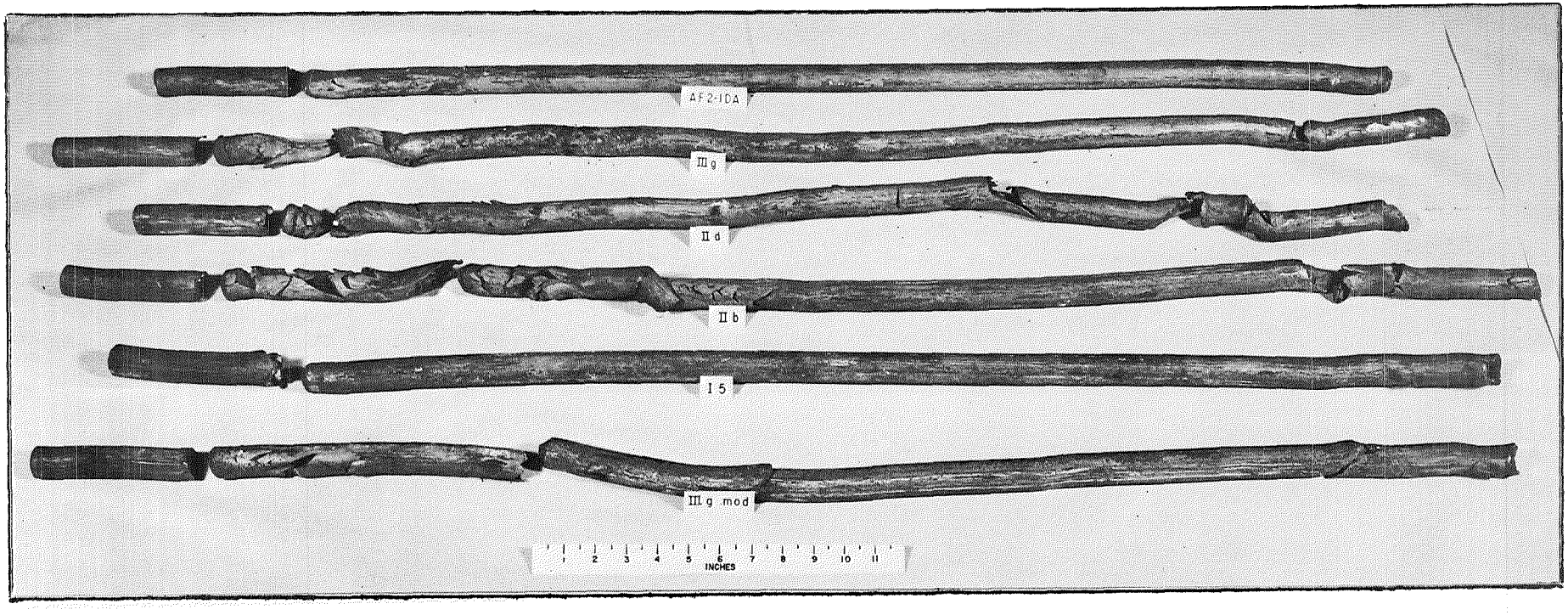


| Alloy | Extrusion Temperature |
|---|---|
| AF2-IDA | 2050°F |
| III g | 2050°F |
| II d | 2000°F |
| II b | 2000°F |
| I 5 | 2000°F |
| III g mod | 2000°F |

FIGURE 6: RESULTS OF SERIES I SINGLE EXTRUSIONS

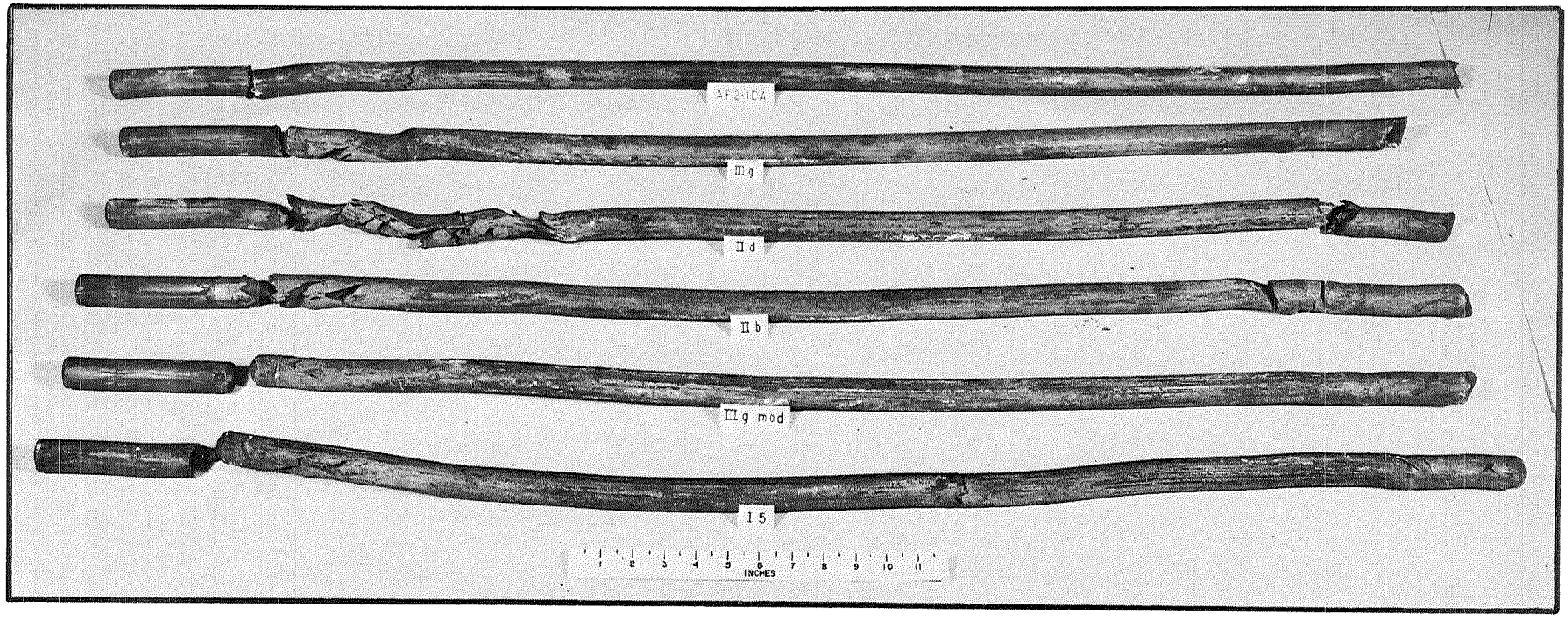


| Alloy | Extrusion Temperature |
|---|---|
| AF2-IDA | 2050°F |
| IIIg | 2050°F |
| IId | 2050°F |
| IIb | 2050°F |
| IIIg mod | 2050°F |
| I 5 | 2000°F |

FIGURE 7: RESULTS OF SERIES II SINGLE EXTRUSIONS

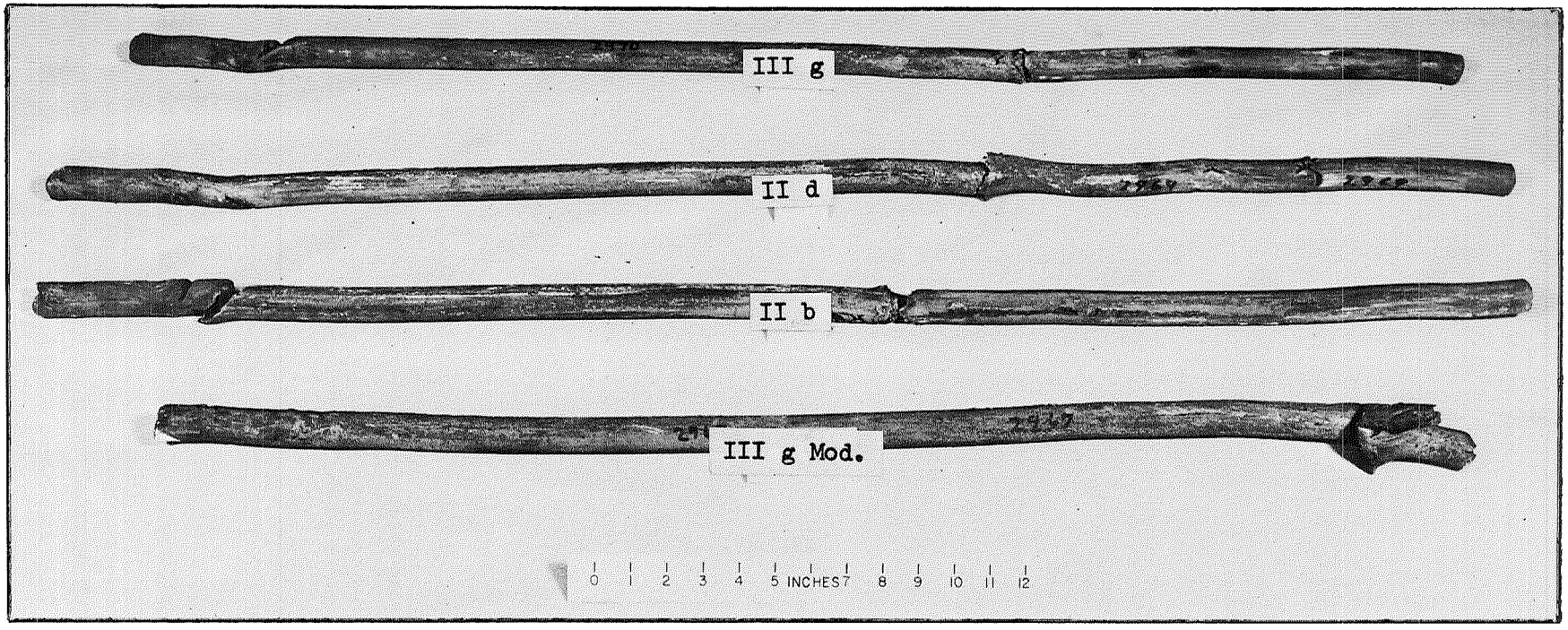


| Alloy | Extrusion Temperature |
|---|---|
| III g | 2100°F |
| II d | 2100°F |
| II b | 2100°F |
| III g mod | 2100°F |

FIGURE 8: RESULTS OF SERIES III SINGLE EXTRUSIONS

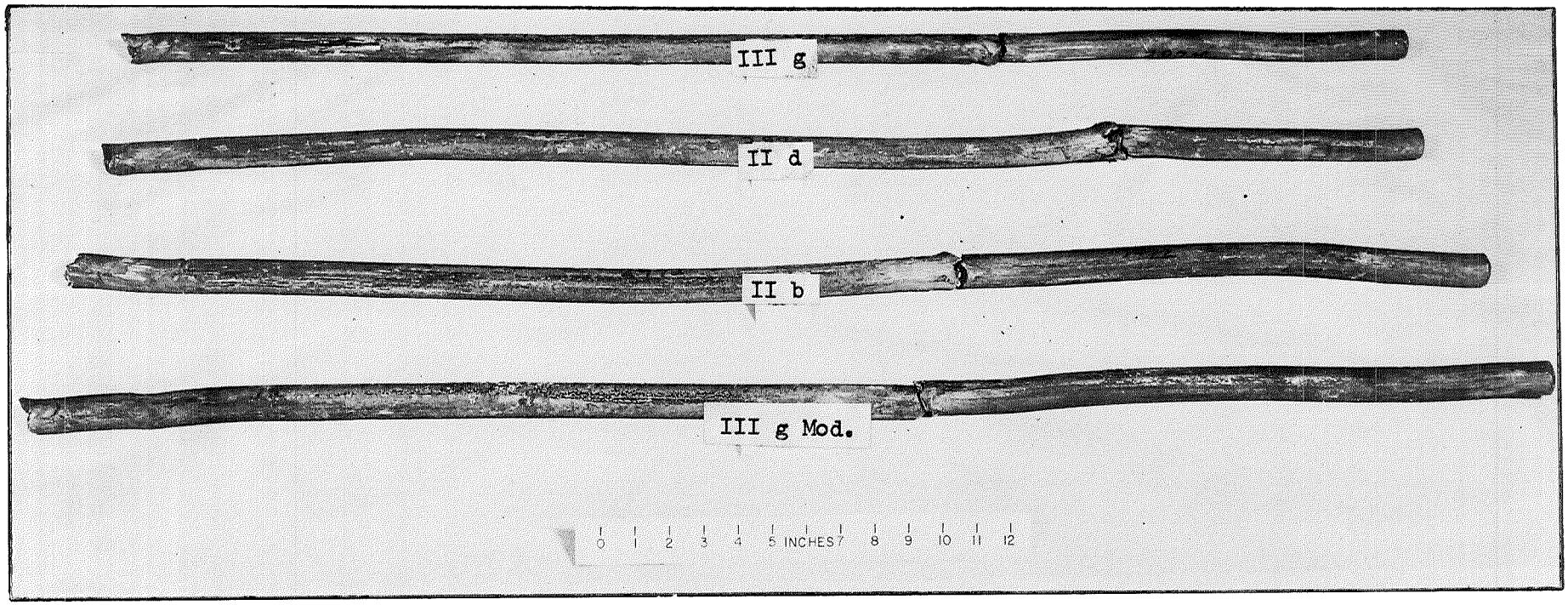


| Alloy | Extrusion Temperature |
|---|---|
| III g | 2125°F |
| II d | 2125°F |
| II b | 2125°F |
| III g mod | 2125°F |

FIGURE 9: RESULTS OF SERIES IV SINGLE EXTRUSIONS

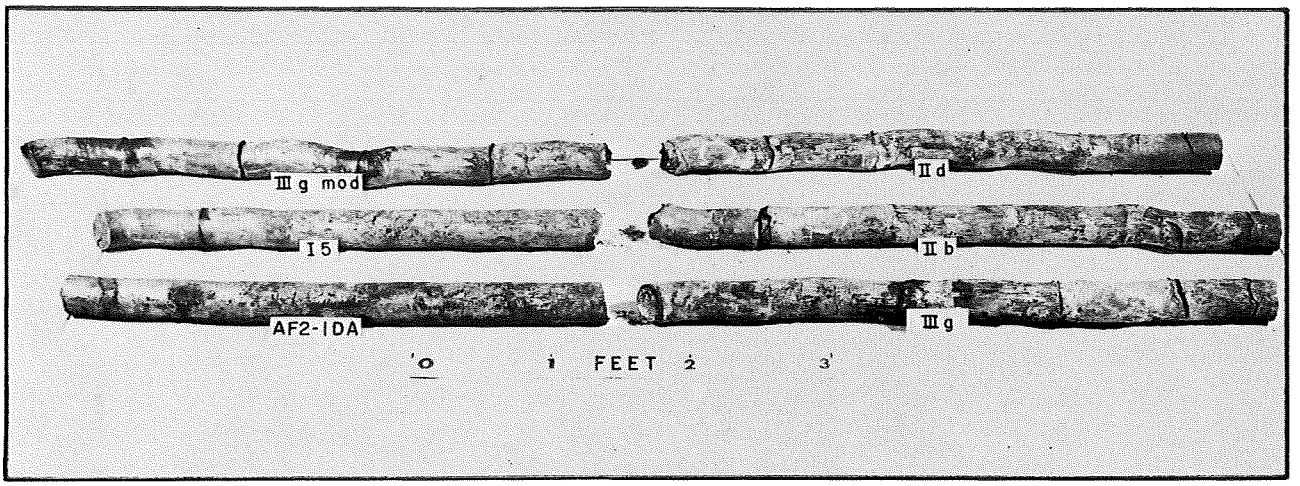


A) Initial Trials

| Alloys | Extrusion Temperature |
|---|---|
| III g mod<br>II d | 2000°F |
| I 5<br>II b | 2000°F |
| AF2-IDA<br>III g | 2050°F |

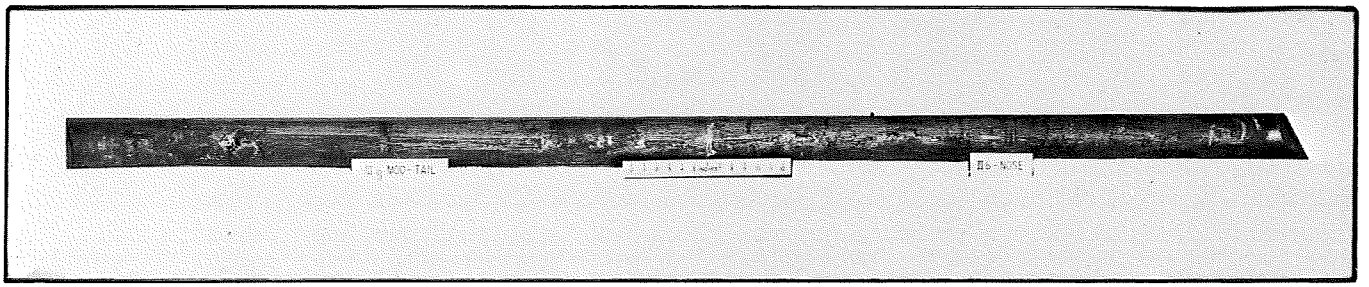

B) Second Trial

| | |
|---|---|
| II b<br>III g mod | 2100°F |

FIGURE 10: RESULTS OF FIRST PHASE OF DOUBLE EXTRUSIONS

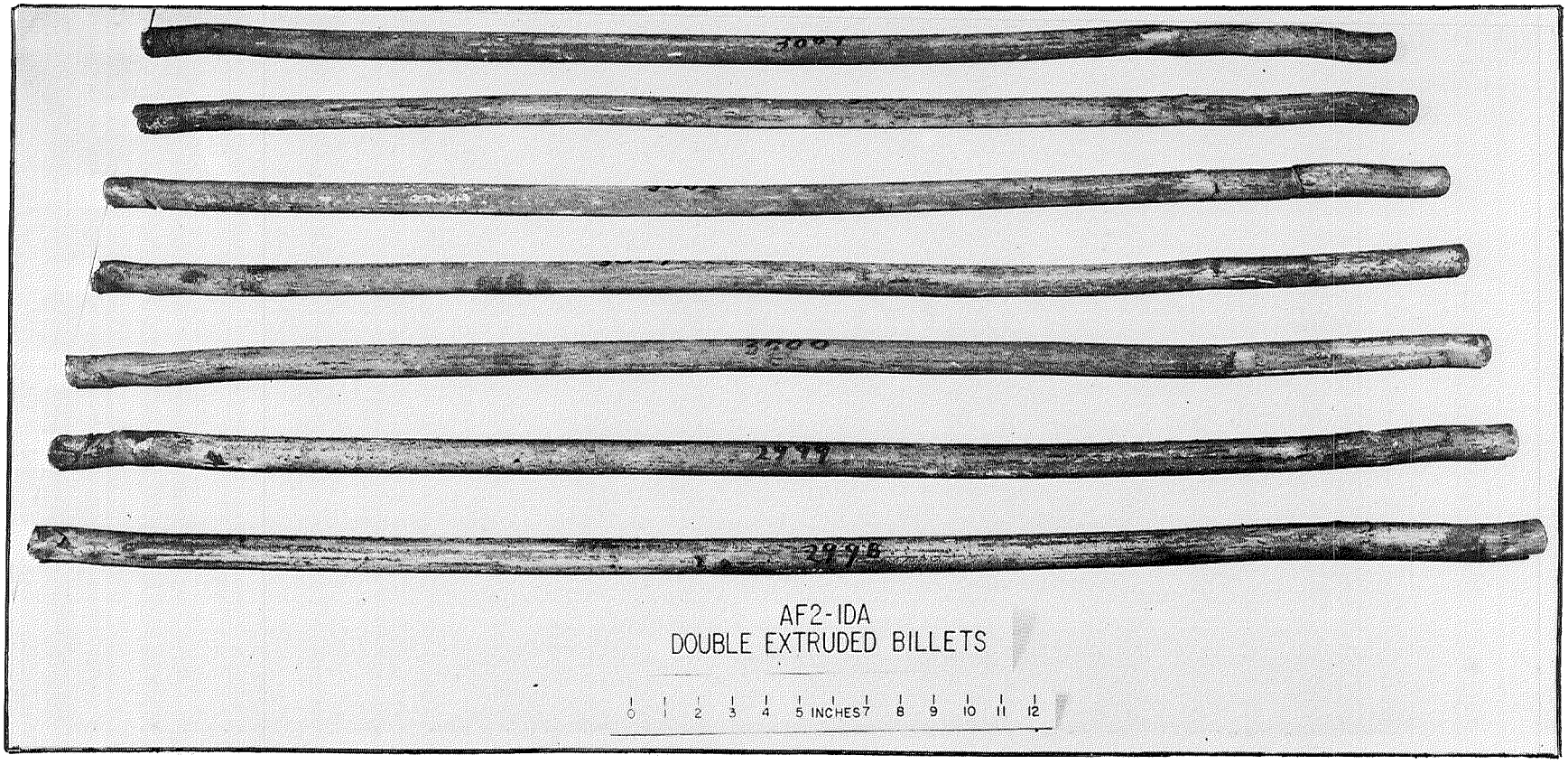


| Alloy | Extrusion Temperature |
|---|---|
| AF2-IDA | 2050°F |

FIGURE 11: RESULTS OF SECOND PHASE OF UNITEMP AF2-IDA DOUBLE EXTRUSIONS

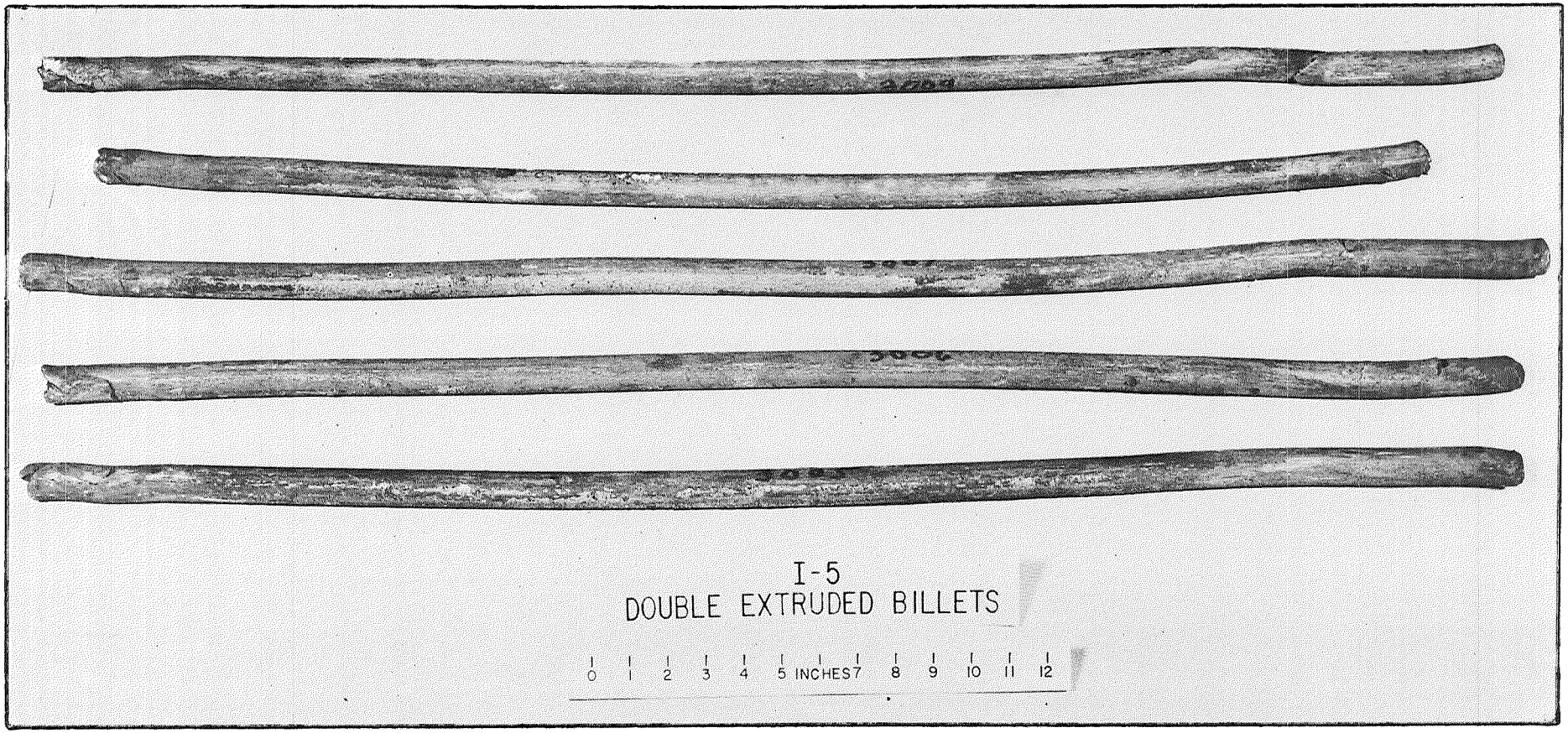


| Alloy | Extrusion Temperature |
|---|---|
| I 5 | 2050°F |

FIGURE 12: RESULTS OF SECOND PHASE OF I 5 DOUBLE EXTRUSIONS

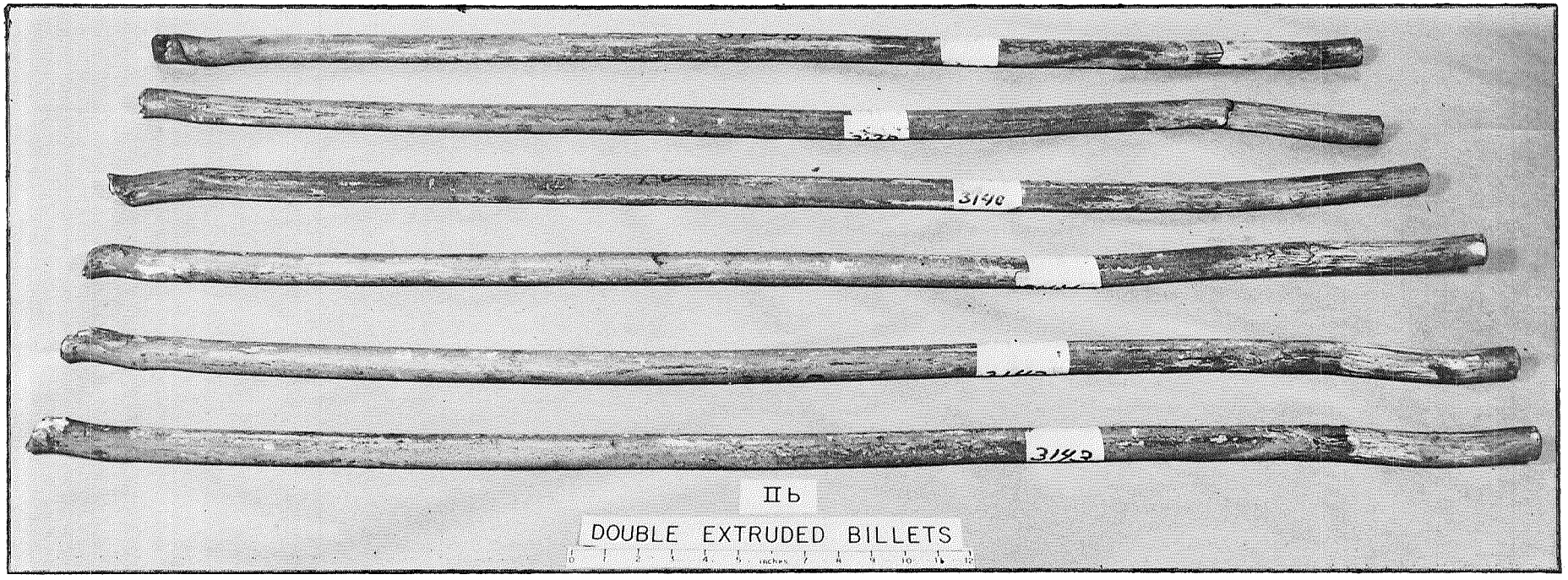


| Alloy | Extrusion Temperature |
|---|---|
| II b | 2100°F |

FIGURE 13: RESULTS OF SECOND PHASE OF II b DOUBLE EXTRUSIONS

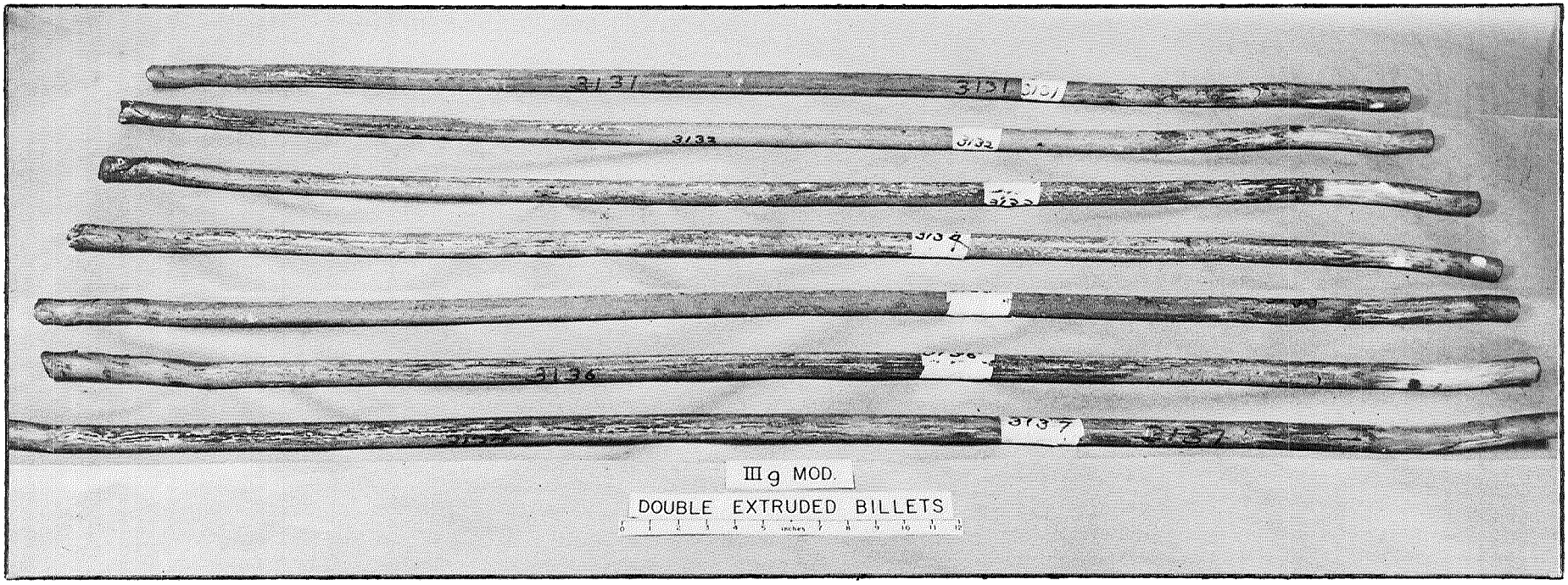


| Alloy | Extrusion Temperature |
|---|---|
| III g mod | 2100°F |

FIGURE 14: RESULTS OF SECOND PHASE OF III g mod DOUBLE EXTRUSIONS

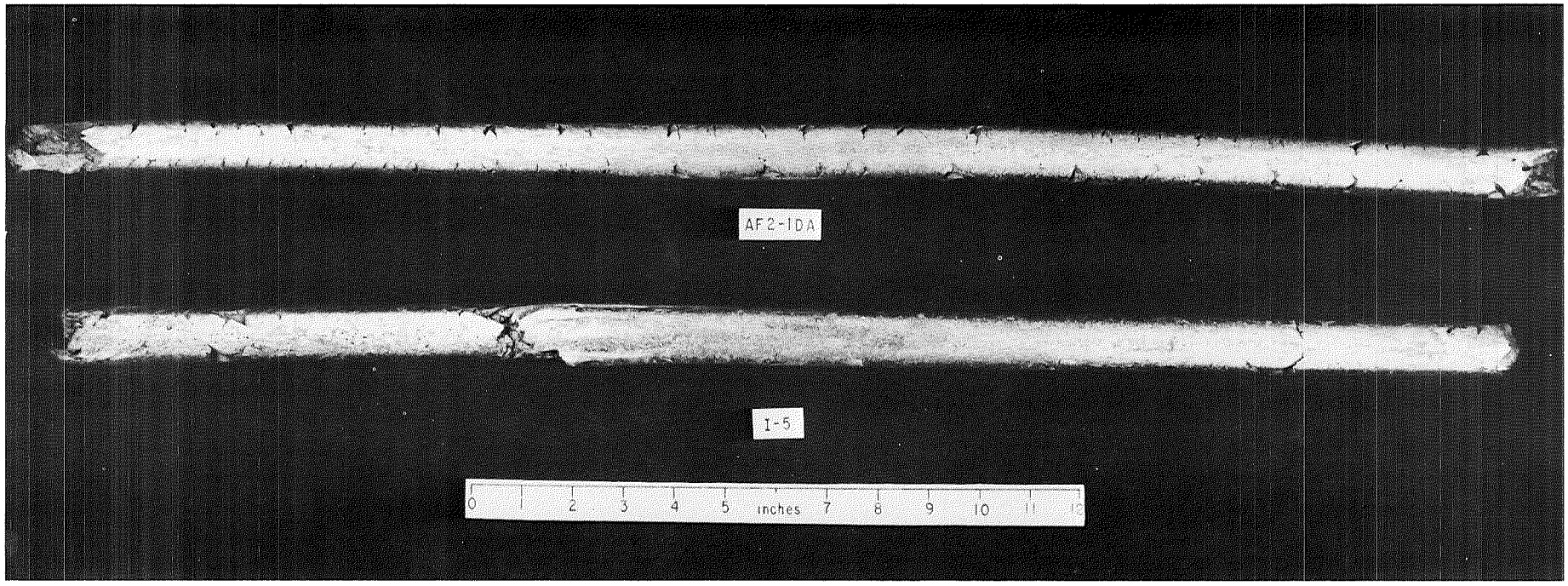


M1251

FIGURE 15: UNITEMP AF2-IDA AND I 5 BARS ROLLED FROM $3\frac{1}{8}$ INCH DIAMETER INGOTS TO ONE INCH DIAMETER ROUND CORNERED SQUARE BARS.

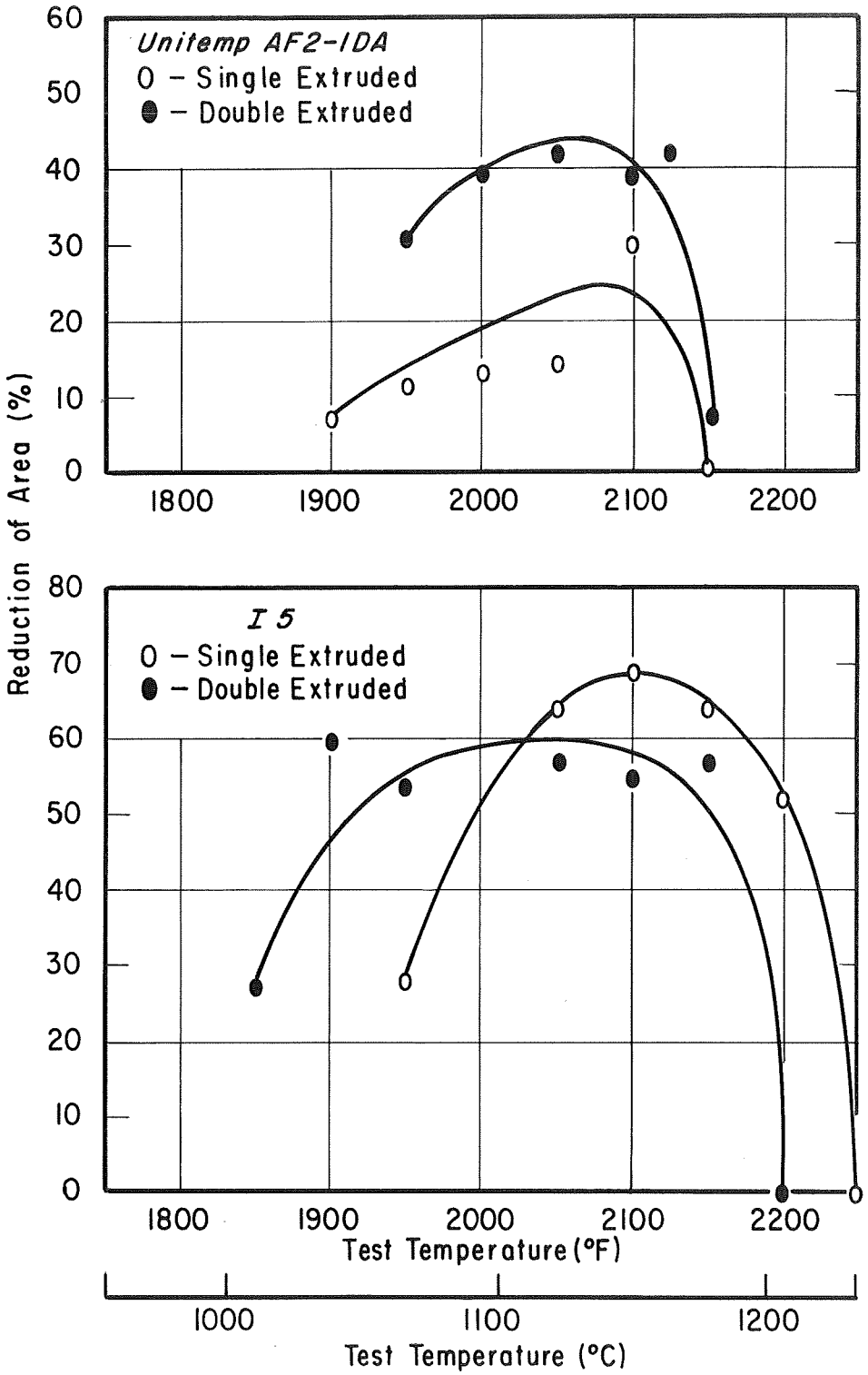


FIGURE 16: GLEEBLE HOT WORKABILITY CURVES FOR EXTRUDED UNITEMP AF2-IDA AND I 5.

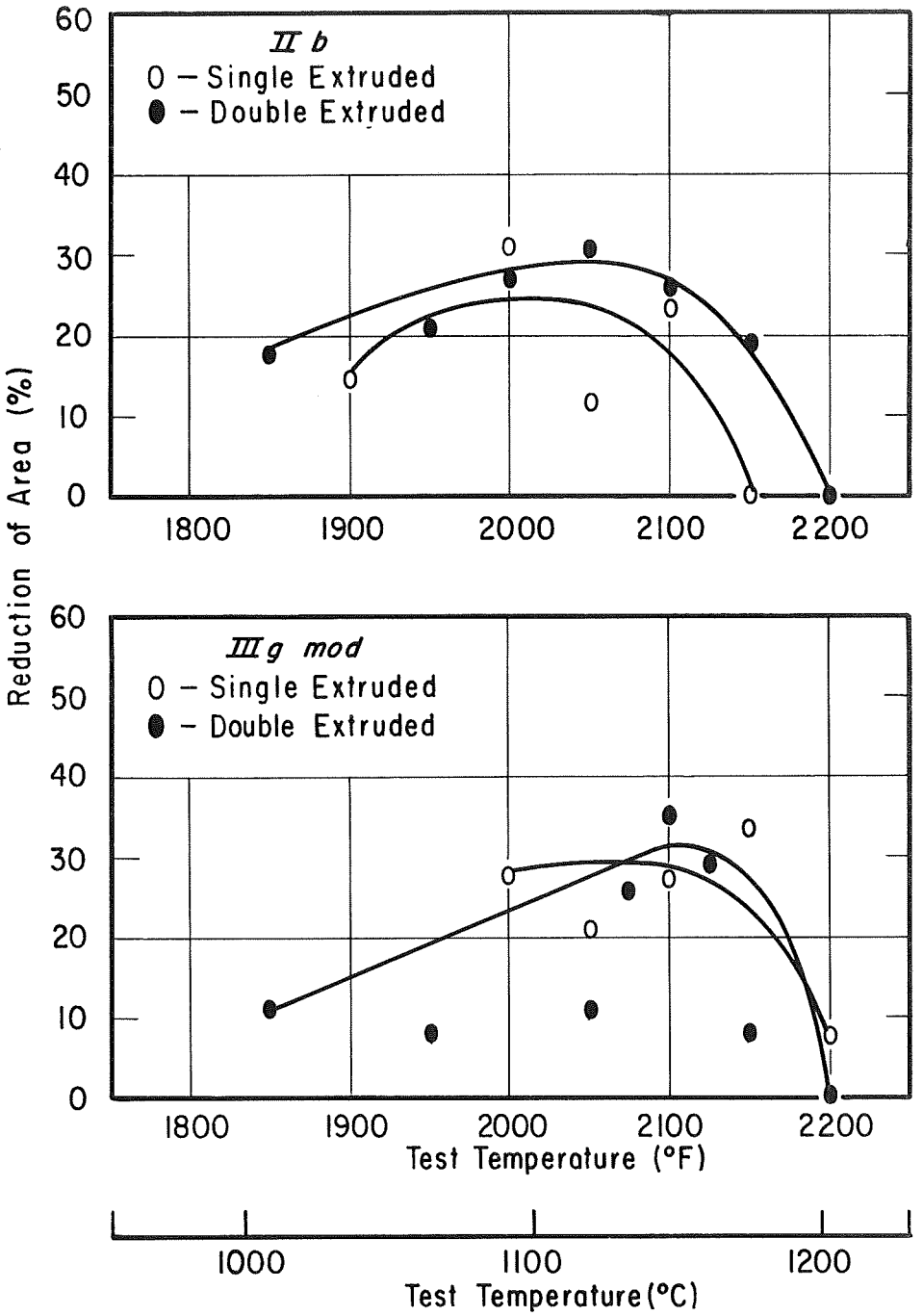


FIGURE 17: GLEEBLE HOT WORKABILITY CURVES FOR EXTRUDED IIb AND IIIg mod.

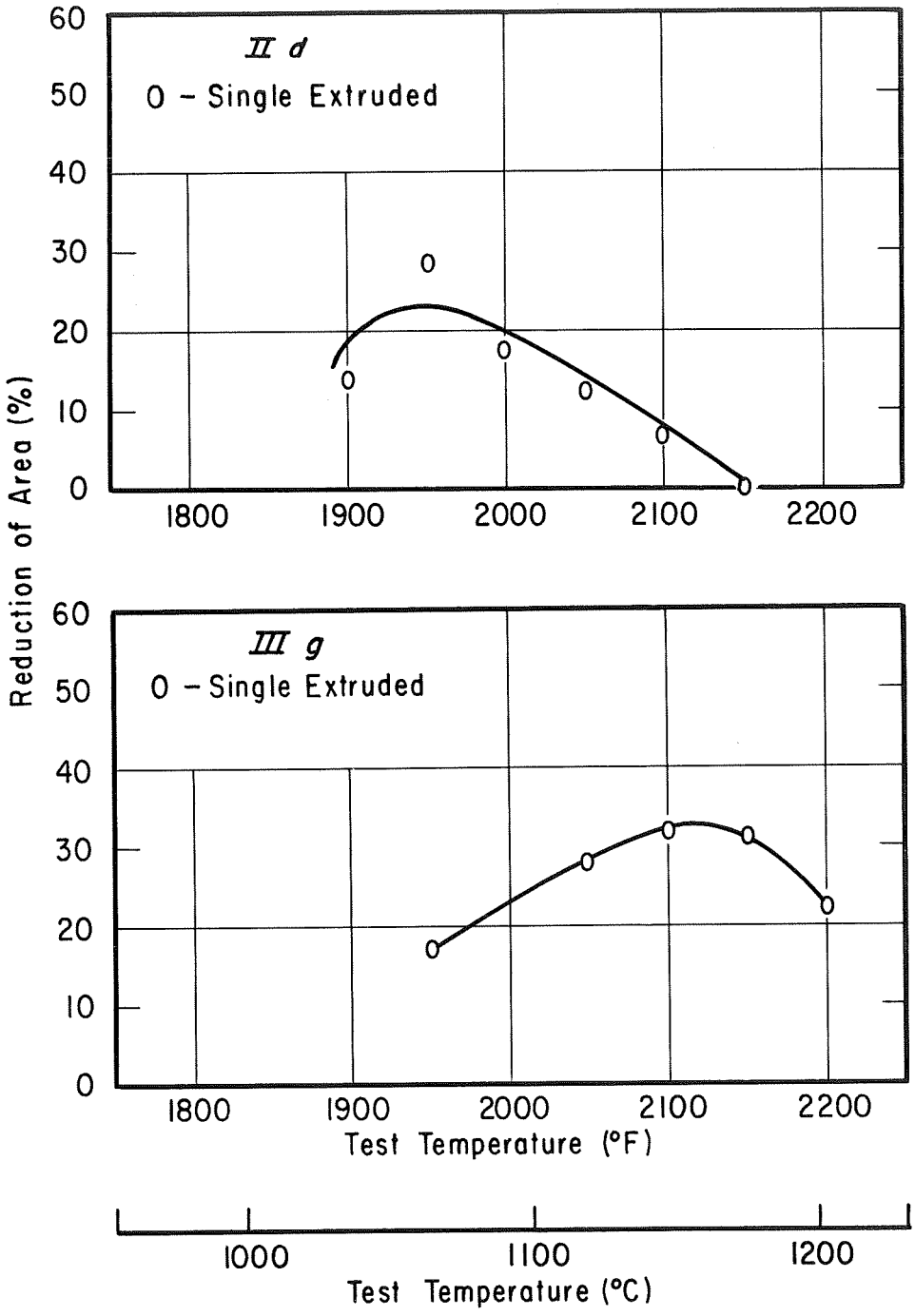


FIGURE 18: GLEEBLE HOT WORKABILITY CURVES FOR EXTRUDED IId AND IIIg.

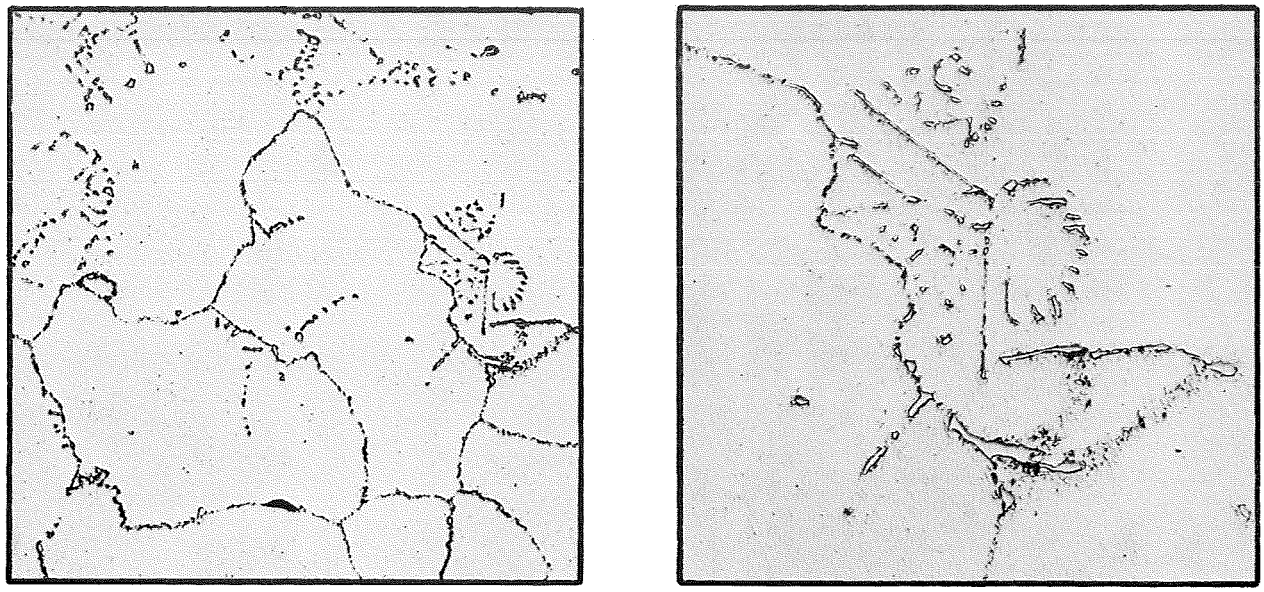

R21275 200X R21276 500X

I 5

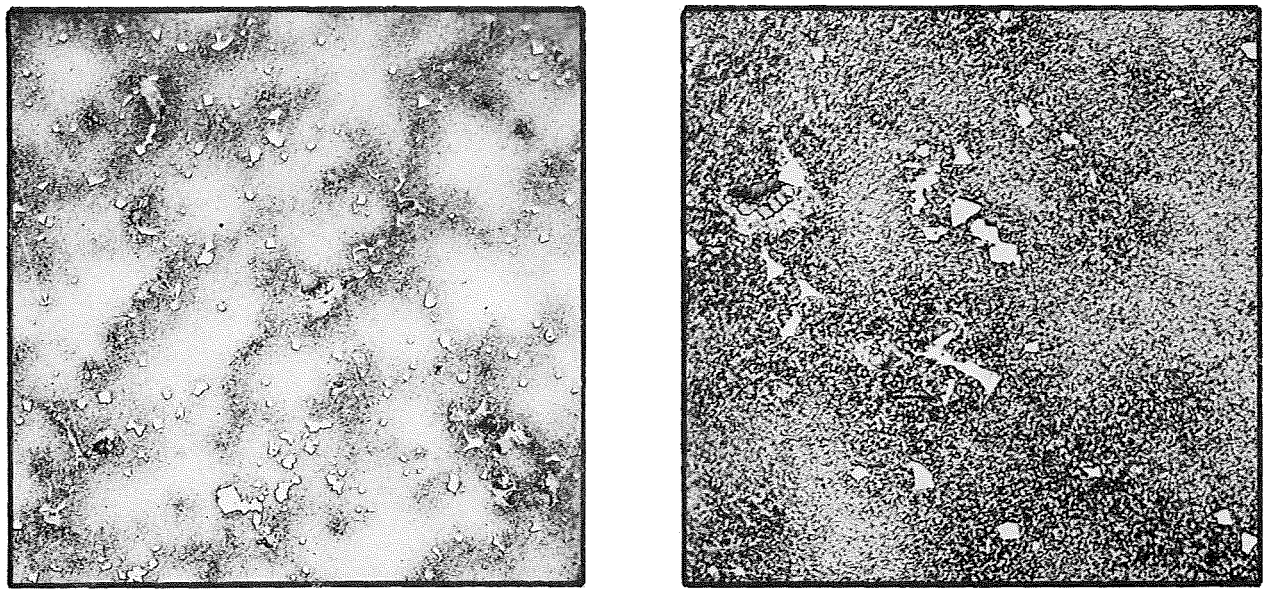

R21277 200X R21278 500X

Unitemp AF2-IDA

FIGURE 19: PHOTOMICROGRAPHS REPRESENTING THE BASIC VARIATIONS IN THE AS-CAST MICROSTRUCTURES OF THE EXPERIMENTAL ALLOYS.

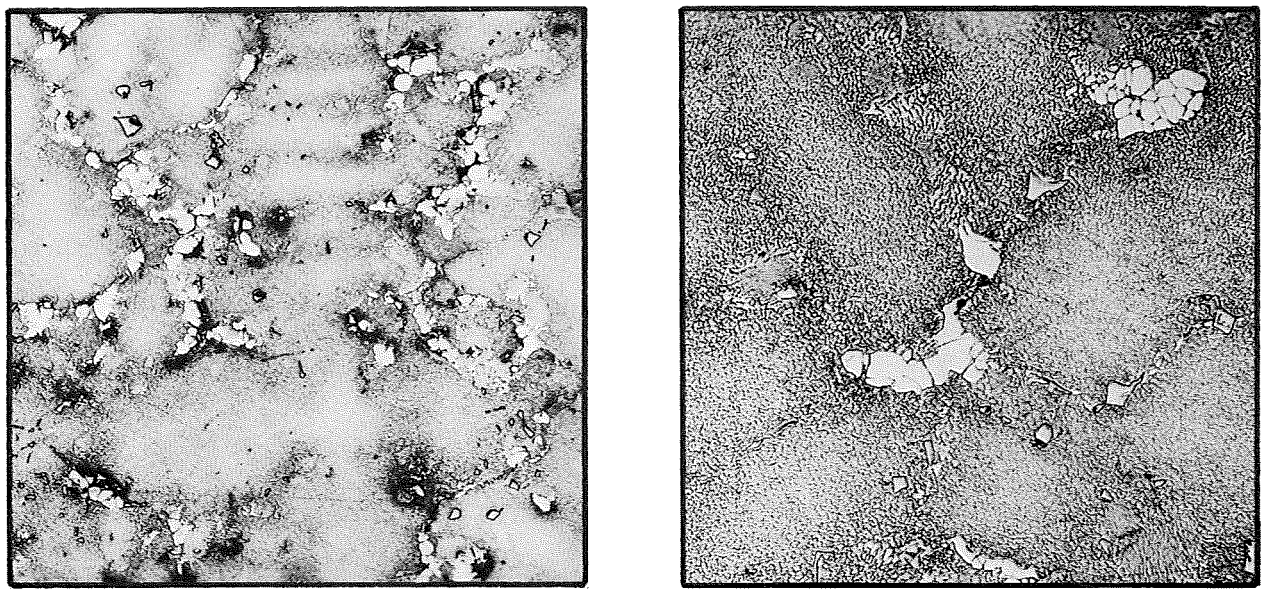

R21279 200X R21280 500X

II d

FIGURE 19 :(continued) PHOTOMICROGRAPHS REPRESENTING THE BASIC VARIATIONS IN THE AS-CAST MICROSTRUCTURES OF THE EXPERIMENTAL ALLOYS.

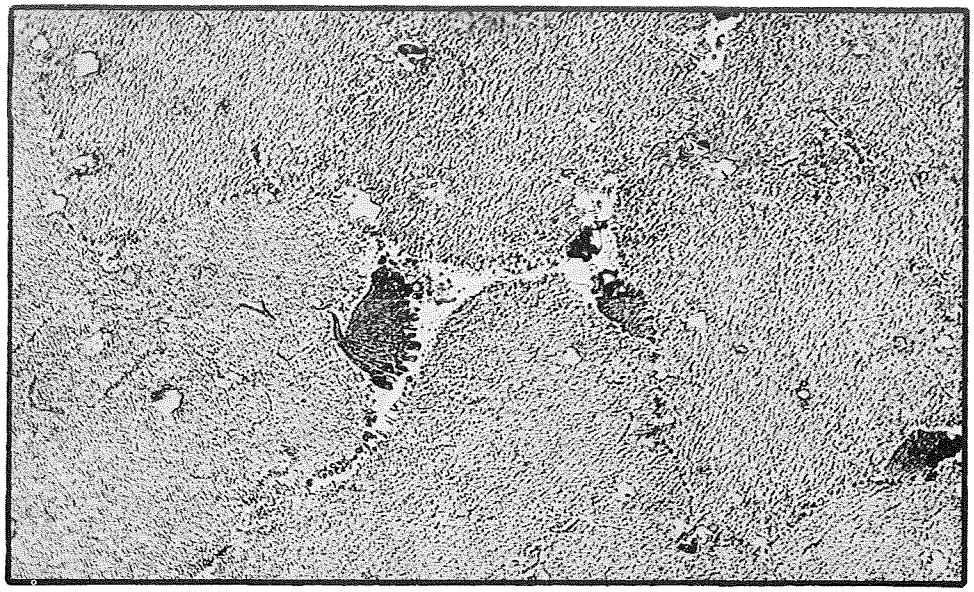

R21308 III g 500X

Quenched from 2050°F

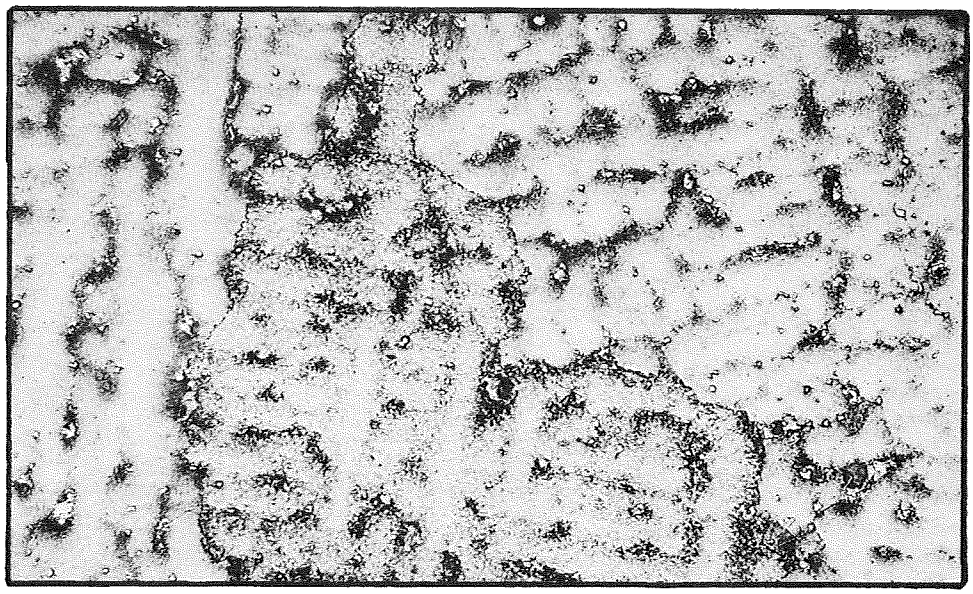

R21309 200X

Unitemp AF2-IDA

Quenched from 2050°F

FIGURE 20 : PHOTOMICROGRAPHS OF III g AND UNITEMP AF2-IDA ILLUSTRATING THE SIMILARITY TO THE AS-CAST STRUCTURE AFTER QUENCHING FROM THE OPTIMUM WORKING TEMPERATURE.

R21329 500X

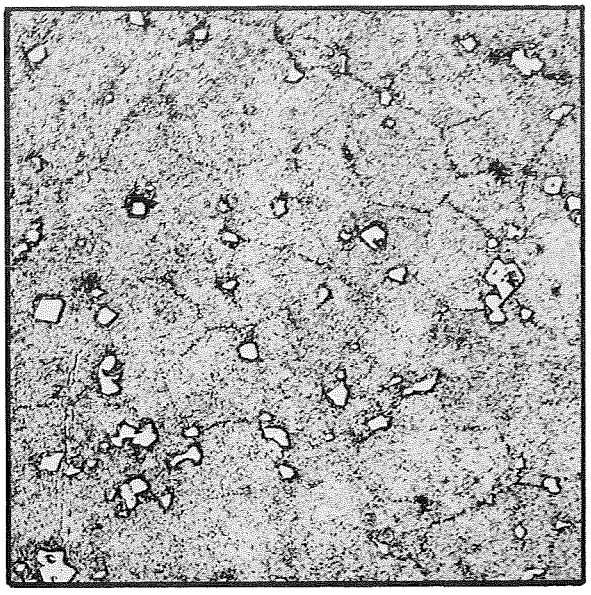

R21328 500X

Unitemp AF2-IDA

Three inch diameter billet

One inch diameter billet

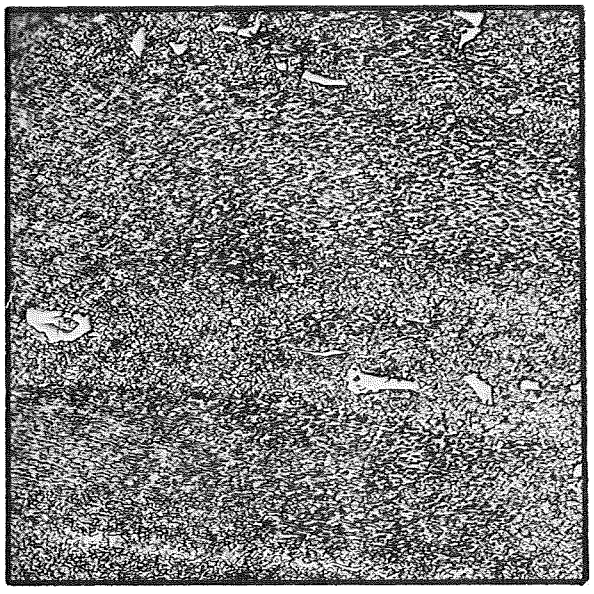

R21401 500X

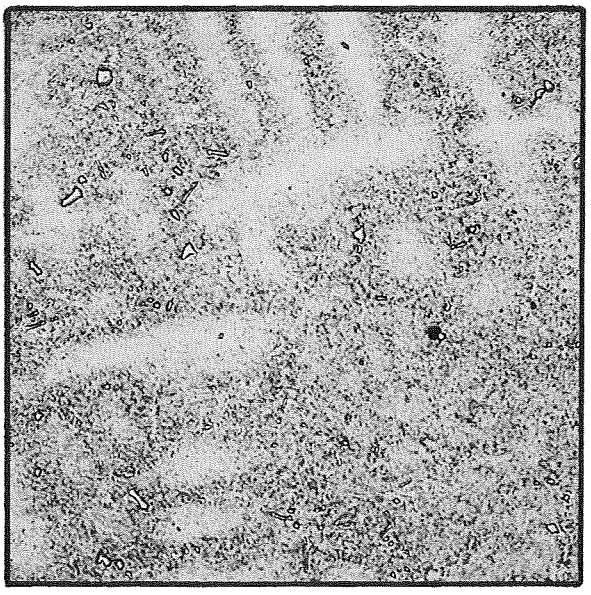

R21402 500X

I 5

Three inch diameter billet

One inch diameter billet

FIGURE 21: PHOTOMICROGRAPHS COMPARING THE STRUCTURES OF THREE ALLOYS AFTER EXTRUSION TO THREE INCH DIAMETER AND ONE INCH DIAMETER BILLETS.

R21335 500X

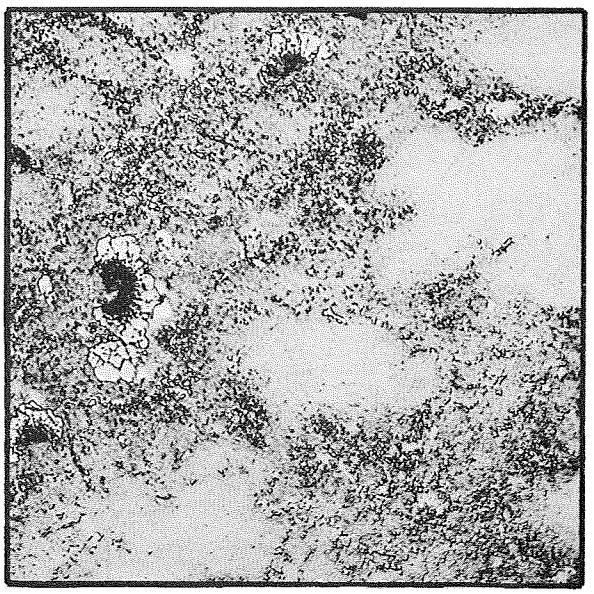

R21334 500X

III g

Three inch diameter billet

One inch diameter billet

FIGURE 21:(continued) PHOTOMICROGRAPHS COMPARING THE STRUCTURES OF THREE ALLOYS AFTER EXTRUSION TO THREE INCH DIAMETER AND ONE INCH DIAMETER BILLETS.

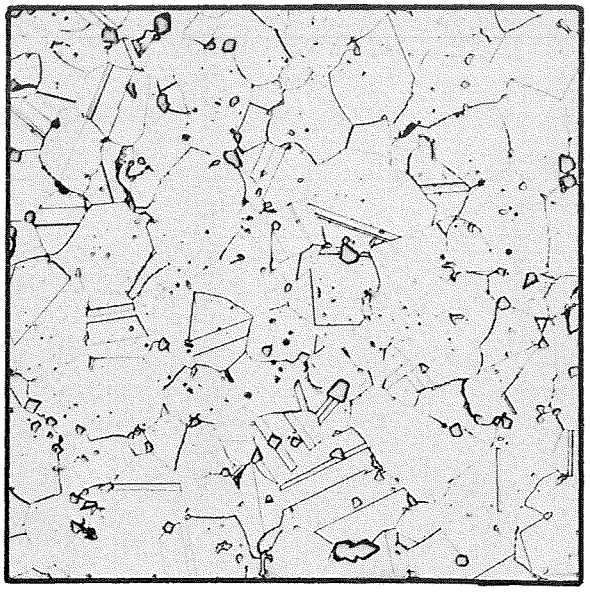

R21608 200X

2175°F/4hours

Grain Size : ASTM 6-7

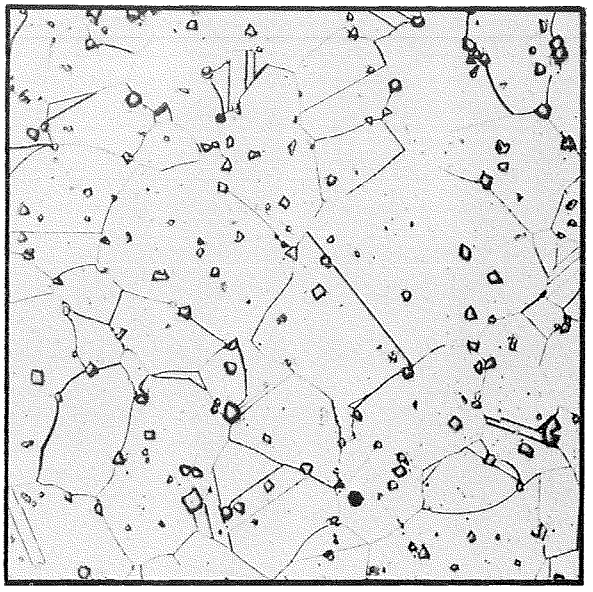

R21586 200X

2200°F / 2 hours

Grain Size : ASTM 4-5

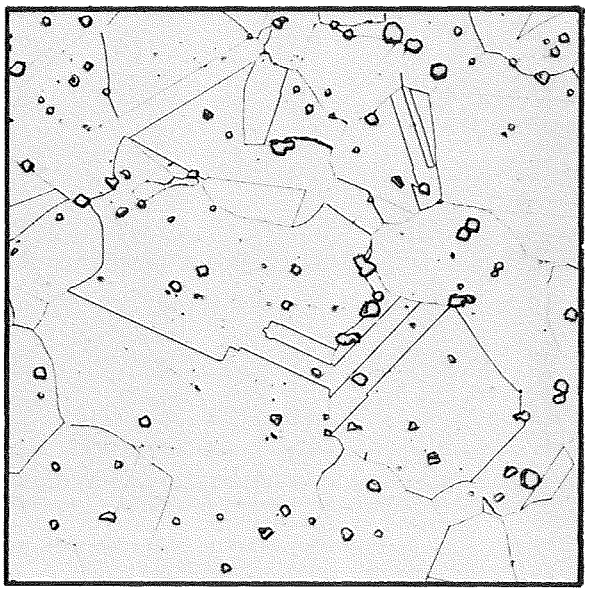

R21610 200X

2250°F / 2 hours

Grain Size : ASTM 3-4

FIGURE 22: OPTICAL MICROGRAPHS OF DOUBLE EXTRUDED UNITEMP AF2-IDA ILLUSTRATING THE EFFECT OF VARIOUS SOLUTION TREATMENTS ON GRAIN SIZE.

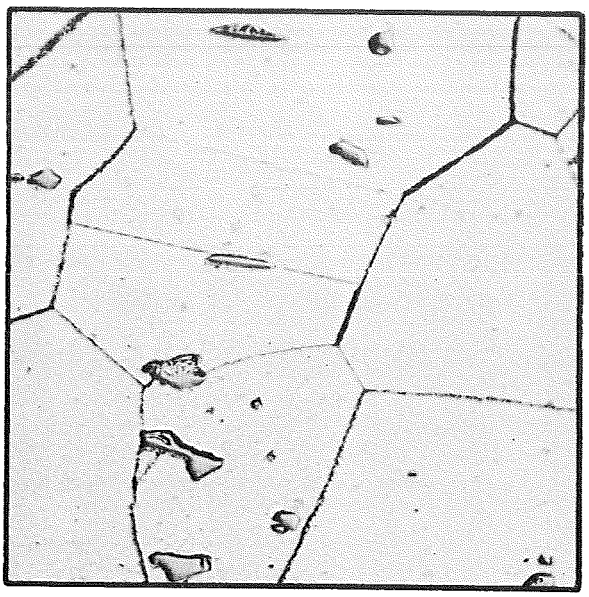

R21615 500X

2225°F/1 hr. + 1950°F/2 hrs.

R21617 500X

2225°F/1 hr. + 2000°F/16 hrs.

R21625 500X

2225°F/1 hr + 1950°F/16 hrs.

FIGURE 23: OPTICAL MICROGRAPHS OF DOUBLE EXTRUDED I5 ILLUSTRATING THE EFFECT OF VARIOUS INTERMEDIATE AGING TREATMENTS ON GAMMA PRIME AND GRAIN BOUNDARY CARBIDE PRECIPITATION.

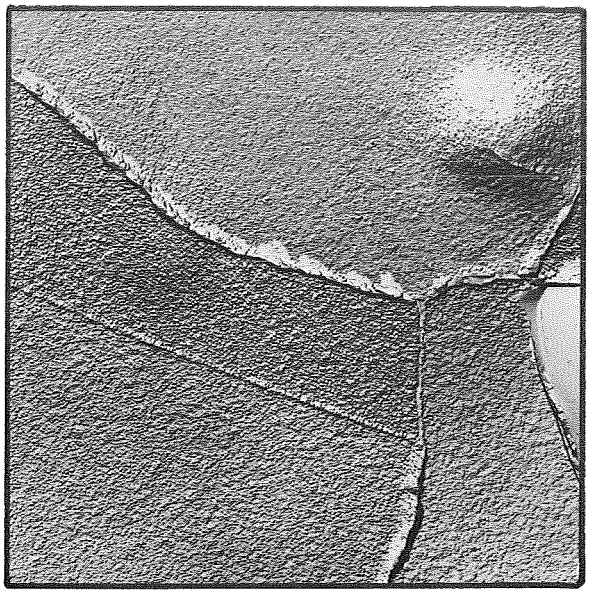

EM1612 5000X

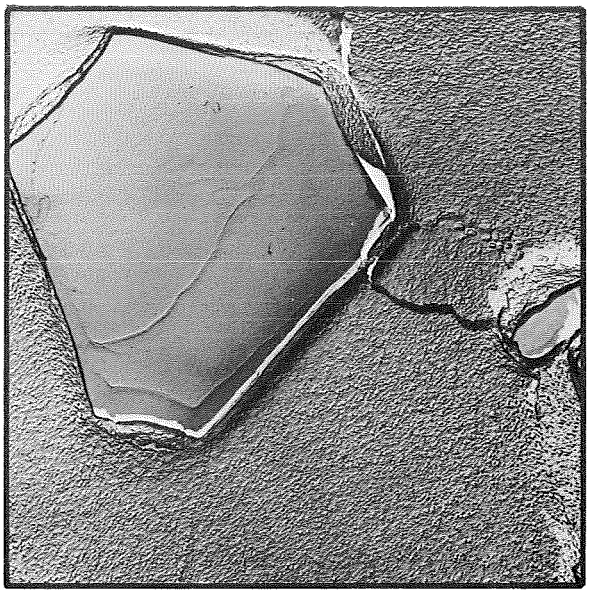

EM1611 5000X

2200°F / 2 hrs.

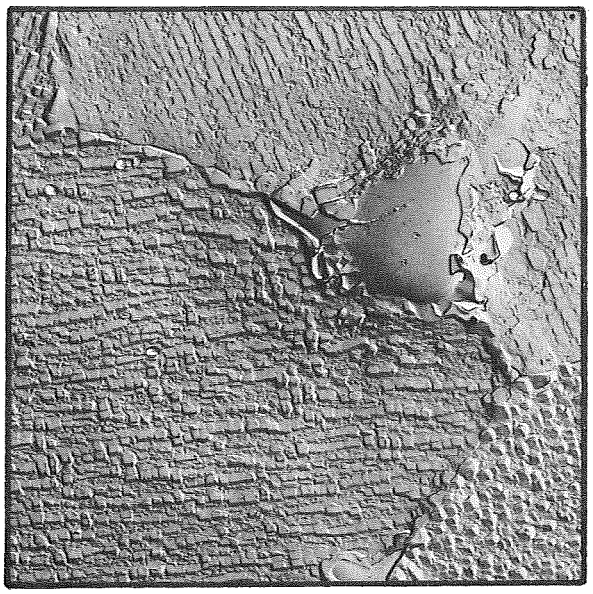

EM1620 5000X

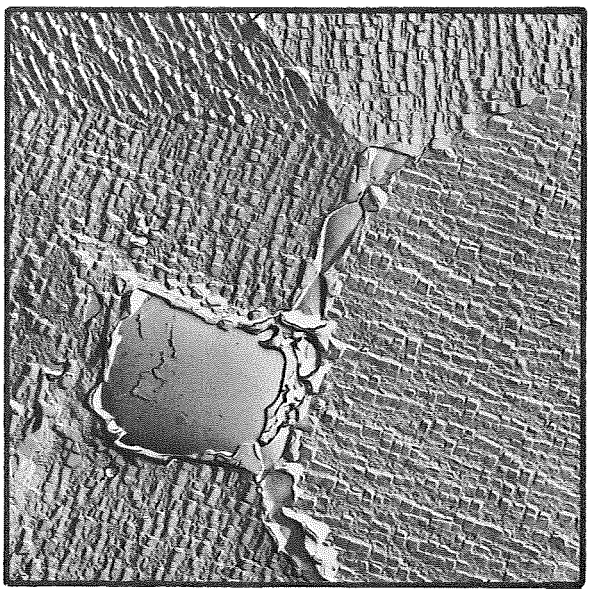

EM1621 5000X

2200°F / 2 hrs. + 1950°F / 2 hrs.

FIGURE 24: ELECTRON MICROGRAPHS OF UNITEMP AF2-1DA ILLUSTRATING THE VARIATIONS IN STRUCTURE AFTER EACH STAGE OF HEAT TREATMENT.

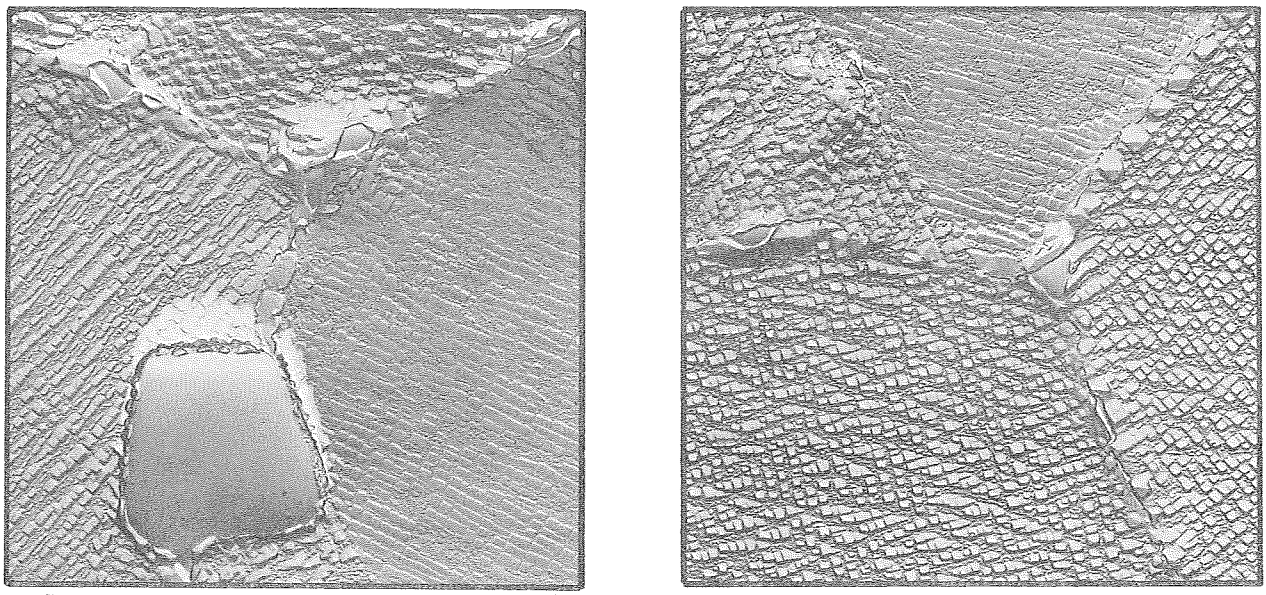

EM 1610 5000X EM1604 5000X

2200°F/2 hrs. + 1950°F/2 hrs. + 1400°F/16 hrs.

FIGURE 24: (continued) ELECTRON MICROGRAPHS OF UNITEMP AF2-IDA ILLUSTRATING THE VARIATIONS IN STRUCTURE AFTER EACH STAGE OF HEAT TREATMENT.

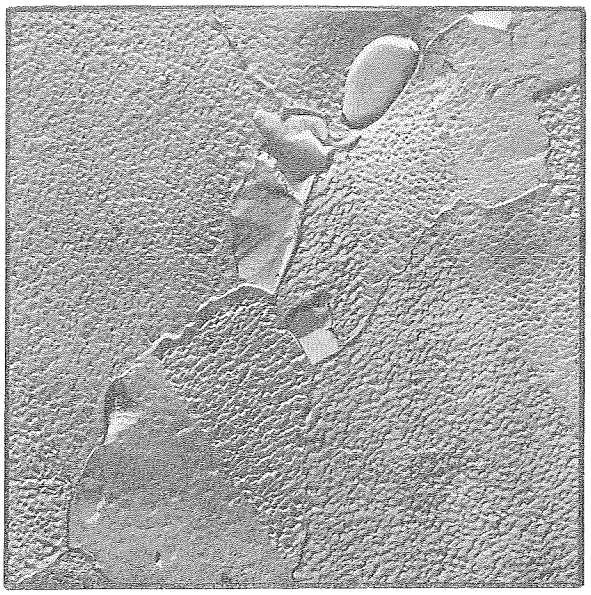

EM1740 5000X

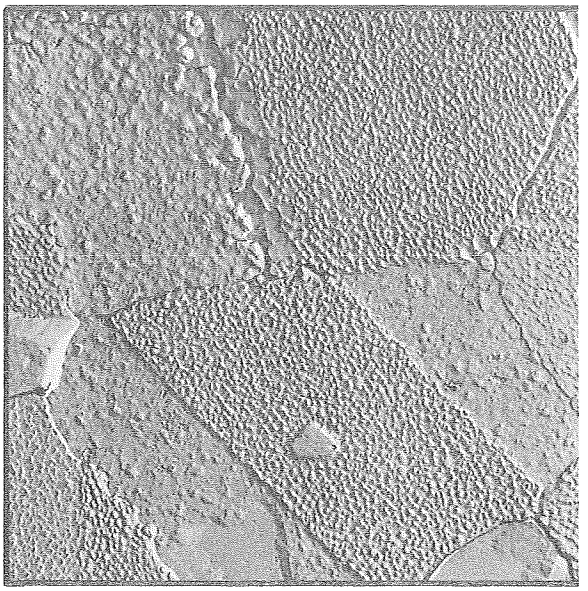

EM1739 5000X

2225°F / 1 hr.

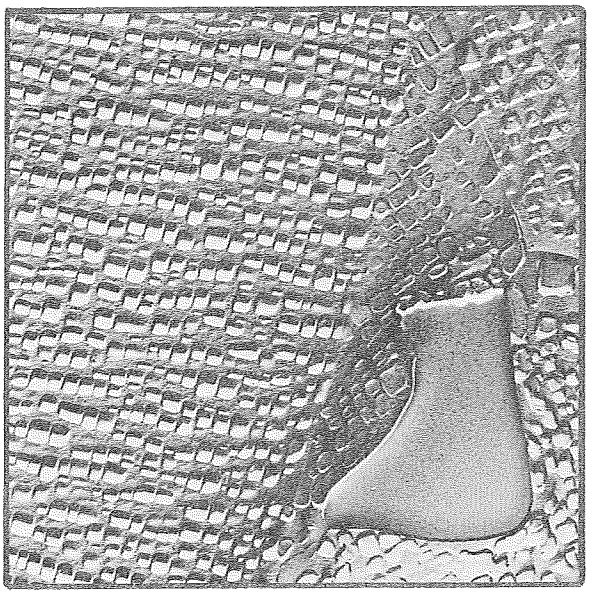

EM1870 5000X

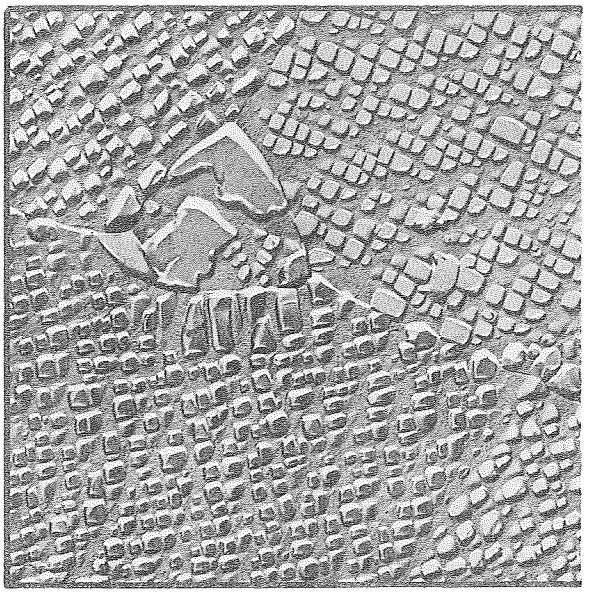

EM1873 5000 X

2225°F / 1 hr. + 1950°F / 16 hrs

FIGURE 25: ELECTRON MICROGRAPHS OF I 5 ILLUSTRATING THE VARIATIONS IN STRUCTURE AFTER EACH STAGE OF HEAT TREATMENT.

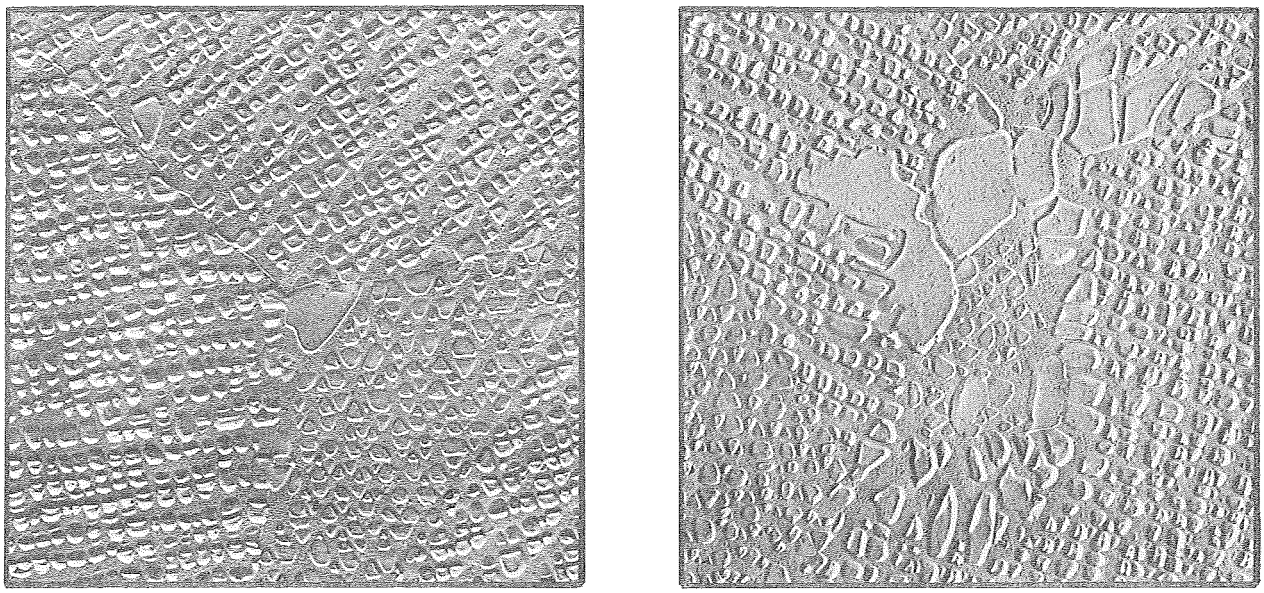

EM2092 5000X EM2096 5000X

2225°F / 1 hr. + 1950°F / 16 hrs. + 1400°F / 16 hrs.

FIGURE 25: (continued) ELECTRON MICROGRAPHS OF I 5 ILLUSTRATING THE VARIATIONS IN STRUCTURE AFTER EACH STAGE OF HEAT TREATMENT.

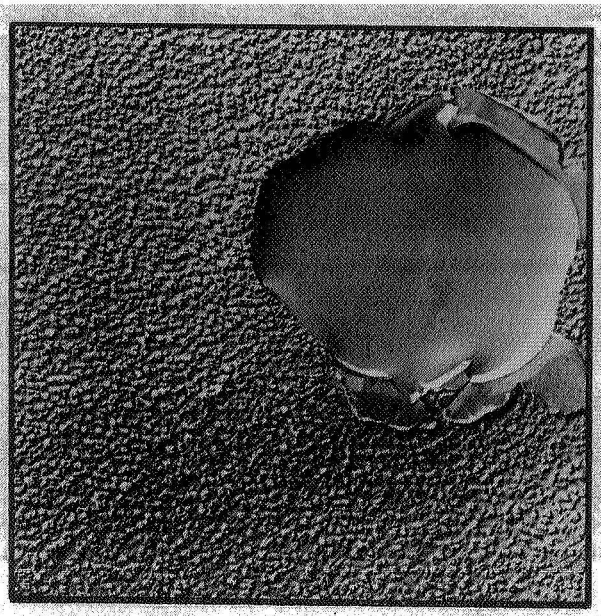

EM2144 5000X

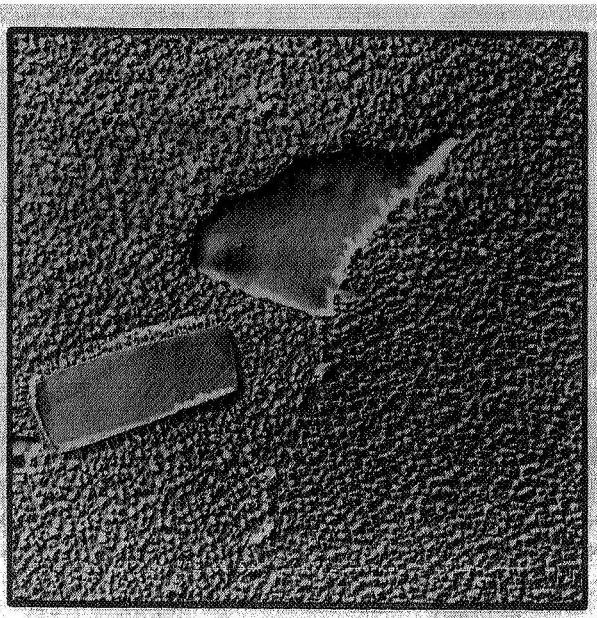

EM2145 5000X

2225°F / 2 hrs.

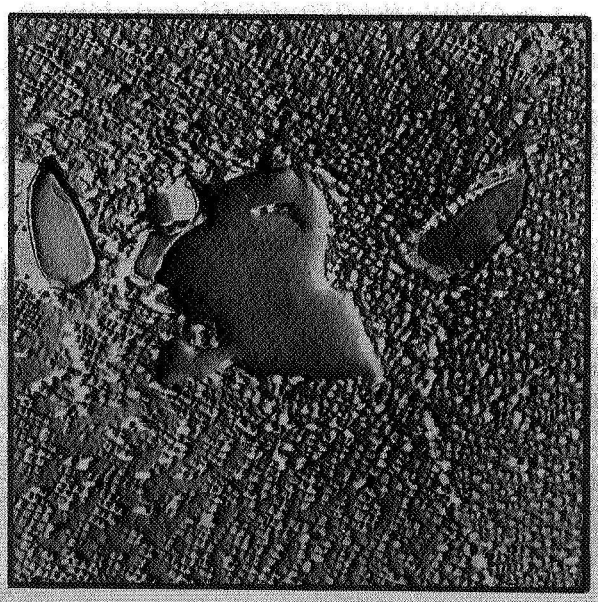

EM2150 5000 X

EM2153 5000 X

2225°F / 2 hrs. + 1900°F / 2 hrs.

FIGURE 26. ELECTRON MICROGRAPHS OF II b ILLUSTRATING THE VARIATIONS IN STRUCTURE AFTER EACH STAGE OF HEAT TREATMENT.

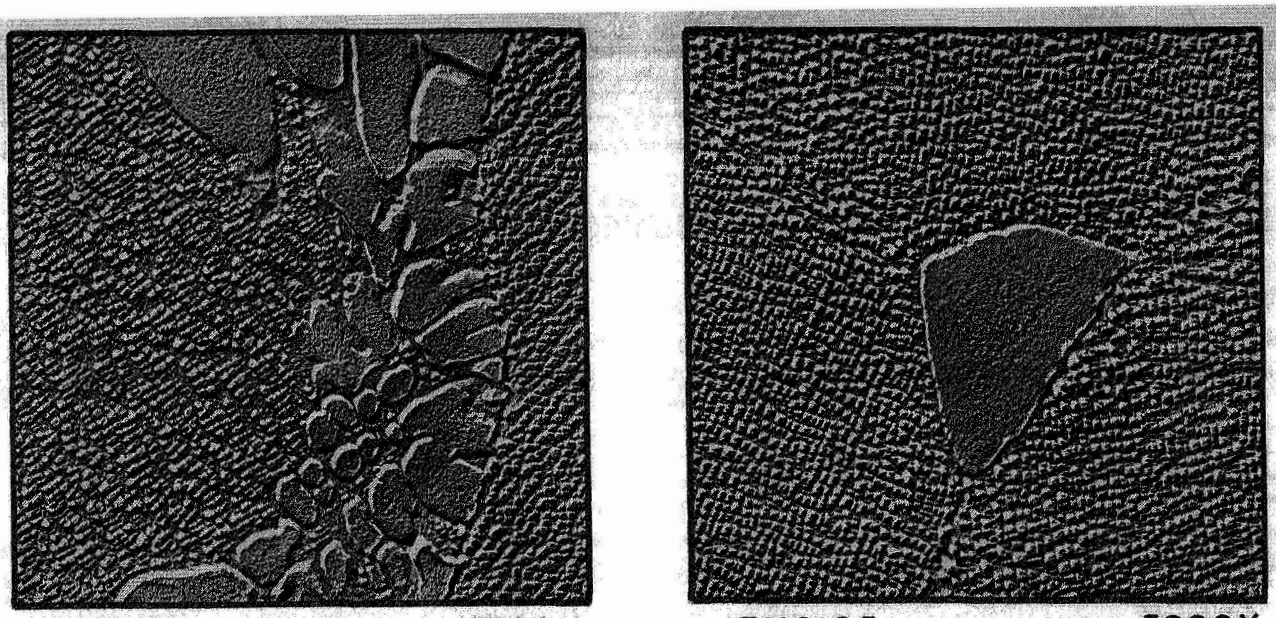


FIGURE 26 (continued) ELECTRON MICROGRAPHS OF II b ILLUSTRATING THE VARIATIONS IN STRUCTURE AFTER EACH STAGE OF HEAT TREATMENT

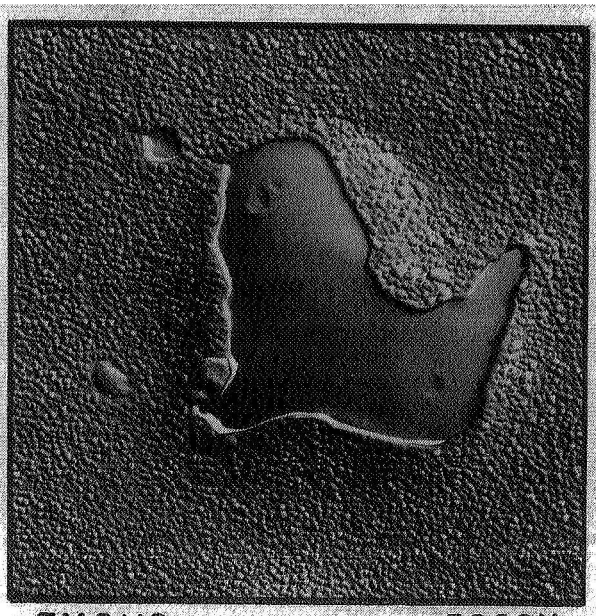

EM2119 5000X

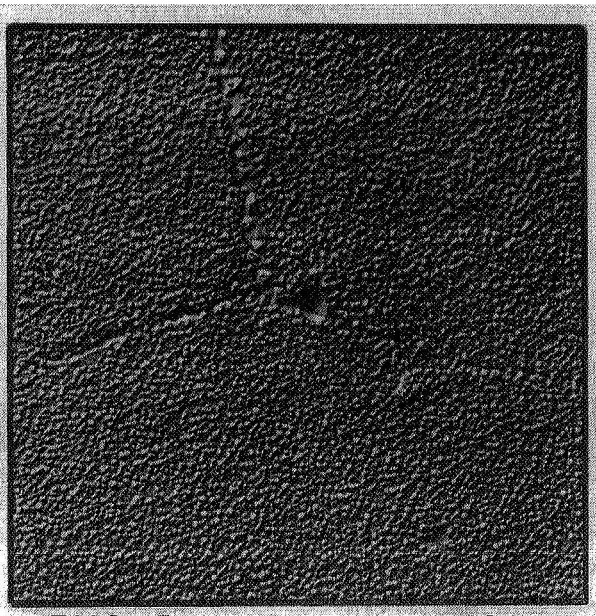

EM2115 5000X

2225°F / 2 hrs.

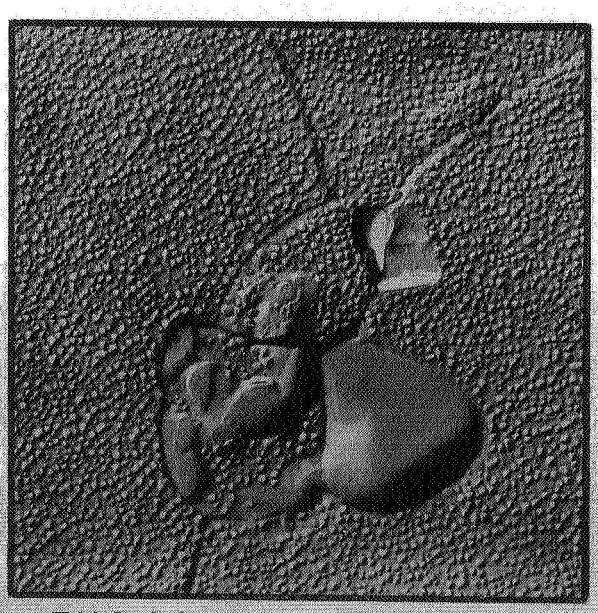

EM2188 5000X

EM2190 5000X

2225°F/2 hrs. + 1950°F / 2 hrs.

FIGURE 27 ELECTRON MICROGRAPHS OF IIIg mod ILLUSTRATING THE VARIATIONS IN STRUCTURE AFTER EACH STAGE OF HEAT TREATMENT

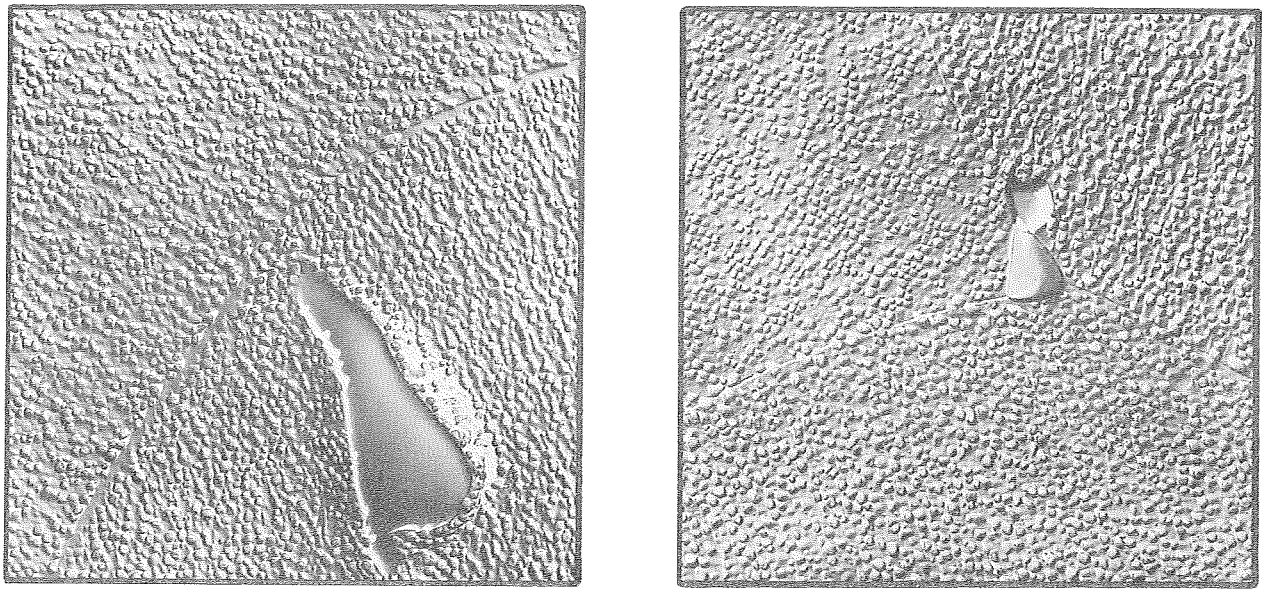

EM2137 5000X EM2139 5000X

2225°F/2 hrs. + 1950°F/2 hrs. + 1400°F/16 hrs.

FIGURE 27: (continued) ELECTRON MICROGRAPHS OF IIIg mod ILLUSTRATING THE VARIATIONS IN STRUCTURE AFTER EACH STAGE OF HEAT TREATMENT.

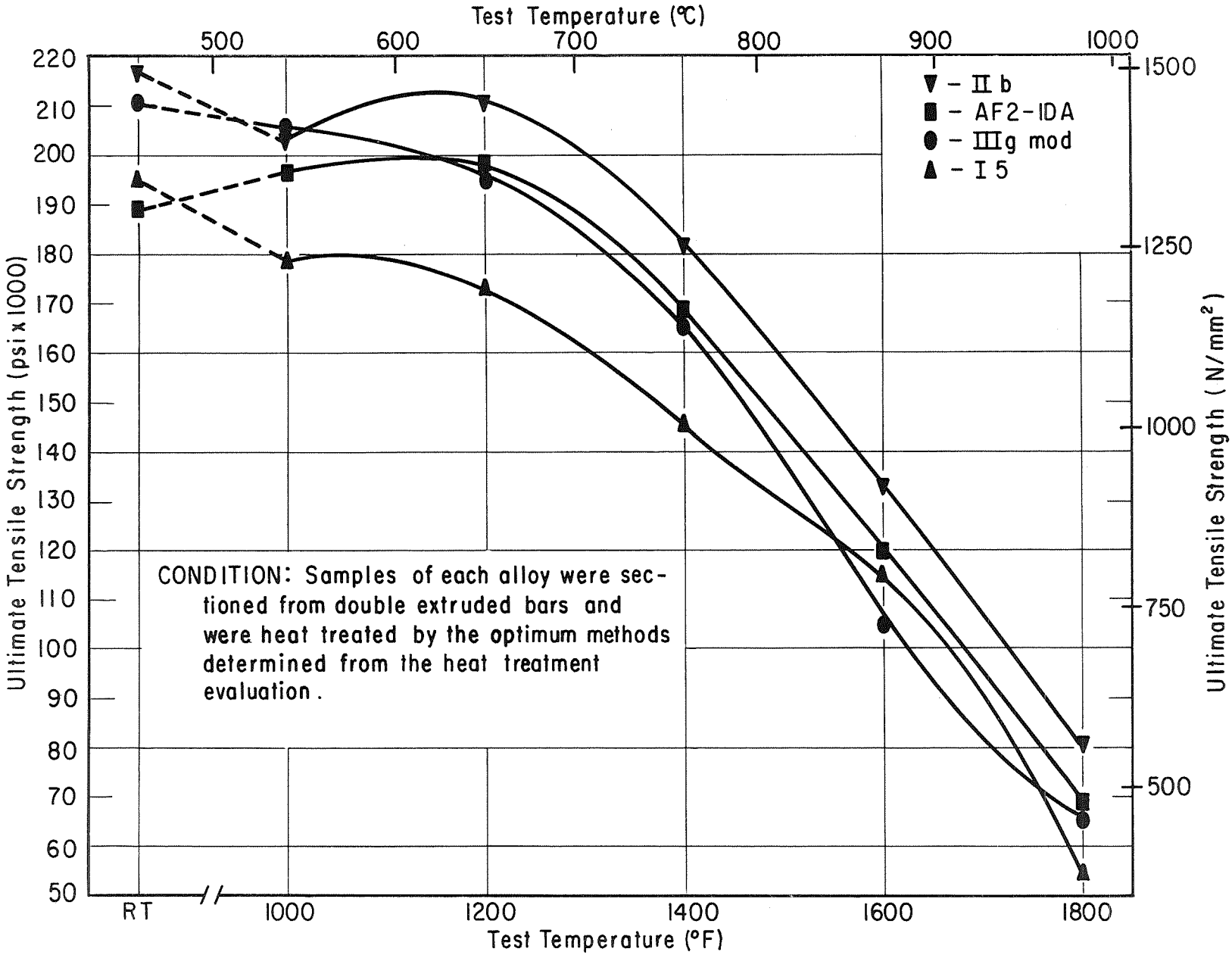


FIGURE 28: ULTIMATE TENSILE STRENGTH versus TEST TEMPERATURE FOR TASK II ALLOYS.

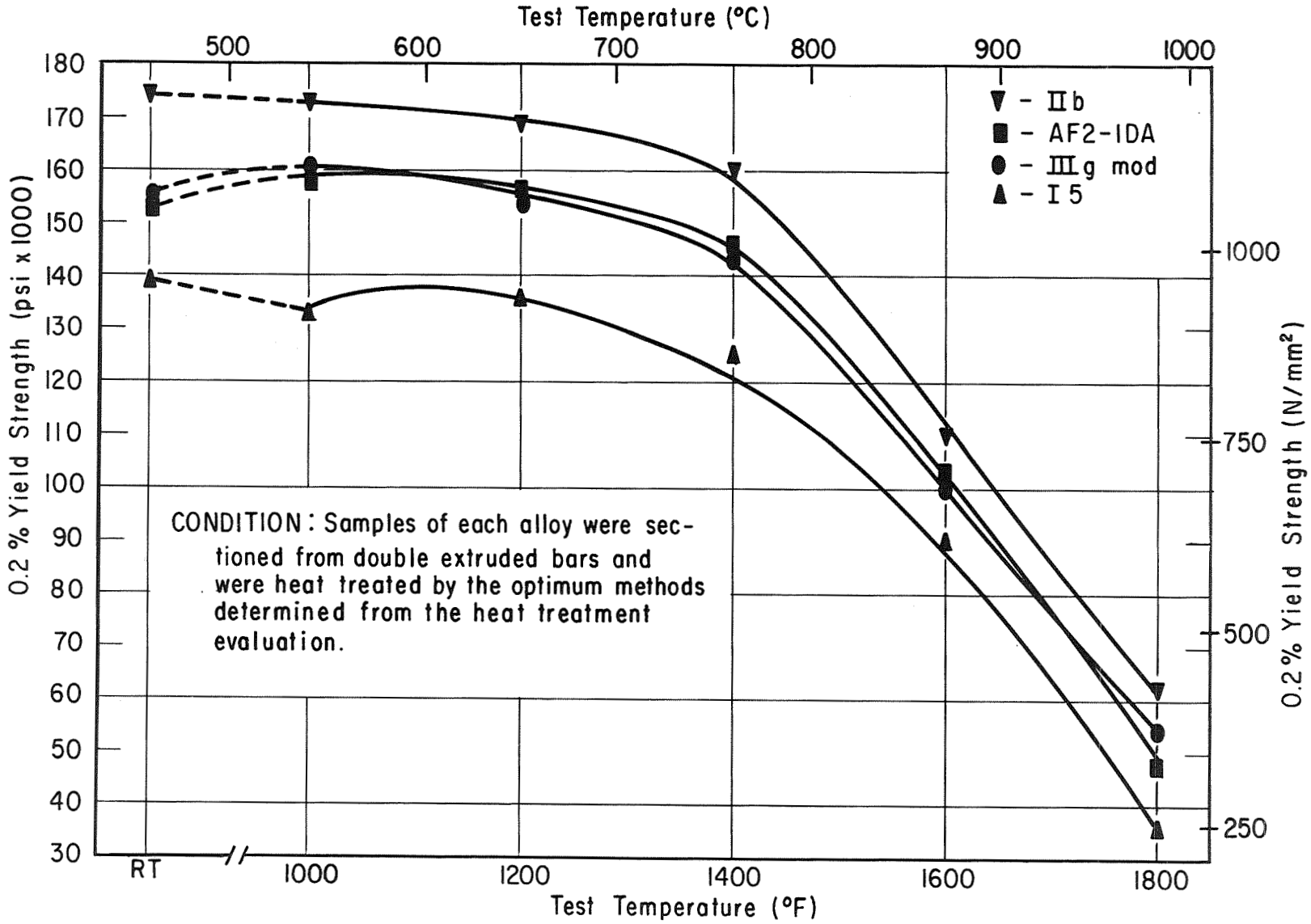


FIGURE 29 : 0.2 PERCENT YIELD STRENGTH versus TEST TEMPERATURE FOR TASK II ALLOYS.

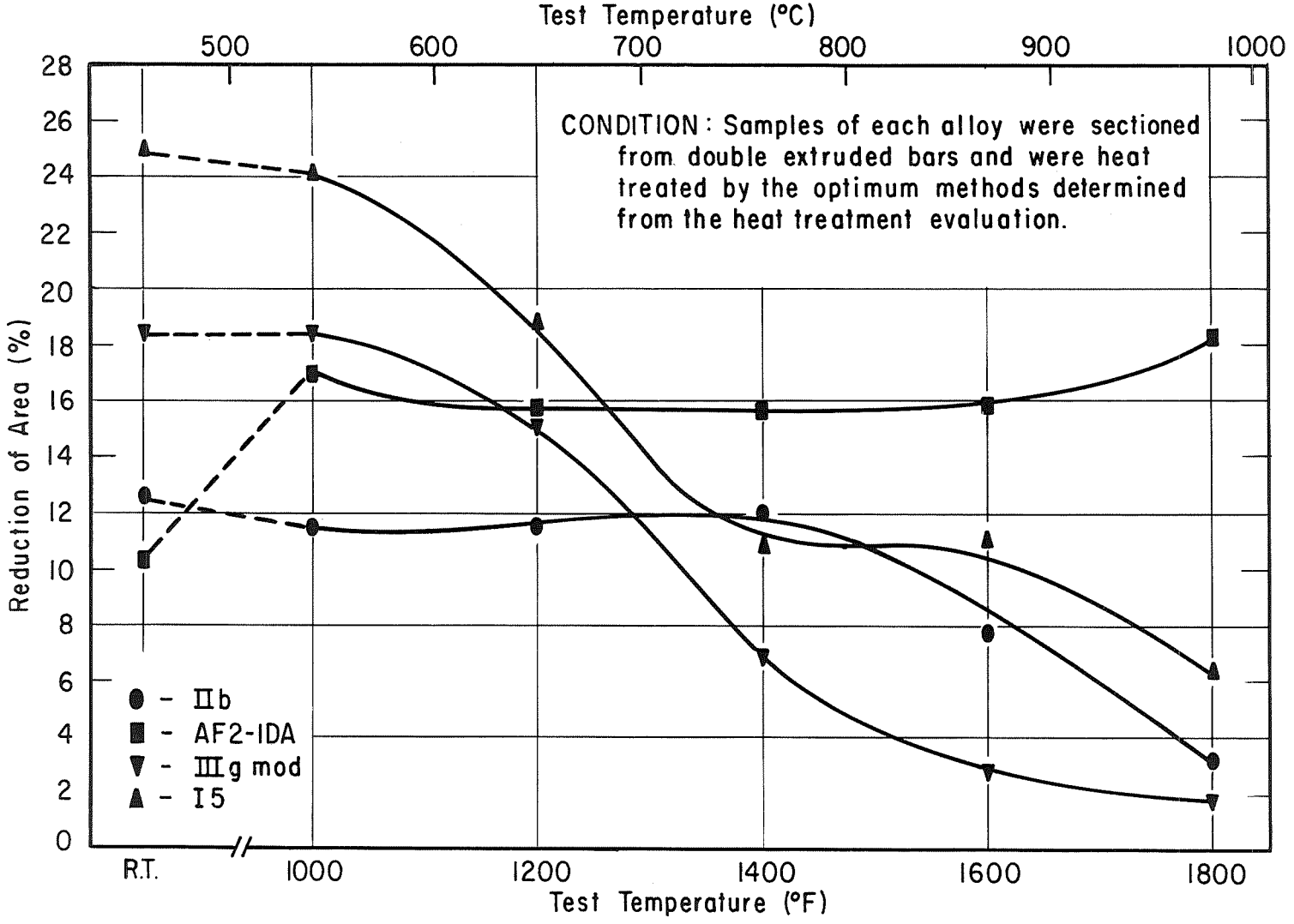


FIGURE 30: TENSILE DUCTILITY VERSUS TEST TEMPERATURE FOR TASK II ALLOYS.

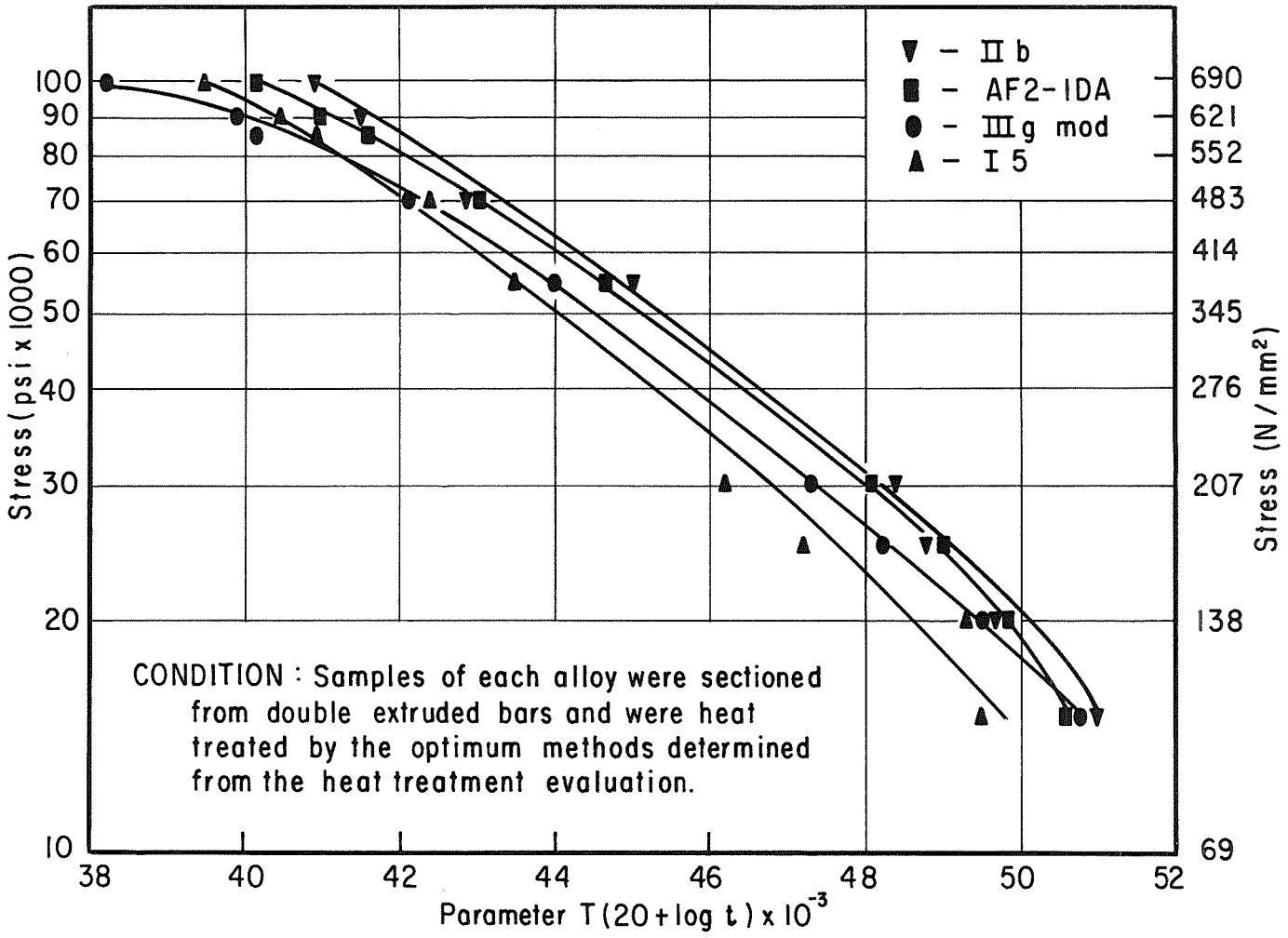


FIGURE 31: LARSON-MILLER PARAMETER CURVES SHOWING STRESS RUPTURE PROPERTIES OF TASK II ALLOYS.

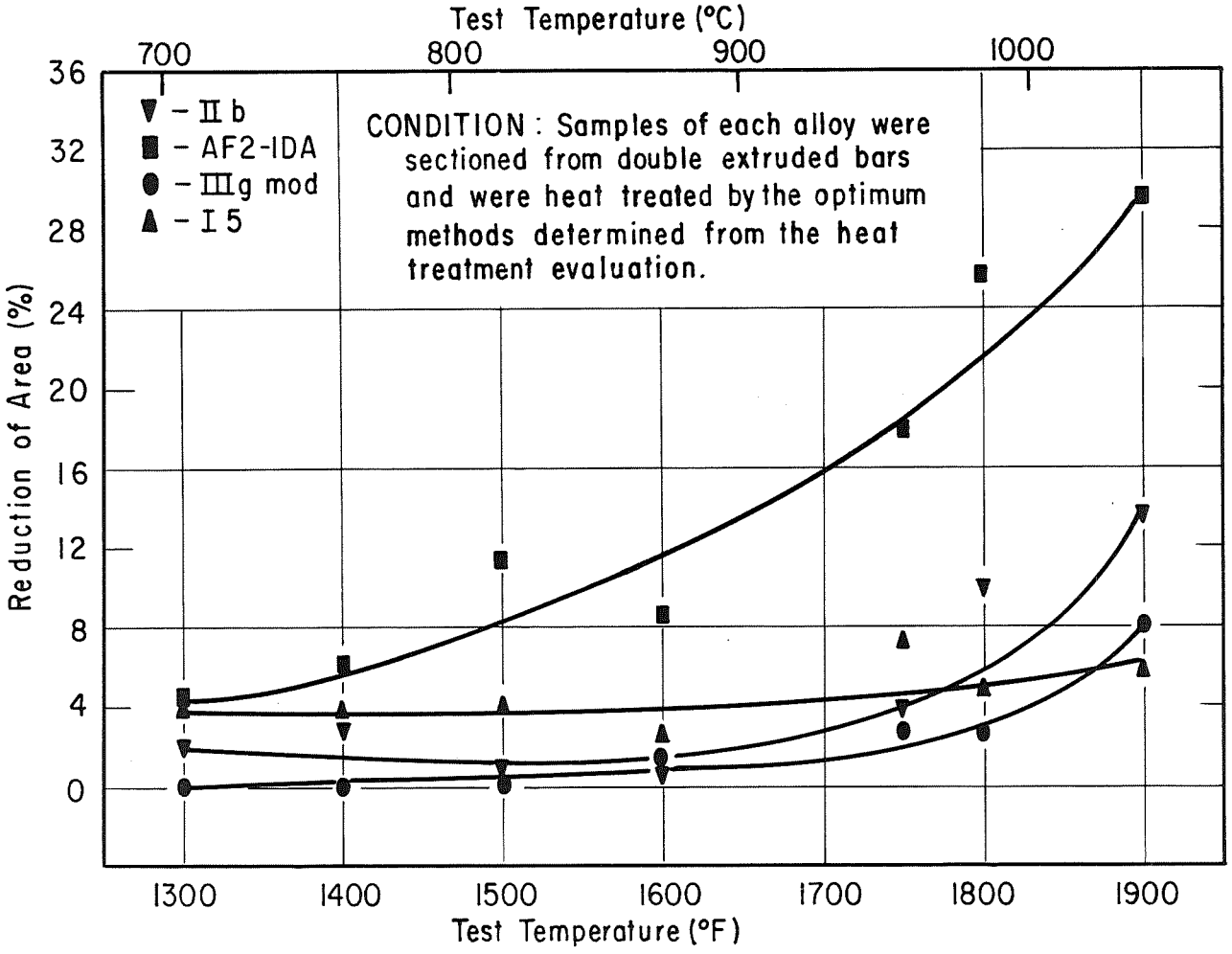


FIGURE 32 : STRESS RUPTURE DUCTILITY versus TEST TEMPERATURE FOR TASK II ALLOYS.

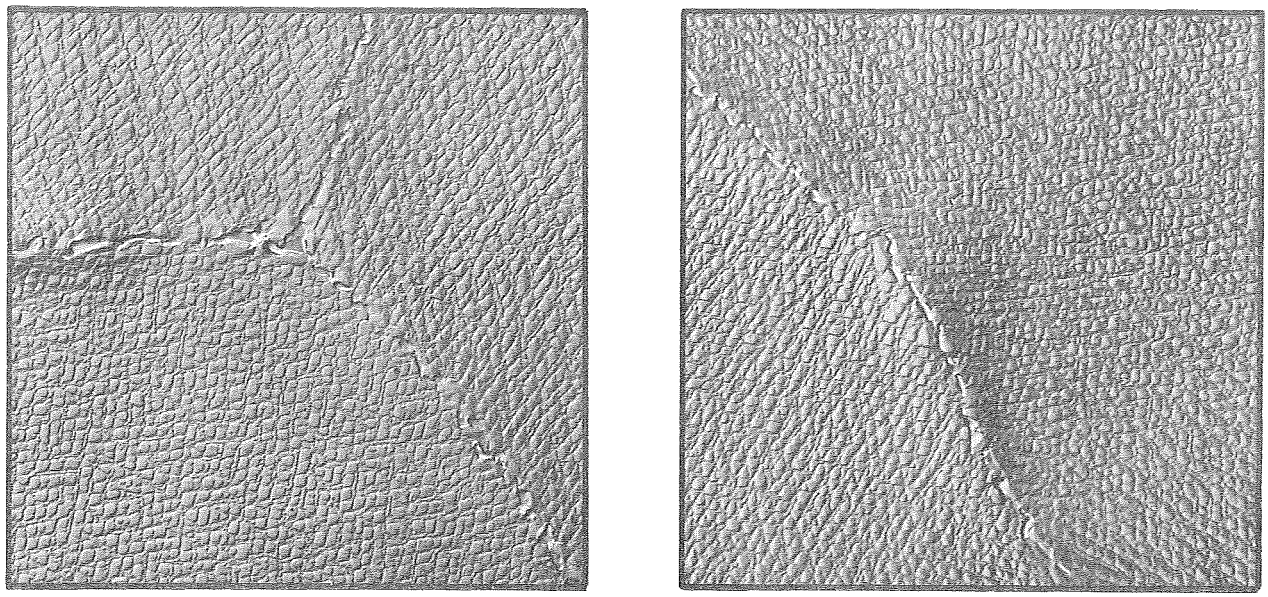

EM1709 5000X EM1710 5000X

1400°F - 90,000 psi
(Rupture Life - 111.2 hours)

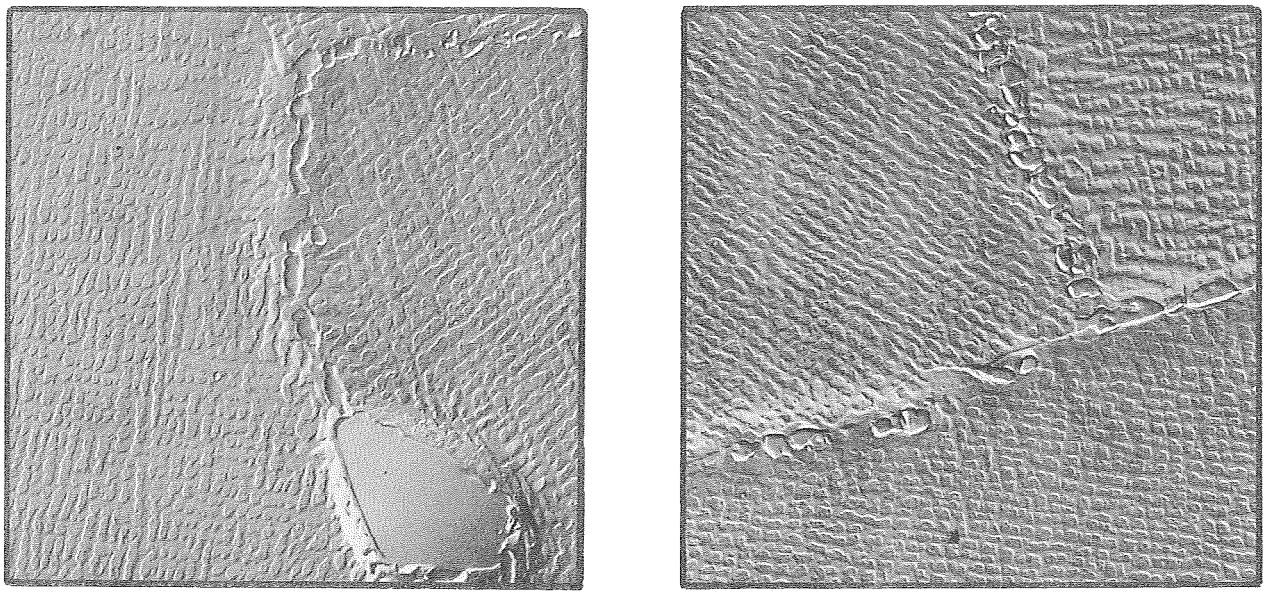

EM1714 5000X EM1713 5000X

1600°F - 55,000 psi
(Rupture Life - 53.3 hours)

FIGURE 33: MICROSTRUCTURES OF DOUBLE EXTRUDED UNITEMP AF2-IDA AFTER STRESS RUPTURE TESTING AT VARIOUS CONDITIONS.

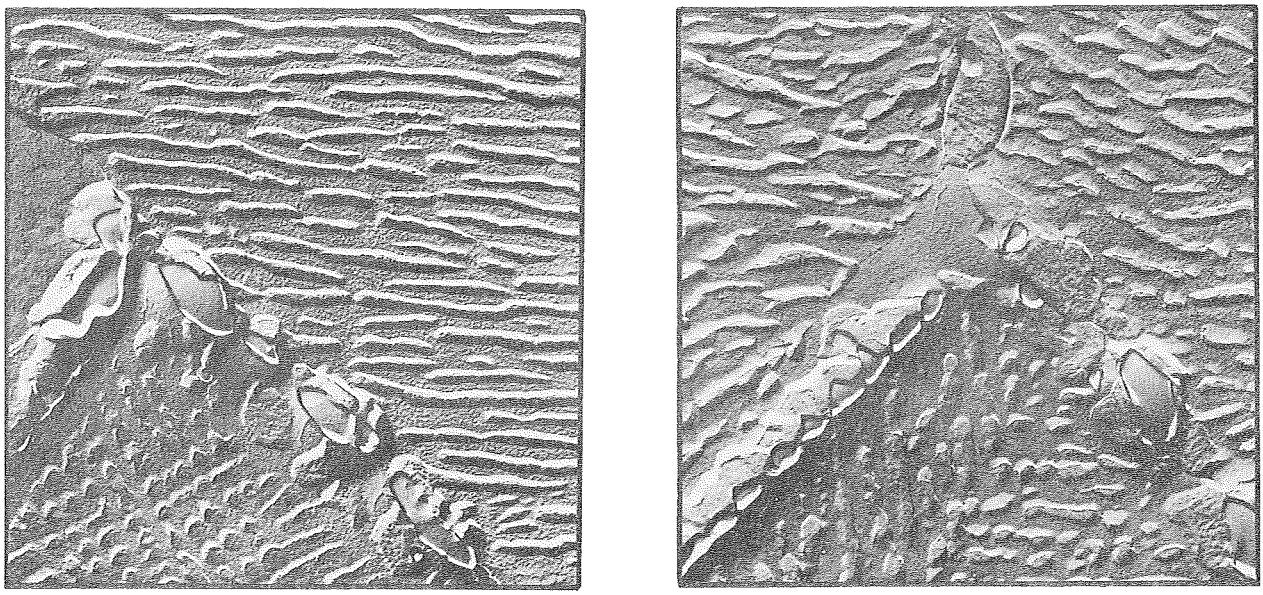

EM1719 5000X EM1722 5000X

1900°F - 15,000 psi
(Rupture Life - 27.7 hours)

FIGURE 33: (continued) MICROSTRUCTURES OF DOUBLE EXTRUDED UNITEMP AF2-IDA AFTER STRESS RUPTURE TESTING AT VARIOUS CONDITIONS.

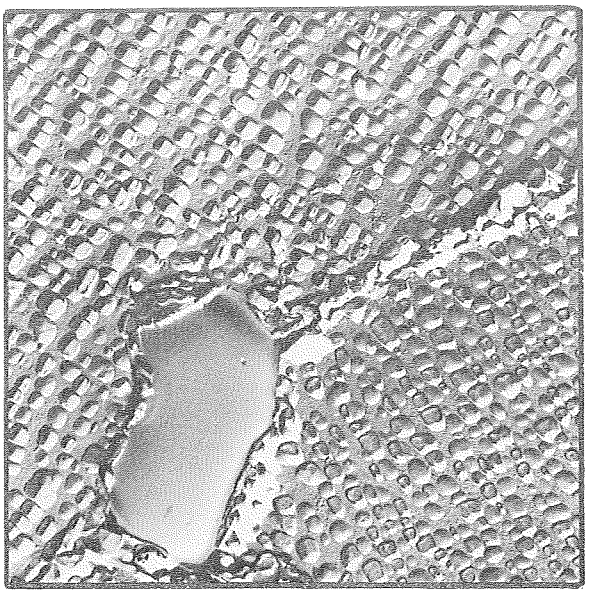

EM1908 5000X

EM1907 5000X

1400°F - 90,000 psi
(Rupture Life - 110.2 hours)

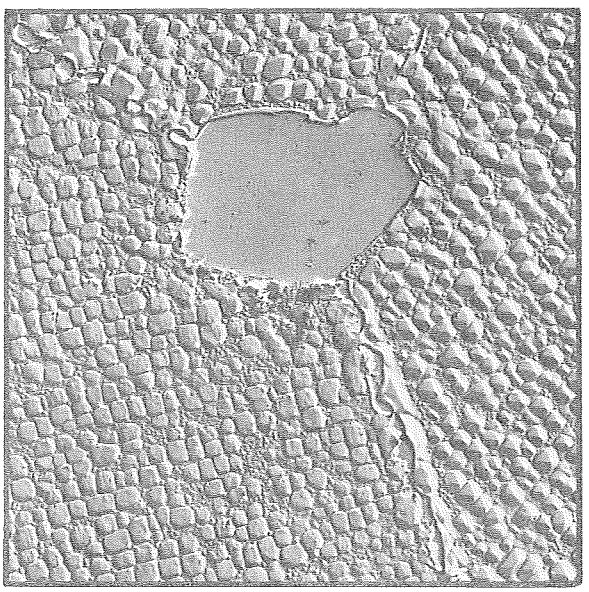

EM1727 5000X

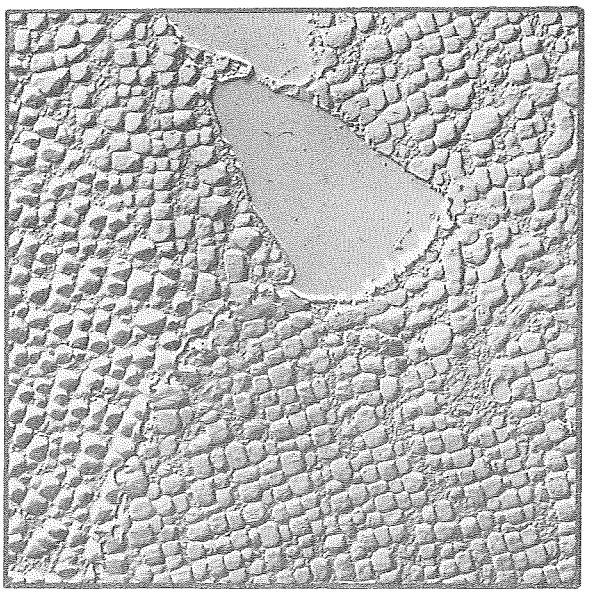

EM1729 5000X

1600°F - 55,000 psi
(Rupture Life - 10.7 hours)

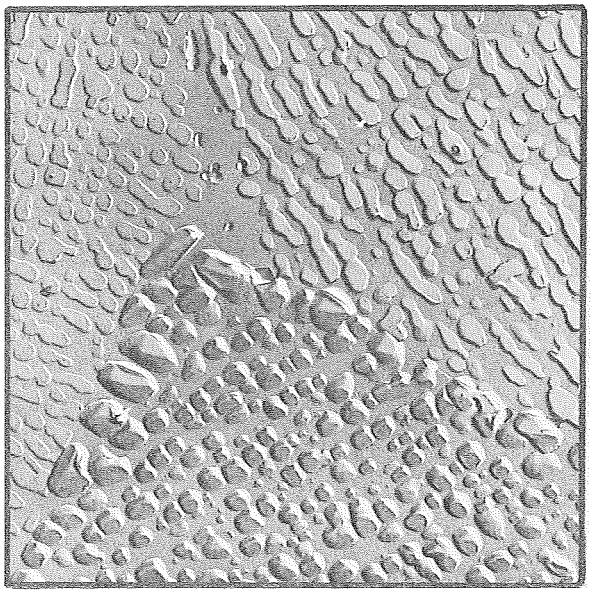

EM 1915 5000 X

EM1916 5000 X

1900°F - 15,000 psi
(Rupture Life - 7.9 hours)

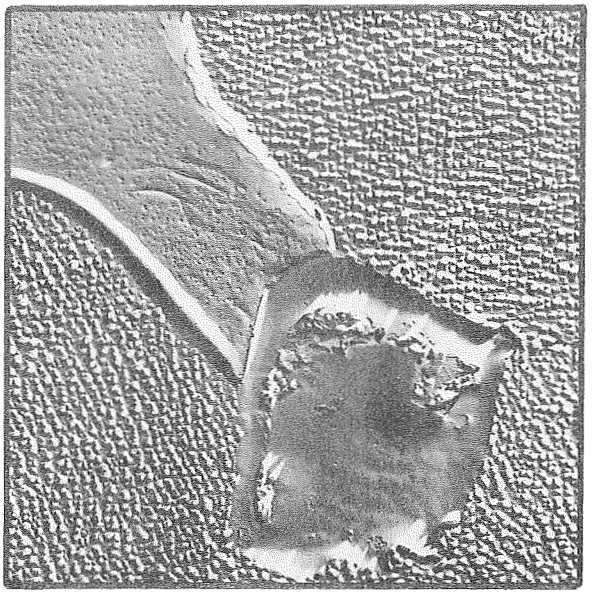

EM2036 5000X

EM2038 5000X

1400°F – 90,000 psi
(Rupture Life – 201.7 hours)

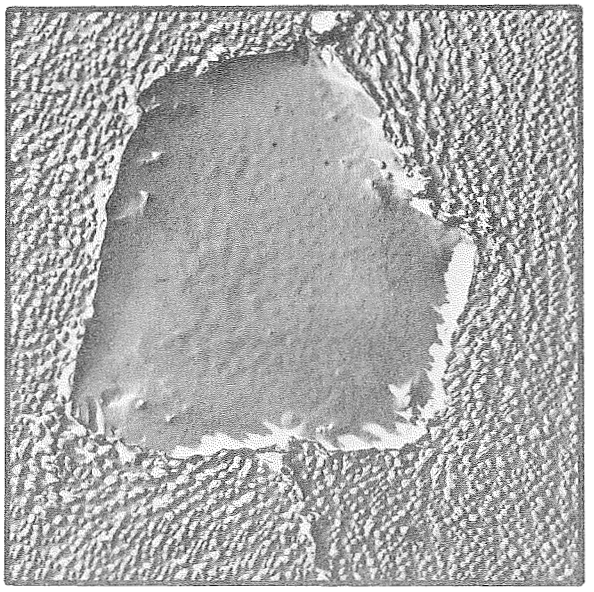

EM2041 5000X

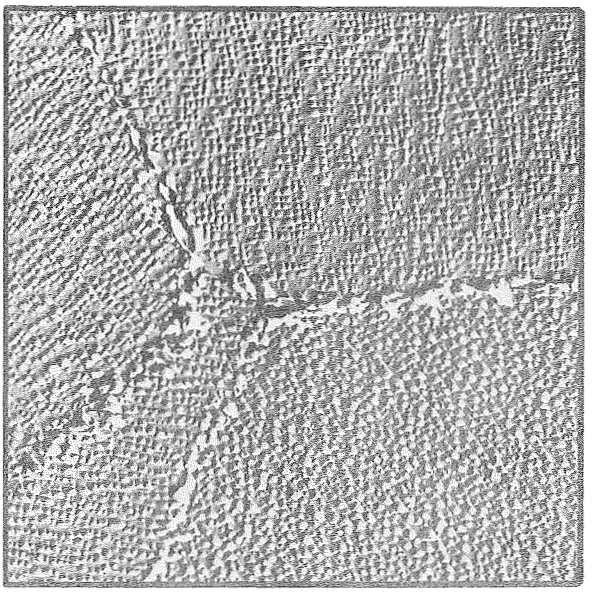

EM2042 5000X

1600°F – 55,000 psi

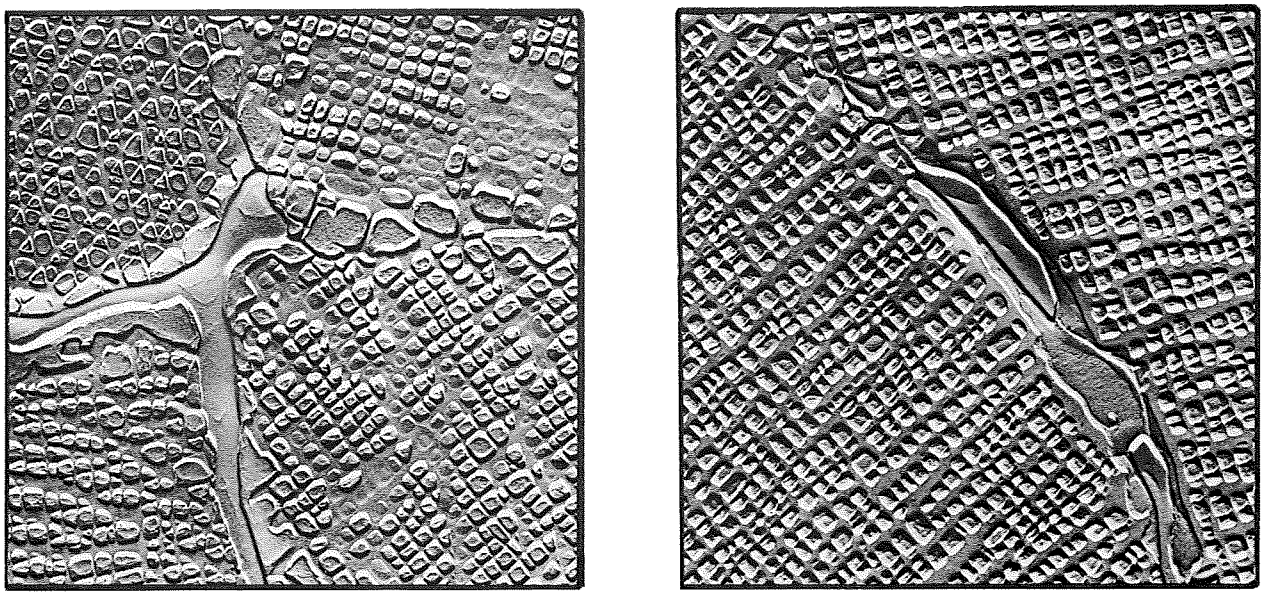

EM2100 5000X EM2099 5000X

1900°F - 15,000 psi

(Rupture Life - 50.1 hours)

FIGURE 35 : (continued) MICROSTRUCTURES OF DOUBLE EXTRUDED IIb AFTER STRESS RUPTURE TESTING AT VARIOUS CONDITIONS.

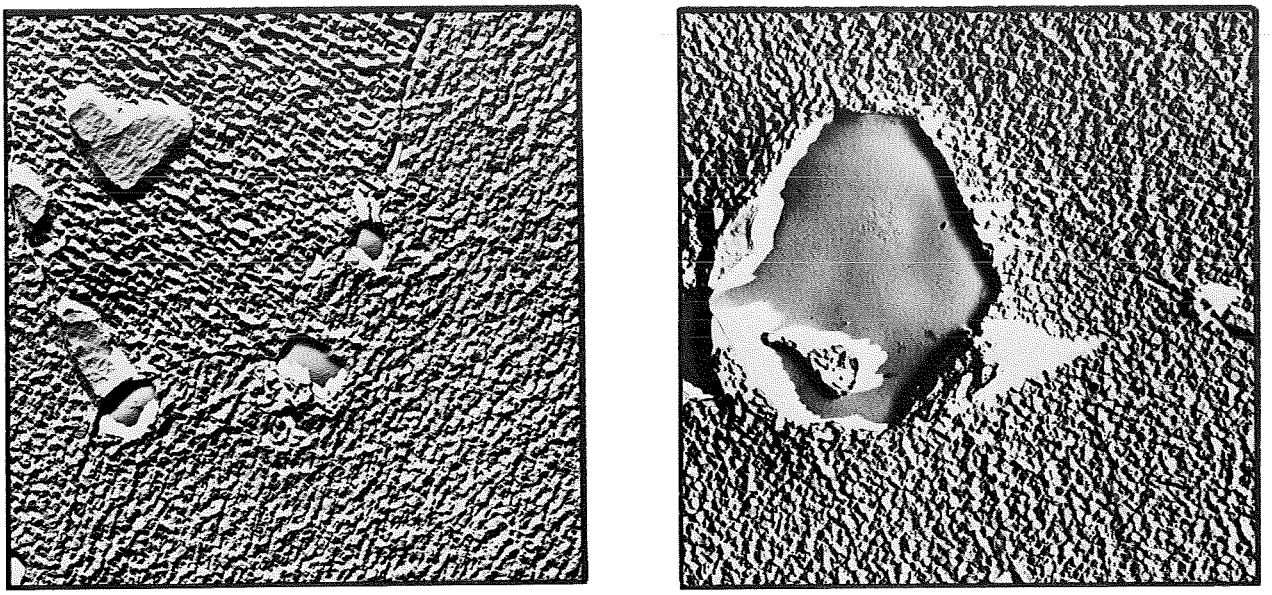

EM2022 5000X EM2023 5000X

1400°F - 90,000 psi
(Rupture Life - 38.5 hours)

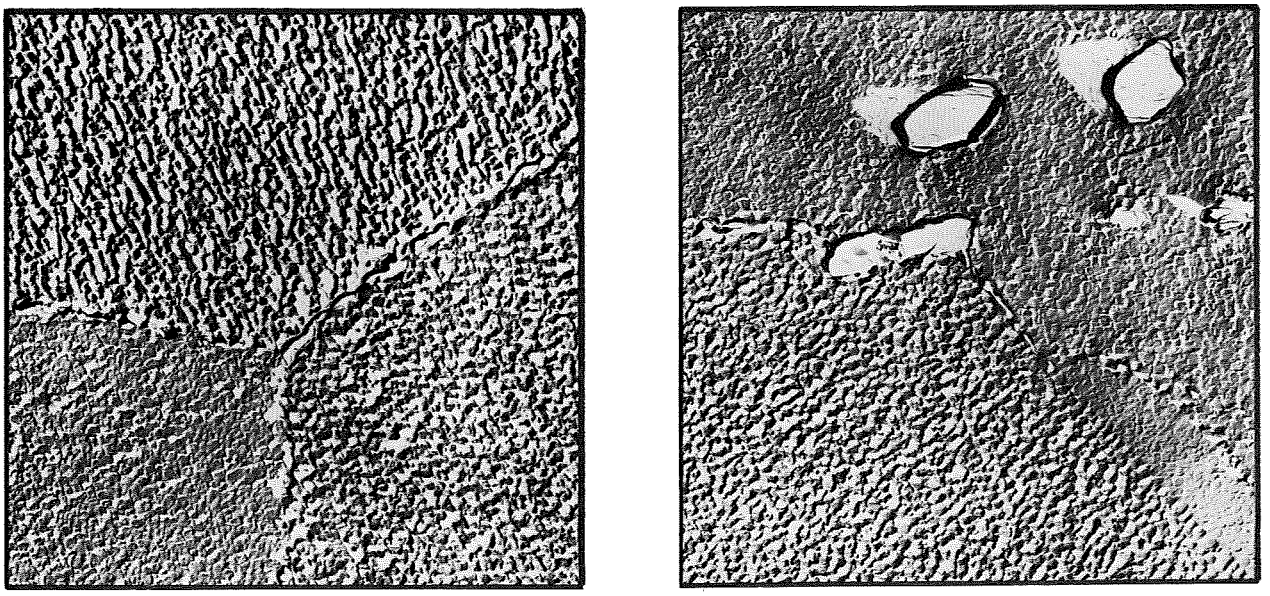

EM2029 5000X EM2030 5000X

1600°F - 55,000 psi
(Rupture Life - 25.6 hours)

FIGURE 36: MICROSTRUCTURES OF DOUBLE EXTRUDED IIIg mod AFTER STRESS RUPTURE TESTING AT VARIOUS CONDITIONS.

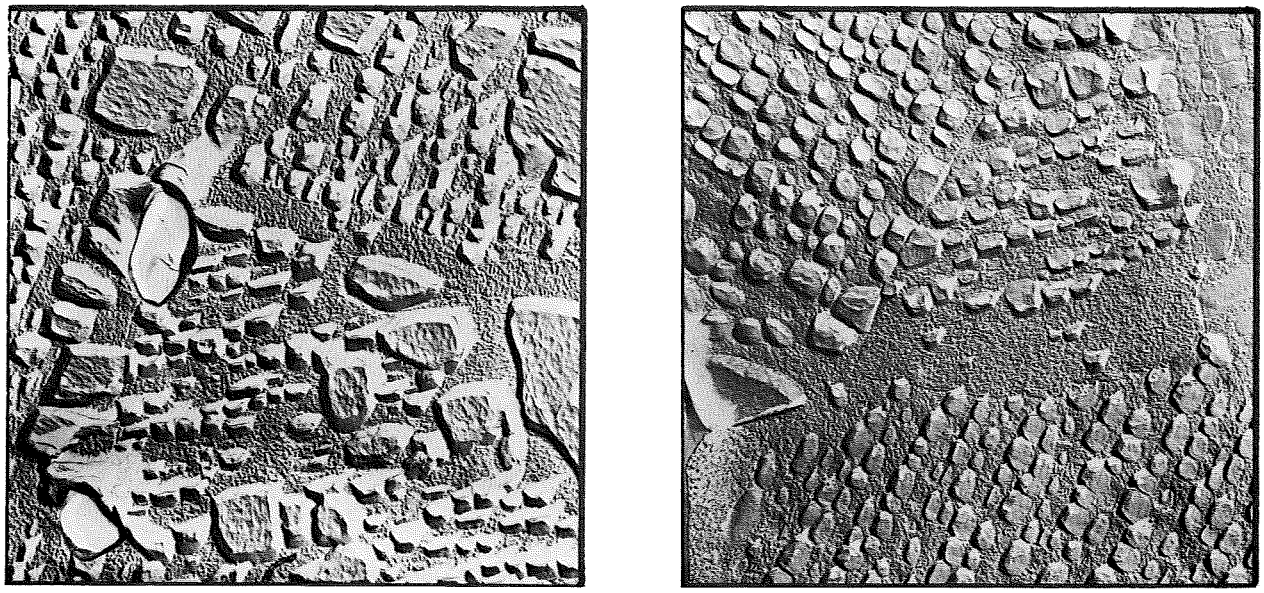

EM 2035 5000X EM2032 5000X

1900°F – 15,000 psi
(Rupture Life – 76.4 hours)

FIGURE 36: (continued) MICROSTRUCTURES OF DOUBLE EXTRUDED IIIg mod AFTER STRESS RUPTURE TESTING AT VARIOUS CONDITIONS.

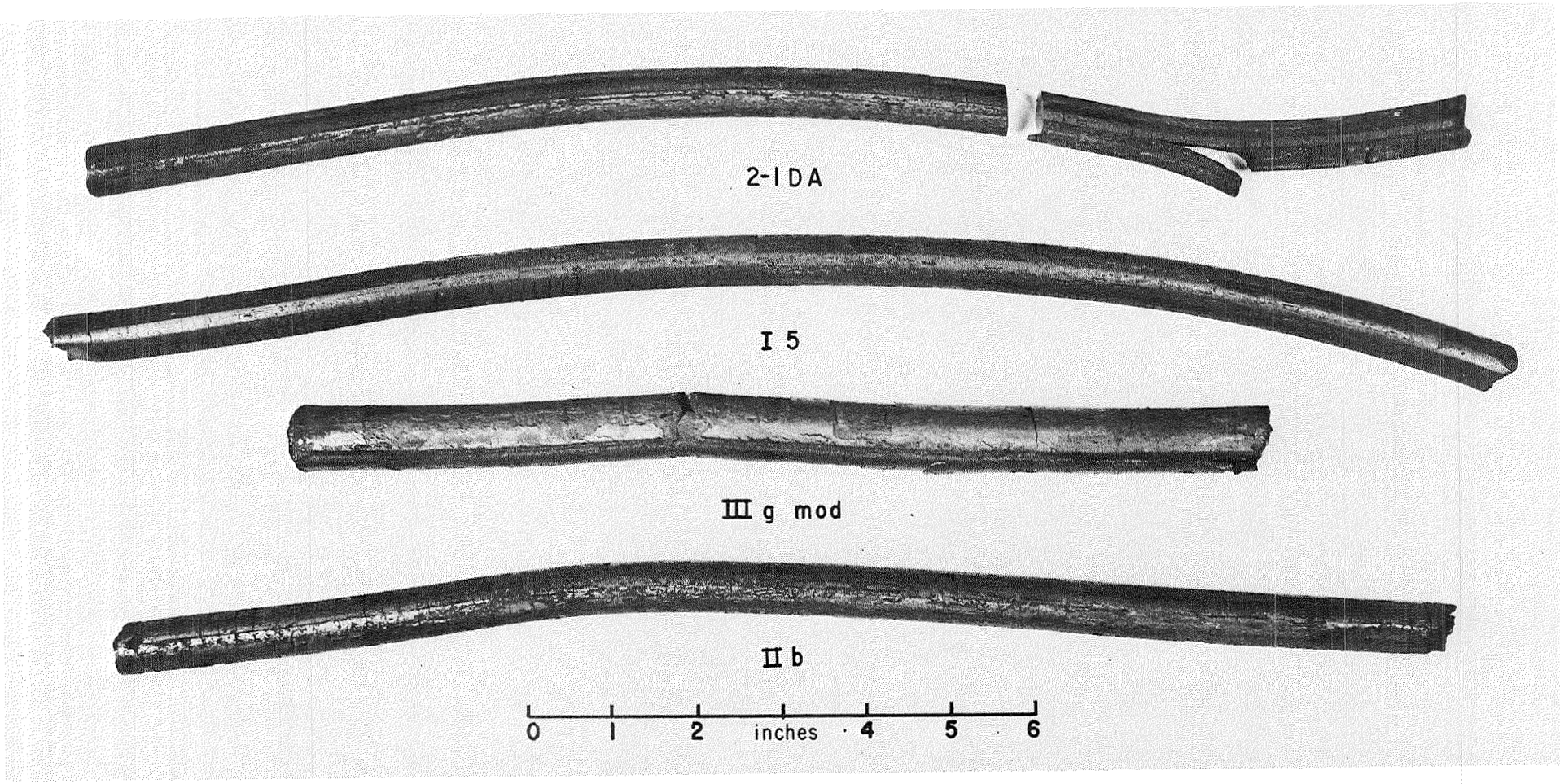


M1359

FIGURE 37: TASK II ALLOYS ROLLED FROM $1\frac{1}{8}$ INCH DIAMETER CANNED SINGLE EXTRUDED BILLETS TO 0.6 INCH DIAMETER BARS.

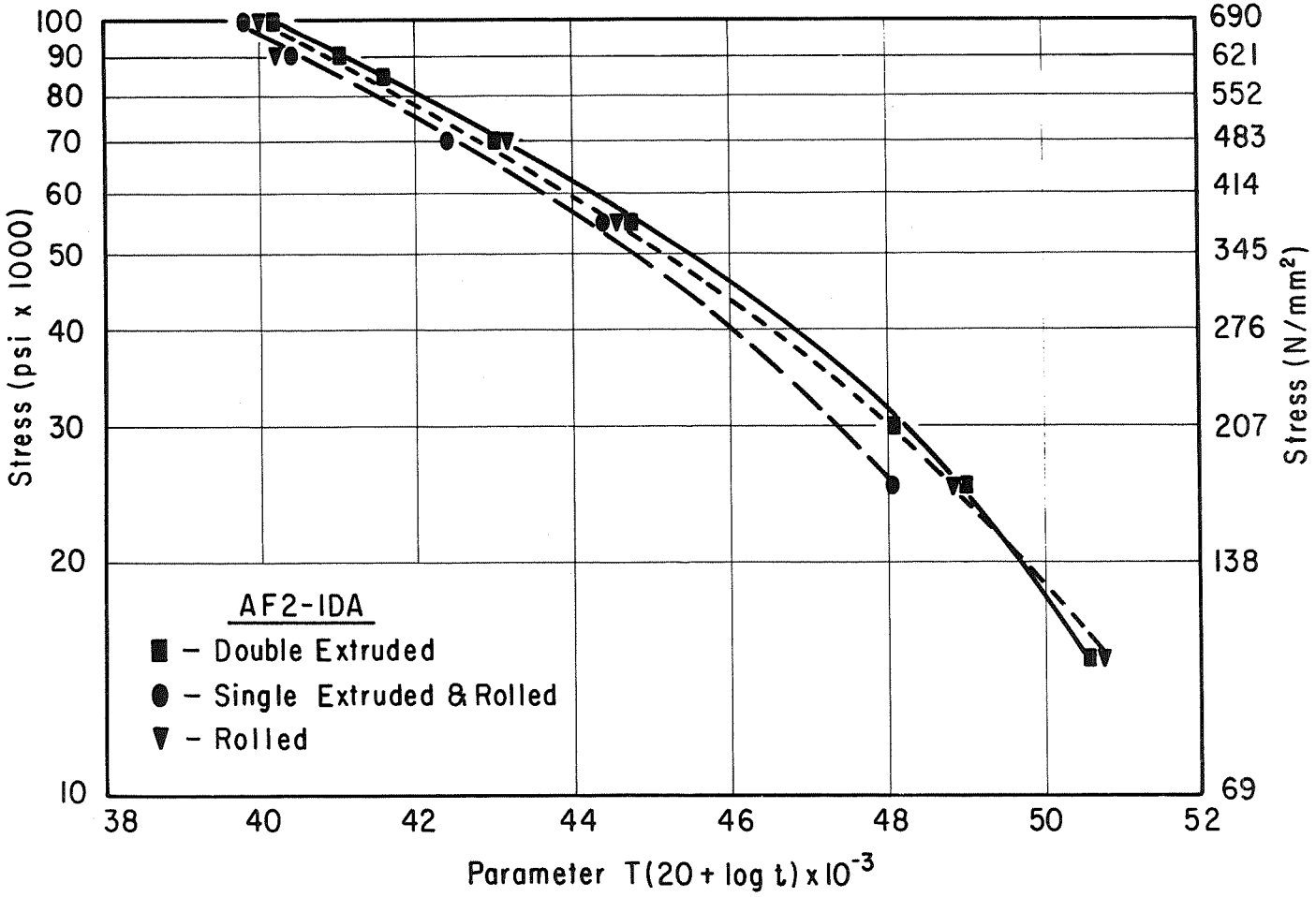


FIGURE 38: LARSON-MILLER PARAMETER CURVES SHOWING STRESS RUPTURE PROPERTIES OF UNITEMP AF2-IDA AFTER VARIOUS METHODS OF PROCESSING.

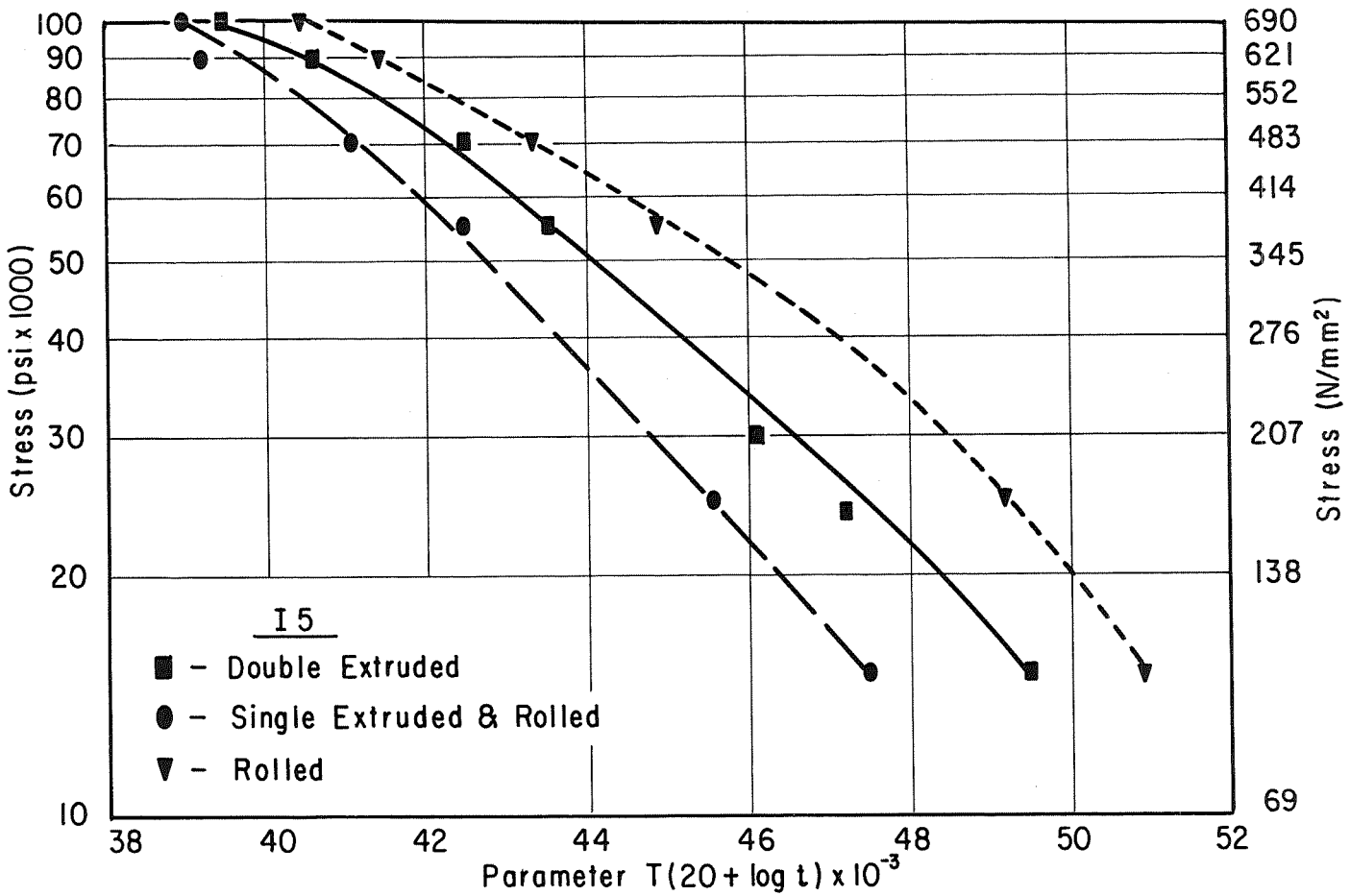


FIGURE 39: LARSON-MILLER PARAMETER CURVES SHOWING STRESS RUPTURE PROPERTIES OF I 5 AFTER VARIOUS METHODS OF PROCESSING.

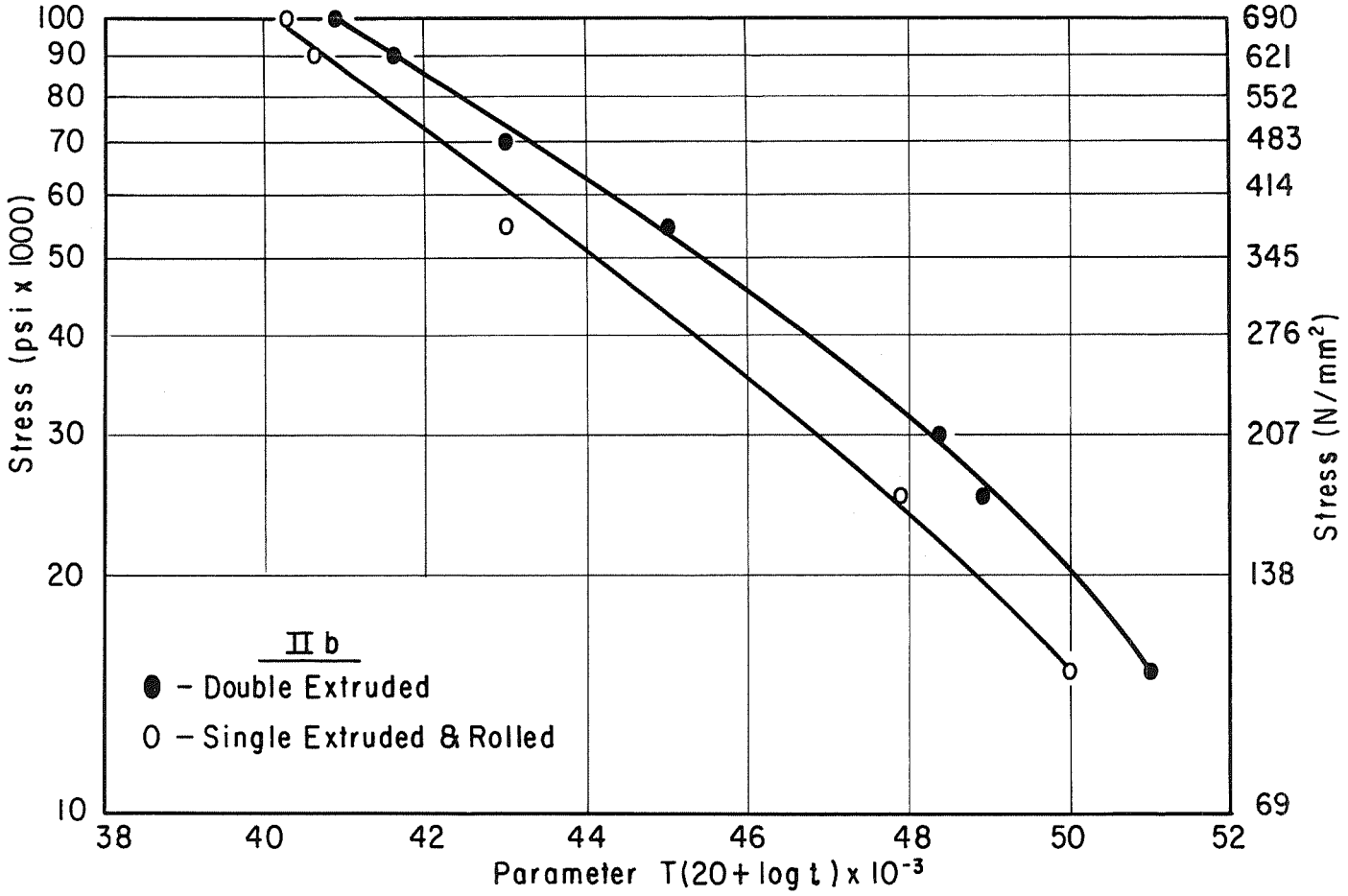


FIGURE 40 : LARSON-MILLER PARAMETER CURVES SHOWING STRESS RUPTURE PROPERTIES OF IIb AFTER VARIOUS METHODS OF PROCESSING.

R21999 200X

Rolled Directly from Ingot
S/R Life at 1300°F/100ksi = 841.5 hours

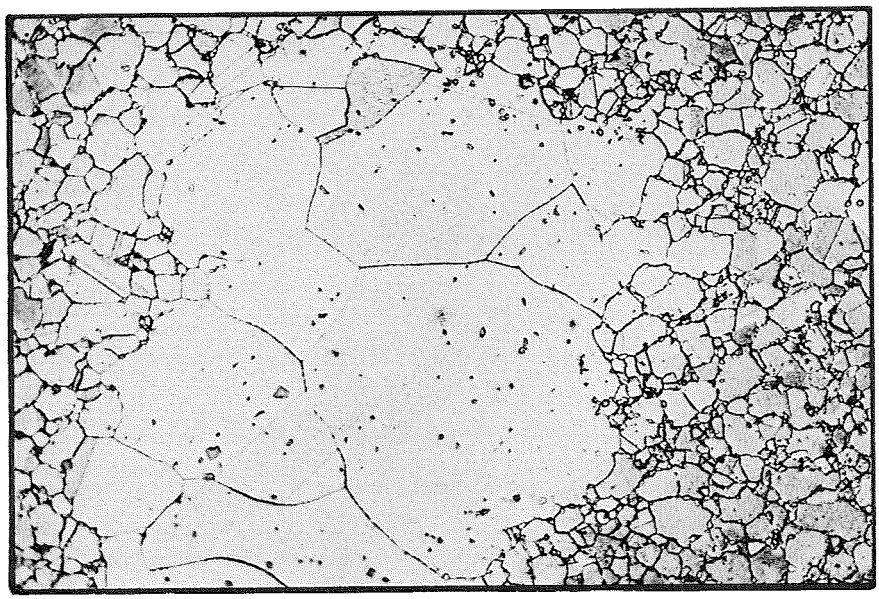

R22002-8 200X

Single Extruded and Rolled
S/R Life at 1300°F/100 ksi = 138.2 hours

FIGURE 41: OPTICAL MICROGRAPHS OF I5 STRESS RUPTURE SAMPLES ILLUSTRATING THE STRUCTURAL VARIATIONS WHICH OCCUR DEPENDING ON THE METHOD OF PROCESSING. SAME HEAT TREATMENT WAS USED FOR BOTH SAMPLES.

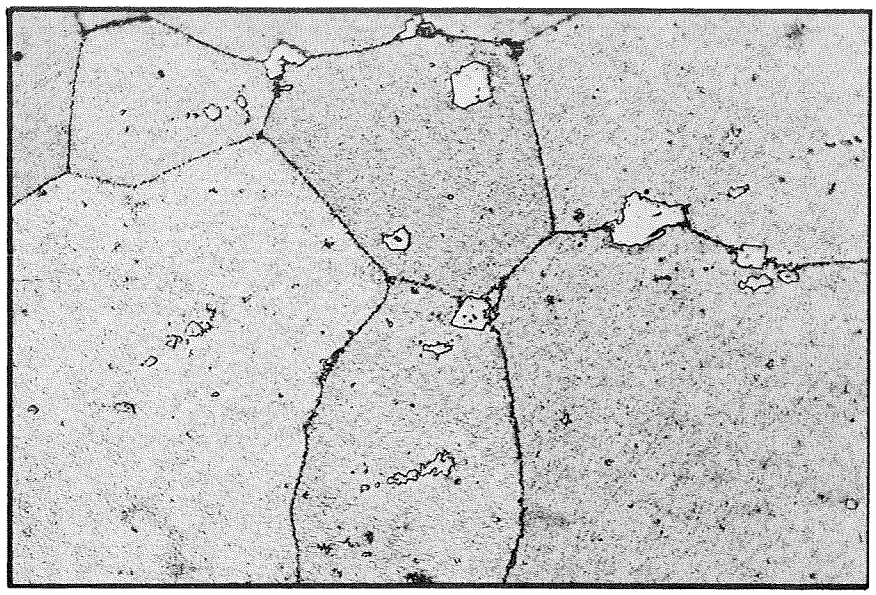

R22516 500X

Double Extruded

S/R Life at 1400°F / 90 ksi = 201.7 hours

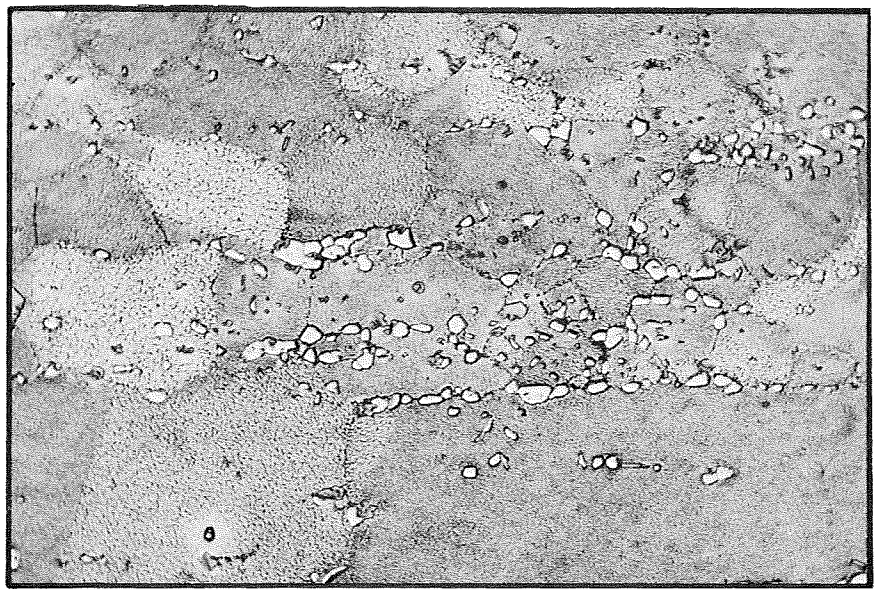

R22513 500X

Single Extruded and Rolled

S/R Life at 1400°F / 90 ksi = 69.7 hours

FIGURE 42: OPTICAL MICROGRAPHS OF IIb STRESS RUPTURE SAMPLES ILLUSTRATING THE STRUCTURAL VARIATIONS WHICH OCCUR DEPENDING ON THE METHOD OF PROCESSING. SAME HEAT TREATMENT WAS USED FOR BOTH SAMPLES.

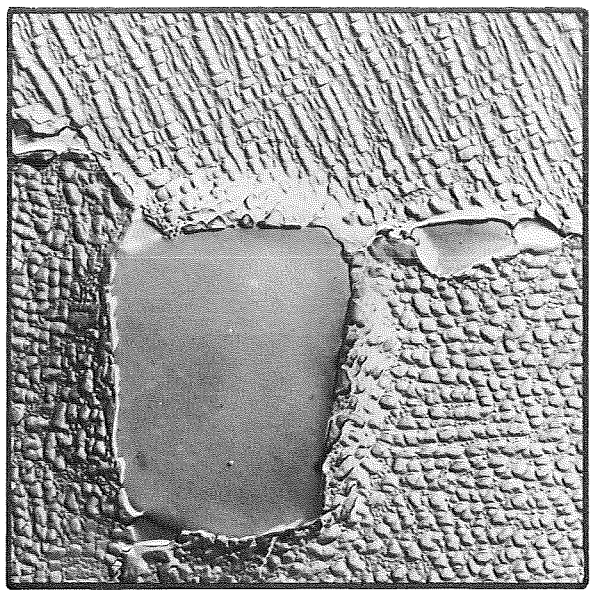

EM1984 5000X

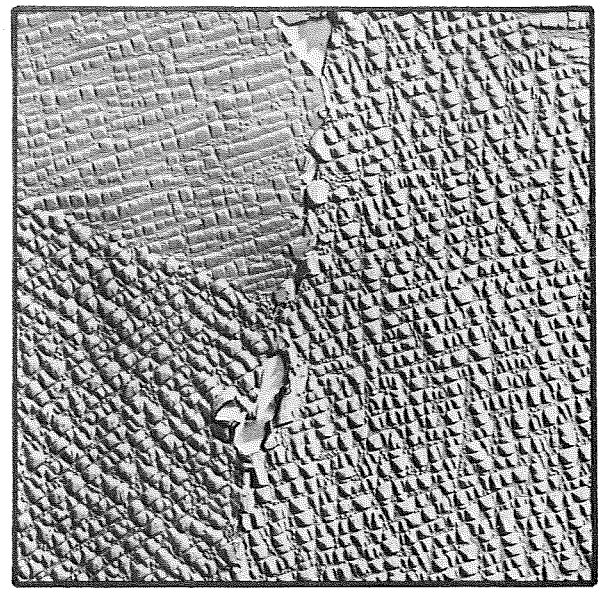

EM1982 5000X

1400°F / 1500 hours

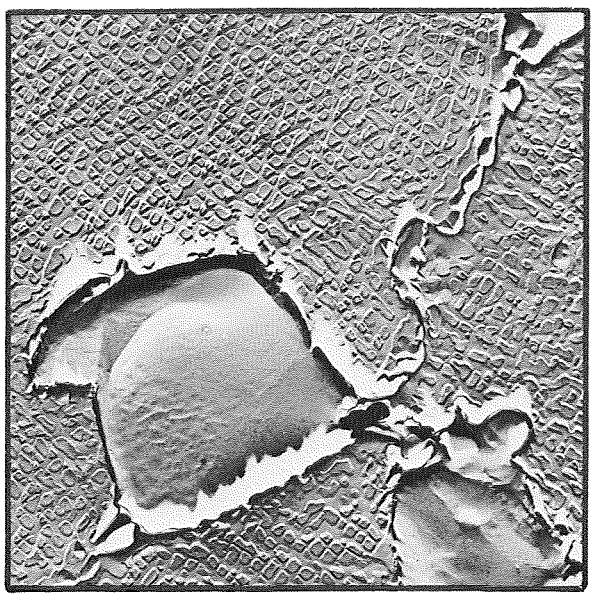

EM2054 5000X

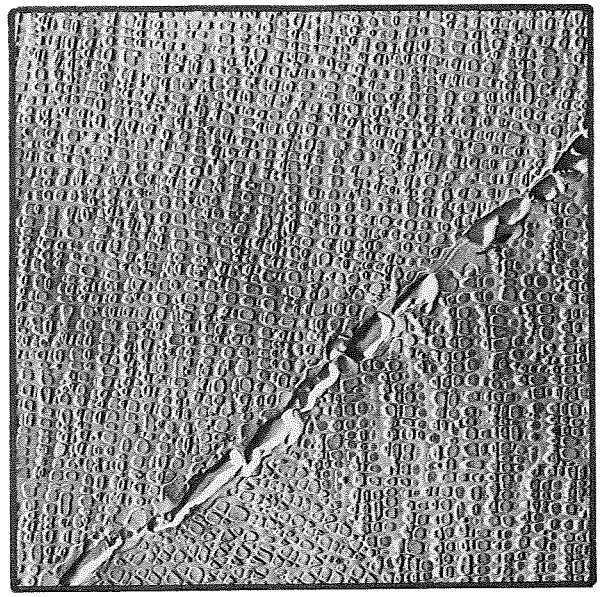

EM2060 5000X

1500°F / 1500 hours

FIGURE 43: ELECTRON MICROGRAPHS ILLUSTRATING THE MICROSTRUCTURE OF UNITEMP AF2-IDA AFTER 1500 HOURS EXPOSURE AT VARIOUS TEMPERATURES.

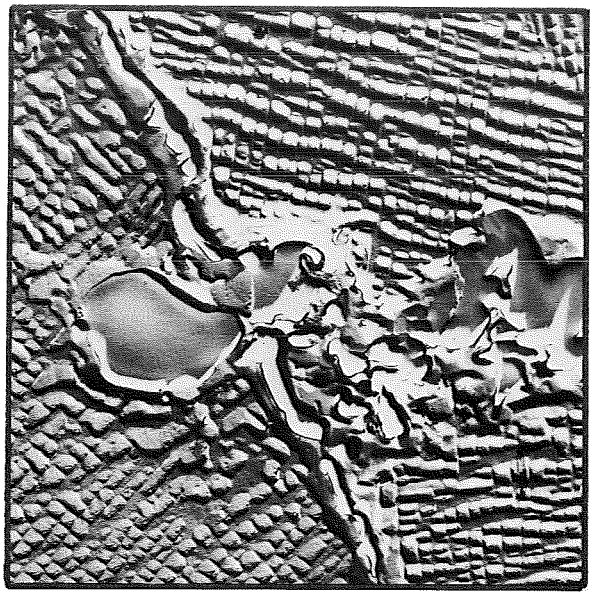

EM1976 5000X

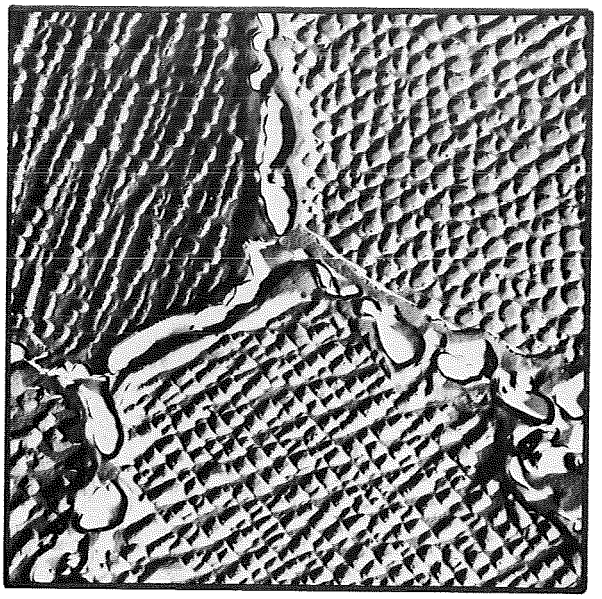

EM1970 5000X

1600°F / 1500 hours

EM1967 5000X

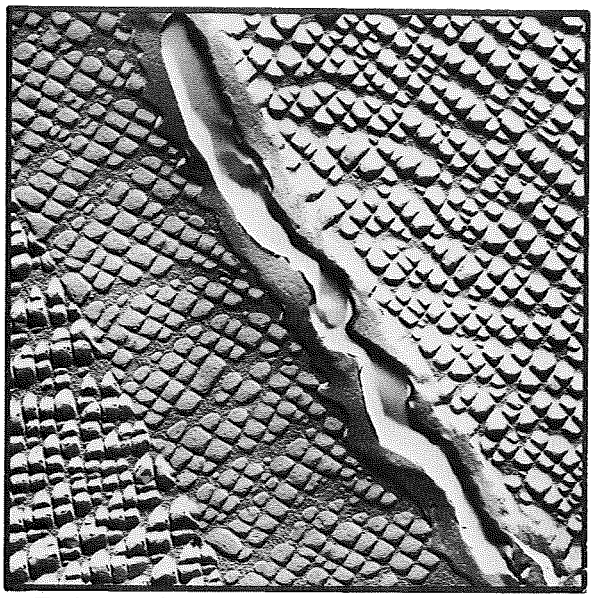

EM1966 5000X

1700°F / 1500 hours

FIGURE 43: (continued) ELECTRON MICROGRAPHS ILLUSTRATING THE MICROSTRUCTURE OF UNITEMP AF2-IDA AFTER 1500 HOURS EXPOSURE AT VARIOUS TEMPERATURES.

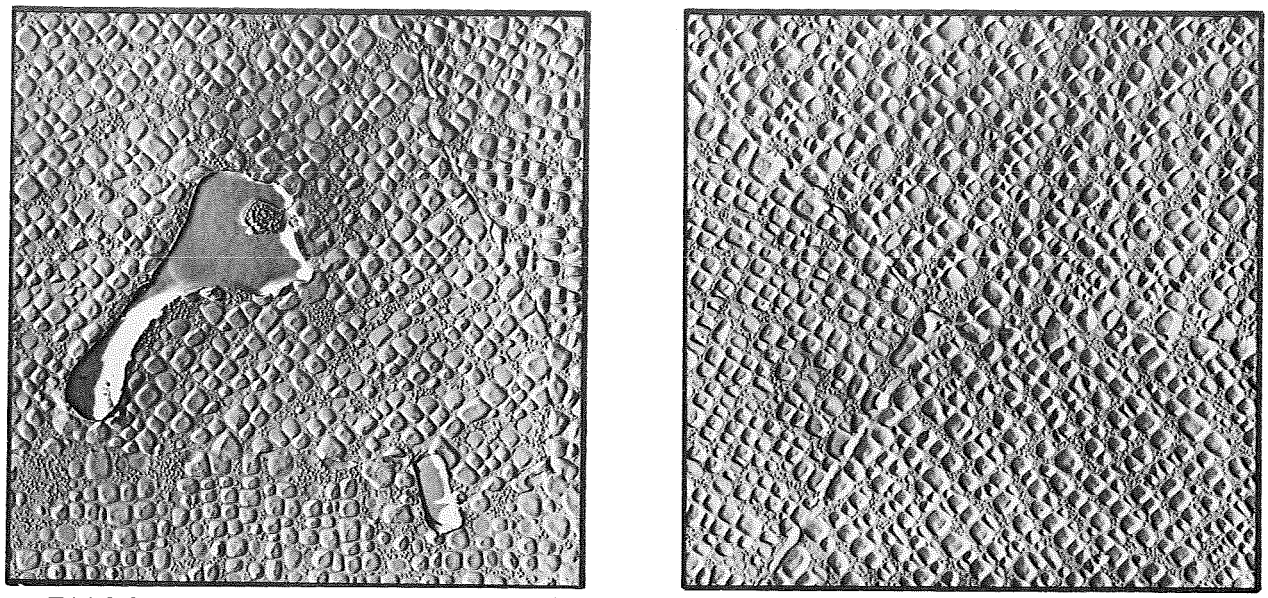

EM2045 5000X EM2046 5000X

1400°F / 1500 hours

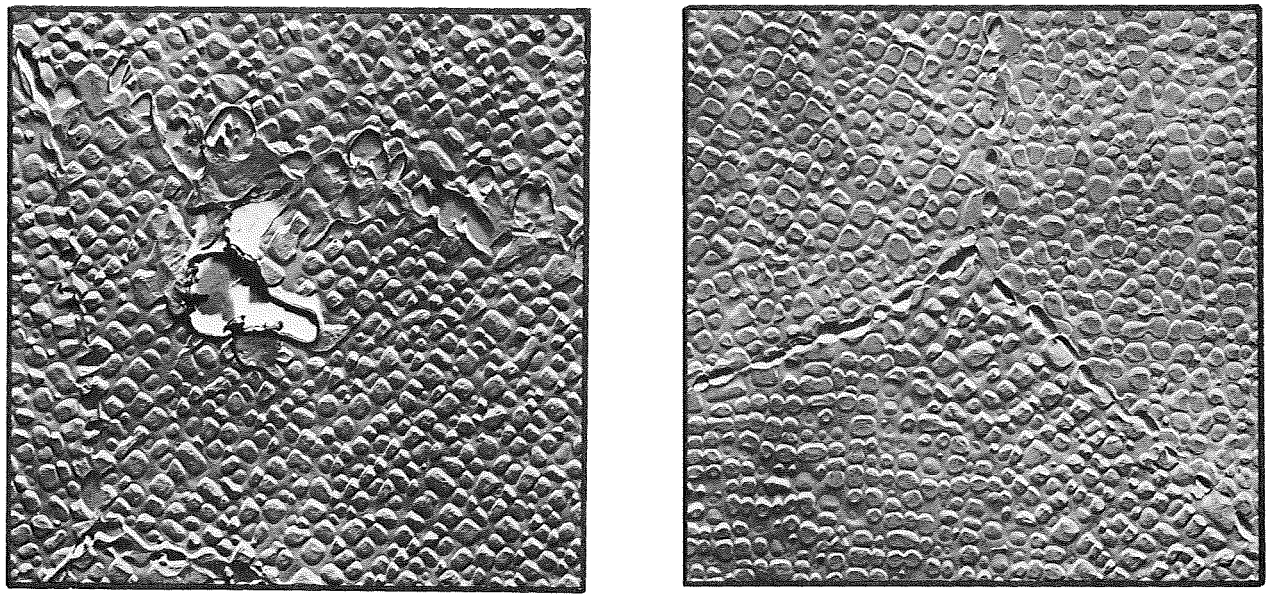

EM2049 5000X EM2047 5000X

1500°F / 1500 hours

FIGURE 44 : ELECTRON MICROGRAPHS ILLUSTRATING THE MICROSTRUCTURE OF I 5 AFTER 1500 HOURS EXPOSURE AT VARIOUS TEMPERATURES.

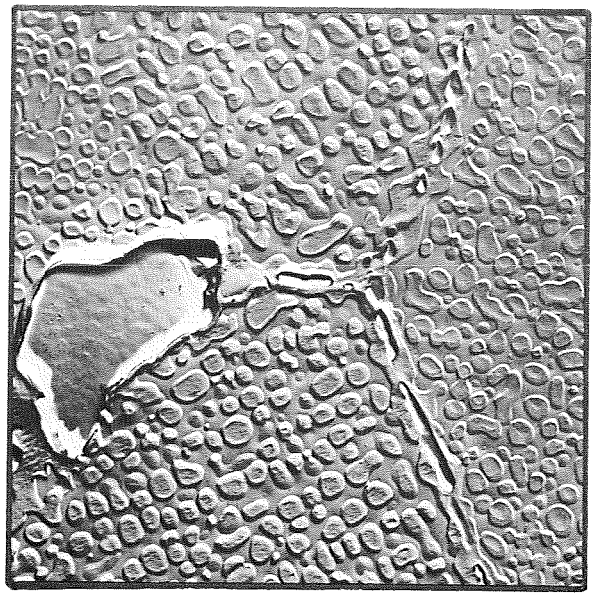

EM2053 5000X

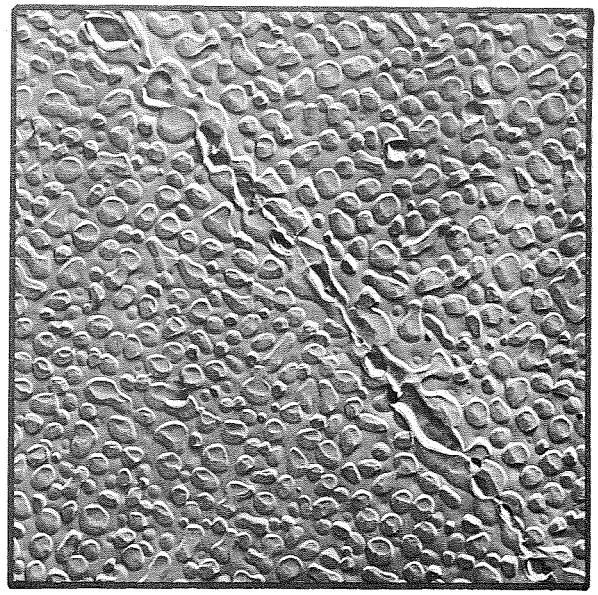

EM2052 5000X

1600°F / 1500 hours

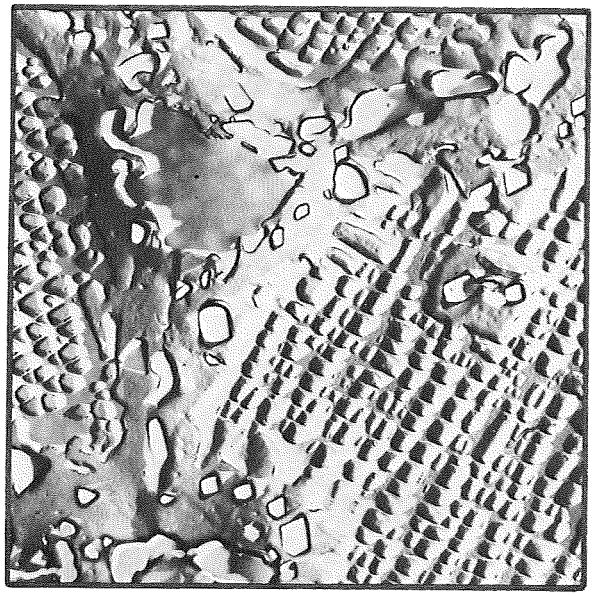

EM 2012 5000X

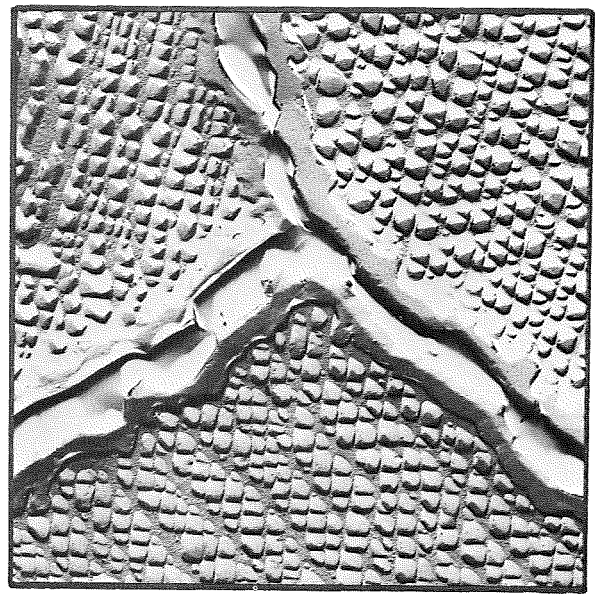

EM2014 5000X

1700°F / 1500 hours

FIGURE 44: (continued) ELECTRON MICROGRAPHS ILLUSTRATING THE MICROSTRUCTURE OF I5 AFTER 1500 HOURS EXPOSURE AT VARIOUS TEMPERATURES.

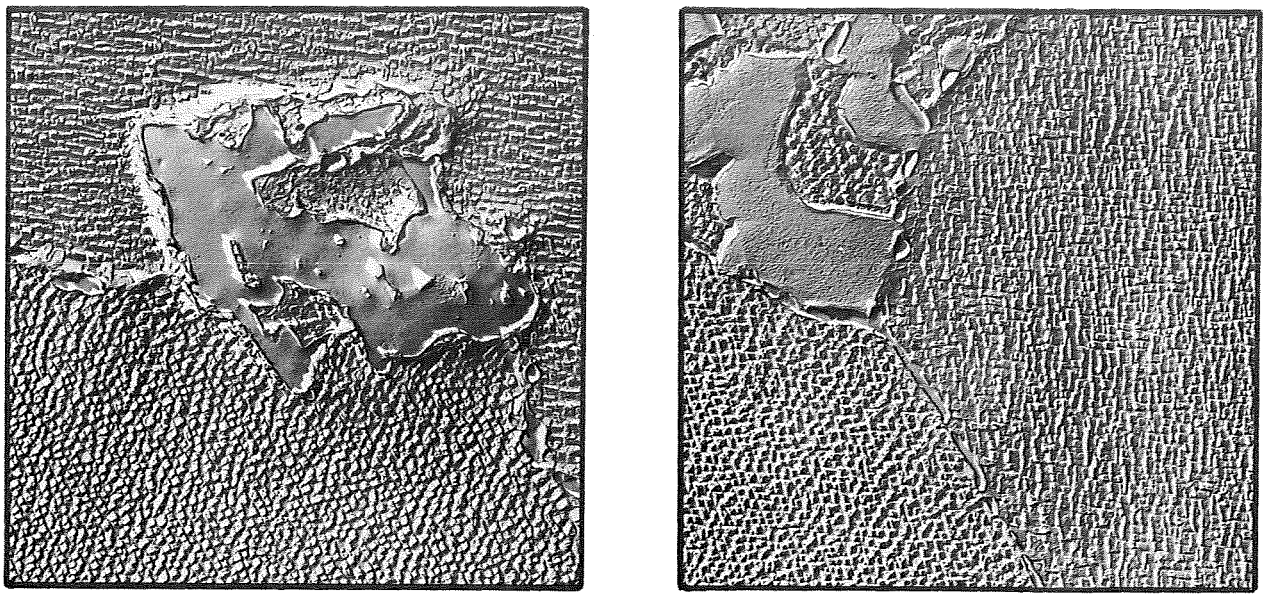

EM2424 5000X EM2426 5000X

1400°F / 1500 hours

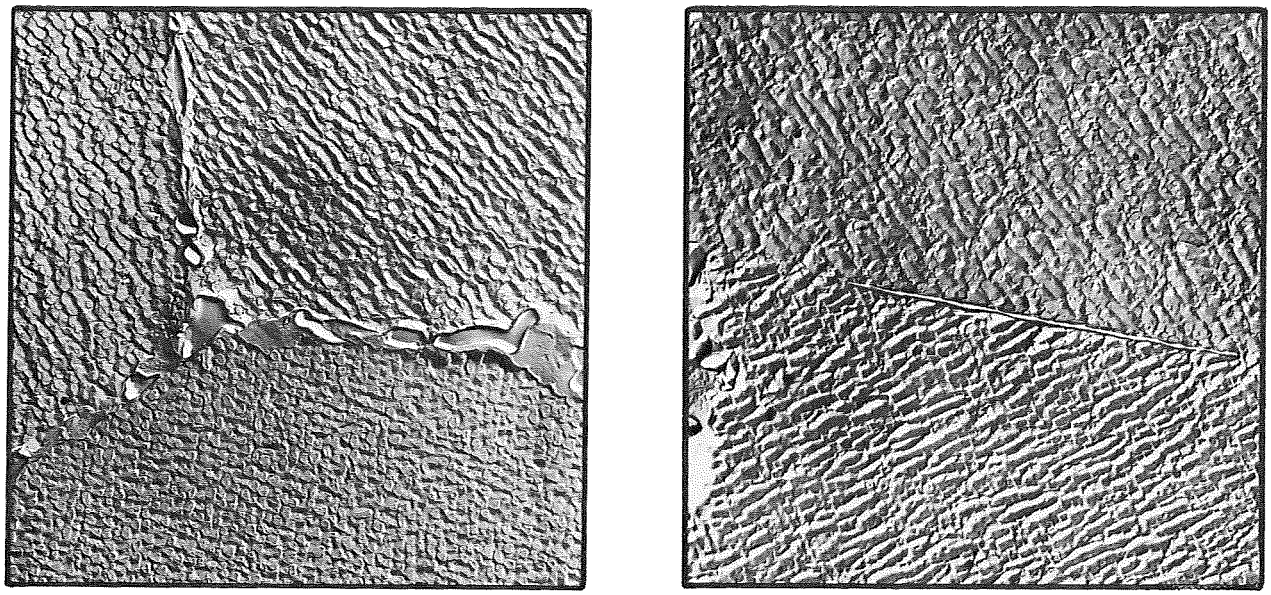

EM2435 5000X EM2573 5000X

1500°F / 1500 hours

FIGURE 45 : ELECTRON MICROGRAPHS ILLUSTRATING THE MICROSTRUCTURE OF IIb AFTER 1500 HOURS EXPOSURE AT VARIOUS TEMPERATURES.

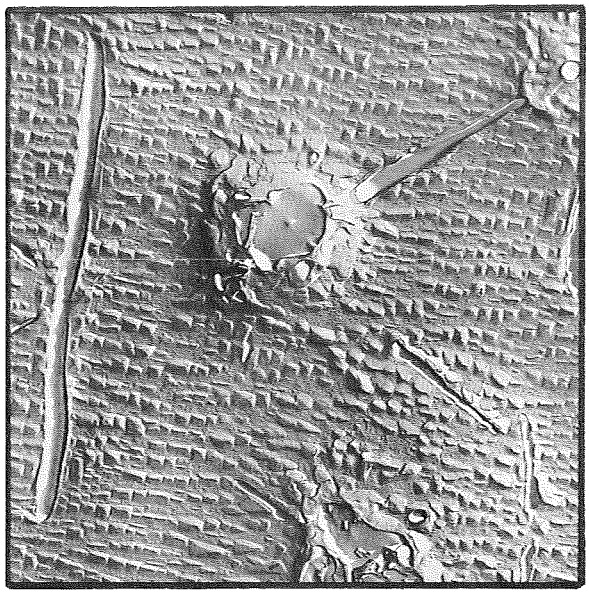

EM2609 5000X

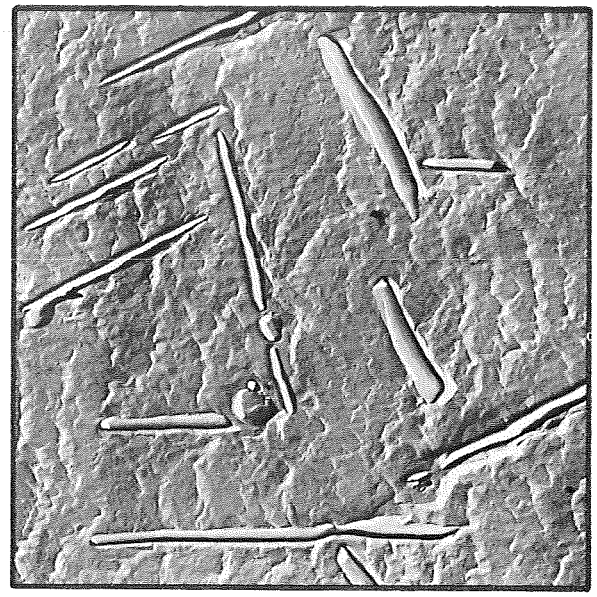

EM2443 5000X

1600°F / 1500 hours

EM2449 5000X

EM2450 5000X

1700°F / 1500 hours

FIGURE 45: (continued) ELECTRON MICROGRAPHS ILLUSTRATING THE MICROSTRUCTURE OF IIb AFTER 1500 HOURS EXPOSURE AT VARIOUS TEMPERATURES.

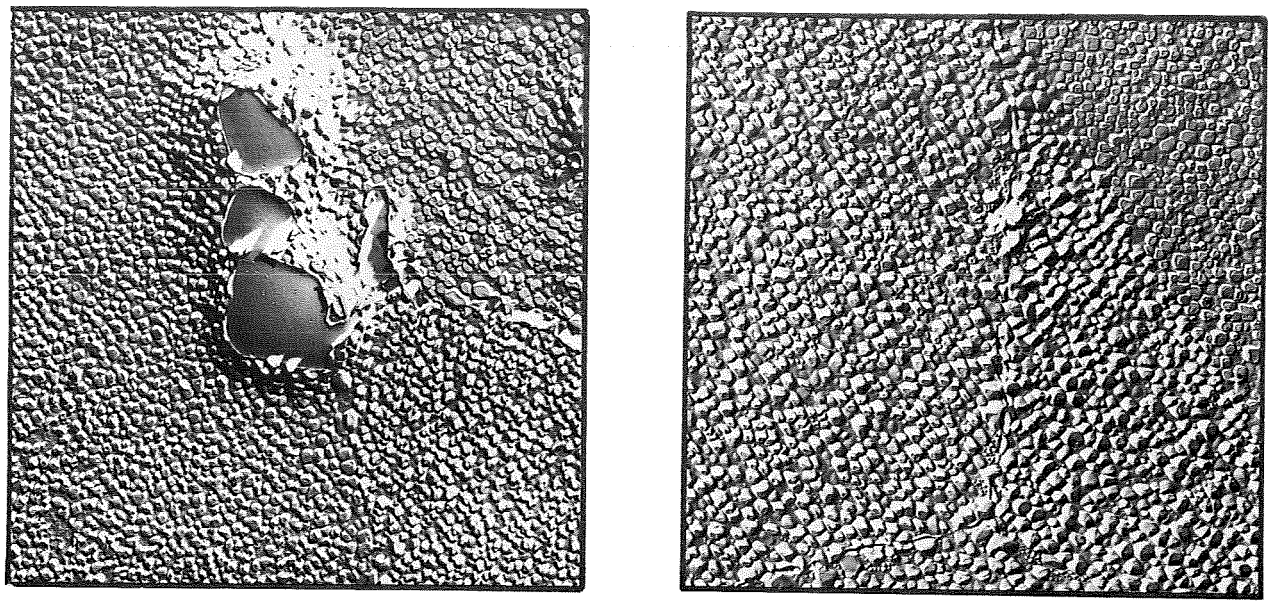

EM2490 5000X EM2489 5000X

1400°F / 1500 hours

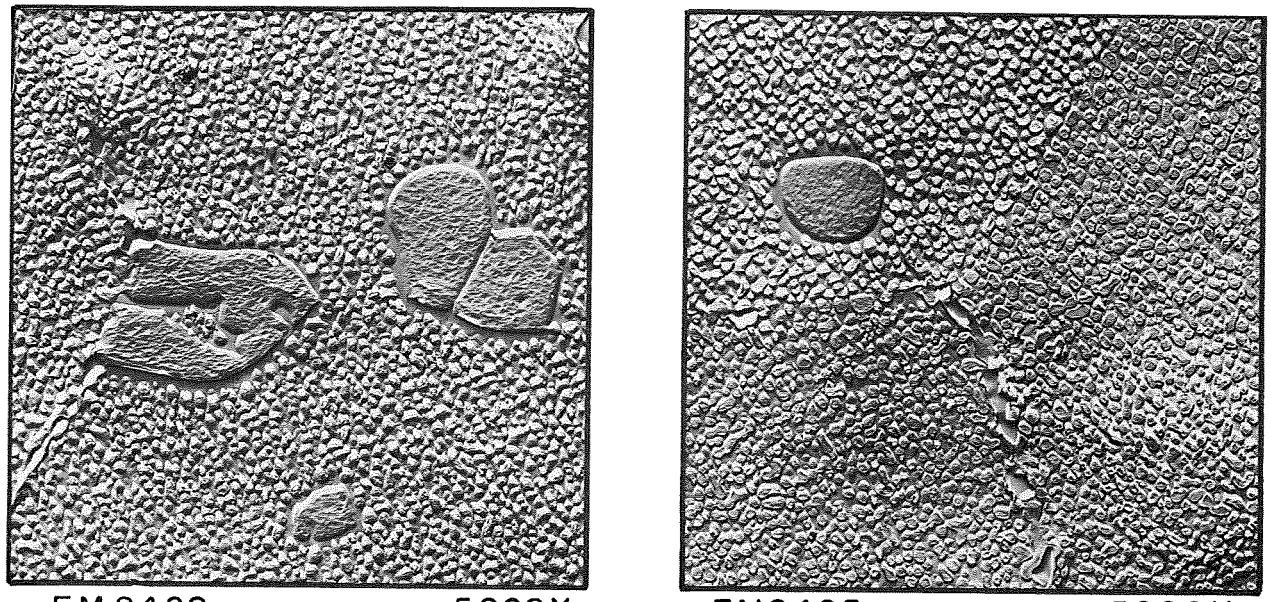

EM 2482 5000X EM2485 5000X

1500°F / 1500 hours

FIGURE 46: ELECTRON MICROGRAPHS ILLUSTRATING THE MICROSTRUCTURE OF IIIg mod AFTER 1500 HOURS EXPOSURE AT VARIOUS TEMPERATURES.

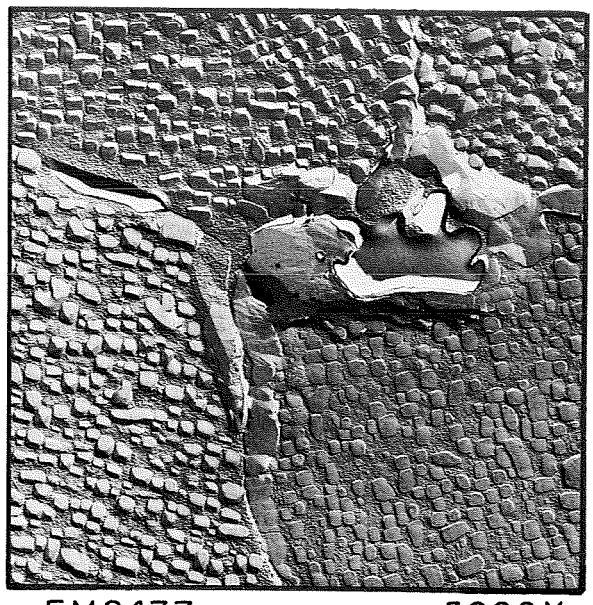

EM2477 5000X

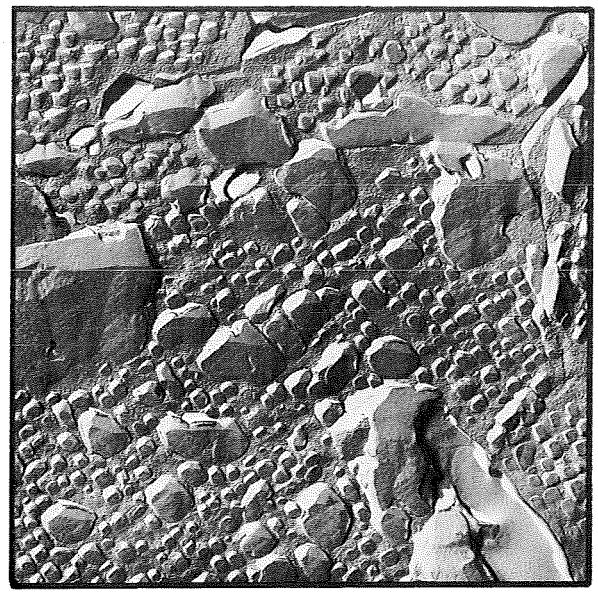

EM2475 5000X

1600°F / 1500 hours

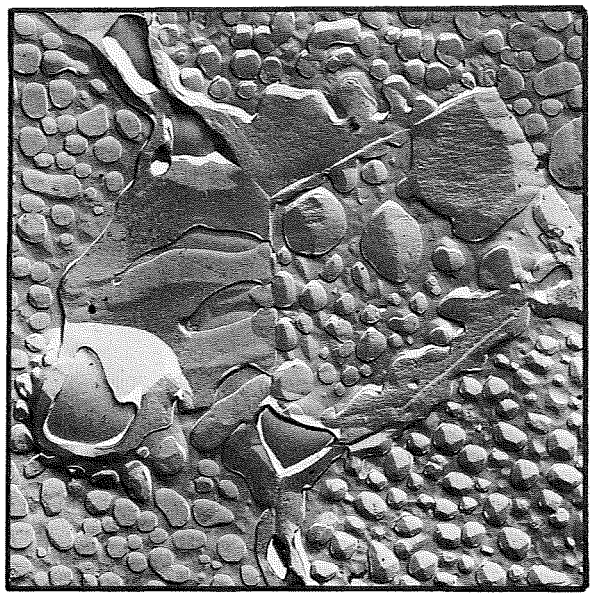

EM2471 5000X

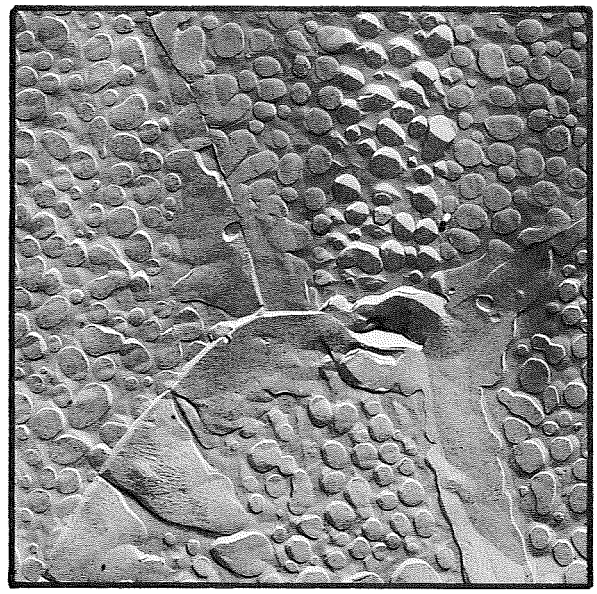

EM2469 5000X

1700°F / 1500 hours

FIGURE 46: (continued) ELECTRON MICROGRAPHS ILLUSTRATING THE MICROSTRUCTURE OF IIIg mod AFTER 1500 HOURS EXPOSURE AT VARIOUS TEMPERATURES.

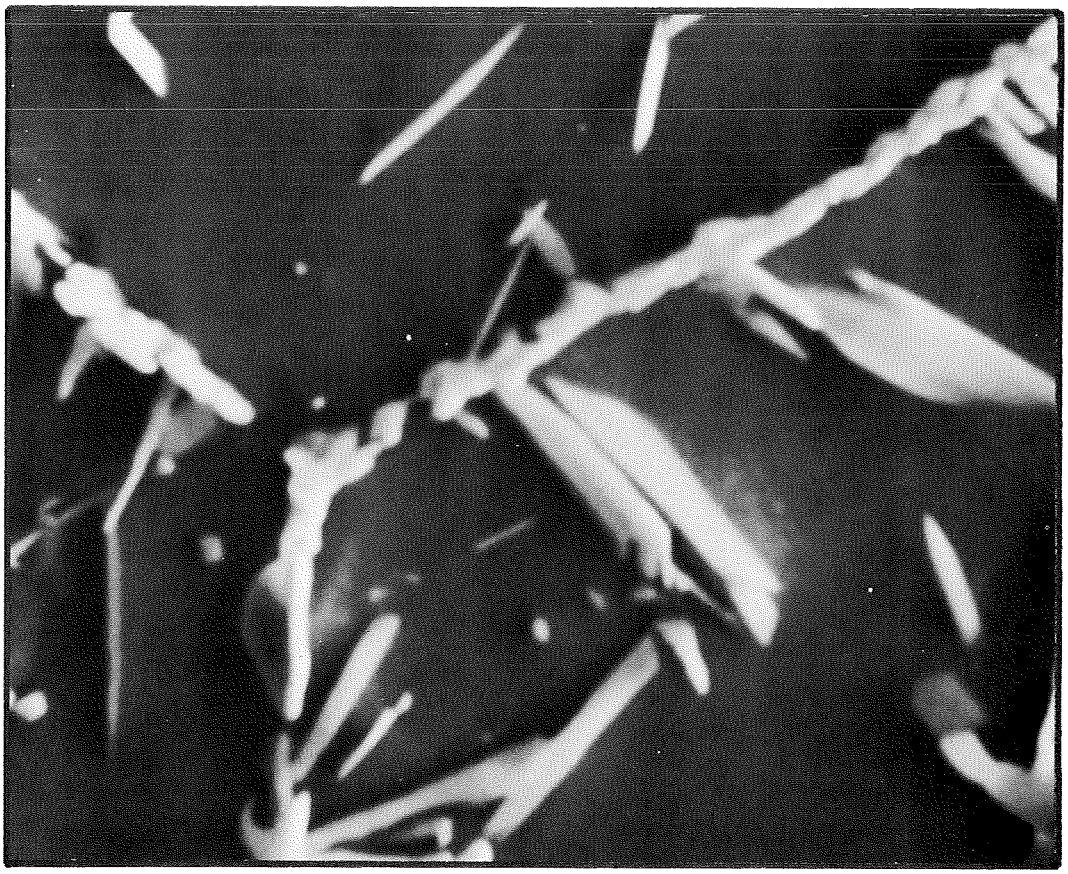

II b 1600°F / 1500 hours 1700X

FIGURE 47: SCANNING ELECTRON MICROGRAPH OF A II b SAMPLE AFTER A 1600°F / 1500 hour EXPOSURE SHOWING HEAVY GRAIN BOUNDARY PRECIPITATE AND NEEDLE-LIKE PLATELETS.

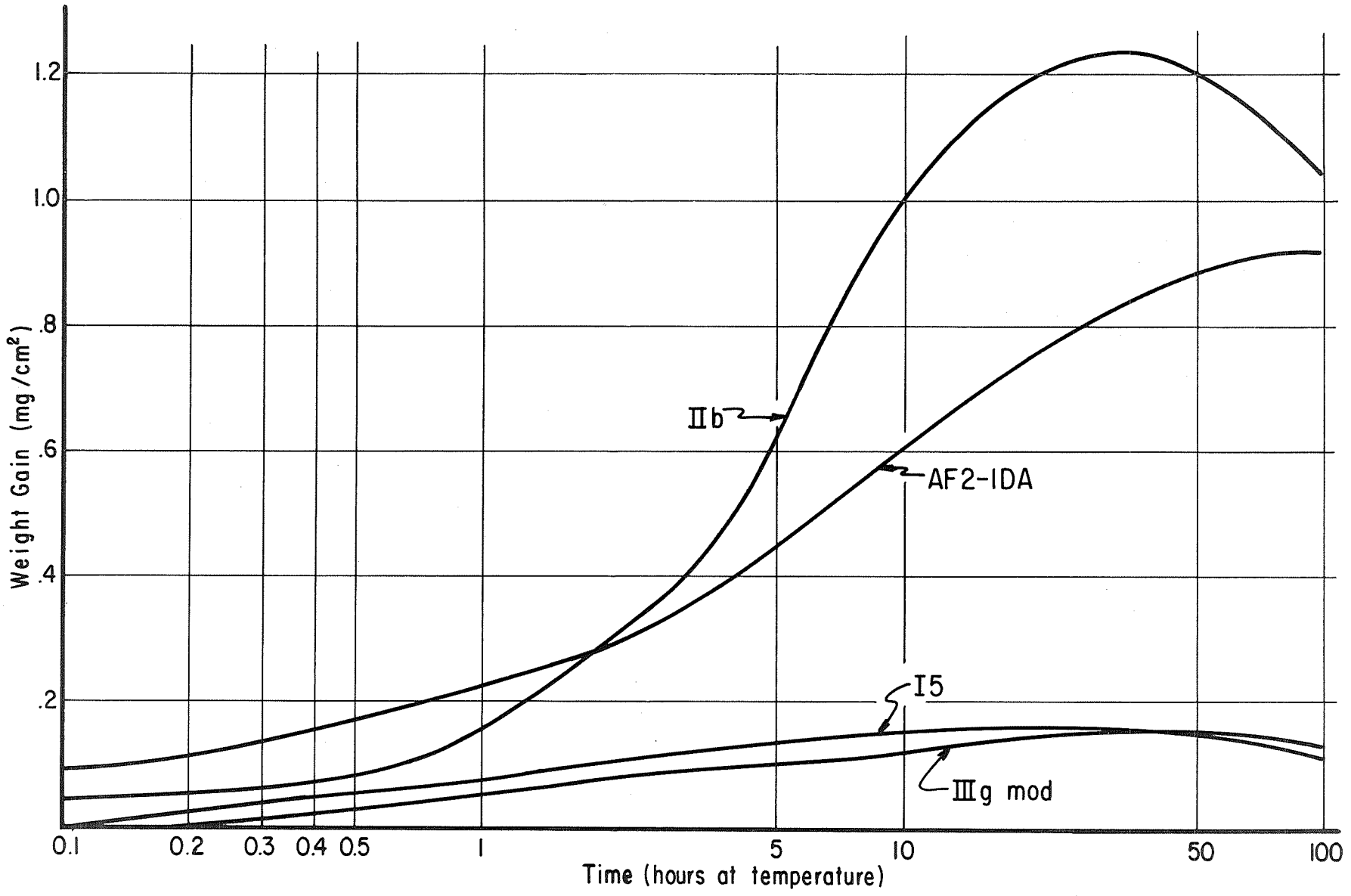


FIGURE 48: OXIDATION RATES OF TASK II ALLOYS FOR CONTINUOUS TESTING AT 1950°F.

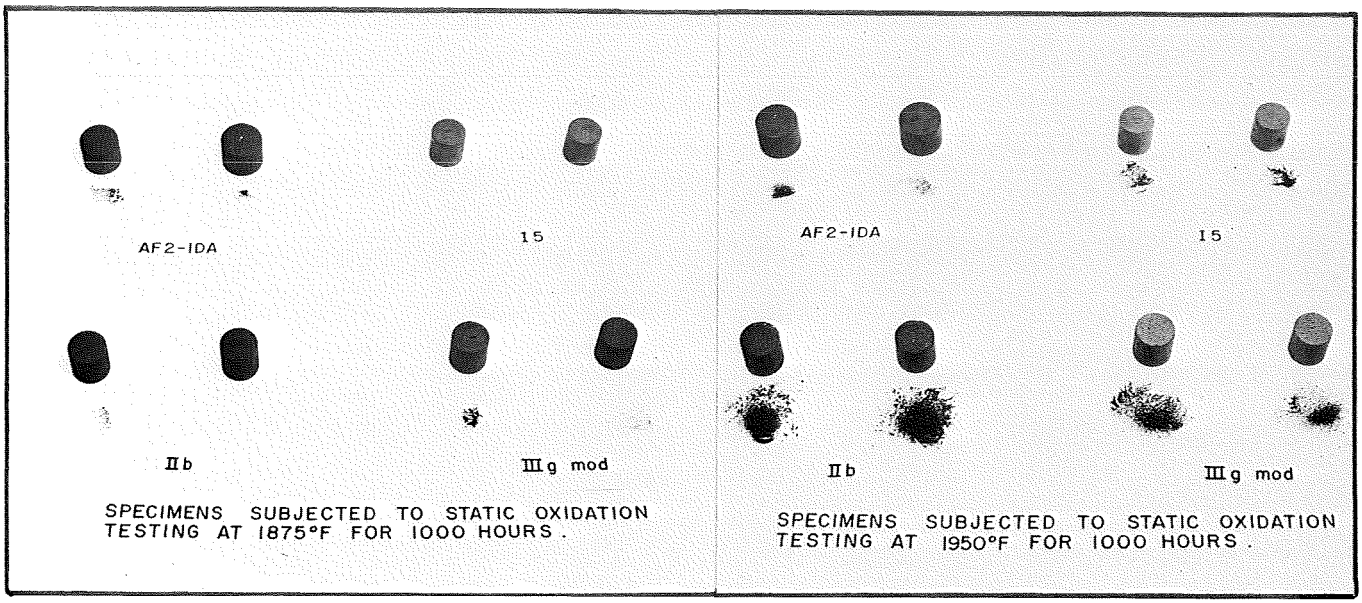


M1735 M1736

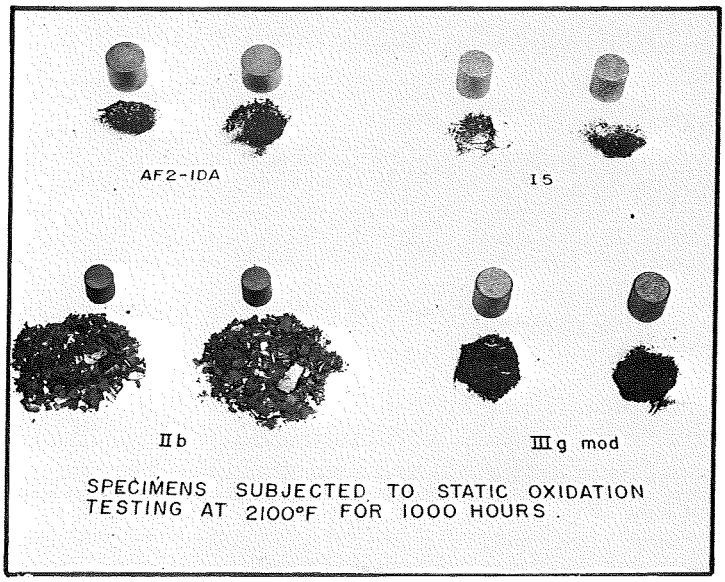


M1737

FIGURE 49: SAMPLES RESULTING FROM 1000 HOUR STATIC OXIDATION TESTS CONDUCTED AT 1875, 1950 AND 2100°F.

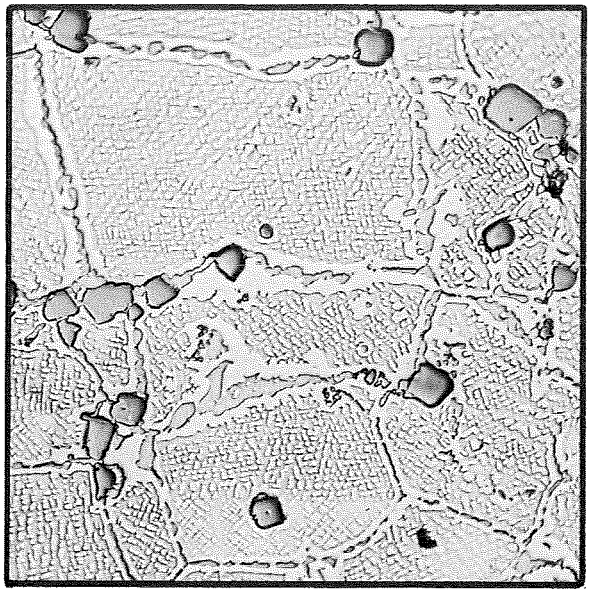

R22522 500X
Test Temperature : 1875°F

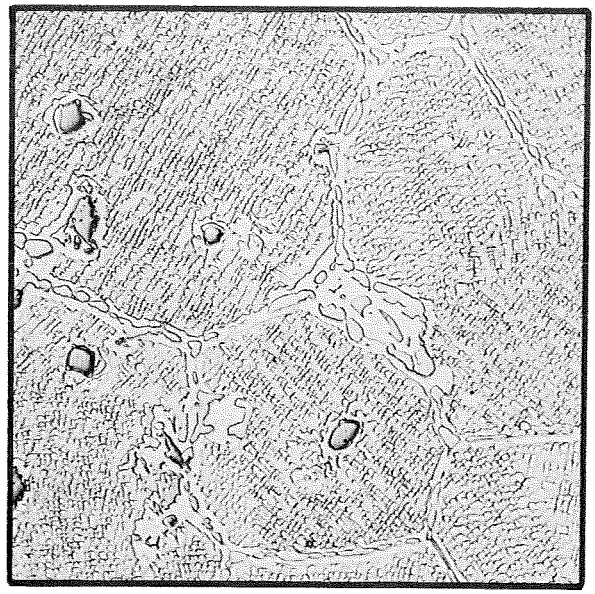

R22530 B 500X
Test Temperature : 1950°F

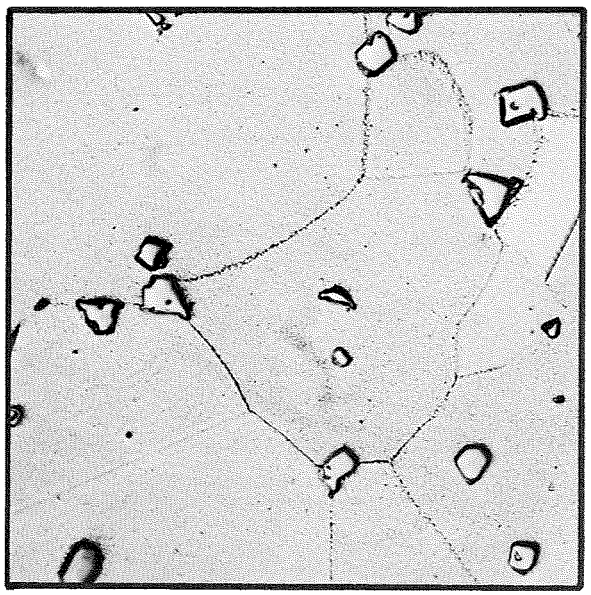

R22538 B 500X
Test Temperature : 2100°F

FIGURE 50 : OPTICAL MICROGRAPHS ILLUSTRATING THE EFFECTS OF 1000 HOUR CYCLIC OXIDATION TESTS CONDUCTED AT VARIOUS TEMPERATURES ON THE MICROSTRUCTURE OF UNITEMP AF2-1DA.

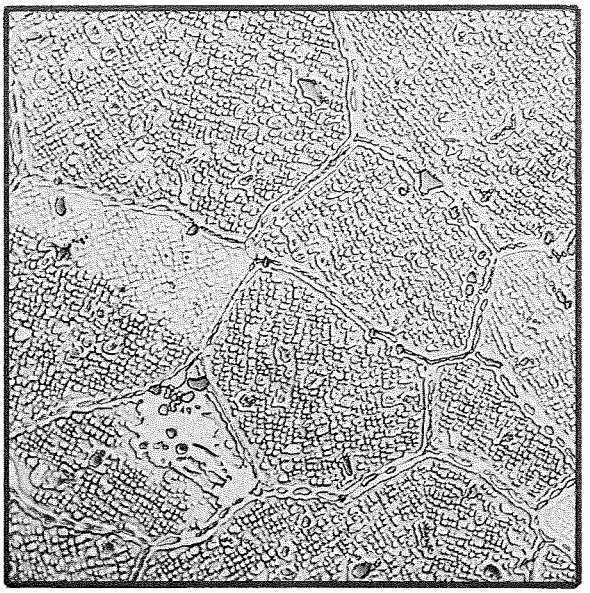

R22523 500X

Test Temperature : 1875°F

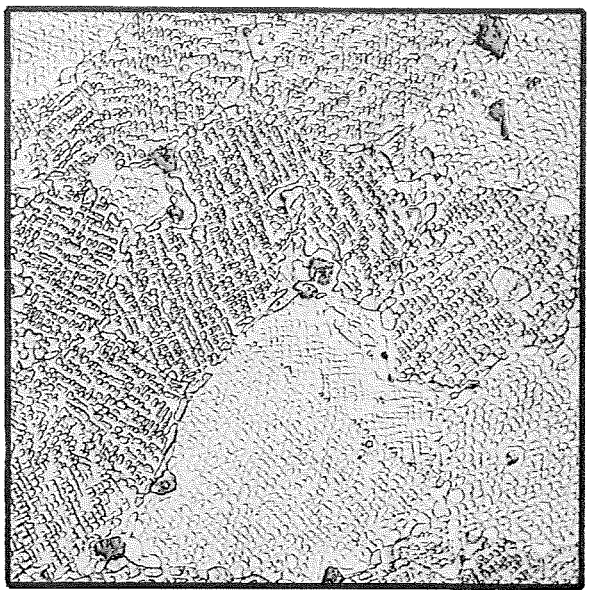

R22531B 500X

Test Temperature : 1950°F

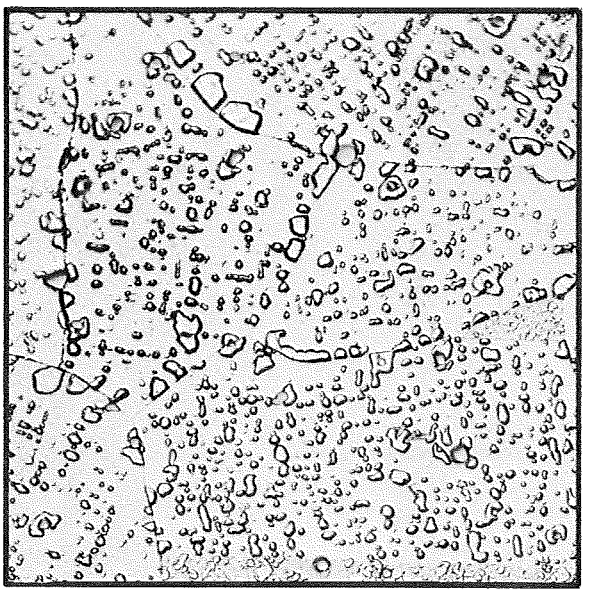

R22534 B 500X

Test Temperature : 2100°F

FIGURE 51: OPTICAL MICROGRAPHS ILLUSTRATING THE EFFECTS OF 1000 HOUR CYCLIC OXIDATION TESTS CONDUCTED AT VARIOUS TEMPERATURES ON THE MICROSTRUCTURE OF I 5.

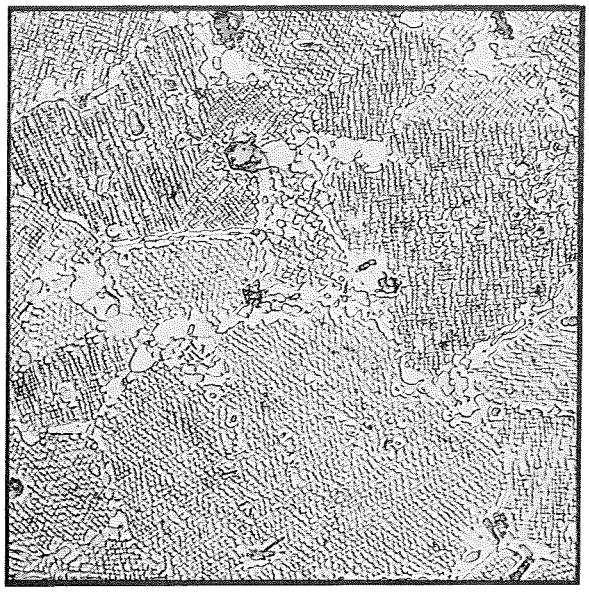

R22524 500X

Test Temperature : 1875°F

R22532 B 500X

Test Temperature : 1950°F

R22535 B 500X

Test Temperature : 2100°F

FIGURE 52 : OPTICAL MICROGRAPHS ILLUSTRATING THE EFFECTS OF 1000 HOUR CYCLIC OXIDATION TESTS CONDUCTED AT VARIOUS TEMPERATURES ON THE MICROSTRUCTURE OF IIb.

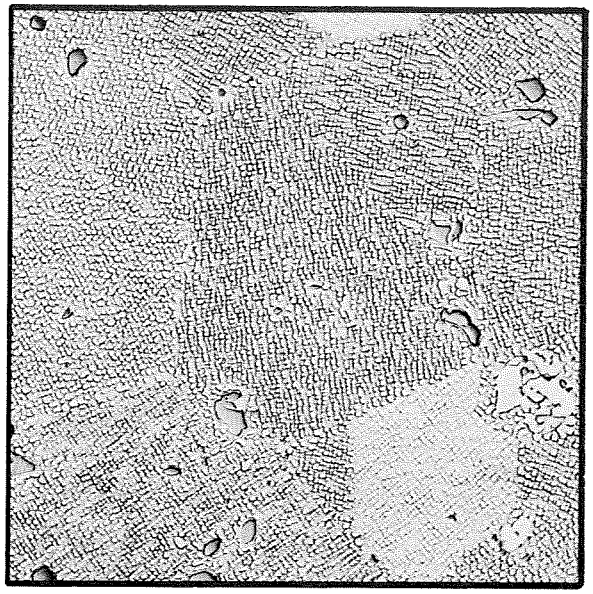

R22525 500X
Test Temperature : 1875°F

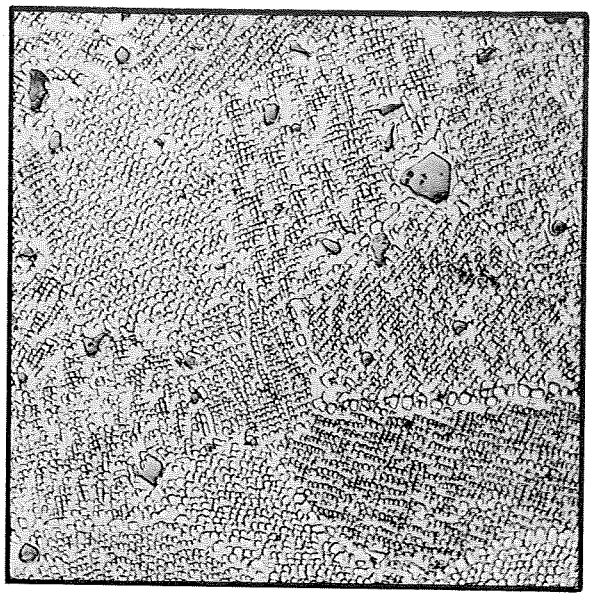

R22533B 500X
Test Temperature : 1950°F

R22539B 500X
Test Temperature : 2100°F

FIGURE 53 : OPTICAL MICROGRAPHS ILLUSTRATING THE EFFECTS OF 1000 HOUR CYCLIC OXIDATION TESTS CONDUCTED AT VARIOUS TEMPERATURES ON THE MICROSTRUCTURE OF IIIg mod.

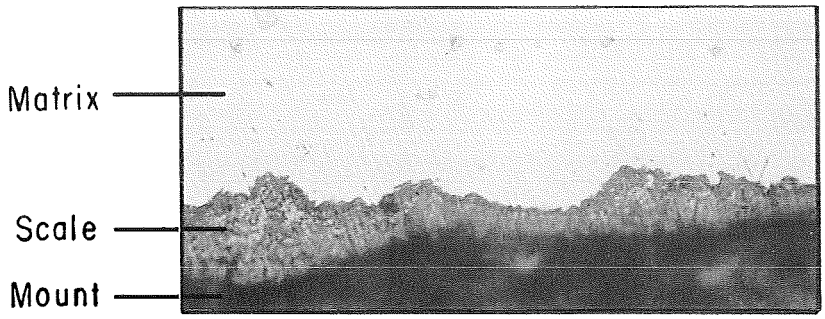


Optical Micrograph 500X

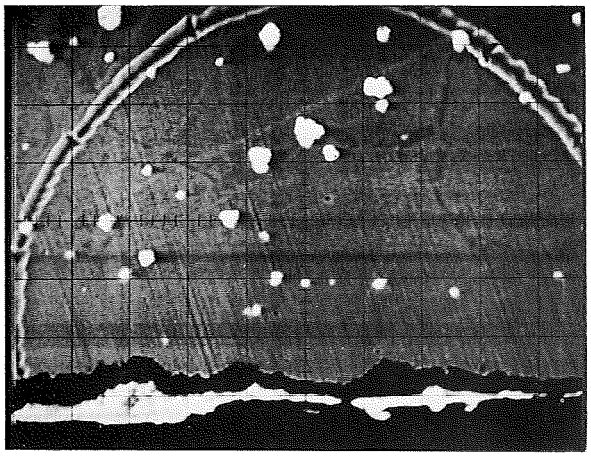

Sample Current Image 400X

Oxygen

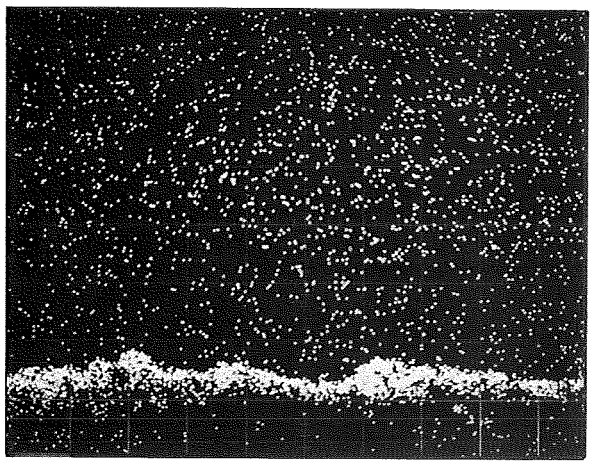

Aluminum

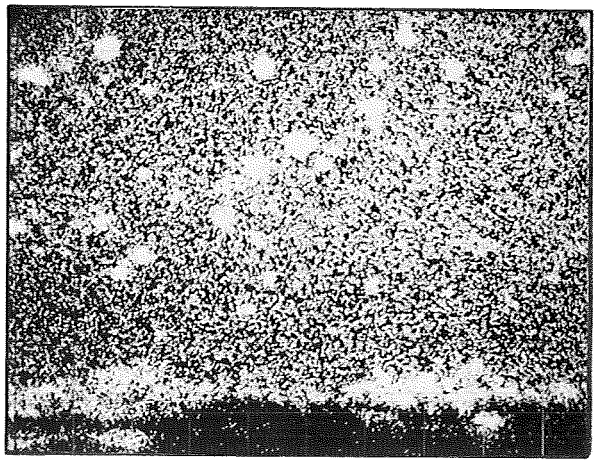

Titanium

FIGURE 54: ELECTRON BEAM MICROPROBE SCANS SHOWING ELEMENT DISTRIBUTION IN MATRIX AND OXIDE SCALE OF A UNITEMP AF2-IDA CYCLIC OXIDATION SAMPLE TESTED FOR 1000 HOURS AT 1950°F.

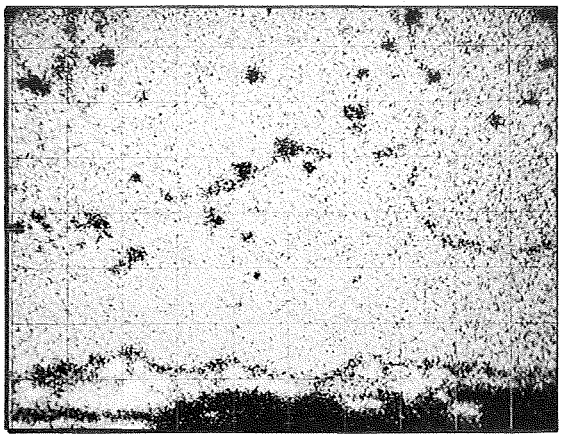

Chromium

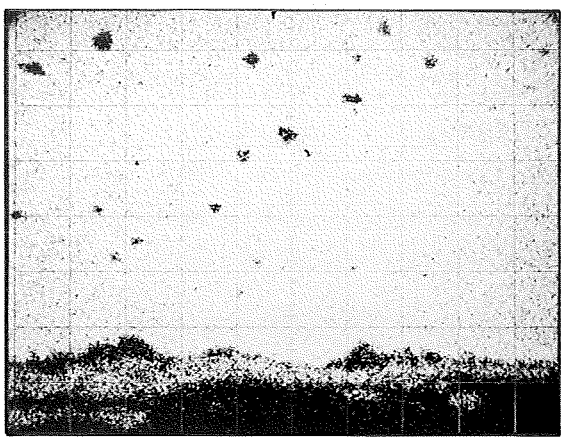

Nickel

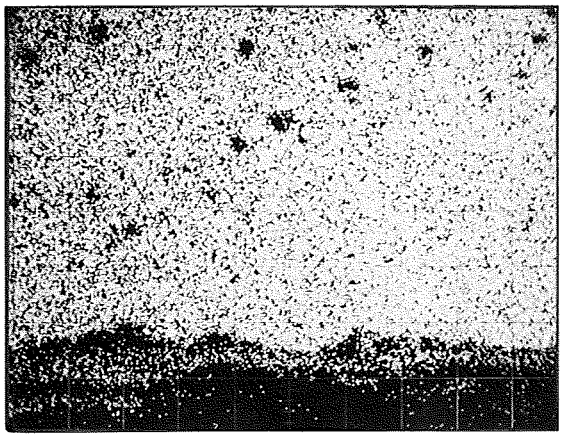

Cobalt

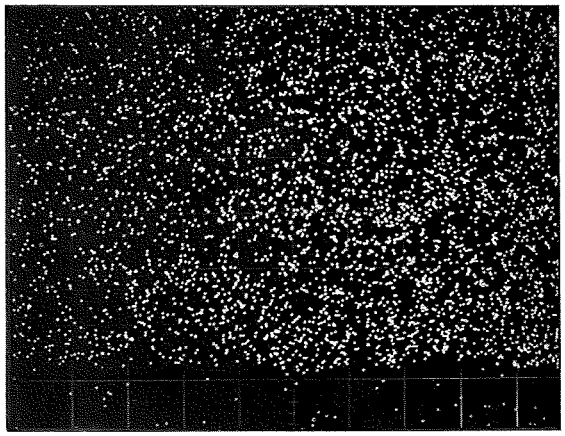

Molybdenum

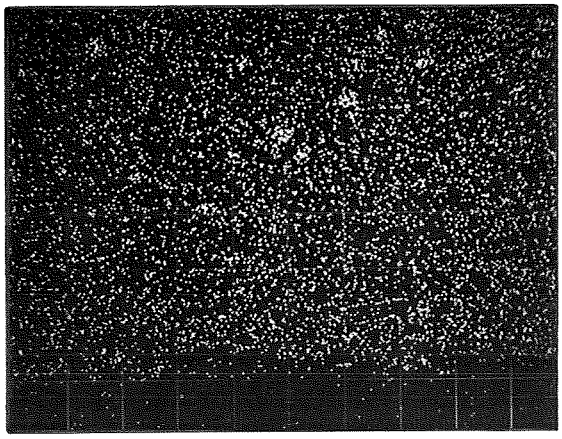

Tungsten

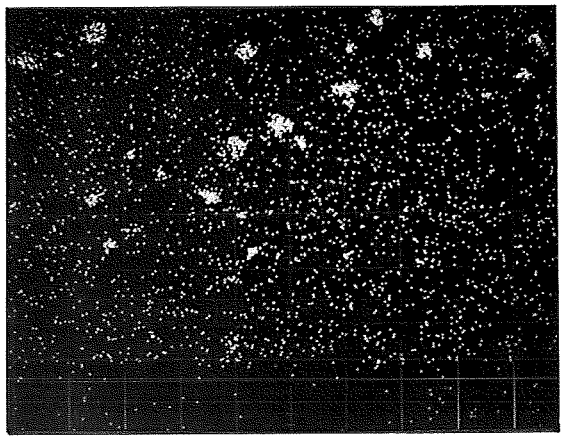

Tantalum

FIGURE 54: (continued) ELECTRON BEAM MICROPROBE SCANS SHOWING ELEMENT DISTRIBUTION IN MATRIX AND OXIDE SCALE OF A UNITEMP AF2-IDA CYCLIC OXIDATION SAMPLE TESTED FOR 1000 HOURS AT 1950°F.

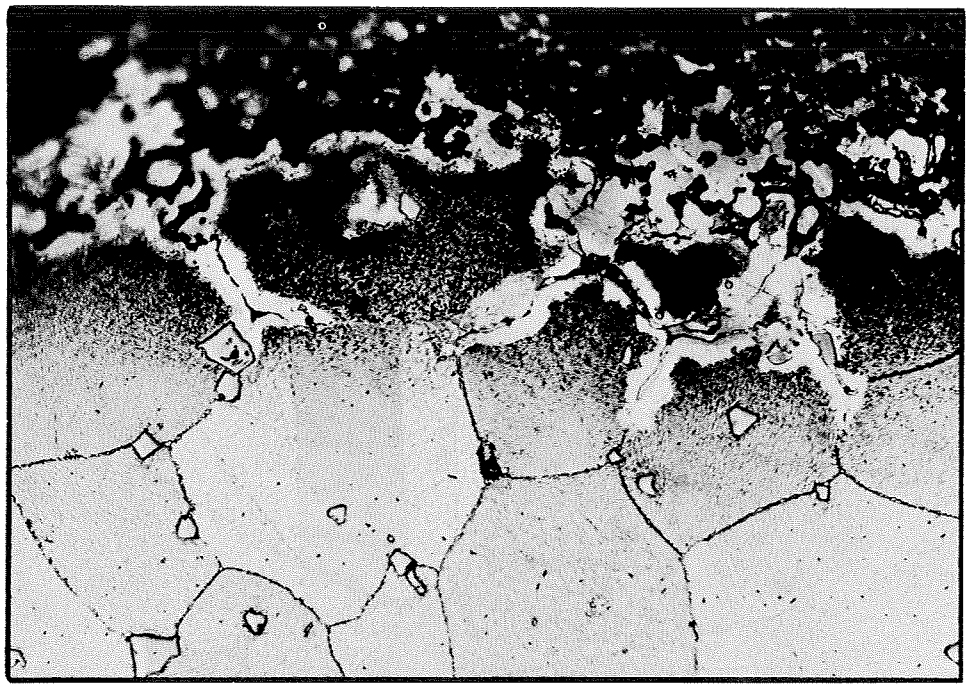

R21871 500X

1800°F Sulfidation Test Specimen

FIGURE 55: OPTICAL MICROGRAPH OF UNITEMP AF2-IDA ILLUSTRATING GRAIN BOUNDARY ATTACK AFTER SULFIDATION TESTING FOR ONE HOUR AT 1800°F.